ACCELERATING THE THAUMASITE FORM OF SULFATE ATTACK AND AN INVESTIGATION OF ITS EFFECTS ON SKIN FRICTION

by

RENÉ BRUECKNER

(Dipl.-Ing.)

A Thesis Submitted to
The University of Birmingham
for the Degree of
DOCTOR OF PHILOSOPHY

School of Civil Engineering
University of Birmingham
Edgbaston
Birmingham B15 2TT
December 2007

Synopsis

The objective of the research was to accelerate the thaumasite form of sulfate attack (TSA) under laboratory conditions in order to identify its effects on skin friction at the soil/concrete interface.

The experimental programme was organised into five series which investigated the formation of TSA under unrestrained and restrained conditions whereby the acceleration of TSA was observed at unrestrained conditions depending on water-cement ratio, cement content, casting face and aggressive solution. Restrained conditions simulated soil/concrete interface interactions and were applied to identify changes of the skin friction affected by the formation of thaumasite.

TSA was successfully accelerated and a linear deterioration progress was monitored using a developed needle test method. Using clay-restrained conditions thaumasite formed attached to the concrete and favoured a more severe deterioration culminating in thaumasite layers of up to 25mm depending on interface pH and applied pressure. Thaumasite at the interface did not decrease the shear strength including skin friction and cohesion. Therefore it was concluded that TSA occurring at piles or foundation bases does not affect the stability of the superstructure regarding loss of friction and settlements, however, continuous loss of concrete can increase the slenderness and cause premature corrosion.

Contents

References

Appendices

Appendix A: Material Properties

Appendix B: Microscopical Investigations

Appendix C: XRD-Analysis Data

Appendix D: Pressure Development – Series I

Appendix E: Ion-Exchange Data

Appendix F: TSA Expansion at Concrete/Clay Interface – Series V

Appendix G: Interface Moisture Content – Series V

List of Figures

Chapter 2

Chapter 3

Chapter 4

Chapter 5

Chapter 6

List of Tables

Chapter 2

Chapter 3

Chapter 4

Chapter 5

Chapter 6

Abbreviations:

Different units may be used in the text and in the notation items of notation are, however, dimensionally identical.

General terms:

A   cross sectional area [mm^2]

ACEC-class   Aggressive Chemical Environment for Concrete

ACR   Aggregate carbonate range

APM   Additional protective measures

BRE   Building Research Establishment

BRECEM   50% ggbs and 50% HAC

CS   cast in-situ

DC-class   Design Chemical class

DETR   Department of the Environment, Transport and the Regions

ECC   English China Clay

EDX   Energy Dispersive X-ray analysis

ESEM   Environmental Scanning Electron Microscopy

ggbs   ground granulated blastfurnace slag

HAC   calcium aluminate cement

LLC   Lower Lias Clay

N   normal force [N]

PC   Portland cement

PC   precast

PCD   popcorn calcite deposition

pfa   pulverised fuel ash

PLC   Portland limestone cement

PPL   plane polarised light

SEM   Scanning Electron Microscopy

SRPC   Sulfate Resisting Portland cement

TEG   Thaumasite Expert Group

TF	Thaumasite Formation
TSA	Thaumasite form of Sulfate Attack
w/c-ratio	water/cement ratio
XPL	crossed polarised light
XRD	X-ray diffraction analyses

Chemical terms:

Afm	tricalcium-aluminate-ferrite-monosulfate
C_3S	alite
C_2S	belite
C_3A	aluminate
C_4AF	aluminateferrit
$CaCO_3$	calcite/aragonite/vaterite
$CaCO_3MgCO_3$	dolomitic limestone
CAH	calcium aluminate hydrate
CO_2	carbon dioxide
$Ca(OH)_2$	portlandite
$3CaO \cdot Al_2O_3 \cdot 3CaSO_4 \cdot 32H_2O$	ettringite
$CaSiO_3 \cdot CaCO_3 \cdot CaSO_4 \cdot 15H_2O$	thaumasite
$CaSO_4$	gypsum/selenite
CSH	calcium silicate hydrate
Fe_2O_3	ferric oxide
Fe_2S	pyrite/marcasite
FeS to $Fe_{1.8}S$	pyrrhotite
H_2SO_4	sulfuric acid
$Mg(OH)_2$	brucite
$MgSO_4$	epsomite
Na_2SO_4	Glauber's salt
pH	potentio hydrogenii

Physical terms:

c'	cohesion $[kN/m^2]$
c_a	peak interface cohesion $[kN/m^2]$
c_b	base cohesion $[kN/m^2]$
c_r	residual cohesion $[kN/m^2]$
c_u	undrained cohesion $[kN/m^2]$
δ	peak skin friction angle $[°]$
δ_r	residual skin friction angle $[°]$
f_{cu}	concrete cube compressive strength $[N/mm^2]$
φ	angle of peak internal clay friction $[°]$
φ_r	angle of residual internal clay friction $[°]$
γ	unit weight of soil $[kN/m^3]$
μ	coefficient of friction $[-]$
p_{CO_2}	partial pressure of CO_2 $[atm]$
Q_p	point resistance $[kN]$
Q_s	skin friction $[kN]$
Q_u	ultimate load $[kN]$
σ	total stress $[kN/m^2]$
τ	peak shear strength $[kN/m^2]$
τ_r	residual shear strength $[kN/m^2]$
w	moisture content $[\%]$

1   Introduction

Engineers have, for many years, been familiar with and designed to protect against the conventional form of sulfate attack which occurs when sulfate in ground water reacts with calcium aluminate hydrates (CAH) in the concrete. Due to its discovery in the foundations of a number of overbridges a second form of sulfate attack – the thaumasite form of sulfate attack (TSA) has received considerable attention in recent years. In the case of TSA the calcium silicate hydrates (CSH), the main binding agent in all Portland cements, are targeted. Where the consumption of CAH during conventional sulfate attack causes expansion and, ultimately, cracking of the cement matrix [1] TSA leads to a transformation of the cement matrix into a mush from the surface inwards. Much of the research effort to date has concentrated very much of the formation mechanisms of TSA and the identification of concrete mixes capable of resisting it.

The work reported here is concerned with the acceleration of TSA in laboratory based concrete samples, its effect on structural behaviour at the concrete/soil interface and, hence, the validity of certain assumptions made during design.

1.1   Background

According to the Building Research Establishment (BRE) [2] over 80 cases of sulfate attack of concrete and mortar have occurred in the UK during the last two decades. The majority (95%) of these cases are caused by the thaumasite form of sulfate attack (TSA) and most of these have been found in buried limestone aggregate concretes exposed to sulfate-bearing Lower Lias Clay in the West of England.

However, the thaumasite form of sulfate attack is not only a problem in the UK, it is a worldwide phenomenon. There are cases of thaumasite formation in building materials in Canada, China, Denmark, France, Germany, Italy, Netherlands, Norway, Slovenia, South Africa, Switzerland and USA [3-17]. The most severe case as a result of the thaumasite form of sulfate attack was found in the Canadian Arctic [3, 4] where structural elements had to be replaced after two years. Despite the number of known cases, the thaumasite form of sulfate attack is a rare cause of concrete deterioration.

Other deterioration mechanisms such as carbonation, freeze-thaw attack, alkali-silica reaction and delayed ettringite formation have a higher rate of occurrence [2].

The first case of thaumasite attack detected was in a grout sample in 1962 and was published with three other cases in 1965 in the USA [16,18]. The thaumasite attack was observed in the cement grout taken from a salt mine, two sanitary sewer pipes and in the base of a core taken from an 11-year old pavement. The sewer pipes were 5 and 32 years old, respectively.

In Europe and UK, the first case of thaumasite attack found was in a mortar in Stoke-on-Trent in 1969 and it was reported by Bensted in 1977 [19]. In the following years several researchers worldwide reported the occurrence of thaumasite in a variety of deteriorated building materials. French workers Lachaud et al. [8] described 69 cases of expansion/deterioration due to sulfate attack and in particular thaumasite attack. In 1983 Oberholster et al. [14] reported the occurrence of thaumasite in concrete blocks in South Africa. In Germany hardly any cases of thaumasite formation in structures are known, however, Leifeld et al. [9] as well as Ludwig and Mehr [10] found damage in lime-gypsum plasters and in mortar encountered in sulfate-containing brickwork in historic buildings after repair, respectively. In 1987, Berra and Baronio [11] reported the occurrence of thaumasite in a 40-year old concrete lining in Italy surrounded by pyrite-containing soil. These early cases of thaumasite formation might have been a small proportion of the actual number of cases where TSA was the main deterioration mechanism but were referred to as conventional sulfate attack.

In the early 1990's BRE investigated several cases of sulfate attack in buried cast in-situ foundations in the Cotswolds area which had, apparently, been designed to resist sulfates. In these cases the reaction product was thaumasite and the coarse and/or fine aggregate was limestone [20]. Additional civil engineering structures, such as the grout in tunnel linings [21-23] or the mortar of a 100-year-old brickwork tunnel wall [21, 24], have also been affected by the thaumasite form of sulfate attack.

Although TSA has been recognised for many years it did not receive any serious attention from either industry or the research community until the discovery of 10 cases of the thaumasite form of sulfate attack in the foundations of motorway bridges in Gloucestershire in 1998. In response to this discovery, the UK Government convened

the Thaumasite Expert Group (TEG) with 'the remit to produce interim advice and guidance on the implications for existing buildings and structures and for the design and specification of new constructions in the UK' [1]. The TEG has also published one year and three year reviews of the original expert group report [25, 26]. The report of the TEG identified areas where research was needed to improve understanding of both TSA and its effects. One of these areas is the effect of TSA on skin friction of piles and base friction of foundations – this is the primary aim of the research reported here. TSA has been found in both foundations [27] and piles [1], however, data about the effects caused by TSA are not available and nor are the mechanisms to accelerate and simulate field conditions and investigate the structural consequences of TSA.

It is necessary to investigate the effects of the thaumasite form of sulfate attack on buildings and structures despite that the cases of thaumasite attack only make up a small proportion of the different kinds of concrete deterioration. Furthermore there is not one case where the structural integrity has been seriously compromised.

1.2   Aims and Objectives

The main aims of this research project are to develop techniques for the production of TSA-affected concrete specimens with thaumasite profiles similar to those observed in the field and to assess the effects of TSA on skin friction at a soil/structure interface. The key output of the project will be guidance and quantitative data of use to those responsible for the management of concrete structures.

The specific research objectives are as follows:

- To develop laboratory techniques for the accelerated synthesis of thaumasite on concrete surfaces, whilst ensuring that the thaumasite formed does not become detached from those surfaces.
- To determine the shear strength parameters of synthesised thaumasite and the effects of TSA on skin friction at the soil/concrete interface.

1.3   Scope of the Thesis

The theoretical background to the thaumasite form of sulfate attack, testing methods for investigation of the soil/structure interface and findings relating to affected and unaffected interfaces is presented in Chapter 2. The methodology for the acceleration of TSA in laboratory conditions, the development of testing methods suitable to TSA and the materials used are found in Chapter 3. Experimental results and discussion of the acceleration of TSA in laboratory studies can be found in Chapter 4 and in Chapter 5 the results and discussion of the effects of TSA on the interface are presented. Chapter 6 presents the practical influence of the findings obtained in Chapter 4 and 5. Conclusions drawn from the results are presented in Chapter 4, 5 and 6, and recommendations for further work can be found in Chapter 7.

2   Literature Review

2.1   Introduction

Deterioration of concrete has become a significant research area with two distinct branches one concerned with design for durability and understanding deterioration mechanisms and the other on the structural effects of deterioration in existing structures. There is a wide knowledge about several types of deterioration and their mechanisms such as physical effects on durability and chemical attack of concrete structures. Physical effects include freeze-thaw damage, lime leaching and fire damage and chemical attack is defined through acid attack, various forms of sulfate attack, alkali-silica reaction and corrosion of reinforcement [28, 29]. Guidance is available for the prevention and treatment of many causes of deterioration including the thaumasite form of sulfate attack (TSA). This was not the case, however, until the publication of a report in 1999 by the Thaumasite Expert Group [1] prompted by the discovery of foundation suffering from an extreme case of TSA that had been deteriorating out of sight, for up to 30 years.

The following sections deal with this special form of sulfate attack occurrence; formation and consequences of thaumasite as well as identification, laboratory testing and prevention methods are described.

2.1.1   Sulfate Attack

Before discussing TSA it is worth revising the causes and effects of the conventional form of sulfate attack.

The damaging influence of sulfates on concrete has been known since 1877 and first investigations were performed by Candlot [30] and Michaelis [31] at the end of the 19th century. They identified a complex water enriched compound in the damaged matrix and described it as:

$$3CaO \cdot Al_2O_3 \cdot 3CaSO_4 \cdot 30H_2O$$
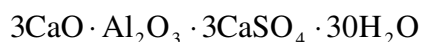
Michaelis called the salt formed 'cement bacillus' and nowadays it is known as 'ettringite', this is the main reaction product in various forms of sulfate attack. The literature recognises several forms of sulfate attack that attack phases of the cement hydration products other than the main strength giving by C-S-H-phases and these are differentiated according their formation product as the following forms [32]:

(i)   The conventional form of sulfate attack with ettringite and/or gypsum formation, primary attack of C_3A, C-A-H-phases and $Ca(OH)_2$;

(ii)   Physical sulfate attack associated with the crystallization of sulfate containing salts at or near an evaporative surface causing surface erosion, primary attack of $Ca(OH)_2$;

(iii)   Delayed ettringite formation (DEF), primary attack of C-A-H-phases and Monosulfatehydrate; and

(iv)   Sulfate attack associated with the formation of Afm phases (Tricalcium-Aluminate-Ferrite-Monosulfate), primary attack of C-A-H-phases.

Sulfate attack can also result in one of two forms of deterioration, the first form is due to leaching of the calcium containing phases, particularly of the portlandite [$Ca(OH)_2$]. The second form is the expansive form caused by formation of more voluminous reaction products such as gypsum, monosulfate and ettringite [28]. The expansive form can be categorised by the location of the supplied sulfate whether there is an external or internal source.

The main reaction products of sulfate attack are gypsum and/or ettringite and the reaction mechanism is generally accepted as portlandite transforms into gypsum and calcium aluminate hydrate into ettringite the latter being the more expansive reaction [28]. These findings allowed the development of sulfate-resisting Portland cement (SRPC - BS 4027-1996) which is mainly characterised by a limited tricalcium aluminate content ($C_3A<3.5\%$). The low presence of the main ingredient for the deteriorative reaction hinders the formation of the more voluminous reaction products which is mainly ettringite. Guidelines, such as BS EN 206, BS EN 1992 and BS 8500, have also been produced resulting in the solution to the majority of problems caused by sulfate attack.

2.1.2   Thaumasite Form of Sulfate Attack

As has already been mentioned the thaumasite form of sulfate attack differs to the forms described above including the conventional sulfate attack that in that the calcium silicate hydrates (C-S-H-phases), the main binding agent in all Portland cement binders, is targeted rather than the calcium aluminate hydrates (C-A-H-phases) and the highly soluble calcium hydroxide (Ca(OH)$_2$) [1].

Although TSA has been recognised for many years it did not receive any serious attention from either industry or the research community until the discovery of 10 cases of the thaumasite form of sulfate attack in the foundations of overbridges along the M5 motorway in Gloucestershire in 1998 [27]. The seriously attacked columns (Figure 2.1) had been all buried in backfilled Lower Lias Clay and were discovered during strengthening works. In response to this discovery the UK Government convened the Thaumasite Expert Group (TEG) with 'the remit to produce interim advice and guidance on the implications for existing buildings and structures and for the design and specification of new constructions in the UK' [1].

Figure 2.1 - Example of 29-year old bridge column exposed to wet, reworked Lower Lias Clay [1]

The Thaumasite Expert Group (TEG) emphasised in their final report [1] that deterioration as a result of the formation of thaumasite has become a separate form of sulfate attack, which has the potential to affect a wide variety of components and a range of building materials. The TEG gave thaumasite two classifications. The first being the 'Thaumasite form of Sulfate Attack' (TSA) where significant damage of the concrete/mortar matrix has occurred as a consequence of replacement of cement hydrates by thaumasite. In this case the TSA-affected concrete transforms into a soft, mushy mass with a distinctive white colouration. The second classification the 'Thaumasite Formation' (TF) refers to the occurrence of thaumasite as precipitations in pre-existing voids and cracks without causing deterioration of the host concrete or mortar. However, thaumasite formation can be a precursor of the thaumasite form of sulfate attack and constitute an early stage in the deterioration process as suggested by Sims and Huntley [33] who suggested changing the term TF to 'incipient TSA'.

In their report the TEG recognised two sets of conditions for the formation of TSA in buried concretes, these are four primary and four secondary risk factors. The TEG emphasises 'that all of the four primary risk factors need to be present before significant TSA will occur within a buried Portland cement based concrete'. The primary risk factors are defined as [1]:

- A source of sulfates and/or sulfides in the ground;
- A source of carbonate;
- Presence of mobile groundwater, and
- Low temperatures (<15°C).

The source of silicate, which is also a necessary component, was not included into the risk factors since it is an actual element in all Portland cement based materials and is mainly present as calcium silicate hydrate phases (C-S-H-phases).

The four secondary risk factors are identified by the TEG as:

- Type and quantity of cement used in concrete;
- Quality of concrete mix, compaction;
- Changes to ground chemistry and water regime resulting from construction;
- Type, depth and geometry of buried concrete.

Based on the findings of the TEG and other researchers conventional sulfate attack and thaumasite form of sulfate attack have to be considered as two separate forms, which occur in different environments. TSA takes mainly place in low temperatures (<15°C) whereas conventional sulfate attack is predominantly at ambient temperatures of >15°C. However, 15°C cannot be considered as a threshold between both types of attack, see Section 2.2.3.5.

The more frequent detection of TSA during the past decades is most probably due to the development of more selective analytical and diagnostic techniques, which are able to differentiate unambiguously between ettringite and thaumasite as well as mixed crystals of both [4, 21]. Hence Crammond [2] suggests that TSA is not a recent phenomenon and has occurred likely in the past, but has not been recognised as such because of several reasons [2]:

- Failure to detect thaumasite in standard sulfate resistance tests;
- Improved analytical techniques;
- Buried concretes rarely inspected;
- Post-construction enhancement of sulfate levels in the ground; and
- Changes in composition of modern cements.

Consequently Crammond [2] and Skalny and Thaulow [4] suggest that many other cases of TSA may remain unidentified or have been reported spuriously as 'sulfate attack' caused by ettringite formation because of misidentification due to the structural similarities. Furthermore the traditional diagnosis 25 years ago was performed using chemical analysis alone and this method is not able to distinguish between ettringite and thaumasite [2]. Nowadays the mechanisms of the different types of sulfate attack are well known and the facilities for an unambiguous identification are available.

Crammond [21] states that '*TSA is by far the most damaging mechanism involving the occurrence of thaumasite in modern constructions. It has been identified in good quality, buried limestone aggregate concretes exposed to sulfate-bearing groundwaters. The fact that most of these buried concretes should have proved sulfate resistant, prompted the UK Government's Thaumasite Expert Group to provide new recommendations in order to minimise the effect of TSA in new constructions* '.

2.2   Occurrence of TSA

The following paragraph deals in the first instance in general with thaumasite formation and then in particular with TSA and its effects on construction materials.

2.2.1   Mineral Thaumasite

Thaumasite was first identified by Nordenskiöld in Sweden in 1878 [34] and its name derives from the Greek word 'θαυμαζειν' (thaumazein) this translates as "to be surprised" or "to wonder at"[1, 27].

The mineral thaumasite is a rare naturally occurring mineral and is usually found in metamorphic rocks as a secondary mineral beside ettringite, aragonite, calcite, portlandite, gypsum, anhydrite, merwinite, gehlenite, spurrite and tobermorite [18, 33, 35]. Therefore it is hardly surprising that it can occur in a variety of building materials. The structure of both thaumasite and ettringite was characterised by Moore and Taylor [36] and Edge and Taylor [37] in 1969. Thaumasite is a calcium silicate carbonate sulfate hydrate and its chemical formula can be expressed in two ways:

$$CaSiO_3 \cdot CaCO_3 \cdot CaSO_4 \cdot 15H_2O \text{ or } Ca_3[Si(OH)_6 \cdot 12H_2O](SO_4)(CO_3)$$
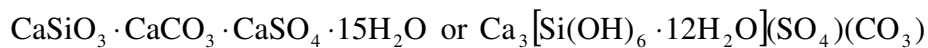
The second way represents better the structural relation between the various components. Thaumasite occurs as acicular (needle like) crystals with a hexagonal structure very similar to that of ettringite and therefore solid solution can form as well in field as in laboratory conditions where thaumasite has been synthesised successfully [2, 35, 38-41]. In laboratory investigations it was shown that thaumasite forms more rapidly in a temperature range below 15°C (ideally about 5°C) while ettringite prefers an environment of more than 15°C, however, both minerals are able to form under opposite conditions.

2.2.2   Consequences of TSA

Thaumasite as a deterioration product has been discovered worldwide and there is still a huge possibility that a vast number of cases have not been identified yet or have been misidentified as conventional sulfate attack, also see Section 1.1.

Deterioration due to TSA can be found on the one hand in buried concretes such as concrete foundations [21, 27, 42], piles [20, 40], tunnel linings [2, 21, 43], floor slabs [2, 21, 44], pavements [2, 18, 21] and lime stabilisations [21]. On the other hand there exist TSA cases of above ground structures such as in gypsum plaster and in brickwork in historical buildings [17, 21, 45, 46, 47]. However, Gaze and Crammond [48] noted that sulfate attack of brickwork in the field is small and should not become a major problem in practice. The formation conditions for TSA in above ground structures hardly differ from buried concretes except for the location of the sulfate, which is already available in the material of above ground constructions with the exception of ground floor slabs in contact with an external source of sulfate.

Structural consequences of TSA in buried concrete structures can be the loss of strength due to reduction of cross-sectional area, possible premature corrosion due to loss of cover concrete, loss of sliding resistance towards lateral movement and reduction in skin friction. Actual cases of loss of structural integrity in the field have not been found but a structure in the Canadian Arctic, where the columns supporting a building had to be replaced after two years in aggressive environment [3, 4].

2.2.2.1   Forms of Degradation

TSA can be accompanied by expansion, cracking, spalling and final disintegration of the concrete from the surface inwards. The loss of integrity of the cement matrix occurs due to the instability of the C-S-H-phases in the presence of gypsum and calcite and consequently thaumasite replaces the main glue at low temperatures resulting, in the worst cases, to the transformation of the cement paste to a soft 'mush' [49, 50]. This soft 'mush' is an incohesive mass with a distinct white colouration and does not possess any binding ability [1]. Aggregate particles found lie loose within that soft bed. It can be easily scraped away and if permitted to dry the surface becomes harder and friable [27]. Deteriorated concrete is occasionally found with a 'crust' of apparently unattacked

concrete, however, underneath this layer the exposed coarse aggregate is surrounded by white rings or haloes of reaction product. In affected buried concrete clay is often strongly adhered to the surface and appears to be desiccated [27].

Expansion of deteriorated concrete due to TSA is caused by the fact that the newly formed compound thaumasite has a larger volume than the originally present hydration products. However, the expansive effect of thaumasite is relatively low compared to its deteriorative effects. The Highways Agency [27] measured a maximum amount of 33mm expansion at the TSA affected 29 year-old Tredington-Ashchurch Bridge in Gloucestershire and Fountain [51] reports typical expansion of about 15mm from the original surface at structures along the M5 motorway. The maximum overall depth of thaumasite formed in these structures was up to 70mm [52] with an average depth of 25mm which corresponds to the worst case of TSA reported in foundations in the UK. BRE reported further field cases where thaumasite occurred with depth up to 40mm at 4 years in an in-situ pile containing sulfate resisting Portland cement (SRPC) [20] and up to 50mm at 9 years at PC strip foundation [53]. The measured depths contain the actual concrete deterioration and the expansion of the more voluminous reaction products over the original surface. The proportion of actual concrete deterioration and expansion can be assumed as 1:1 based on average field measurements undertaken by BRE [20, 52, 53], Halcrow Group [27] and Fountain [51].

The extent of the deterioration of columns of up to 70mm at the Tredington-Ashchurch overbridge at the M5 motorway in Gloucestershire [27, 54, 55] lead to the decision to replace completely the affected concrete. This was a decision based on time management and lack of knowledge about the mechanism of TSA combined with its effects. The basic idea was to restore the load capacity as soon as possible and to limit restrictions to traffic flow during the busy summer vacation time.

TSA of in-situ concrete foundation piles was investigated on site by the Building Research Establishment in 1990 [40]. Deterioration occurred on the tops of the piles to a depth of several centimetres and the cement matrix was transformed into a white incohesive pulpy mass. Further down the sides of the piles TSA was still present to a major degree. It should be noted that knowledge about the occurrence of TSA in concrete piles is very limited because it is very difficult to investigate this type of structure and signs of deterioration are almost invisible due to the non-exposure of the

piles. Though, the consequences can become visible in the form of cracks and settlements of the above ground structure.

Furthermore TSA sometimes has side effects, chloride corrosion occurs when groundwater is enriched in chloride ions through the run-off moisture containing de-icing salts from motorway. Rust staining and breakouts to the reinforcement revealed corrosion in the case of the Tredington-Ashchurch Bridge [27].

2.2.2.2   Deterioration Zones

The concrete affected due to TSA can be divided into four zones of gradually increased degradation with sharp very distinct fronts within high quality structural concrete. These four zones also stand for the progress of the deterioration; Zone 1 is the least affected one and represents the beginning formation stage of the attack with non-deleterious thaumasite formation defined by the Thaumasite Expert Group as TF. Zone 4 represents the softened zone with fully developed TSA on the surface where no binding ability is present and aggregate particles lie loose in the deteriorated bed [38]. Sibbick et al. [38, 54] postulated a simple four stage degradation sequence for TSA based on microscopical observation of affected structures investigated:

• **Zone 1:** This zone is farthest form the surface of the concrete where there is the source of sulfate, the concrete is in very good condition with low paste porosity and few air or adhesion voids. There is no significant internal micro-cracking. Adjacent to this sound part of the concrete can be a narrow band where air voids and adhesion cracks around aggregate particles lined with thaumasite (TF) or ettringite.

• **Zone 2:** TSA, the deleterious form of thaumasite, can be seen in its earliest or most minor form and develops as a fine network of microcracks originating within the cement paste and running sub-parallel to the concrete surface. Microcracks are usually full of thaumasite crystals orientated perpendicular to the walls of the crack and calcium carbonate is sometimes precipitated into these cracks. Little amounts of portlandite are still present within the cement paste. There is no evidence of other sulfate-bearing minerals.

- **Zone 3:** All the aggregate particles are surrounded by a thick halo-like deposit of thaumasite. The network of microcracks develops further and becomes larger. The microcracks can pass into the coarse aggregate particles and contain massive uniformly crystalline deposits of thaumasite. Calcium carbonate can be precipitated into the cracks as well and portlandite is still present, however, only in the greatly reduced unattacked cement paste. There is no evidence of other sulfate-bearing minerals. The crystals within the thaumasite deposits are more randomly orientated and appear to demonstrate a type of 'flow structure'. The residual cement paste in these highly affected areas has an isotropic, milky appearance with a total loss of internal features, such as unhydrated clinker grains.

- **Zone 4:** TSA degradation is fully developed and the transformation of the cement paste into thaumasite is completed. Residual islands of heavily depleted cement paste can be observed at different depths and occasional aggregate particles are embedded in extremely soft white mush. However, the microcracking observed in Zone 3 is virtually no longer present due to the massive nature of the thaumasite and the lack of rigid material through which microcracks can pass.

The different zones of TSA within a high quality concrete structure are idealised in Figure 2.2.

Sibbick et al. [38] observed that the degradation zones 1-4 can also be found within concrete where a still largely intact outer crust of 'sound' concrete is available, however, which will very easily debond from the underlying degraded concrete. The development of the four zones can still be observed but they are generally less well defined within lesser quality cementitious materials, which are generally characterised by lower cement contents and higher capillary porosity and therefore higher water to cement ratios.

Wide cracks filled
with thaumasite and
haloes of thaumasite
around coarse and
fine aggregates

Thin cracks
infilled with
thaumasite

Needles of
thaumasite and
occasional
ettringite within
voids

Thaumasite

Coarse aggregate
particles only

Surface of
concrete

Unaffected
concrete

Reinforcement

SO₄ in groundwater
from oxidation of
FeS₂ in clay

Effective cover
before repair

Zone 4   Zone 3   Zone 2   Zone 1

Figure 2.2 - Sketch of the idealised four zones of TSA degradation with high quality concrete [38]

2.2.2.3   Rate of Deterioration

The determination of the rate of TSA deterioration is very complicated due to the many interrelated factors that affect it these include; the availability and concentration of both sulfate and carbonate ions dissolved in groundwater, the quality and type of concrete, and the range of temperature [1, 2]. Field cases have shown clearly the dependency on the different factors, e.g. the case of TSA in the Canadian Arctic where the structure had to be replaced two years after construction in a very cold and aggressive environment [3]. In the case of the Tredington-Ashchurch bridge there was a maximum thaumasite development of up to 70mm and the average was given with 25mm after 29-years, however, the actual maximum concrete deterioration was reported as 33mm based on the difference between softening and expansion [27, 56]. These findings lead to an average rate of about 1mm/year over a long period as suggested by the TEG [1] and

Erikson [7] estimated the rate of TSA of 0.2 mm/year based on the deteriorated zone of a 69-year old structure. However, these estimations have to be considered very carefully. As it is not possible to determine the initial dormant period in the case studies reported it is only possible to estimate an average deterioration rate.

Laboratory experiments with constant conditions during deterioration can reveal much better descriptions for the rate of deterioration. Significant signs of TSA generated in laboratory conditions have been observed within several weeks in small cement paste samples and within 6 to 12 months for concretes and this resulting in up to several millimetres of softening after a couple of years [2, 57]. According to data found in literature [40, 58] it is suggested that significant deterioration starts after an initial dormant period, which is accompanied by saturation of cement paste with penetrating ions. It is speculated that thaumasite formation (TF) occurs before expansion pressure exceeds the tensile strength of concrete and deterioration is visible. Crammond and Nixon [40] observed a dormant period of six months before deterioration started in mortar samples and Monteiro [58] reported dormant periods which could last up to 15 years in samples with low w/c-ratio.

The slow rate of formation of thaumasite is beneficial in the sense that it allows plenty of time for warnings whether the structure is endangered and, if so, to carry out safely and efficiently remedial works [59].

2.2.2.4   Measurement of Deterioration

To date standard methods for the measurement of deterioration caused by TSA and resistance of concrete to TSA have not been published. There are test methods, which estimate the resistance of concrete and mortar to the conventional sulfate attack, however, the fact that the thaumasite form of sulfate attack occurs at low temperatures has not been considered.

Mulenga et al. [60] developed a test method which contains storage of test prisms in a high sulfate-containing solution at 8°C and the characteristic value of deterioration is the relative axial tensile strength. The tensile strength is a very expressive value for the measurement of resistance against TSA because the generally used determination measurements are the expansion, the reduction in compressive strength and the loss of mass [45, 47, 61]. Ultrasonic pulse velocity can be also used to assess the level of

deterioration as performed by Tsivilis et al. [62]. The measurement of expansion and the determination of the reduction in strength parameters such as compressive and flexural strength are the most common methods used for assessing sulfate attack but damage due to microcracking can be better expressed using the tensile strength.

The methods described above measure predominantly the pure structural effects caused by TSA, see Section 2.8.1. Other aspects of deterioration that are not measured but are of interest are the effects of deterioration on soil/structure interactions and the extent of deterioration.

The Building Research Establishment [63] introduced the 'wear rating' method to assess the resistance of concrete cubes to TSA. This method was used for comparative studies between field trials and laboratory. The average depth of erosion or damage for one corner of a cube is determined by the difference of the sum of length between the four known undamaged diagonals and their damaged counterparts on the struck face and its opposite face divided by 8. However, BRE concluded that this method is relatively insensitive for assessing TSA because erosion occurs across the face and is not concentrated on corners where damage occurs initially due to conventional sulfate attack. For the conventional sulfate attack it is a useful measurement but by a combination of thaumasite form and conventional sulfate attack, 'the wear ratings are disproportionately influenced by the degree of conventional sulfate attack and any tendency to TSA could easily be masked' [63].

The Halcrow Group under Slater [61] assessed TSA in the field using the severity of the attack on the whole structure and classified four different attack ratings based on the area of softening and the maximum depth of attack:

- Rating 1 (No attack): No softening in areas surveyed and no damage due to thaumasite attack observed
- Rating 2 (Slight attack): Less than 15% of buried area surveyed is softened or maximum depth of attack does not exceed 15 mm.
- Rating 3 (Moderate attack): At least 15% of buried area surveyed is softened or maximum depth of attack exceeds 15 mm.
- Rating 4 (Severe attack): At least 25% of buried areas surveyed are softened and maximum depth of attack exceeds 25 mm.

This visual form of estimation of damage due to TSA is a very pragmatic method of initial investigation in the field and it is not relevant for the description of thaumasite progress in laboratory conditions. TSA is expected to occur at the full sample area exposed to aggressive solution.

An appropriate test method for the determination of concrete deterioration due to TSA including the ability for an estimation of the rate of progress, and the effects on the soil/structure interface has not been found in the current literature.

2.2.3 Risk Factors

The formation of thaumasite occurs in buried concrete structures under certain conditions as identified by the TEG [1] and described in Section 2.1.2. These four primary risk factors including the one general condition of a silicate source are described in detail in the following paragraphs.

2.2.3.1 Source of Silicate

The silicate needed for the formation of thaumasite originates from the silicate-containing phases in the cement paste. These are on the one hand the primary source the calcium silicate hydrates (C-S-H-phases) which represent the main binding agent in all Portland cement based materials including SRPC. On the other hand remnant unhydrated clinker grains such as alite (C_3S) and belite (C_2S) form a secondary source [1, 2, 28].

2.2.3.2 Source of Sulfate

Sulfur is the ninth most abundant element in the Earth's crust [64] and therefore exists as various forms present around and inside of structural elements. The main external source is in the adjacent soil. However, internal sources can also supply sulfate for the formation of thaumasite as found in field cases and shown thermodynamically by Bellmann [49, 50].

The external available sulfate-ions in the soil can be present in a variety of different sulfur minerals either already as sulfates or as sulfides which are able to oxidise to sulfate-ions. Sulfates occur primarily in soils as calcium sulfates (gypsum, selenite); however, other secondary compounds such as magnesium sulfate (epsomite) and sodium sulfate (Glauber's salt) may also be present [1, 64, 65]. Sulfate compounds with magnesium ($MgSO_4$), sodium (Na_2SO_4) and potassium (K_2SO_4) are much more soluble compared to calcium sulfate ($CaSO_4$) which has a solubility of 1.4g SO_4/l, these compounds provide much higher concentrations of SO_4^{2-}-ions in the transportation medium, the groundwater [1, 39, 66].

The presence of sulfides, which are generally found in natural ground as the mineral pyrite (FeS_2) and other less common minerals such as marcasite (FeS_2) and pyrrhotite (FeS to $FeS_{1.8}$), can contribute to the source of SO_4^{2-}-ions [1, 66]. Sulfide-bearing clays contain in their unweathered state a negligible amount of sulfate-bearing phases but appreciable amounts of pyrite and these had been categorised as harmless regarding sulfate attack in the past [2]. However, oxidation of pyrite to sulfate increases significantly the sulfate level in the ground and this reaction has been described by Longworth [66] as:

"If oxygen in air or groundwater has access to unweathered pyritic soil/rock it oxidises the pyrite (FeS_2) to form red-brown ferric oxide (Fe_2O_3) usually as a hydrated form, together with sulfuric acid (H_2SO_4). The latter is the initial source of sulfate. If calcium carbonate ($CaCO_3$) is present in the material, the H_2SO_4 will react with it further to produce calcium sulfate which crystallises as gypsum ($CaSO_4 \cdot 2H_2O$)."

Detailed pyrite oxidation mechanism descriptions are widely available in the literature, e.g. by Czerewko et al. [64] or Floyd et al. [67]. The gypsum reservoir formed during the oxidation dissolves in groundwater up to 1.4g SO_4/l and to higher concentrations if cations such as magnesium, sodium and potassium are present this is the case with a variety of clays where sulfuric acid is able to leach clay minerals and release these cations.

Oxidation and weathering, respectively, occur when the ground is disturbed during construction work (one secondary risk factor), i.e. when soil is excavated, exposed to atmosphere due to stockpiling and then backfilled against the structure [1, 64, 66, 68].

This process can take place within a few years and can be considered as relatively quick compared to the natural progress of weathering accompanied by pyrite oxidation which is extremely slow and can take of the order of thousands of years to penetrate several metres below ground surface [69].

According to Czerewko et al. [64] there are sulfate- and sulfide-bearing lithologies in the UK which are several marine Mesozoic and Cenozoic sedimentary clay deposits, including Lower Lias Clay, Kimmeridge Clay, Oxford Clay, Gault Clay, Weald Clay, Lambeth Clay and London Clay. Further soils with potential to contain sulfates are named by the TEG [1]. Lower Lias Clay (LLC) is the strata where most of the TSA cases have occurred in the UK.

Additional sources of sulfate-bearing material in ground or in contact with the structure are bedding materials such as cinder and ash hardcore, furnace bottom ash, spoil from mining of coal and oil shale which are found around old industrial areas as well as seabed [1, 2, 21]. Aggregates, cements and cement products (bricks, concrete blocks) as well as sulfate-based binder such as plaster and render are potential locations for the formation of thaumasite in above ground constructions [33].

2.2.3.3   Source of Carbonate

Carbonate is an essential ingredient for the formation of thaumasite and can be derived both internally and/or externally. The main sources of carbonate ions are internal, available either in limestone-containing aggregates or cement filler within the cement or mortar itself. Furthermore there are secondary sources which are both internal and external.

The most common forms of carbonate in aggregates are calcareous limestone ($CaCO_3$) and dolomitic limestone ($CaCO_3MgCO_3$) and can be encountered as crushed limestone, crushed dolomite, and as limestone, chalk and shell fragments in sands and gravels [1]. Limestone filler is also a considerable source for carbonate ions; modern UK and European Portland cements (CEM I), BS EN 197-1:2004, are permitted to contain up to 5% limestone filler as a minor addition leading to an even higher susceptibility to thaumasite formation [1, 70].

Initially it was thought that only fine dust carbonate particles had contributed to TSA but investigations on affected concretes in the laboratory and field have shown that

good quality carbonate aggregates are also able to initiate deterioration [2]. However, smaller limestone particles are the more reactive [1, 2, 40].

A secondary internal source is the carbonation layer in concrete, which is caused externally by atmospheric CO_2. The carbonated zone in concretes, including buried concretes, can provide the carbonate ions needed for thaumasite formation. Several authors [33, 39, 48, 57, 68, 70-72] concluded from investigations that atmospheric CO_2 and the consequent carbonation of concrete/mortar could have been the only available carbonate source and Sahu et al. [44] showed using microstructural analyses that thaumasite occurred adjacent to carbonated layer.

Another source for the supply of carbonate ions derives from the groundwater where both dissolved CO_2 as bi-carbonate (HCO_3^-):

$$CO_2 + H_2O \Leftrightarrow H_2CO_3 \Leftrightarrow H^+ + HCO_3^- \Leftrightarrow 2H^+ + CO_3^{2-} \tag{1}$$
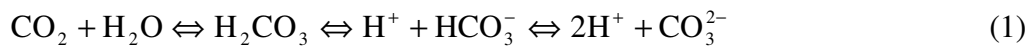
and the partially soluble calcite as carbonate CO_3^{2-} are present [1, 11, 39]:

$$CaCO_3 \Leftrightarrow Ca^{2+} + CO_3^{2-} \tag{2}$$

The reaction what proceeds in the ground and involves rainwater can be described through the combination of Equations (1) and (2):

$$CaCO_3 + CO_2 + H_2O \Leftrightarrow Ca^{2+} + 2HCO_3^- \tag{3}$$
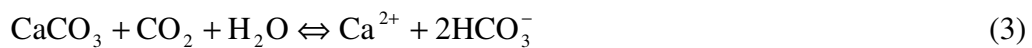
It is to note that all these reactions are reversible and depend on equilibrium between ambient conditions, i.e. on temperature, pH and the amount and nature of the carbon dioxide in solution [39].

2.2.3.4   Source of Water

All forms of sulfate attack require water in order to both provide the transport medium for the sulfate-ions and to assist in the chemical reaction. The water does not have to be mobile, especially when the source of sulfate and carbonate are both internal [33]. The

source of water in the case of TSA in buried concretes is mobile groundwater, which occurs naturally. However, the amount of water may be increased due to certain construction processes, including the formation of a sump during foundation works, or at a later stage if motorway drainage is faulty [1, 2, 55].

The groundwater flow depends on the depth in the clay strata and is greater in the upper ground layers; however, in the top-most metre of the ground there is usually a very low sulfate content because of the natural leaching process. Furthermore it is necessary to note that thaumasite attack is strongly related to the groundwater level [56]. No attack was usually observed above the maximum water level (i.e. permanently dry, except percolating water) and full attack usually occurred below the minimum water level (i.e. permanently wet).

In the UK the groundwater is usually saturated with respect to calcium sulfate (1.4g SO_4/l) and can contain highly soluble sulfates such as magnesium, sodium and potassium. Additional to the mentioned cations Na^+, K^+, Ca^{2+}, Mg^{2+} anions of Cl^-, CO_3^{2-}, HCO_3^- and sulfate SO_4^{2-} are the major ion species in most natural waters [56].

The groundwater chemistry has a significant influence on the aggressiveness of TSA be that the higher solubility of magnesium-, sodium and potassium sulfate or the presence of sulfuric acid formed during pyrite oxidation. The latter could lead to a combined sulfuric acid attack, however, the current literature is in disagreement about the fact whether this contributes to TSA [2], is a precursor [73] or is involved at all [74] and this is discussed further in Section 2.3.4. The dependence of the kind of cations present is also an important factor since magnesium has been found to be the most aggressive of the most common cations. Several laboratory investigations have shown that magnesium sulfate solutions are more aggressive and that they act as a catalyst and stimulate the growth of thaumasite [40, 73, 75-77].

2.2.3.5   Temperature

Low temperatures favour the formation of thaumasite where generally less than 15°C are necessary with an optimum value of approximately 5°C. The formation ability increases with the decrease of the temperature, i.e. the lower the temperature the faster the formation of thaumasite.

One reason for the increase in deterioration rate with reduced temperature is solubility. The solubility of carbon dioxide increases with decreasing temperature leading to about twice the amount of dissolved carbonate in solution at 0°C than at 25°C portlandite is also more soluble at low temperatures whereas thaumasite is in the order of a hundred times less soluble. From this follows an increased rate of deterioration at low temperatures [2, 20, 39, 78]. On the other hand lower temperatures lead to a better stability of the six-co-ordinated $[Si(OH)_6]^{2-}$ groups as Bensted [79] states, which are present in the structure of thaumasite, see Section 2.2.1.

Crammond [2] has found the cut off point where the mineral formed changes from thaumasite to ettringite to be between 15°C and 20°C, notwithstanding thaumasite is able to form at higher temperatures, however, at a much slower rate [8, 79]. Several cases of thaumasite have occurred in areas/conditions where the temperature had been more than the threshold of about 15°C [4].

The typical temperature conditions in the ground at foundation depth in the UK range from about 9 to 12°C and are therefore in the optimum range of below 15°C [2, 80].

2.2.3.6   Secondary Risk Factors

Due to the consumption of calcium silicate during the thaumasite formation all Portland cement based binders are at risk, even sulfate resisting Portland cement (SRPC). Nevertheless, there are some cements which perform well in situations where the risk of TSA is high and the literature states that concrete with lower cement contents are more susceptible to TSA [1]. An additional factor is the type and quantity of the filler used, i.e. limestone filler serves as a carbonate source and does not prevent the onset of TSA even with a high density of concrete.

The quality of the concrete, including water-cement ratio, compaction and curing has a very important role in the performance of each concrete since the permeability is ruled by the density. A low water/cement ratio, good compaction and sufficient curing increase the density and reduce the permeability of concrete. The British Cement Association recommends water/cement ratios of 0.40 and 0.45 when SRPC and carbonate aggregates are used in concrete [28, in 1].

Further risk factors are changes to ground chemistry and water regime resulting from construction as sulfate classes in ground can change through oxidation of sulfides as

described in Section 2.2.3.2. Furthermore, changes in groundwater conditions can be caused by soil disturbance due to excavation resulting in increased permeability and therefore a higher mobility of groundwater with wetter conditions around the structure, see also Section 2.2.3.4.

The type, depth and geometry of underground structures depends on the load to be carried and in general the greater the load, the deeper the foundations, the better the quality of the concrete and the larger the dimensions. Structures of high quality concrete founded below sulfate bearing strata and with large dimensions have reduced vulnerability to TSA [1].

2.2.3.7   Comment

It is important to note that the risk factors described need not all be satisfied for TSA to occur. Cases have been reported [33] where TSA occurred in situations where only one of the risk factors was present. Sims and Huntley [33] reported anonymous cases where sulfate was always present but there was no direct source of carbonate, water was either abundant or mobile and temperatures were not always low. Furthermore TSA was also observed in Mediterranean-type climatic regions. Desk studies aimed to identify the risk of TSA consider mainly soil strata, type of aggregate, water level and temperature and will generally exclude structures from risk when one of the four risk factors is not present. As it has been shown that all four factors need not be present for TSA to occur structures that have been classified as not at risk using the method described above may actually be suffering from TSA.

It should be remembered that TSA is a rare form of deterioration with a small number of structures in the UK potentially at risk and that the overall structural integrity has not seriously been affected in cases to date and if it were then signs of structural deformation would be evident well before there was a risk of collapse [1, 2].

2.3   Formation Mechanism

2.3.1   Formation Theories

The formation of thaumasite has been investigated by several authors; however, the actual formation route has not been identified yet. Bensted [75] suggests that there are two possible formation routes, the direct route and the woodfordite route, and Crammond [2] considers three different theories that (i) thaumasite forms by a topochemical replacement of ettringite; (ii) thaumasite uses ettringite only as a template for its initial nucleation; and (iii) thaumasite forms through a solution mechanism.

- *Direct route according to Bensted [75]:* Thaumasite forms by the general reaction of sulfate with carbonate, silicate and excess water in the presence of calcium ions. However, the reaction is very slow and it can take up to several months until a significant yield is obtained.

- *Woodfordite route according to Bensted [75]:* Thaumasite and ettringite form as end members from a solid solution, called woodfordite, which occurred through the reaction between ettringite, silicate and carbonate in the presence of excess water. This reaction is again very slow but after an initial period when thaumasite has started to form the rate rises significantly. It is to note that the solid solution between ettringite and thaumasite is not continuous.

- *Topochemical replacement of ettringite by thaumasite according to Crammond [2]:* It is suggested that alumina needs to be present in a small amount that through topochemical interchange of [Si] for [Al] and [CO_3^{2-}+SO_4^{2-}] for [SO_4^{2-}+H_2O] a solid solution series between ettringite and thaumasite forms. The released aluminium goes back into solution, where it can form more ettringite and the interchange can continue. Crammond considers this way as less likely.

- *Ettringite as a template according to Crammond [2]:* Thaumasite uses ettringite only as a template for its initial nucleation and when it nucleates additional thaumasite would continue to form directly from solution.

- *Through solution mechanism according to Crammond [2]:* Sulfate attack occurs in the conventional way until the alumina is used up and ettringite stops to precipitate. Further penetrating sulfate ions will be forced to find a new sulfate-bearing host, which will be the portlandite, however, if carbonate or bicarbonate ions are present the end product formed will be thaumasite instead of gypsum.

Koehler et al. [78] remark that Crammond's first theory is too slow to be the likely formation mechanism for the huge amounts of thaumasite observed during investigations. They suggest that thaumasite formation occurs through the heterogeneous nucleation of thaumasite on the surface of ettringite, however, Nobst and Stark [72] observed in cement pastes that the supply of ettringite did not influence the amount of thaumasite.

To summarise, formation theories generally fall into one of two categories and these are that either formation occurs through the decomposition of ettringite or that thaumasite forms directly from the pore solution. However, it should be noted that formation of thaumasite in real cementitious systems results in an impure thaumasite since none of the reactants are pure [75]. Other influencing factors include ambient conditions and further reactions occurring in close proximity. There is the hypothesis that sulfuric acid attack is also involved in addition to the above [2, 73] and combined reactions during magnesium sulfate attack are also possible.

2.3.2   Reaction Products

The most common reaction products occurring from the thaumasite form of sulfate attack in buried concretes beside thaumasite are ettringite, gypsum, quartz and calcite. It is possible in laboratory conditions, to produce thaumasite as a single reaction product. Further reaction products found in analyses of TSA affected concretes are brucite and aragonite. Brucite ($Mg(OH)_2$) is frequently observed in near surface regions of concrete exposed to magnesium-containing solutions, such as seawater and results in an additional magnesium sulfate attack. In the presence of magnesium salts the thaumasite formation is modified in that brucite is normally produced alongside thaumasite as a deterioration product as it has a lower solubility than portlandite [40, 75, 81].

$$MgSO_4 + Ca(OH)_2 \Rightarrow CaSO_4 \cdot 2H_2O + Mg(OH)_2 \qquad\qquad (4)$$
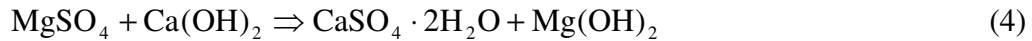
Freyburg and Berninger [43] conclude that aragonite derives from the carbonation process of thaumasite. Sibbick and Crammond [82] also observed it during de-calcification processes. However, aragonite is not found as a primary product and Hartshorn [83] states that crystallisation of aragonite from solution is favoured by higher temperatures and in the presence of calcium sulfate.

2.3.3   Stability of Thaumasite

The stability of the formation process and of the thaumasite formed is dependent on the pH-value and temperature. Gaze and Crammond [48] suggest that thaumasite does not appear to form at a pH of below 10.5 but will form readily at a pH of 13, however, once formed it is able to survive in contact with pH solutions up to 7 or even 6. Crammond [2] continues that thaumasite becomes less stable the more it approaches pH 7. There is evidence in the work of Hill et al. [84] that pH values lower than 7 can be tolerated. Sahu et al. [44] observed in a concrete slab thaumasite and gypsum coexisting at a pH of 10-11, whereas it was likely that thaumasite and ettringite would coexist in the pH range 11-12 and the zone with a pH greater than 12 contained only ettringite. Ettringite becomes unstable at lower alkalinity and will eventually decompose to gypsum when the pH falls below about 10.5-10.7 [28, 48, 85, 86]. The dominant presence of gypsum as a degradation product in acid conditions in laboratory conditions also shows the dependence on pH and according to Zhou et al. [57] does not support the hypothesis that TSA favours acid conditions. Zhou et al. [57] suggested that the gypsum formed through the reaction between sulfuric acid and calcite which is present in alkaline conditions, and only traces of thaumasite were detected.

The dependence of the stability of thaumasite on temperature can be considered as negligible since only an upper bound value of 110°C is found in literature and ground conditions cannot reach this temperature [47, 75].

It should be noted that ettringite is also not a stable phase in the presence of carbonates, sulfates and silica in the pore solution at a temperature of 5°C according to Torres et al. [70].

2.3.4   Combined Degradation Forms

Thaumasite formation may be accompanied by one of three other main degradation processes the magnesium sulfate attack, sulfuric acid attack and decalcification.

Magnesium sulfate attack has already been mentioned in Section 2.3.2 and it has been noted that this kind of attack reinforces the thaumasite form of sulfate attack and makes the overall deterioration worse [75]. Apart from ammonia, generally only found in agricultural situations, the magnesium cation is the most aggressive ion encountered (aggressiveness: $NH_4^+>Mg^{2+}>Na^+>Ca^{2+}$) [28]. Magnesium sulfate reacts with portlandite and forms brucite and gypsum where hydroxyl ions are removed from the solution and consequently the pH in the pore solution reduces. Below critical pH of 12.5 the C-S-H-phases break down and are replaced by hydrated magnesium silicate which has no cementitious binding properties [12, 40, 81]. Crammond and Nixon [40] suggest that even low concentrations of magnesium play an important role in the initiation of the degradation process because magnesium is not present within the thaumasite structure and the ions are released back into the solution for further reaction. According to Crammond and Nixon [40] the breakdown of C-S-H-phases is probably an important intermediate reaction product within the process of thaumasite formation.

The research community is still in doubt about the role of sulfuric acid attack whether it contributes to TSA [2], is a precursor [73] or is involved at all [57, 87]. Hobbs and Taylor [73] suggest the extreme case that sulfuric acid attack is the primary cause of deterioration derived from the pyritic oxidation where the acid reduces the pH of the groundwater and these results in attack of the foundations. Zhou et al. [57] concluded from their laboratory study that the primary cause of the deterioration observed in field studies is unlikely to be the low pH, but instead the increased levels of sulfate ions present in the ground due to pyrite oxidation. However, further investigations are necessary to clarify the role of the sulfuric acid formed in weathered soil during the thaumasite form of sulfate attack.

De-calcification often occurs in combination with pH reduction, this can be caused by several degradation processes common in Portland cement materials, such as

conventional sulfate attack, TSA, seawater attack, alkali-silica reaction, leaching due to excessive groundwater flow and the action of aggressive carbon dioxide within flowing ground. De-calcification is often associated with an unusual form of carbonate deposition within the cement paste matrix, this has been given several notations. Thaulow and Jakobson [88] called it popcorn calcite deposition 'PCD', Sibbick and Crammond [89], Bromley and Pettifer [90] Cornflake calcite deposition, Thaulow et al. [91] bi-carbonation and French [92] described it as secondary calcite precipitation as a result of sub-aqueous carbonation. Due to the better description the term popcorn calcite deposition has more often been used in recent years. There appears a close relationship between TSA and PCD degradation process such as large amounts of water are required and both processes can occur below ground.

The ingress of hydrogen carbonate (bi-carbonate, HCO_3^-) into the matrix results in the reduction of pH as Thaulow [in 82] states that the pH of the pore solution depends on the ingress of dissolved carbon dioxide and not on the presence of calcium hydroxide. Decalcification of calcium bearing compounds ($Ca(OH)_2$ and C-S-H-phases) occurs when the pH drops below 10.5 and thaumasite stops forming. Further reduction of pH towards the neutral value of 7 leads to a decrease in the stability of thaumasite and the only stable calcium-bearing phase, which can form, is calcite (PCD). During this process sulfate ions will be released back into the pore solution the whole process including thaumasite formation can continue into the still sound concrete [2, 82]. The popcorn calcite formed has just as little binding ability as thaumasite and according to Crammond [2] can be considered as the final degradation process associated with TSA.

Finally, physical processes can also affect TSA, for example, in cases observed in the Arctic where forms of freezing and thawing probably contributed to the degradation process [20].

The magnesium sulfate attack plays a decisive role during TSA so that it enhances the breakdown of the C-S-H-phase and initiates the degradation process. De-calcification processes can be assumed as being the final step during TSA and thaumasite can be considered as an intermediate reaction product. The role of the sulfuric acid attack has not been clarified yet but it is suggested that sulfuric acid is involved as initiator of

TSA, attacking the cement phases, and that it plays a role during the final step. Thaumasite is not a stable phase in acidic conditions and so it might be decomposed.

2.4   Identification of TSA

2.4.1   General

The identification of TSA and its reaction products can be unambiguously performed using a combination of techniques, i.e. X-ray diffraction (XRD) and optical microscopy such as scanning electron microscopy (SEM) and polarisation microscopy are usual techniques. A combination of either XRD and polarisation microscopy or SEM with energy dispersive X-ray analysis (EDX) can also be used for the identification of TSA reaction products [43].

Before the development of these techniques it was very difficult to distinguish the main reaction products of the conventional and the thaumasite form of sulfate attack and misidentification was common [2]. Both deterioration products ettringite and thaumasite, respectively, have very close similarities in their structure and differ principally in the aluminium and silicon content, see Table 2.1 and therefore it is difficult to identify unambiguously ettringite or thaumasite using only one technique. Additionally there is the necessity to confirm the presence and the extent of deterioration using a second technique, microscopy is used to distinguish between TSA and TF.

Table 2.1: Chemical composition of ettringite and thaumasite [68]

	Ettringite	Thaumasite
SiO_2	0.0	19.4
Al_2O_3	15.0	0.0
CaO	49.5	54.5
SO_3	35.5	26.1

Note: Compositions are normalised to 100% and exclude CO_2 and H_2O.

2.4.2   X-ray Diffraction

X-ray diffraction analysis identifies the mineralogical phase composition present in materials and is a significant component in analysing building materials. Identification using XRD-analysis is a very powerful tool since it represents a fingerprint analysis of the material investigated; however, a sufficient concentration of the mineral is necessary if the technique is to be effective. Before scanning samples are dried and then ground to 50μm. The scanning range for the examination is preferred to be from 5-65°2Θ, however the strong peaks for thaumasite occur at low angles where the errors in 2Θ values are more pronounced and therefore can cause problems leading to misidentification [35, 57].

The XRD pattern can show unavoidable deviation in peak position and this must be corrected by orientation on other peaks, such as quartz and calcite, or using an internal standard, before the final evaluation and if applicable semi-quantitative analysis of the sample [43]. Due to the similarity of thaumasite and ettringite the primary peaks at about 9°2Θ are almost identical and therefore the differences of the secondary peaks serve as distinction angles [18]. The peak position of the general reaction products according to literature [18, 83, 84, 93] are listed below:

Aragonite	26.3°2Θ
Brucite	18.5 ; 38.0°2Θ
Calcite	29.4°2Θ
Ettringite	9.0; 15.8; 18.9°2Θ
Gypsum	11.6°2Θ
Portlandite	18.0; 34.0°2Θ
Quartz	26.5°2Θ
Thaumasite	9.2; 16.0; 19.4°2Θ

Gaze and Crammond [48] used a semi-quantitative analysis for the evaluation of samples and expressed the relative strength of the XRD peaks in nine different steps from traces, very weak, weak, moderately weak, moderate, moderately strong, strong, very strong and very very strong, see Figure 2.3. This method is able to illustrate semi-quantitative changes over different dates during the formation.
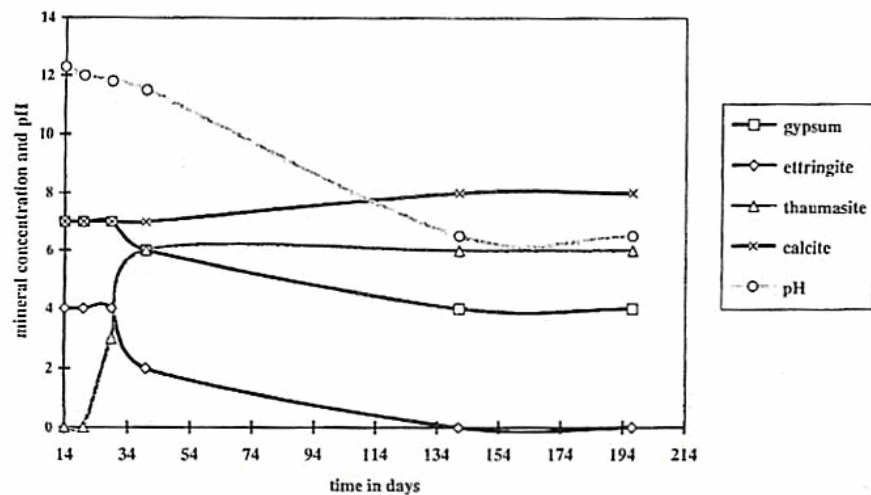
Figure 2.3 - Semi quantitative mineral concentration analysis by Gaze and Crammond [48]

2.4.3   Polarisation Microscopy

Petrographic analysis represents probably the most versatile and cost effective technique to analyse concrete properties in both sound and damaged conditions. The use of thin sections gives the opportunity to map features such as microcrack development and changes in porosity caused by deterioration mechanisms [68]. Eden [68] described the information that can be gained by petrographic analysis if thaumasite attack occurs:

- Determination of the maximum depth of deterioration;
- Classification of the severity of thaumasite-related deterioration based on Figure 2.2;
- Determination of the composition of the concrete including water/cement ratio and cement content;
- Identification of aggregate type and classification of the 'Carbonate Range' of the combined coarse and fine aggregates based on TEG report [1];
- Identification of other forms of deterioration such as ASR or leaching;
- Determination of the general condition of the concrete at depth;
- Estimation of compressive strength of the concrete from petrographically determined composition and void content.

However, the unambiguous distinction of thaumasite and ettringite is not always possible using microscopy and for that reason petrographic analysis should be combined with either microprobe or X-ray diffraction analysis [43, 68, 94].

The distinction problem is based on the quite similar habit (fibrous character) and density of thaumasite (ρ=1.83g/cm^3) and ettringite (ρ=1.75g/cm^3) as well as nearly identical values for the birefringence under Polarisation microscopes with plane polarised light (PPL) and crossed polarised light (XPL). Birefringence is the effect on polarised light of variations in the refractive index of different minerals and minerals are often distinguished by different levels of birefringence (refraction) [38, 43, 94].

Sibbick at el. [38] identified petrographically three different types of thaumasite Type I, Type II and Type III. Type I is a needle-like crystalline material where the crystals are more poorly formed, randomly orientated and associated with large amounts of voidage and it appears as colourless to very pale yellow in PPL and white in XPL. Type II has needle-like crystals similar to Type I but they are more closely spaced and exhibit a more massive structure. The colour ranges in PPL from light straw yellow to bright yellow and in XPL from creamy white to pale yellow. Type III is much denser and has well ordered needle-like crystals, running in preferentially oriented sheets around aggregate particles and within microcracks. They are yellow tinted in PPL and have a much higher birefringence under XPL which can results in areas of up to at least second order green. The authors concluded that all three forms are closely associated but the most common type is Type II.

2.4.4   Scanning Electron Microscopy

The identification of materials using scanning electron microscopy (SEM) and environmental scanning electron microscopy (ESEM), respectively, is becoming more popular in material science. Deterioration products, such as thaumasite, can be identified without problems using the included energy dispersive x-ray analysis (EDX) but this method is not appropriate for keeping costs in low budget. Thin sections produced for conventional light microscopy can be used in SEM and through a pre-selection of interesting areas under the conventional microscope cracks and therein containing reaction products can be represented very clearly in pictures [94].

Because of the high costs of using this apparatus, the combination of polarisation microscopy and XRD is currently the most common identification method.

2.4.5   Sampling

Sampling is one of the most important steps within the analytical process. It is important to achieve a representative and complete sample of the area investigated.

In case of XRD where the identification is qualitative and semi-quantitative the products of sulfate attack need to be present in sufficient quantities and sampling needs to be well distributed within the affected area. However, there is the risk of diluting the sample when a part of the collected surface concrete has not yet undergone any deterioration. The preparation includes drying and grinding of the sample and is important in that drying at high temperatures can cause structural changes [68].

Sampling plays a more important role in the identification using microscopy since the transition from sound concrete to very substantially deteriorated concrete that has undergone TSA is very sharp. This can cause loss of the deteriorated zone when core samples are taken and leading to an inaccurate assessment of the depth of the four deterioration zones described in Section 2.2.2.2 [65, 68]. Eden [68] suggested that any surface material for laboratory analysis should be removed by hand and then transported under controlled conditions, i.e. sealed in plastic bags in order to prevent moisture loss and carbonation. The drying of the samples has to be done slowly at room temperature to prevent changes in the structure such as drying-induced microcracking and degradation [54, 68].

After drying, concrete samples for microscopy are vacuum impregnated with coloured araldite resin and only then can the actual thin section preparation begin [68]. It is usual to use fluorescent resins in thin section preparation, however, the characteristic creamy yellow colour of thaumasite in plane polarised light can be masked by the strong colour fluorescent resin. Sibbick et al. [54] has shown that blue resin is the most effective resin colour for use in thaumasite identification.

2.5   Thaumasite Prevention

2.5.1   General

The resistance of limestone-containing concrete structures to the thaumasite form of sulfate attack is based on chemical and physical properties. Physical resistance, i.e. the resistance to sulfate-ion ingress, is governed by cement content and water-cement ratio and chemical resistance can be improved using appropriate binders [95]. Beside cement content and w/c-ratio, compaction and curing play an important role in the physical resistance to TSA as well, also see Section 2.2.3.6.

2.5.2   Binder

Due to the susceptibility of all Portland cement based binders, resistance is achieved chemically with the use of composite cements containing different fillers. Thereby the type and amount of the filler used is crucial. Pozzolanas can reduce the susceptibility of binders due to the improvement of physical properties and the conversion of the portlandite into C-S-H-phases [50].

Crammond [2] suggests that TSA can be avoided in buried concrete containing limestone aggregate when either slag cement or BRECEM is used. However, the slag cement should contain at least 70% ground granulated blastfurnace slag (ggbs) and 30% PC to perform well. Laboratory studies showed that slag cements with lower amounts of ggbs did not perform well [2]. The second alternative, the BRECEM contains 50% calcium aluminate cement and 50% ggbs but this cement is not commercially available. Additional filler which prevent successfully TSA are nanosilica and, to a lesser extent, metakaolin due to the pozzolanic reaction with portlandite to C-S-H-phases [70, 85, 93]. However, the use of microsilica is disadvantageous on the contrary to nanosilica because microsilica accelerates strongly the thaumasite formation at low temperatures while the pozzolanic reaction is retarded as shown experimentally by Nobst and Stark [72, 93]. The role of fly ash has not been clearly identified in the current literature yet. Torres et al. [70] suggest that fly ash enhance successfully the durability whereas Bellmann and Stark [95] talk about an improvement in the physical properties but not in the chemical resistance. Therefore fly ash was found to perform well in field conditions

but laboratory studies showed great susceptibility to TSA, i.e. fly ash delays rather than prevents TSA [49, 80].

2.5.3   Aggregate

Aggregate plays a major role in the occurrence of thaumasite since it is the main source of carbonate ions. The use of non-carbonate containing aggregates isolates the main source of the carbonate ions, however, thaumasite is able to form in concrete containing siliceous aggregate due to external derived sources, also see Section 2.2.3.3. If carbonate containing aggregate is used then precaution needs to be considered.

The TEG divided carbonate containing aggregates into three ranges regarding their carbonate content, Range C with the lowest carbonate content which will not in general be prone to TSA. Range B has a higher carbonate content and if sulfate ground conditions of above Class 2 occur then some additional precautionary measures are recommended depending on the structural performance level as shown in TEG report Table 9.3 [1]. Range A has the highest carbonate content and additional preventive measures are necessary. However, the concept of the aggregate carbonate range is no longer included in BRE Special Digest 1 [96] because of the ever-present possibility of exposure to an external source of carbonate (principally bicarbonate in groundwater).

Even that fine and coarse limestone aggregate particles are involved in TSA a better resistance can be achieved using limestone dust free aggregates [2].

2.5.4   Additional Preventive Measures

To ensure the resistance to TSA, high quality workmanship is necessary to achieve good physical properties and additional passive preventive measures can be applied. That includes for instance the application of an effective moisture barrier, of a waterproof bituminous coating or of a spray-applied membrane [27]. Furthermore Crammond [2] suggests that initial air-curing prevents the onset of TSA as well. At the counterpart to the concrete constructional measures at the environment the soil also decrease the risk of TSA. Longworth [66] recommends to minimise disturbance of the ground during construction; to design the excavation process in order to prevent the formation of high sulfate-containing groundwater sumps; to use constructions such as

piles and trenchfill foundations to avoid backfilling of excavated material; and to design
ground drainage. The TEG [1] suggests to apply an additional outer concrete skin with
low-carbonate aggregate or to substitute sulfide/sulfate-bearing backfill material if other
measures cannot be applied.

2.5.5   Guidance

Guidance for the prevention of TSA is available and has been revised after the
publication of the Thaumasite Expert Group report [1] in 1999. Building Research
Establishment published the BRE Special Digest 1 – 'Concrete in aggressive ground'
[96] as successor of the BRE Digest 363 – 'Sulfate and acid resistance to concrete in the
ground' [97] and therein BRE took into account the occurrence of TSA. In BRE Special
Digest 1 the Aggregate Carbonate Range (ACR) classification and the Design Chemical
classes (DC class) were introduced. Furthermore additional protective measures (APM)
were extended by the TEG to previous BRE guidance. Amendments to BS 5328 –
'Concrete' were issued in 2001 as well, however, the concrete standard BS 8500 –
'Concrete – Complementary British Standard to BS EN 206-1' has still to be taken into
account due to more detailed information on the use of concrete in aggressive ground
conditions. The European standard is BS EN 206-1 – 'Concrete'. Other relevant
standards are BS 882 – 'Specification for aggregates from natural sources for concrete'
for aggregates and BS EN 197-1 – 'Cement'.

2.6   Thaumasite in Laboratory Conditions – Accelerated Tests

2.6.1   General

To produce thaumasite in the laboratory, in addition to creating an external environment
that is conducive to the development of thaumasite, the concrete mix must be
susceptible to attack. This means creating a concrete with a reasonably high
permeability so that the external sulfate ions can penetrate into the cement paste and
react with dissolved carbonate and silicate ions in the pore solution. The main factor
governing permeability and, incidentally, strength of concrete is the water-cement (w/c)

ratio. BRE Special Digest 1 [96] gives maximum free water/cement ratios for prevention of sulfate attack according to this guide w/c-ratios of 0.35 for the most aggressive environments and should not exceed 0.55 for slightly aggressive conditions. However, if there is no potential for attack the w/c-ratio is not limited. It can be inferred from this guidance that to encourage and accelerate attack the w/c-ratio should be over 0.55.

2.6.2   Binder

All binders based on Portland cement are susceptible to the thaumasite form of sulfate attack as thaumasite consumes the calcium silicate hydrates that are the main strength giving agent in all these binders. The time of onset of deterioration can be influenced by the type of filler used as this has physical as well as chemical effects on the cement paste, see Section 2.5.2.

For the acceleration of TSA in laboratory based experiments the most vulnerable binder is Portland limestone cement (PLC) as shown by Lipus and Punkte [98, 99] and Tsivilis et al. [62]. Portland cement pastes are susceptible in a lower degree to TSA than Portland limestone cement pastes and Tsivilis et al. [62] concluded that the deterioration is more severe the higher the limestone content.

Crammond [35] suggests that the binder used should have an initial reactive Al_2O_3 content of between 0.4 and 1.0% in order to form ettringite as this serves as an important initiator for the growth of thaumasite. Nobst and Stark [93] demonstrated experimentally that the amount of thaumasite formed is directly proportional to the total amount of Al_2O_3 and C_3A, respectively, but Blanco-Varela et al. [100] and Herfort et al. [101] showed the opposite that low C_3A cements produce higher amounts of thaumasite than high C_3A cements suggesting that SRPC concretes may be more susceptible to attack than those with Portland cement.

At the thaumasite field trial at Shipston-on-Stour, after three years BRE [80] observed that concretes based on Portland cement and Portland limestone cement showed the worst signs of sulfate attack of all the binders investigated, these are listed in Table 2.2. BRE could not find significant differences in the severity of attack at the concretes containing PC with 6.6% and 9.9% C_3A. The SRPC with 1.4% C_3A performed slightly

better than its PC counterparts and this is in agreement with the observations of Nobst and Stark [93] but disagrees with Blanco-Varela et al. [100] and Herfort et al. [101]. Binder under which buried concrete performs satisfactory are described more in detail in Section 2.5.2. The term binder is used for both cements and composite cements.

Table 2.2: Binder type used by BRE at Shipston-on-Stour [80, 102]

Binder type	Cement type to BS EN 197-1: 2000
Portland cement (PC): 9.9% C_3A	CEM I 42.5
Portland cement (PC): 6.6% C_3A	CEM I 42.5
Sulfate-resisting PC (SRPC): 1.4% C_3A	CEM I 42.5
Combination of 70% PC and 30% pfa	CEM II/B-V
Combination of 60% PC and 40% ggbs	CEM III/A
Combination of 30% PC and 70% ggbs	CEM III/B
Portland limestone cement (PLC) containing 15% limestone	CEM II/A-LL
BRECEM (50% HAC + 50% ggbs)	-
PC-silica fume (microsilica): 90% PC + 10% microsilica	CEM II/A-D
Portland metakaolin cement: 75% PC + 25% metakaolin	-

2.6.3   Aggregate

To accelerate TSA in laboratory conditions it is appropriate to provide the highest source of carbonate ions possible, i.e. the aggregate should contain of up to 100% of calcite. Aggregate types used by BRE [102] in a field trial at the Shipston-on-Stour field trial are crushed magnesian limestone, Jurassic Oolitic limestone gravel and crushed carboniferous limestone. Siliceous aggregates, such as flint gravel, were used for control mixes. The magnesian limestone consisted mineralogically of mainly dolomite and traces of quartz; the Jurassic limestone mainly of calcite, traces of quartz and some traces of dolomite; the carboniferous limestone mainly of calcite, some traces of quartz and minor dolomite. The field trial showed after three years that the Jurassic Oolitic limestone concrete had suffered the most deterioration. Significant differences between the other limestone aggregates could not be observed [80].

The categorisation of aggregates susceptible to the thaumasite form of sulfate attack is represented in Section 2.5.3.

2.6.4   Mix Design

Laboratory susceptibility tests of binders are often performed using mortars with a variety of water/cement ratios up to one and sometimes higher. Few large-scale concrete trials have been performed and this is mainly due to costs for the amount and size of samples stored in environmental chambers. Building Research Establishment have performed several large-scale concrete trials during the last 10 years [102, 103, 104] these concrete trials were designed to satisfy then current requirements of BRE Digest 250 or 363 [105, 97] and this is to investigate the sulfate resistance of general concretes used under TSA conditions. In 1996 the BRE [103] reported the results of a trial intended to obtain more evidence on TSA. In this three different cement contents with a w/c-ratio of about 0.5 were used. The cement contents used were referred to as low (290 kg/m^3), medium (330 kg/m^3) and high (370 kg/m^3). A further trial, reported in 2000 [104], investigated the performance of a series of concrete mixes designed for good sulfate resistance as specified in BRE Digest 363 [97]. The concrete mixes were designed to 0.5 free water/cement ratio and 350 kg/m^3 cement content with different types of binder, changing grades of carbonate aggregates and stored in a series of aggressive solutions at 5°C and 20°C.

The Shipston-on-Stour field trial [102], initiated in 1998, aimed to compare data obtained by TSA deterioration simulated in laboratory conditions with deterioration caused by TSA in the field. Several different mixes with a uniform binder content of 320 kg/m^3 and a slump of 50±20mm, i.e. a free water/binder ratio of 0.53-0.58, were designed for field and laboratory conditions. To investigate the effects of TSA in poor quality concretes, mixes were included in which the binder content was reduced to 290 kg/m^3 and the slump increased to 75±20mm (free water/binder ratio of about 0.75).

The trials performed by BRE aimed to investigate the vulnerability of different binders, mix designs and the aggressiveness of several solutions. The extent of deterioration was reported as a 'wear-rating' these and further findings are discussed Section 2.7.2.

2.6.5   Casting

In the Shipston-on-Stour field trial [80, 102] two types of concrete cubes were buried, these were described as either precast or cast in-situ. The precast cubes were cast, air-

cured for 14 days and then placed in the trench so that some faces were in contact with undisturbed Lower Lias Clay and some with backfilled material. The aim of these specimens was to investigate the effect of an initial air-cure as it is known that this is a beneficial factor for concretes affected by conventional sulfate attack [63], the effect of curing is discussed further in Section 2.6.6. This method represents precast manufacturing for instance the case of precast concrete piles. In the second method of casting cubes were cast directly against either undisturbed Lower Lias Clay or the shuttering and then backfilled with disturbed material to simulate trench fill, strip foundations and cast in-place concrete piles.

2.6.6   Curing

Different types of curing can be found in the literature, these are air-, moist-, water-, autoclave-, and seal-curing. BRE [63, 80] investigated the effects on TSA of air-, water- and seal-curing and concluded that the most reactive type regarding TSA is seal-curing. In seal curing, specimens are wrapped in three layers of cling film and then put in a polythene bag immediately after demoulding for 27 days at 20°C. Previous investigations of BRE [63] showed that initial air-cured specimens are more resistant to TSA than water-cured specimens and that the degree of TSA at faces which were in direct contact with surfaces other specimens was even worse, irrespective of whether the specimens were air- or water-cured.

The beneficial effect of air-curing is caused by the formation of a protective carbonated layer. Differences between 'contact' and 'free' faces during water-curing occur due to the different extent of leaching of calcium hydroxide which is restricted at contact faces [63]. Further investigations at BRE [80, 102] included seal-curing to simulate the contact faces and field and laboratory experiments, such as the Shipston-on-Stour field trial, showed that seal-cured cubes were the most susceptible to TSA. BRE explains this behaviour with the main difference that carbonation is prevented and therefore the alkalinity in the pore solution remains high and conducive to TSA [2].

Oberholster et al. [47] investigated the effect of curing using water-cured and autoclave-cured specimens and it was observed that the latter showed faster deterioration than the cubes cured in water. However, there is no comparison with seal-cured specimens

available. Thomas et al. [71] cured specimens in a moist environment of 100% humidity but no comparable data have been found.

2.6.7   Storage Solution

For TSA to occur specimens must be stored in an aggressive solution with a sufficient concentration of aggressive ions. There is, however, no linear dependency between aggressiveness and concentration [28]. According to Wittekindt [106] sulfate attack does not increase over a limit of 10000mg SO_4^{2-}/l.

In addition to concentration the type of cation is an important factor for aggressiveness, as already mentioned in Section 2.3.4 magnesium is the second most aggressive cation after ammonium and the most common in laboratory research. According to Bensted [75] magnesium sulfate attack enhances TSA and increases the deterioration. However, sodium, potassium and calcium sulfate solutions as well as combinations of these have been used in laboratory studies [48, 63]. It was observed that these solutions provoke thaumasite but the formation occurred much later and then potassium accelerates the 'alkali carbonation' where alkali metal hydroxides readily absorb carbon dioxide [48], see also Section 2.3.4. Some concentrations used in laboratory investigations are summarised in Table 2.3.

Table 2.3: Sulfate solution concentrations

Concentration	Reference
1.53g/l CaSO$_4$·2H$_2$O, 2.56g/l MgSO$_4$·7H$_2$O, 0.77g/l Na$_2$SO$_4$, 0.05g/l K$_2$SO$_4$ and 370mg CO$_3^{2-}$/l	Crammond and Halliwell, BRE [102]
0.42% SO$_4^{2-}$; 1.8% SO$_4^{2-}$ as MgSO$_4$ 1.8% SO$_4^{2-}$ as Na$_2$SO$_4$	Crammond and Nixon, BRE [40]
0.42% SO$_4^{2-}$; 1.99% SO$_4^{2-}$ as MgSO$_4$ 0.42% SO$_4^{2-}$; 1.99% SO$_4^{2-}$ as K$_2$SO$_4$	Gaze and Crammond, BRE [48]
0.42% SO$_4^{2-}$; 1.27% SO$_4^{2-}$; 4.24% SO$_4^{2-}$ as MgSO$_4$	Lee et al. [85]
29800mg SO$_4^{2-}$/l	Lipus and Sylla [45]
1.44% SO$_4^{2-}$ as MgSO$_4$	Torres et al. [70]
1.4g SO$_4^{2-}$/l as CaSO$_4$ + 1.6g SO$_4^{2-}$/l as MgSO$_4$	Zhou et al. [57]

Gaze and Crammond [48] confirmed Wittekindts [106] statement that an increase in solution strength increases the amount of reaction but only up to a limit and they stated that weaker solutions are more efficient, comparable damage being achieved with smaller amounts of sulfate.

Besides the sulfate BRE [102] also used carbonate as an ingredient for lab-based solution in order to simulate field situations and to supply another source of carbonate ions. Chemical characterisations showed that bi-carbonate is dissolved in groundwater and therefore can serve as a secondary source of carbonate. Another type of solution used in laboratory conditions was sulfuric acid. Zhou et al. [57] used sulfuric acid as an aggressive solution to investigate whether the sulfuric acid formed during pyrite oxidation favours TSA and it was concluded that the acid does not promote the formation of thaumasite.

In the majority of studies reported in the literature solutions were renewed every three months to maintain a constant concentration of sulfate ions.

2.6.8   Storage

Specimens are in general stored at temperatures at about 4-6°C with a high humidity in environmental chambers but dry-wet cycles are also a possibility [71, 107]. The dry-wet cycles [71] are based on test methods to investigate the resistance of concrete to freeze-thawing which is the most effective in this case, however, in the case of TSA it could not accelerate testing. Specimens are separated in order to avoid cross-contamination between cubes containing different aggregates and binders [80]. Gaze and Crammond [48] stored specimens in air-tight containers in order to minimise the influence of atmospheric CO_2 as a source of carbonate ions.

2.7   Results of Comparable Field/Laboratory Trials at BRE

2.7.1   General

The Building Research Establishment has undertaken two large-scale field trials funded by DETR following the findings of the Thaumasite Expert Group, one at Shipston-on-

Stour in the Cotswold area which is supported by a parallel laboratory trial and another field trial at Moreton Valence on the M5 motorway.

2.7.2   Shipston-on-Stour

The Shipston-on-Stour field trial has been divided into two sets, one set was excavated after three years in buried exposed conditions and the second set will be excavated and investigated after 10 years, this set was buried during Spring 1998. The parallel laboratory trial assessed concrete cubes after one and two years in exposed conditions. The materials used and the design of the concrete is described in Section 2.6 and summarised in Table 2.4:

Table 2.4: Specifications for Shipston-on-Stour field and parallel laboratory trial [80, 102]

Field conditions:	
Binder	Table 2.2
Aggregate	Flint gravel
	Crushed magnesian limestone
	Jurassic limestone gravel
	Crushed carboniferous limestone
Mix design	Main mixes: 320 kg binder/m^3; w/c = 0.53-0.58
	Outlier mixes: 290 kg binder/m^3; w/c = 0.72-0.78
Casting	Cast in-situ
	Precast
Exposure	1.5-1.8g SO_4^{2-}/l (Sulfate Class 3); 0.7g Mg^{2+}/l i.e. Design Sulfate Classes DS-4m and DS-5m; pH=7.5; T=9.5-12.5°C
Additional lab-specifications:	
Curing	Water-, air- and seal-cured
Exposure:	1.53g/l $CaSO_4\cdot2H_2O$, 2.56g/l $MgSO_4\cdot7H_2O$, 0.77g/l Na_2SO_4, 0.05g/l K_2SO_4 and 370mg CO_3^{2-}/l; T=5°C

Relevant findings from both trials are summarised below [80]:

- The timescale of three years in a field trial is sufficient to assess resistance of concrete mixes;

- Visual results of field trial correlate well with laboratory results, except for concretes containing pfa and 40% ggbs;

- Even after the relatively short period of exposure on site many of the test specimens were covered with a white coloured reaction product;

- Precast concrete masonry blocks containing Jurassic Oolitic limestone were coated with thaumasite;

- The precast concrete cubes performed much better than their cast in-situ counterparts;

- The poor quality outlier mixes showed more surface deterioration;

- The worst attack was found on the corners and edges of the top struck face, which had been in contact with the back-fill clay;

- All cast in-situ concrete cubes made with either PC or PLC (Portland limestone cement) have shown significant signs of sulfate attack irrespective of aggregate type.

The deterioration measurement used by BRE, the wear rating method described in Section 2.2.2.4 revealed the following results for seal-cured concrete cubes [108]:

Table 2.5: Wear ratings after one year laboratory exposure [108]

Binder Type	Free w/b-ratio	Aggregate	Water-cured cubes wear rating	Seal-cured cubes wear rating
PC (10% C_3A)	0.53	Siliceous	0.0, 0.0	6.0, 7.5
PC (10% C_3A)	0.55	Magnesian limestone	0.0, 0.0	4.0, 5.0
PC (10% C_3A)	0.58	Carboniferous limestone	0.0, 0.0	3.5, 4.0
PC (7% C_3A)	0.53	Siliceous	0.0, 0.0	6.5, 9.0
PC (7% C_3A)	0.55	Magnesian limestone	3.0, 3.0	6.0, 7.0
PC (7% C_3A)	0.58	Carboniferous limestone	0.0, 0.0	4.5, 5.0
SRPC (1.4% C_3A)	0.53	Siliceous	0.0, 0.0	1.0, 1.5
SRPC (1.4% C_3A)	0.55	Magnesian limestone	0.0, 0.0	4.5, 5.0
SRPC (1.4% C_3A)	0.58	Carboniferous limestone	0.0, 0.0	2.5, 4.0

Note: Wear rating thresholds after one year: >5 – imply low sulfate resistance; 2-5 imply satisfactory sulfate resistance; <2 imply good sulfate resistance

Significant differences can be seen between the two types of curing, however, it should be noted that the wear rating method does not express well the features of the thaumasite form of sulfate attack and the results could be affected by deterioration caused by conventional sulfate attack.

2.7.3   Moreton Valence

The field trial at Moreton Valence is a long term trial funded by DETR and has the intention to investigate the durability of repaired column pieces extracted from the Tredington-Ashchurch Bridge and to assess whether the various repair techniques are viable. Beside this, a geotechnical survey is being carried out to observe the soil and groundwater conditions over the long term [55]. Additionally the weathering progress of the present Lower Lias Clay is investigated by means of pyrite oxidation.

The trial started in 2001 and is based on an exposure time of 10 years and therefore results are not yet available.

2.8   Structural Effects

Structural effects of the thaumasite form of sulfate attack due to loss of strength, stiffness and resistance to ionic diffusion of the gradual progressive deterioration zone were described in the report of the Thaumasite Expert Group [1]. The main effects are as follows:

(i)   loss of concrete cross-sectional area;

(ii)   loss of cover concrete to the reinforcing bars and, possibly, beyond the bars;

(iii)   loss of bond between reinforcement and concrete in affected zones;

(iv)   loss of pile skin friction;

(v)   loss of foundation base friction;

(vi)   settlement, inducing structural damage;

(vii)   loss of durability as a result of a loss of protection against reinforcement corrosion.

The TEG classifies effects (i) to (iii) as purely structural, (iv) to (vi) as soil-structure system and effect (vii) as durability issues which may have structural implication.

The effects listed above are able to affect the structural integrity; however, public safety will be rarely endangered due to the gradual nature of TSA. Signs of deterioration of a substructure will be visible in the superstructure above through e.g. progressive cracking before significant loss of stability occurs.

2.8.1   Pure Structural Effects

The softening due to TSA leads to a reduction in the cross-sectional area of sound concrete, in compression members one of the consequences of this is an increase in effective slenderness. Wallace [109] reported a case where there was a risk that the designated 'fixed end' condition of a buried reinforcement lap just above the base may have converted to a less effective 'pinned end' due to loss of bond strength. There occurred a reduction of the concrete compression area though the core concrete was sound and the reinforcement was still likely to be effective in resisting buckling.

Bond strength depends on the nett cover as shown experimentally by Gorst and Clark [110] and therefore depends on the extent of the softened zone. They performed full size pullout test on plain round reinforcement bars embedded in two unaffected and four TSA-affected reinforced concrete elements. These elements were sections of columns which were removed from the thaumasite-affected Tredington-Ashchurch Bridge on the M5 in Gloucestershire. Experimental data indicated a reduction of the mean experimental bond coefficient of 24% for corner bars and 10% for non-corner bars leading to an average reduction of the mean experimental bond coefficient of 15% for all bars including corner bars.

Structural members which would be most affected by TSA are, according to TEG [1]:

- Slender columns, piles and beams, which would be more likely to buckle and have reduced compression capacity.
- Structures with a significant reliance on bond for their structural integrity. The TEG gives an example of a buried column/foundation connection where starter bars from the foundation are lapped with the main column bars. A moment in

such a connection is transmitted through the capacity of the transmissible tensile force and therefore depending on bond.

- Vulnerable structural details, such as Freyssinet hinges, and tension members such as 'tie downs'.

2.8.2   Soil-Structure Effects

Changes in soil-structure interactions caused by softening of the concrete surface due to TSA can be defined [1] on the one hand as the loss of friction at the affected areas, i.e. reduction of sliding resistance to lateral loads, as for instance in foundations and retaining walls, and reduction of load capacity of piles which is characterised by skin friction. On the other hand the loss of effective cross-section can reduce the capacity and increase element slenderness as described in Section 2.8.1.

There have not been reported investigations of the effect of TSA on friction characteristics of substructures and it has not been possible to locate in the literature any information regarding field cases. The TEG [1] reported a case of cast-in-place concrete piles in Lower Lias Clay where the pile had been affected up to 50% of the exposed area and a general softening of less than 20mm occurred but at one location the softening progressed up to 70mm. Beside this, corrosion was found, this was not severe and was caused by carriageway surface run-off.

To date there is little evidence of a negative impact on the stability of foundations caused by TSA. Substantial loss of structural integrity did not occur at the severe TSA affected cast in-situ concrete piles as reported by the TEG [1]. This may be partly due to the safety factor which is used during the design of the piles. This factor is generally two or greater and includes allowance for uncertain ground conditions as well as for concrete piles the uncertainties of workmanship and long term durability below ground. However, the probability of the worst case is very low and, before substantial loss of integrity occurs, the piles would need to be affected massively. In addition there is the lack of knowledge about the effects of TSA on skin friction which may be either negative or positive nature.

Negative effects should become obvious in the superstructure in the form of settlement/deformation induced distress before the whole structural integrity is affected.

In the case of base foundations subjected to lateral load there exists little practical knowledge about the effects of TSA, however, field experience showed that base friction can be mobilised fully on unweathered or undisturbed clay due to the absence of TSA [1, 27]. Minor thaumasite formation (TF) was merely detected on a base of a M5 bridge foundation and this after an exposure to an aggressive environment for 29 years.

The skin friction at the soil-structure interface forms one important part in the assessment of the stability of structures as discussed above. Hence this lack of knowledge needs to be addressed to allow the engineering community to make informed assessments of the likely impact of TSA on soil/structure interaction.

The relevant theories of soil structure interaction and the influence of TSA on these are discussed in the next section.

2.9 Soil/Structure Interaction

2.9.1 General

Buried concrete structures are usually foundations whose function is to transfer the load of the superstructure to the underlying soil formation without overstressing the soil [111]. Beside these there are other structures such as retaining walls which depend on interface interactions which can derive from both physical and chemical nature. In the following paragraphs these interactions are described more in detail.

2.9.2 Types of Foundations

Foundations are divided into two types the first type is referred to as shallow foundations where light to moderate foundation loads are transmitted directly to either a rock formation or a safe bearing soil. Ordinary spread footings or wall footings are common in these cases for residential, commercial, and even industrial structures. The second type are deep foundations that transfer loads through weak ground to strata that has sufficient capacity to carry the required loads. This can be achieved through the use of piles, drilled piers or caissons as foundations [111, 112]. The differentiation between

shallow and deep foundations derives from the physical size and the method of installation. Piles can be made of concrete, steel or timber and concrete piles can be divided further into two basic categories; precast piles and cast-in-situ piles [113].

2.9.3   Physical Interactions

The focus of this study is on skin friction and its influence on the bearing capacity of piles and stability of structures subjected to lateral earth pressure. These depend on several factors [111]:

(i)   The physical properties of the soil;

(ii)   The time-dependent nature of soil strength;

(iii)   The interaction between the soil and the retaining structure at the interface;

(iv)   The general characteristics of the deformation in the soil-structure composite; and

(v)   The imposed loading (e.g. height of backfill).

Structures which undergo lateral earth pressure can be defined as various types of retaining walls, basement or pit walls as well as sheet pilings [112]. These structures can be affected by two types of earth pressure, active and passive pressure as shown in Figure 2.4. Beside the passive resistance, the friction force at the basement is another factor which determines the sliding resistance against active earth pressure.
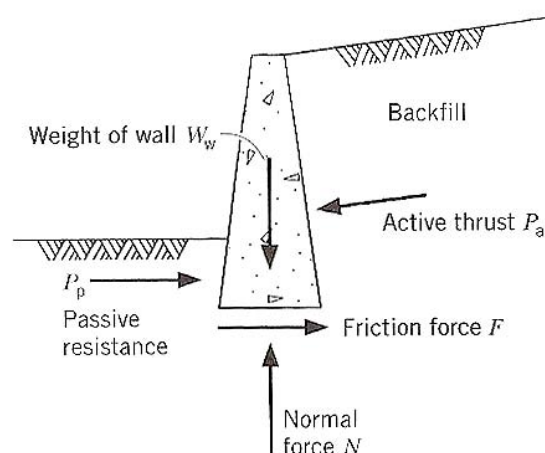
Figure 2.4 - Forces on gravity retaining wall [112]

The resisting force to lateral movement is provided by the horizontal force F, composed of friction and adhesion, and by the passive resistance P_p and can be expressed as

$$F = \mu N + c_b A \qquad (5)$$

where $\mu =$ coefficient of friction

          $N =$ normal force

          $c_b =$ base cohesion ($0.5c \leq c_b \leq 0.75c$)

          $A =$ base area

The coefficient of friction μ depends on the friction angle φ and on the type of casting the structure, i.e. whether the structure was precast or cast in-situ on site. The coefficients can be expressed as follows [112, 114]:

$$\mu = \tan \delta = \tan \varphi \left(\max .35° \right) \qquad \text{cast in-situ elements}$$

$$\mu = \tan \delta = \tan \frac{2}{3} \varphi \qquad \text{precast elements}$$

The sliding resistance according to BS EN 1997-1:2004 is calculated using the same friction coefficients and any effective cohesion should be neglected so that:

$$R_d = V_d' \tan \delta_d$$

Deep foundations which encompass piles, drilled piers and caissons are mainly subjected to an axial compressive load and the load transfer to the ground is achieved through skin friction, end-bearing capacity or a combination of both. Drilled piers and caissons are designed as end-bearing members and the side friction is neglected. Piles can be differentiated between friction and end-bearing piles; however, the load capacity is derived from a combination of end-bearing and skin friction [112].
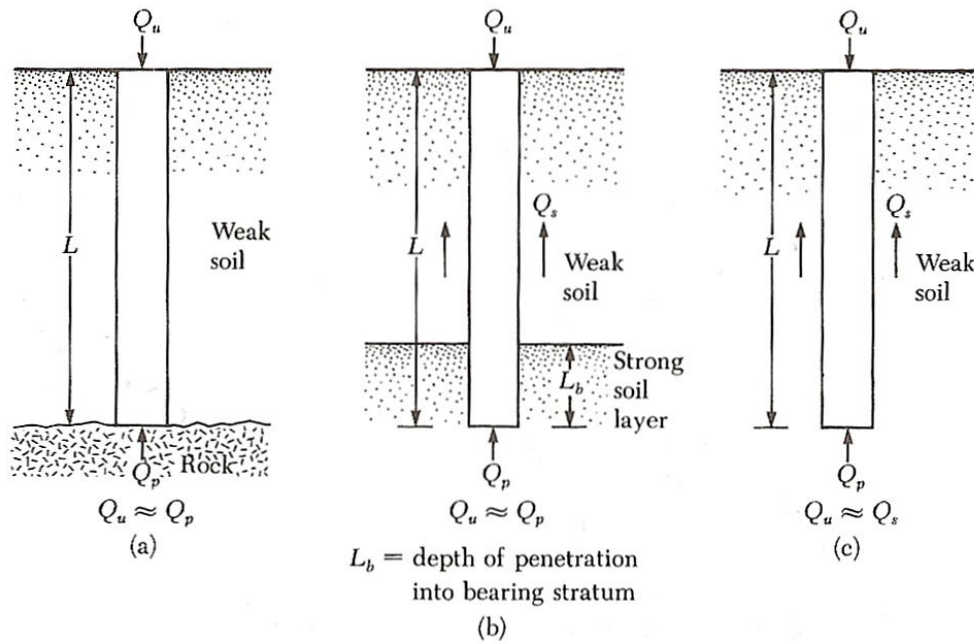
Figure 2.5 - Pile categories: (a) and (b) point bearing piles; (c) friction piles [113]

Figure 2.5 shows the three load capacity categories, where (a) represents point bearing piles; (b) shows the combination of point bearing and friction pile if the shear resistance of the strong soil layer is large enough to be included and (c) represents friction piles. Friction piles are used as foundations when no layer of rock or rocklike material is present at a reasonable depth and point bearing piles become very long and uneconomical [113]. The ultimate load of a single pile can be generally expressed as

$$Q_u = Q_p + Q_s \tag{6}$$

where Q_p = point resistance (end-bearing)

Q_s = skin friction resistance developed at the side of the pile (caused by shearing resistance between the soil and the pile)

If the point or skin friction resistance is very small their part of the capacity can be neglected as it is shown in Figure 2.5(c).

The resistance of friction piles is mostly derived from skin friction, however, in clayey soils the resistance is also caused by adhesion. The load capacity of friction piles depends on the shear strength of the soil as well as the size and lengths of the pile [113].

The estimation of the load capacity caused by skin friction can be generally expressed for a layered system and/or varied sections as

$$Q_s = \sum (\Delta L) p_i s_{si} \qquad (7)$$

where L =   total length of embedment of pile

p_i =   perimeter of pile in contact with soil at any point

s_{si} =   shaft resistance per unit area at any point along pile

In the case of cohesive soils (clay) the shaft resistance s_s is expressed as unit skin friction resistance f_s and according to Meyerhof [115] this value can be estimated for driven piles as

$$f_s = 1.5 c_u \tan \varphi \qquad (8)$$

And for bored piles as

$$f_s = c_u \tan \varphi \qquad (9)$$

where c_u =   average cohesion, undrained conditions

φ =   angle of internal friction of clay

Chandler [116] suggests that the effective stresses in the ground control the magnitude of pile shaft friction if loading is slow enough to ensure drained conditions in the clay along the pile shaft by horizontal effective stress, σ_h'. According to the basic shear stress equation for soil:

$$\tau_s = c' + \sigma_h' \tan \varphi' \qquad (10)$$

Chandler [116] and Burland [117] neglected the influence of the cohesion c' with the reason that it is likely being destroyed during pile installation and as a result the shaft friction τ_s at any point is given as:

$$\tau_s = \sigma_h' \tan \delta' \qquad (11)$$

where δ' is the effective angle of friction between clay and the pile shaft. This friction angle depends on the soil type and the properties of the pile surface. BS EN 1997-1:2004 neglects any effective cohesion present at interface and considers only the skin friction for load capacity calculations.

Other physical interactions which occur when piles are driven into soft saturated clays are according to Cernica [112]:

- Disturbance of the clay around the pile;
- Increase of pore water pressure, however, it dissipates rather rapidly;
- Increase of compressibility in the clay, and
- Remoulding the clay to varying degrees for a distance of approximately one pile diameter.

The apparent loss of pile capacity after installation is temporary and the shear strength is regained generally after 30 days and frequently exceeds the initial values [112]. The increase in density, consolidation effects and the increased horizontal stress after pile driving leads to an increase of skin friction between soil and pile [112].

2.9.4   Physical Testing

2.9.4.1   Theory of Pure Clay Shear Tests

The parameters relevant for the estimation of the frictional resistance, such as the shear strength parameter, internal friction 'φ' and cohesion 'c', of soil are determined experimentally using different shear strength tests in the laboratory. These are the direct shear test, the triaxial compression test and the unconfined compression test [111]. The direct shear test is a simple and widely used test for the determination of the shear strength parameter of the soil itself and of skin friction at interface systems. The direct shear test is relevant to the current investigation.
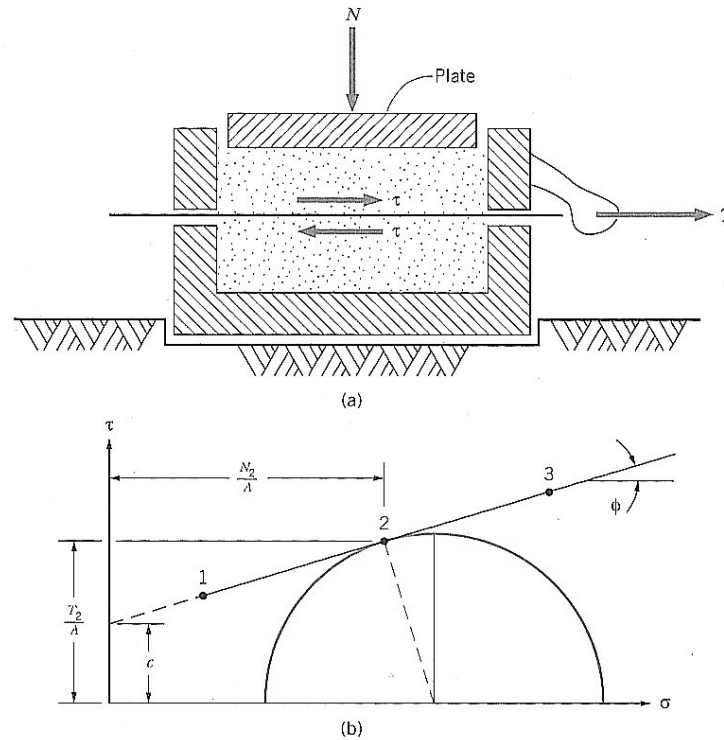
Figure 2.6 - (a) Schematic direct shear apparatus (b) Representation of results using Mohr circle [111]

Figure 2.6 (a) shows a schematic representation of the direct shear apparatus which consists of an upper and a lower section. In this case the lower section is fixed to a frame and the upper moves horizontally relative to the lower section. A shear force, T, pulls the upper section and creates a shear plane with corresponding shear stresses determined by the normal force, N. The test is performed either at a constant speed (strain-controlled test) or at a constant load (stress-controlled test) until failure is induced. Several repetitions with different values of normal force N are necessary to plot the results and obtain a failure envelope as shown in Figure 2.6 (b). Using Mohr circles the shear strength parameters φ and c can be obtained directly from the corresponding tangent in the graph [111].

There are three different kinds of testing which determine the values of φ and c. The undrained shear test is defined as the test where the sample has not undergone substantial water drainage and the load is applied soon after the placement of the specimens in the shear box. If the sample was allowed to consolidate before the test, however, the test is run quickly and pore pressure develops then it is referred to as consolidated undrained test. In the case of a very slow performance where no pore pressure develops the test is referred to as consolidated drained [111].

The consolidated drained test is very time consuming but it is not affected by excess hydrostatic pore-water pressure and therefore the effective friction is significantly larger. However, the actual strength may lie somewhere between the strength measured at consolidated drained and undrained conditions since total drainage is unlikely [111].

2.9.4.2 Soil-Structural Interface Tests

To date soil-structure interface tests have been performed mainly to investigate the structural integrity of foundations or chemical interactions at the interface. The majority of the research work to date has considered the shear behaviour of solid surface and cohesionless soils such as sand. Over recent years the computational simulation of interface behaviour has developed to a much greater extent applying frictional laws for instance to investigate interface shearing between soil and concrete [118], interface shearing along different planes [119] and to estimate the reduction in load capacity caused by minor flaws [120].

The methods for the measurement of the shear strength of soils have served as a means of determining the skin friction at the interface between construction material and soil. The direct shear box, see Section 2.9.4.1, is the test used most commonly for the determination of wall or shaft friction for retaining walls and piles and is useful for the design of soil reinforcement [121].

In 1961 Potyondy [122] realised the lack of experimental skin friction data and carried out a variety of experiments to the effect on skin friction of soil type, type of construction material, surface condition and moisture content of the soil. He determined the shear strength parameter between structural materials: steel, wood and concrete with smooth and rough surface finish and soil types: sand, clay, cohesive granular soil and silt. As a result of this investigation Potyondy [122] concluded that skin friction is dependent on:

(i)   The moisture content of soils;

(ii)   The roughness of surface;

(iii)   The composition of soils; and

(iv)   The intensity of normal load.

The investigation of skin friction on concrete-clay showed that after a certain increase of normal load the skin resistance achieved a constant value, see Figure 2.7, and the maximum shearing strength on smooth concrete reached nearly the strength of the clay itself. In every other case the skin friction was lower than the shearing strength of the soil, Table 2.6. Furthermore Potyondy calculated the relative changes of the shear strength parameters at the interface (δ, c_a) to the parameter obtained from the pure clay (φ, c), $\dfrac{\delta}{\varphi}$ and $\dfrac{c_a}{c}$ (Table 2.6). This showed reduced shear strength at interfaces. Based on this Potyondy [122] concluded that the skin friction values should be reduced in cases where the skin friction is responsible for the bearing capacity. It should be noted, however, that these tests were performed without allowing long term interactions between construction material and soil.
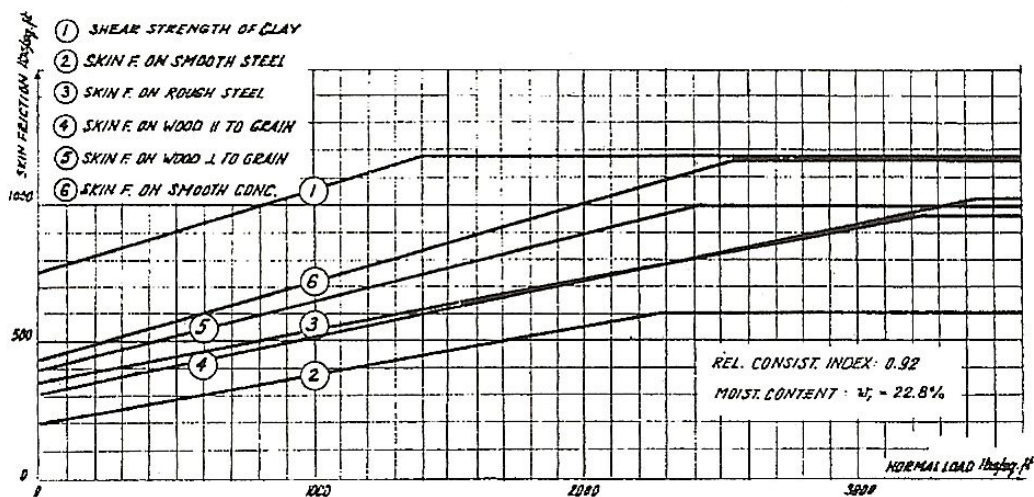
Figure 2.7 - Skin friction/normal load relationship of clay [122]

Zong-Ze et al. [119], Clough and Duncan [123], Peterson et al. [124], Lemos and Vaughan [125], Lee [126] and Frost et al. [127] all carried out direct shear box tests on concrete/soil interfaces where the soil was situated on top of the concrete. However, Clough and Duncan [123], Peterson et al. [124] and Frost et al. [127] performed the interface tests using sand wherefore the results are not comparable with clay interfaces. Lemos and Vaughan [125] investigated the interface resistance at clay interfaces and it was observed that the ultimate interface shear resistance normally approximated to the soil-on-soil residual strength, however, samples were tested immediately after consolidation and before any chemical interaction between the soil and concrete could

take place. Lee [126] cast the concrete against the clay and allowed curing times of up
to 28 days in order to mobilise interactions caused by casting and curing. The interface
shear strength increased with increasing curing time and exceeded the values of the clay
itself, see Figure 2.8.

Table 2.6: Values of shear strength and skin friction of clay [122]

		Friction on	ϕ or δ	c or c_a lb/sq. ft	$c$max $c_a$max lb/sq. ft	$\frac{\delta}{\phi}$	$\frac{c_a}{c}$	$\frac{c_a\text{max}}{c\text{max}}$
Cons. Index: 0·94, Moist. Cont.=22·8%	1	Soil	16° 30′	750	1,175	—	—	—
	2	Smooth steel	9° 00′	200	600	0·55	0·27	0·51
	3	Rough steel	10° 00′	350	350	0·61	0·47	0·84
	4	Wood par. to grain	11° 00′	300	1,020	0·67	0·40	0·87
	5	Wood at right angles to grain	13° 50′	390	1,000	0·82	0·52	0·85
	6	Smooth concrete	16° 10′	425	1,175	0·97	0·57	1·00
Cons. Index: 0·73, Moist. Cont. 26·1%	1	Soil	11° 30′	460	675	—	—	—
	2	Smooth steel	6° 30′	140	360	0·56	0·30	0·53
	3	Rough steel	5° 50′	265	580	0·50	0·58	0·86
	4	Wood par. to grain	7° 00′	210	600	0·61	0·46	0·89
	5	Wood at right angles to grain	8° 00′	230	620	0·69	0·50	0·92
	6	Smooth concrete	9° 30′	240	675	0·82	0·52	1·00
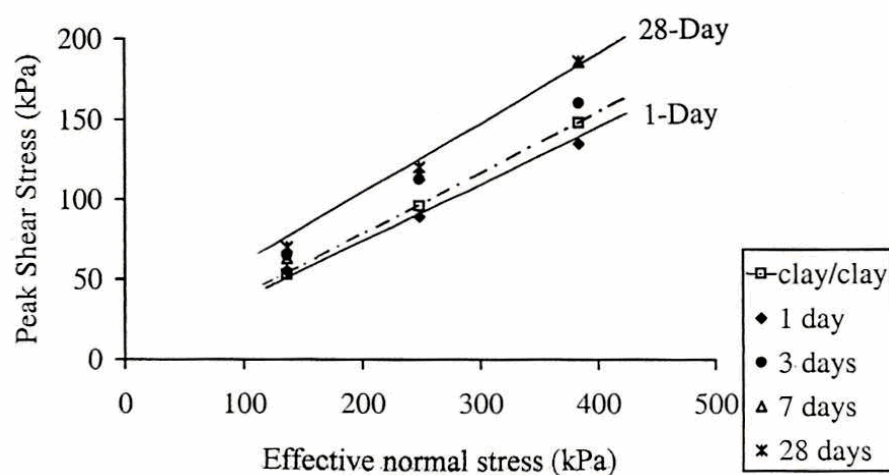
Figure 2.8 - Skin friction/normal load relationship of concrete/clay interface depending on curing time [126]

Zong-Ze et al. [119] assumed for the numerical simulation of interface deformation that sliding may occur in the soil close to the interface and described three different forms: (a) slide takes place just along the wall surface if the interface is smooth; (b) the slide surface is located in the soil adjacent to the wall if the wall surface is rough; and (c) there exists a failure area, which consists of a lot of slide surfaces and they may intersect with the wall surface at an angle. This assumption was based on preceding concrete/soil interface tests using a large direct shear box. Useugi and Kishida [128] observed a transfer of the shear plane into the adjacent soil body, however, their tests were performed on a steel/sand interface. Furthermore they reported that above a critical surface roughness there was no additional effect of increases in surface roughness.

There has been found a second type of interface testing in the literature. Chandler and Martins [129], Johnston et al. [130], Rojas et al. [131, 132] and Lee [126] modelled the development of shear resistance on axially loaded friction piles driven into soil either in the field or in laboratory conditions. Rojas et al. [132] described changes of the initial conditions of clay caused by pile driving:

(i)   A radial stress relaxation on the walls of the hole when preboring is performed;

(ii)   Downdrag and plastification of soil around the pile shaft during driving;

(iii)   Pore pressure increase in saturated soils;

(iv)   Reconsolidation of the soil due to pore pressure dissipation;

(v)   In the case of concrete piles, adherence of a fine crust of material; and

(vi)   Development of positive and negative residual friction loads once the pile has been installed.

The initial loss of bearing capacity during pile driving as mentioned by Cernica [112], see Section 2.9.3, and Rojas et al. [132] which is caused by an increase of pore pressure was considered during pile shear resistance interface tests. The excess pore water pressure has to be allowed to dissipate before loading tests can begin. This is reflected in drained conditions using the direct shear box test which is mainly controlled by the test rate. Cohesive soils, such as clay, require for drained conditions a very slow testing rate as used by Lee [126] with 0.0026mm/min or Chandler and Hamilton [133] with

0.005mm/min. The test rate can be estimated according to BS 1377:7-1990, Clause 4. Beside this Burland [117] and Rao et al.[134] stated that the shear deformation occurs within a relatively thin zone around the pile shaft where drainage can take place rapidly and therefore most pile loading situations tend towards drained conditions.

There exist some main differences between laboratory based direct shear box tests and pile model tests in field conditions. Rojas et al. [132] described the main differences as:

(i)   Horizontal stresses (which represent the vertical stresses in the field) cannot be controlled during the test; and

(ii)   The horizontal confinement of the specimen (which represents the vertical direction in the field) is rigid, avoiding any displacement in that direction, while soil in the field suffers important vertical displacements.

They concluded that data gained from direct shear tests should be considered with caution in friction pile capacity calculations.

Data about skin friction affected by forms of concrete deterioration, such as the thaumasite form of sulfate attack have not been found in the current literature.

2.9.5   Chemical Interactions

Beside the physical interactions, which are mainly responsible for the stability, there are also chemical interactions between soil and concrete piles which occur at the interface or reach inwards the clay. The presence of calcium and hydroxyl ions in the pore water of the soil due to leaching from the cement paste causes a sequence of reactions that vary with soil composition, mineralogy and pore water chemistry and results in the following changes of the soil according to Webster and Sheary [135]:

(i)   Reduction of the Plasticity Index;

(ii)   Reduction of volume change;

(iii)   Flocculation of clay particles to make soils more friable;

(iv)   Increase in optimum moisture content, allowing compaction under more moist conditions (soils dry out more rapidly); and

(v)   Some increase in strength and stability.

Furthermore the presence of hydroxyl ions (OH⁻) increases the pH of the soil this favours a solidification process as result of pozzolanic reactions where dissolution of silicon and aluminium from the clay takes place [136]. The dissolved components react with the calcium ions present in the pore water and form calcium silicate hydrates (CSH) and calcium aluminate hydrates (CAH) this results in a significant long-term increase in shear strength and often a reduction in permeability [137]. That feature has made successful the use of lime and cement in the improvement of clay properties, such as stabilisation.

Investigations on soil-structure interactions have been performed by several authors. Milititsky et al. [138] investigated the moisture movement between fresh concrete and clay where they observed an increase in moisture content of up to 4% after 7 days, Figure 2 9. Furthermore they confirmed the findings of several researchers [139-141] that the moisture content increase falls off rapidly as the sampling point moves away from the interface.
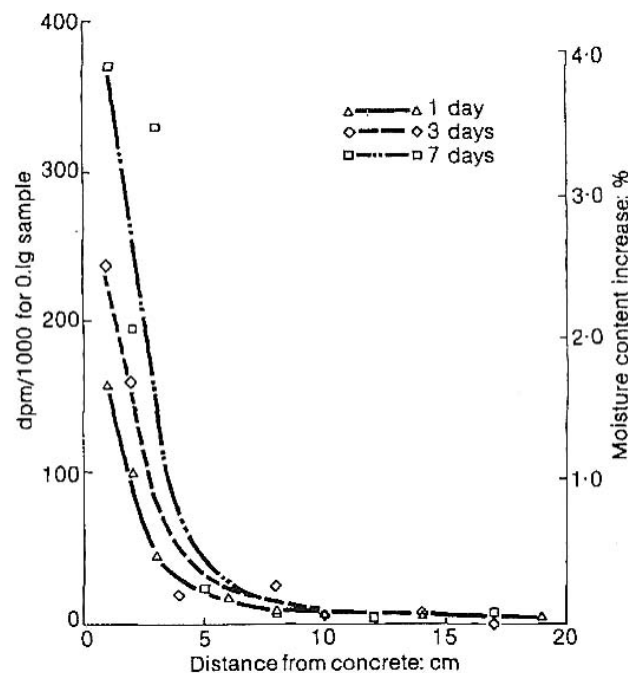
Figure 2 9 - Moisture content increase according to Milititsky et al. [138]

Lee [126] confirmed this trend of moisture content distribution close to the interface, however, she observed that the increase in moisture content decreases with time, in this case tests were performed after 1 to 10 months compared to the 1, 3 and 7 days in Milititsky et al.'s investigations. The same trend was observed for pH which reached the natural soil value at a distance of approximately 25mm similarly to the distance where

the moisture increase is reduced to zero. The influence of calcium ions was observed in increased concentrations in the surrounding clay up to a distance of 75mm over a period of 10 months and this reflected in the plasticity of the clay.

Hill et al. [84] have started measurements on changes in pH and chemical composition of the clay surrounding a pile which is affected by sulfate attack, however, final data could not been found yet.

2.9.6   Effect of TSA on the Concrete/Clay Interface

The Halcrow Group [27] and Slater et al. [56] investigated the clay environment around the TSA-affected bridge foundations along the M5 motorway in Gloucestershire. There could not been found significant relationships between chemical, mineralogical or physical soil parameters and distance from the concrete or degree of thaumasite attack. However, several trends were identified and those are relating to pure soil-structure interactions on the one hand:

(i)   Increase of moisture content towards the concrete;

(ii)   Increase of pH value towards the concrete; and

(iii)   Increase of calcium concentration towards the concrete, what derives from leaching of the calcium hydroxide from the concrete.

On the other hand trends were observed in the clay adjacent to the structure which were in relation to factors and features of the thaumasite form of sulfate attack:

(i)   Water-soluble magnesium decreased closer to the concrete and had an inverse relationship with pH;

(ii)   Pyrite and indirect sulfide concentration decreased with increasing attack, i.e. most thaumasite attack occurred where there was most pyrite oxidation;

(iii)   Sulfates and total sulfur increased with increasing attack;

(iv)   Gypsum values were highest where there was partial attack and depleted where there was full attack; and

(v)   The pH value and water-soluble magnesium increased and decreased respectively with increasing attack.

The trends developed regarding the availability of the transport medium, i.e. they are dependent on the groundwater level. No attack was found above the maximum water level and full attack was encountered below the minimum water level what corresponds to permanently wet conditions.

2.10   Summary

The literature review has shown the current state of knowledge of the thaumasite form of sulfate attack as well as physical and chemical interaction occurring at the soil/concrete interface. The review demonstrated that there is currently a lack of understanding the effects of TSA on skin friction at the soil/concrete interface. The basic knowledge to TSA and interface behaviour as well as the gaps regarding interface deterioration caused by TSA are summarised as follows:

- The most significant difference between TSA and the conventional form of sulfate attack is that TSA attacks the C-S-H-phases which are the main binding agent in Portland cement binders whereas conventional sulfate attack affects only the C-A-H-phases. TSA can be accompanied by expansion, cracking, spalling and final disintegration of the concrete from the surface inwards. The degradation product of the cement paste transformed is often described as a distinctly white coloured, soft, mushy, incohesive mass without any binding ability.

- Risk factors for TSA in buried concrete structures are a source of silicate, present in every Portland cement based binder; a source of sulfate, mostly from the soil; a source of carbonate, mostly supplied by the aggregate; a source of water, the groundwater present in the soil; and the ambient temperature has to be below 15°C. Secondary risk factors are identified as type and quantity of cement used in concrete; the quality of concrete mix; changes to ground chemistry and water regime from construction and type, depth and geometry of buried concrete.

- TSA can attack buried structures such as concrete foundations, piles, tunnel linings, floor slabs, pavements as well as it can be found in lime stabilisations. On the other hand TSA can occur in above ground structures such as in gypsum plaster and in brickwork in historical buildings.

- TSA can occur within a few years of exposure to aggressive environments and progress quickly or gradually depending on the environment. Initial 'dormant' periods of low activity have been observed before deterioration started which could last up to 15 years. Definite deterioration data such as rate and progress characteristics have not been found.

- TSA reaction products are mainly thaumasite, ettringite, gypsum, calcite and quartz and secondly aragonite and brucite can occur. TSA may be accompanied by further reactions such as magnesium sulfate attack, sulfuric acid attack and de-calcification processes. The status of thaumasite as final degradation product of TSA has not been explicitly clarified yet.

- Thaumasite stops to form below pH 10.5, it is, however, able to survive in lower alkalinity. Its stability reduces as pH approaches 7 and it gradually decomposes to gypsum and calcite.

- An unambiguous identification between thaumasite and ettringite requires the use of both microscopy and X-ray diffraction or scanning electron microscopy with combined EDX. The sampling of TSA affected material is significant for the correct identification of the deterioration process.

- Acceleration of TSA in laboratory conditions is combined with the use of susceptible concrete mixes, i.e. high permeability caused by low cement content and high water/cement ratio, susceptible binder and carbonate supplying limestone aggregate; TSA favouring curing method – seal-curing; as well as highly aggressive environment, i.e. highly concentrated magnesium sulfate solution stored at optimum temperature of 5-6°C.

- There is a lack of data about the effect of an additional external carbonate source on the deterioration rate and the ion exchange between aggressive solution and concrete.

- Buried concrete structures can be affected by TSA due to pure structural effects such as loss of concrete cross-sectional area leading to increased slenderness, loss of cover concrete and bond between reinforcement and concrete. On the other hand the structural integrity can be affected by soil-structure interface effects such as loss of pile skin friction and foundation base friction when subjected to vertical and lateral loads; and can cause durability issues resulting in structural implications.

- Investigations of soil-structure interactions, mainly the skin friction, affected by TSA form a gap of knowledge in the current literature.

- Skin friction investigations at the soil/structure interfaces are performed using the direct shear test under consolidated drained conditions or model friction pile tests.

- Skin friction depends on the soil moisture content, surface roughness, soil composition and intensity of the normal load.

- Moisture content, pH-value and calcium concentration increase in the soil adjacent to the concrete towards the interface.

- Skin friction was often observed to be less or equal than internal friction of the clay adjacent to the concrete, i.e. the interface represented the weakest plane, the shear plane. However, other sources reported an increased skin friction compared to internal clay friction. This increase depended on the curing time of the interface as it is caused by cementation processes due to reactions between soil minerals and ions derived from the concrete.

- Loss of structural integrity due to TSA on foundations has not been encountered yet in the field. Only few field cases are known and it is impossible to inspect buried structures at risk, therefore the engineering community needs to be aware of possible changes of the shear strength parameter.

3   Methodology and Materials

This chapter gives an overview of the experimental work. The methodology for the acceleration of thaumasite formation, the determination of its progress and its effects are described. Changes in the methodology and scope of experimental programme made in response to initial results are also described.

3.1   Experimental Programme and Test Specimens

3.1.1   General

To accelerate TSA and investigate the effects of TSA on skin friction at the soil/concrete interface of foundations and piles a number of variables were studied – these are concrete mix, clay type, method of casting – precast or in-situ, pressure applied during thaumasite formation and storage solution. The ultimate aim of the project was to measure the effect of TSA on skin friction at the clay/concrete interface. To achieve this a number of key criteria had to be met. These are listed below:

- thaumasite must form in a reasonable amount of time,
- thaumasite must not become detached from specimen,
- to simulate underground conditions thaumasite must form under some pressure and,
- the specimen must be transferred to the shear strength measurement equipment, a large shear box, without disturbing the clay/thaumasite/concrete interfaces.

The experimental programme was organised into five series, the aim of the first (Series I) was to investigate the effect of concrete mix on the rate of the progress of TSA, the second (Series II) looked for the effect of the casting position and in Series III the exchange of sulfate and carbonate ions between the solution and the concrete was investigated. The main objective of the project, the shear strength parameter, was investigated with Series V. Specimens in Series V consisted of a layer of concrete and a layer of clay which was confined and placed under pressure during thaumasite formation. Specimens in series I, II and III contained only concrete and solution, to

provide a link between these and the shear strength specimens a further series was developed – Series IV which contained both concrete and clay.

The aims and variables investigated in each of the test series are summarised in Table 3.1 and described in detail in the following sections.

Table 3.1: Aims and variables investigated in each test series

Series	Sub-specimen type	Aim	Variables
I	*Effect of mix type and solution on rate of deterioration*		
	"Needle"-specimen, Stage 1	Th.-progress – PC face XRD, Microscopy	5 mixes Precast 1.8% SO_4^{2-}-solution 1.8% SO_4^{2-} + 370mgCO_3^{2-}/l-solution
	Pressure specimens, Stage 2	Attached thaumasite XRD, Microscopy	2 mixes (most reactive mixes: 3, 5) Precast/cast in-situ Pressure of 70kPa (load of 3.5m soil) 1.8% SO_4^{2-}-solution
II	*Effect of casting position*		
	"Needle"-specimen, Stage 2	Th.-progress – CS face XRD, Microscopy	2 mixes (most reactive mixes: 3, 5) Cast in-situ 1.8% SO_4^{2-}-solution
III	*Ion exchange between solution and concrete*		
	Ion exchange	Solution uptake	5 mixes Precast/ cast in-situ 1.8% SO_4^{2-}-solution 1.8% SO_4^{2-} + 370mgCO_3^{2-}/l-solution
	Carbonate migration I (3monthly renewal)	Carbonate migration into H_2O	5 mixes Precast H_2O-solution
	Carbonate migration II (no renewal)	Carbonate migration into H_2O	5 mixes Precast H_2O-solution
	Aggregate in H_2O	Solubility of limestone aggregate	Fine aggregate (0-4mm) Coarse aggregate (4-20mm)
IV	*Providing a link between Series I, II, III and V*		
		Visual measurement of Th.-progress XRD, Microscopy	5 mixes Precast/ cast in-situ Lower Lias Clay (reactive) English China Clay (inert) 1.8% SO_4^{2-}-solution
V	*Determination of the shear strength*		
		Shear strength parameter	3 mixes (most reactive mixes: 3, 5 and most resistant: 4) Precast/ cast in-situ Lower Lias Clay (reactive) English China Clay (inert) 1.8% SO_4^{2-}-solution H_2O-solution Pressure: 10, 40, 70 kPa (load of 0.5, 2.0, 3.5m soil)

3.1.2   Test Series

3.1.2.1   Series I

The main focus of Series I was the investigation of the effects of the concrete mix on the rate of the progress of TSA. Five different concrete mixes were chosen in order to establish a relationship between water/cement ratio and cement content on the rate of progress of TSA. Cement contents of 290 kg/m³ and 320 kg/m³ and water/cement ratios of 0.55, 0.65 and 0.75 were used, see Table 3.2 for details of the mixes used. To allow comparison with work undertaken by BRE two of the mixes conform to mixes used by BRE at the Shipston-on-Stour field trial [80, 102]. A sulfate solution and a carbonate-sulfate solution, served as reaction medium. The concrete mixes and reaction solutions are described fully in Section 3.1.3 and 3.3.1 respectively.

Table 3.2: Mix parameter for Series I specimens

Mix	1	2	3 (BRE)	4 (BRE)	5
Cement content [kg/m^3]	290	290	290	320	320
Water / cement ratio	0.55	0.65	0.75	0.55	0.75
Aggregate content [kg/m^3]	1890	1820	1740	1830	1660
Percentage fine [%]	40	49	52	48	52
Percentage coarse [%]	60	51	48	52	48

Series I specimens were cylindrical with an internal diameter of 57mm and a height of 120mm and were filled with concrete to about 60mm and, after 28 days curing, were immersed into one of two solutions – sulfate, as magnesium sulfate, or carbonate-sulfate ($MgSO_4$) solution. A typical Series I specimen is illustrated in Figure 3.1. The progress of deterioration was determined from the surface inwards towards using a needle apparatus which is described in Section 3.2.1.
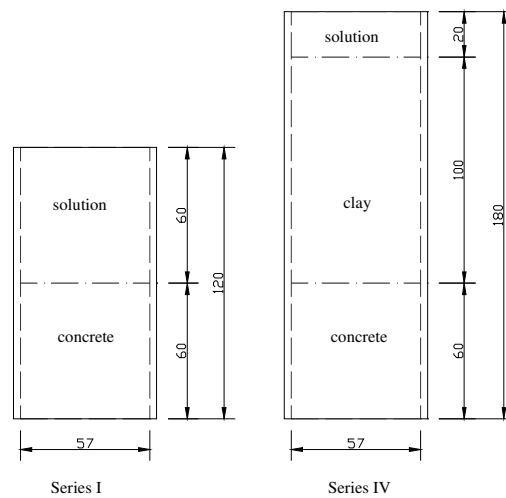
Figure 3.1 - Specimen type for Series I (left) and Series IV (right)

An additional specimen type was developed for Series I to investigate thaumasite formation under application of pressure. In the case of Series IV specimens the thaumasite formed under the pressure due to 100mm of clay at the interface between concrete and clay and in these specimens the thaumasite remained on the surface of the specimen whereas on the initial Series I "Needle"-specimens where no pressure was available the thaumasite became detached from the surface of the specimen. The Series I, Stage 2 specimen applied a pressure to the concrete surface during thaumasite formation, this type of specimen is illustrated in Figure 3.2 and Figure 3.3.
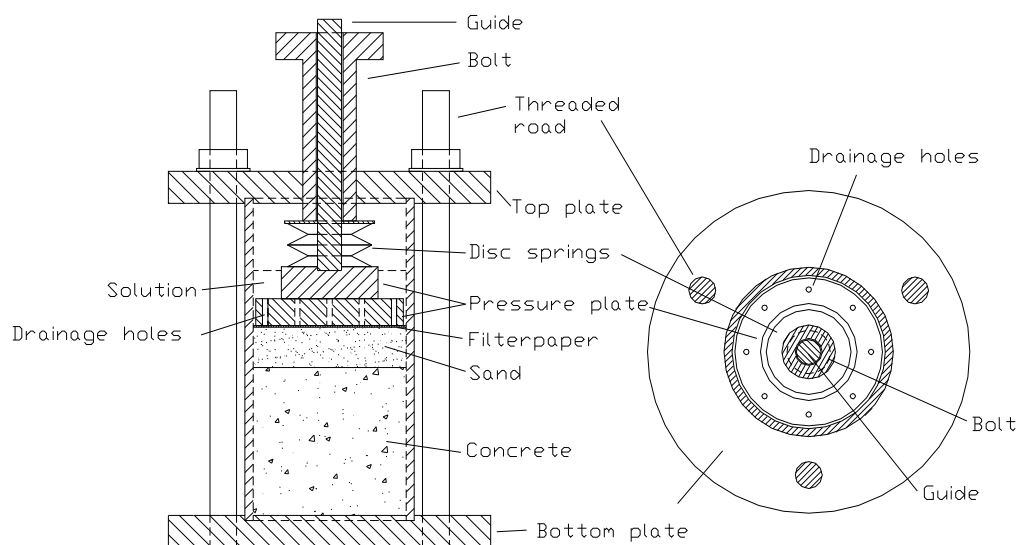
Figure 3.2 - Series specimen with pressure application frame

Figure 3.3 - Specimen with pressure application

The dimensions of the Series I, Stage 2 specimen are the same as Stage 1. These specimens were filled with concrete (Mix 3 and 5) to a height of about 60mm. On top of the concrete was a layer of quartz sand of 15-20mm. The purpose of the sand was to distribute the force from the reaction frame to the top of the concrete. Quartz sand was chosen as it is inert as a source for thaumasite formation. The Series I, Stage 2 specimens were divided into two sub-types the first one does not have a physical barrier to stop thaumasite penetrating in the sand and the second does. The pressure frame simulates a height of soil (γ=20kN/m³) on top of the concrete of 3.5 metres. This value is in accordance with the maximum applied load on the Series V specimens. The pressure is transferred to the surface using an arrangement of disc springs which are loaded with the travel of a bolt in the reaction frame. A schematic drawing is shown in Figure 3.2 and all variables are summarised in the table below. 1.8% sulfate solution, as magnesium sulfate, was used as the aggressive solution.

The methods used for the determination of the identification of thaumasite and determination of its progress were X-ray diffraction, polarisation microscopy, described in Section 3.2.6 and 3.2.7, respectively, and a "Needle-test", developed as part of this test programme and described in Section 3.2.1.

Table 3.3: Variables of Series I & II specimens

	"Needle"- specimen, Stage 1	Pressure specimens, Stage 2	"Needle"- specimen, Stage 2 (see 3.1.2.2)
Variables:	- 5 mixes - Precast - 1.8 % SO_4^{2-}-solution and 1.8 % SO_4^{2-} + 370 $mgCO_3^{2-}/l$ –solution	- 2 mixes (most reactive mixes: 3, 5) - Precast/cast in-situ - Pressure of 3.5m soil - 1.8 % SO_4^{2-}-solution	- 2 mixes (most reactive mixes: 3, 5) - Cast in-situ - 1.8% SO_4^{2-}-solution
Aims:	- Th.-progress – PC face - XRD - Microscopy	- Attached thaumasite - XRD - Microscopy	- Th.-progress – CS face - XRD - Microscopy

3.1.2.2   Series II

The aim of Series II was the investigation of the effect of the casting position on thaumasite formation. Two different methods of casting were investigated; casting methods chosen are similar to those used by BRE at the Shipston-on-Stour field trial [80]. The first, is designated precast (PC) and was designed to represent the case where concrete is precast (i.e. precast pile manufacturing) or cast against shuttering which is then stripped and backfilled, in this case the concrete was cast in the moulds, cured and, after a curing time of 28 days, backfilled with the weathered clay. The method of curing was based on the seal curing method found by BRE [2, 80, 108] to be the most effective type of curing for the development of TSA. Seal curing is described in Section 2.5.6. The specimen types used in this study meant that it was not possible to achieve the full seal and cling film was placed around the specimen as shown in Figure 3.4. It can be seen for this figure that the precast concrete surface is in contact with air, hence, carbonation can occur; this would not be the case had the specimens been fully seal cured. However, seal curing was achieved for the specimens cast in-situ where concrete was cast against cling film.
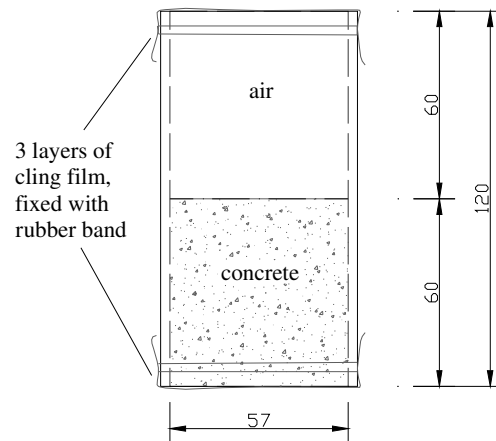
Figure 3.4 - Principal curing arrangement of Series I specimens

The second method of casting involved placing the clay first and casting the concrete directly against it. This method has been called cast in-situ (CS) and models the direct casting of foundations or other structural elements in the field. It should be noted that the clay against which the concrete in the in-situ specimens was cast not undisturbed but had been taken from a stockpile of weathered material and then placed into the mould and compacted in three layers. In the in-situ specimens the bottom cast face is in contact with the clay whereas in the pre-cast specimens the backfill clay is placed against the top cast face. Figure 3.5 illustrates the casting faces.
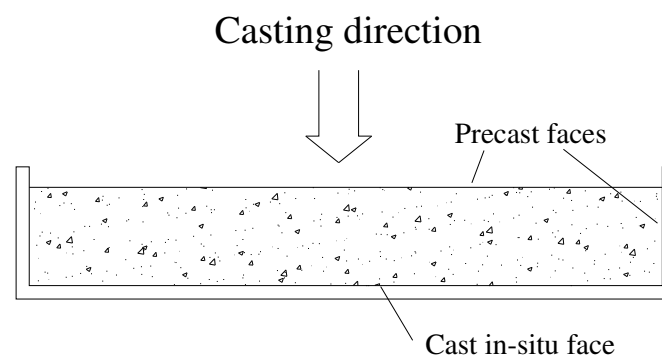
Figure 3.5 - Casting surfaces

The effect of casting position was investigated in all specimen types; it was however a main variable in Series II where the deterioration of the concrete surface was measured for specimens immersed in either a sulfate or a combined carbonate-sulfate solution, see

Table 3.4. The effects of casting position on the deterioration progress were determined using the needle apparatus described in Section 3.2.1; however, the sharp separated deterioration zones as described in the report of the Thaumasite Expert Group [1] and from other authors [21, 27, 38, 42, 56, 68] were detected using polarisation microscopy. Additionally on Series II, Stage 2 – pressure specimens (Table 3.3) these effects of application of pressure on thaumasite formation were observed visually via polarisation microscopy.

Table 3.4: Variables for Series II, Stage 1 – Effects of casting position

Concrete Mix	Sulfate solution		Carbonate-sulfate solution	
	Pre-cast	In-situ	Pre-cast	In-situ
1 (290-0.55)	x	x	x	-
2 (290-0.65)	x	x	x	-
3 (290-0.75)	x	x	x	-
4 (320-0.55)	x	x	x	-
5 (320-0.75)	x	x	x	-

3.1.2.3   Series III

The aim of Series III was the investigation of the exchange of sulfate- and carbonate-ions between solution and concrete. Samples in this series were concrete immersed in either; sulfate, carbonate-sulfate or distilled water solutions. Additionally, the solubility of the limestone aggregate in distilled water was examined in order to determine its yield as a carbonate source.

It was initially intended that the Series I specimens would be used for the determination of carbonate and sulfate exchange. After the first run of tests, however, it was realised that the small cylindrical specimen was not suitable for this test. The results showed an uptake of sulfate of nearly zero and to the trend of consumption contradictory to that expected. The reason for these results is the ratio of volume of solution to the concrete surface area in contact with solution, the ratio is about 7-8 litres to 16x25.5cm² which translates to 17-20 ml/cm². On the one hand this ratio is satisfactory for a constant high source of sulfate and carbonate; however, on the other hand it is too high to be able to

achieve meaningful results. The modified specimens used in Series III were cast in quadratic boxes to a height of about 70mm, 'seal cured' for 28 days and then filled up with solution, see Figure 3.6. The cast face has an area of about $125x125mm^2$ and the specimens were cast using the precast and cast in-situ methods. The solution content for this type of specimen was 0.5-0.75 litres and this resulted in a solution/surface area ratio of 3.2-4.8 ml/cm^2. The variables were the same as Series I, i.e. five different mixes and two different solutions, these are summarised in Table 3.5.

Table 3.5: Series III - Variables and aims of "Ion exchange" specimens

	Ion exchange specimens	**Carbonate migration** (3monthly renewal)	**Carbonate migration** (no renewal)
Variables:	- 5 mixes - Precast - Cast in-situ - 1.8 % SO_4^{2-}-solution - 1.8 % SO_4^{2-} + 370 $mgCO_3^{2-}/l$ -solution	- 5 mixes - Precast - H_2O	- 5 mixes - Precast - H_2O
Aims:	- Solution uptake	- Carbonate migration into H_2O	- Carbonate migration into H_2O

After an increase in the amount of carbonate in solution was observed it was decided that additional specimens would be cast to investigate the percentage of soluble carbonate migrating out of the concrete. Specimens used for the carbonate dissolution tests were cast in boxes with an area of about 125x125mm² and only the pre-cast method of casting was used because in the field it is this face that is in contact with the weathered backfill material. Specimens were submerged in distilled water which was either changed every three months or left for the duration of the test. This was to allow comparison of the behaviour of carbon ion exchange between concrete and water.

The last specimen type belonging to this series was used to investigate the solubility of the two aggregate fractions. Aggregate was immersed in distilled water and the solubility of the limestone was determined, without influence of the alkaline environment in the concrete.

Figure 3.6 - Series III specimen

The results of the exchange test were obtained using the Turbidimetric Method [142] for the sulfates and the Total Carbon Analyser for the carbonate content, both these techniques are described in Section 3.2.5. The change of the SO_4^{2-}- and CO_3^{2-}- content was tested and the solution renewed every three months. According to experimental work of the BRE [143] a three monthly replacement of the solution appears to be optimum to maintain a constant high aggressive environment.

3.1.2.4   Series IV

Series IV was designed to provide a link between Series I-III, specimens of which were not in contact with clay, and Series V, where the specimens were designed to allow testing of the shear strength at the clay/concrete interface. Specimens with the same variables as in Series I and II were placed in contact with two different types of clay, one of which was inert and one reactive and immersed in sulfate solution. The aims of Series V and the variables investigated are summarised in Table 3.6. Both the precast and cast in-situ methods described in Section 3.1.2.2 were used for each of the five concrete mixes. Precast specimens were cast, cured for 28 days, then backfilled with clay and immersed in solution. Cast in-situ specimens were cast against the clay, cured for one day and then immersed in solution. The clays used were one sulfate-containing clay, Lower Lias Clay, and one inert clay, English China Clay. Using a sulfate-bearing and a non-sulfate-bearing clay allows investigation of the effect of different reaction mineral supply by the clay which can influence the thaumasite formation. However, all specimens were immersed in sulfate solution. Both clays were placed at their proctor

density and compacted in three layers each receiving 20 blows with a 4.5kg rammer. The proctor test determines the optimum moisture content to achieve the maximum density for a proper soil compaction [144, BS 1377-4:1990]. This is important to prevent soil settlement and provide stability that conforms to field conditions.

Table 3.6: Series IV - Variables and aims of "link" specimens

Variables:	- 5 mixes
	- Precast
	- Cast in-situ
	- Lower Lias Clay (reactive)
	- English China Clay (inert)
	- 1.8 % SO_4^{2-}-solution
Aims:	- XRD
	- Polarisation microscopy

The thaumasite forms under the influence of solution and adjacent clay as in Series V specimens; however, in this case the pressure was due to only 100mm of clay, Figure 3.1. The presence of thaumasite in these specimens was confirmed with X-ray diffraction and polarisation microscopy was used to measure the progress of deterioration, see Section 3.2.6 and 3.2.7, respectively. As thaumasite formed under identical conditions in the Series IV & V specimens, the results of the XRD and polarisation microscopy tests on the Series IV specimens could be used to infer the rate of deterioration on the Series V specimens. It should be noted that it was not possible to take samples from the Series V specimens as they had to remain intact for shear box testing.

3.1.2.5   Series V

The specimens of Series V were used to measure skin friction at the clay/concrete interface; the ultimate aim of the project. For this series a special type of specimen, a square box that fits into the large shear box apparatus, was developed, also see Section 3.2.3. Only three different mixes, 3, 4 and 5 (see Table 3.2 for details) were used in this series. Two of these (3 and 4) correspond to mixes used by BRE in the Shipston-on-Stour field trial [80, 102]. Mix 5 was chosen to facilitate comparison having the same

cement content as Mix 4 and the same water/cement ratio as Mix 3. Two clays were used - a sulfate-bearing Lower Lias Clay and an inert English China Clay all specimens were immersed in magnesium sulfate solution. Series V variables are summarised in Table 3.7. The procedure for placing the clay was the same as that described for Series IV, i.e. the clay was placed at its proctor density and compacted in three layers.

To achieve values for the shear strength and to produce portable boxes, a shear area of $200 \times 200 mm^2$ was chosen. The height of concrete in these specimens was 60mm, on top of which was approximately 100mm of clay, then 50mm of solution. Overall the PVC-box was 230mm high. As Figure 3.7 shows, the box was divided into 3 parts, a lower box (h=50mm), an upper box (h=160mm) and a removable middle part (h=20mm). During the shear box test the middle part of the box was unfastened.

Table 3.7: Variables for Series V shear strength specimens

	Applied Pressure (kN/m^2)			Method of Casting		Clay Type		Storage Solution	
Concrete Mix	**10**	**40**	**70**	**Pre-cast**	**In-situ**	**Lower Lias**	**ECC**	**Sulfate Solution**	**Water**
3 (290-0.75)	x	x	x	x	x	x	x	x	x
4 (320-0.55)	x	x	x	x	x	x	x	x	
5 (320-0.75)	x	x	x		x	x	x	x	

The skin friction tests were performed using a large shear box and the procedure was in accordance with BS 1377-7:1990. The equipment was modified so that failure would be allowed to occur on the weaker of the following planes:

> (i)   at the concrete/thaumasite interface,
>
> (ii)   within the thaumasite,
>
> (iii)   at the soil/thaumasite interface, or
>
> (iv)   within the clay.

This is in contrast to a typical shear test where the failure plane is determined by the interface between the upper and lower parts of the shear box. The removable section was provided so that it was not necessary to demould the whole specimen before the test. This avoided unnecessary disturbance which would influence the result of the shear strength test. The central section of the box was unfastened after the box was fixed in

the test equipment the reason for this and the test method are described fully in Section 3.2.4.
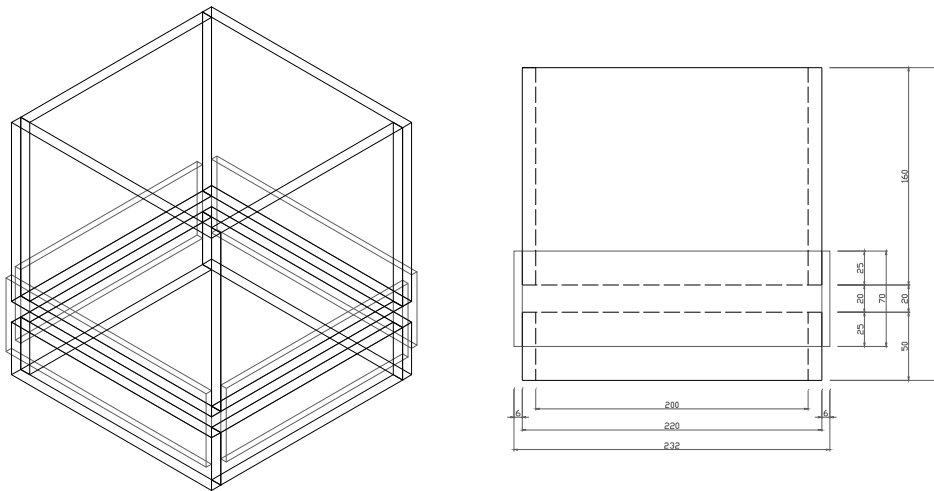
Figure 3.7 - Shear test specimen

To simulate the effect of lateral earth pressure in a foundation it was necessary to develop a method of applying a constant pressure throughout the thaumasite formation period. Assuming a unit weight of $\gamma=20kN/m^3$ three different depths were simulated – 0.5, 2.0 and 3.5 metres, see Table 3.8. The maximum applied pressure was governed by the strength of the test equipment. Pressure was applied to the top surface of the clay using an arrangement of disc springs and a reaction frame where the required pressure was applied by compressing the springs to a required displacement, which could then be adjusted using hollow nut and bolt arrangement. The pressure frame is illustrated in Figure 3.8 and Figure 3.9.

To avoid excessive settlement of the clay after application of the pressure using the disc springs the clay was consolidated, the consolidation procedure is described in Section 3.2.2.

The shear tests, described in Section 3.2.4, were performed 18 months after the load was applied through the pressure frame and in total 27 months after the storage period in the environmental chamber started.
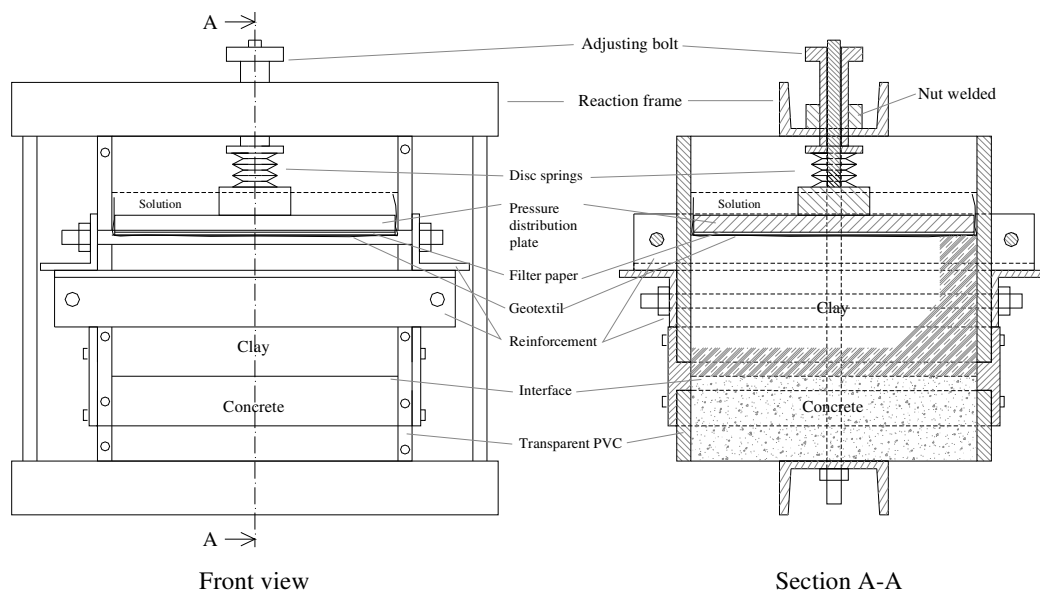
Figure 3.8 - Schematic representation of shear test specimen with pressure frame

Figure 3.9 - Shear test specimen with pressure frame

Table 3.8: Superimposed load on concrete surface

Depth	kN/m^2 = kPa	Load/0.04m^2
0.5 m	10	400 N
2.0 m	40	1600 N
3.5 m	70	2800 N
5.0 m	100	4000 N

3.1.3   Solution

The solutions used in the tests have two different purposes, the first is the simulation of field conditions in laboratory experiments and the second is to cause an acceleration of the reaction processes. The investigation of durability problems in a reasonable period in the laboratory requires the use of highly concentrated solutions since the stronger a solution the more aggressive but the less like the real situation.

Three different types of solutions were used, each relate to the field situation in the fact that they contain both sulfate and carbonate. The concentration used was chosen to be consistent with work undertaken at BRE [20, 40, 63, 82, 143], and hence, facilitate comparison of results. The first solution contains a high amount of sulfate (1.8% SO_4^{2-}), the second solution has a high content of sulfate and carbonate (1.8% SO_4^{2-} and 370 mg CO_3^{2-}) and the third solution was distilled water. The amount of 1.8% SO_4^{2-} as $MgSO_4$ is three times stronger than the maximum for 'Sulfate Class 4m' in BRE Special Digest 1 [96] and the 370 mg/l CO_3^{2-} serve as an additional source of carbonate ions beside the aggregate.

The solutions used in each test series have been described in the preceding sections and are summarised in Table 3.1.

For the production of the sulfate-containing solution, $MgSO_4*7H_2O$, magnesium sulfate hydrate and distilled water were used. The sulfate-carbonate-containing solution contains magnesium sulfate hydrate, $MgSO_4*7H_2O$, sodium hydrogen carbonate, $NaHCO_3$, and distilled water. Required concentrations were achieved as follows:

$$1.8\% \ SO_4^{2-} \quad = \quad 46.17 \ g/l \ MgSO_4*7H_2O$$
$$370 \ mg \ CO_3^{2-}/l \quad = \quad 518 \ mg/l \ NaHCO_3$$

3.1.4   Storage

All specimens were stored in an environmental chamber at a constant temperature of 6°C over a total period of time of between 15 and 27 months. The actual storage time of the main, the Series V – shear test specimens, was governed by the rate of the formation of thaumasite observed at Series IV specimens. The temperature used is in accordance

with the optimum experienced temperature of about 5°C of the formation of thaumasite, see Section 2.6.8.

3.2   Test Methods

3.2.1   Needle Test Rig

The extent of thaumasite formation was measured in two ways. First, the depth of the deterioration was manually measured using the 'Needle-PC/CS' specimens of Series I and II and secondly polarisation microscopy was used to assess the development of thaumasite formation, this is described in Section 3.2.7.

Manual measurement of the depth of attack was performed using a needle test rig where the depth of the deterioration was measured with a needle at nine defined points on the specimen's surface. Formation of thaumasite causes the cement matrix to change into a soft white paste which, in the initial stages, causes the surface of the concrete to heave. The depth of deterioration was determined by pushing the needle into the concrete until solid concrete was reached and measuring the movement relative to a zero measurement describing the distance between template and needle end taken at the start of the investigation period. Illustrations of the test rig are shown in Figure 3.10 to Figure 3.12.
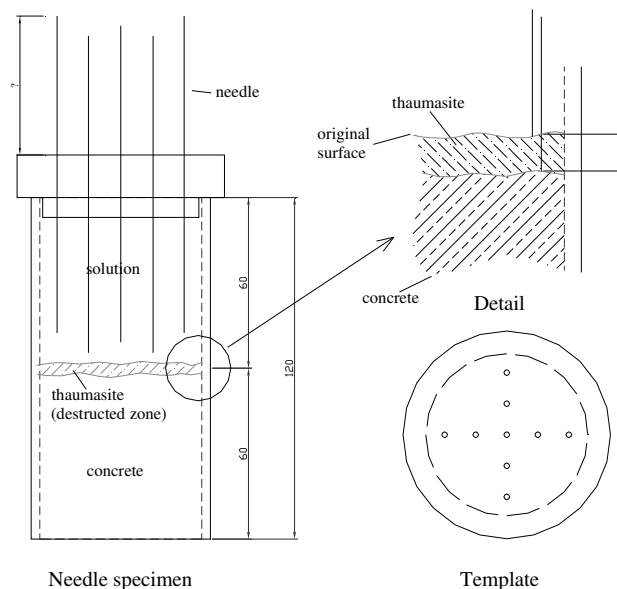
Figure 3.10 - 'Needle'-test apparatus

Figure 3.11 - Needle test specimen
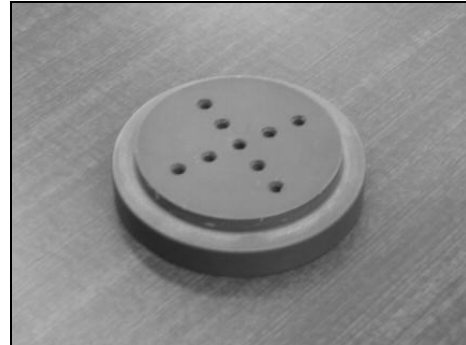
Figure 3.12 - Needle template

3.2.2   Consolidation of Clay

Before application of the long term pressure it was necessary to consolidate the specimens to avoid excessive settlement. The specimens were loaded with an initial weight of 80N for 12 hours and this was followed by a doubling the weight every 12 hours until the required pressure was achieved. The consolidation programme for each of the three final pressures is shown in Table 3.9 and the rig is illustrated in Figure 3.13. The applied consolidation loads (Table 3.9) are 80N less than the interface pressures presented in Table 3.8. This is because the pressure at the interface includes pressure due to the 100mm deep clay.

Table 3.9: Consolidation program of Series V-specimens for clay area of 200x200mm^2

Load [N]			Time [h]	Total time [h]
10kPa (0.5m)	40kPa (2.0m)	70kPa (3.5m)		
80	80	80	12	12
160	160	160	12	24
320	320	320	12	36
	640	640	12	48
	1520	1280	12	60
		2720	12	72

Figure 3.13 - Consolidation rig

Figure 3.14 - Disc spring arrangement

3.2.3   Pressure Rig

The pressure rig applied to Series V – specimens consists of two channels connected by threaded bar. The frame provides a reaction to compressed disc springs which are used to apply a pressure to the top surface of the specimen. The disc spring arrangement is illustrated in Figure 3.8 and Figure 3.14. A 12mm thick PVC-plate was used to distribute the load over the surface of the clay. The pressure plate distributed the load equally over the clay and was located over a layer of geotextile and filter paper which were directly on top of the clay. A system of drainage holes were provided in the pressure plate to allow the pore water to drain off and, hence, the pore water pressure to decrease to zero during every step of the consolidation. Drainage holes were also required to maintain the supply of aggressive solution at the concrete/clay interface. For the different pressures three kinds of stainless disc springs (Belleville Washer) were used in their optimum loading range and arranged in series which means that, for any given applied force the total deflection is the sum of that for each individual spring [145]. Disc springs were chosen in order to maintain pressure on the sample and to have the possibility of readjusting the load and monitoring the effects of settlement and creep in the clay of the mould and heave caused by thaumasite expansion.

Table 3.10: Disc spring types - Belleville Washer [145]

Disc spring type		
0.4m = 320N	1.9m = 1520N	3.4m = 2720N
S31516308	S315163175	S3551832

3.2.4   Shear Strength

The determination of the shear strength was performed with the direct shear test according to BS 1377-7:1990 using a modified large shear box apparatus. In the following paragraphs the preparation of specimen, the installation in the shear box and the shear test are described in detail.

3.2.4.1   Preparation of Specimen for Installation in Shear Box

The first step during the preparation was that each test specimen was removed from the environmental chamber 12 hours before the test was started to acclimatise the sample to ambient temperature. After the pressure frame was removed, each side of the central section (described in Section 3.1.2.5) was opened separately and prepared so that the lower box could slide without experiencing additional friction other than the interface friction as illustrated in Figure 3.15. The stages of specimen preparation are illustrated and described in Table 3.11.
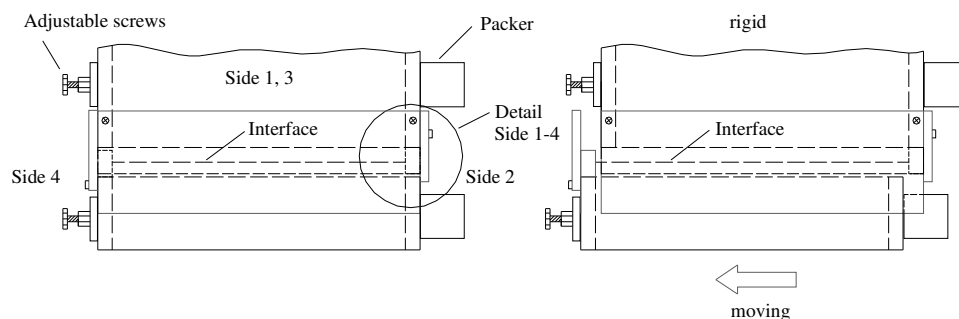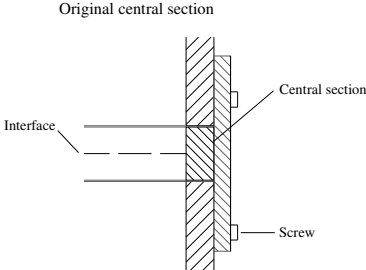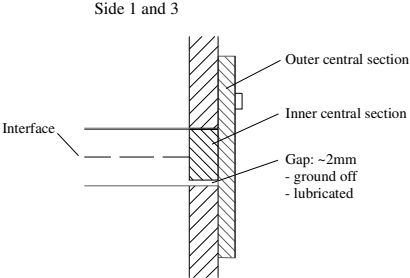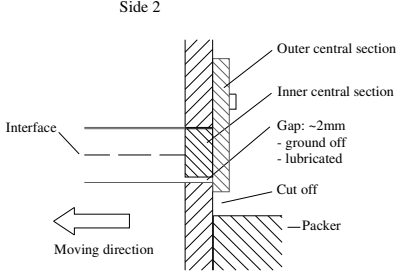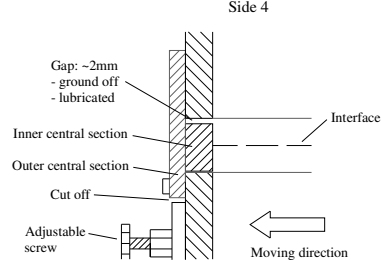
Figure 3.15 - Mould movement, Details see Table 3.11

Table 3.11: Steps of shear box specimen preparation

Original central section Interface —— Central section Screw	**Starting point** of the preparation method for each side, Detail refers to Figure 3.15
Side 1 and 3 Interface Outer central section Inner central section Gap: ~2mm - ground off - lubricated	**Step 1:** - Unfasten the screws of Side 1 and 3, respectively, and remove central sections - Grind off 2mm of the inner central section at the bottom face - Lubricating the gap and the face towards the clay - Insert and refasten Side 1 and 3 of central section
Side 2 Interface Outer central section Inner central section Gap: ~2mm - ground off - lubricated Cut off Moving direction Packer	**Step 2:** - Unfasten/remove Side 2 - Grinding off 2mm of the inner central section at the bottom face - Cutting off the outer part of the central section due to the dimension of the packer - Lubricating the gap and the face towards the clay - Insert/refasten
Side 4 Gap: ~2mm - ground off - lubricated Inner central section Outer central section Cut off Adjustable screw Interface Moving direction	**Step 3:** - Unfasten/remove Side 4 - Grinding off 2mm of the inner central section at the upper face - Cutting off the outer part of the central section due to the dimension of the adjustable screw system - Lubricating the gap and the face towards the clay - Insert/refasten

3.2.4.2   Installation in Shear Box

After preparation was completed the specimen was moved to the shear box and fixed in the centre with packers on one side and an adjustable screw system on the opposite side, see Figure 3.16. The two sides parallel to the shear direction were held in position with wooden wedges so that expansion/creep of the box was prevented.

Before the test was started the screws of the middle part at the lower box were removed to allow the top and bottom boxes to move relative to each other and while still providing some restraint against lateral expansion of the clay, see Figure 3.15, due to the application of normal load and when the test was in progress.

At the end of the installation process the pressure frame of the shear box apparatus was applied and adjusted to the required load. Additionally two LVDT displacement transducers were installed to measure the horizontal movement of the specimen and the vertical settlement of the clay.
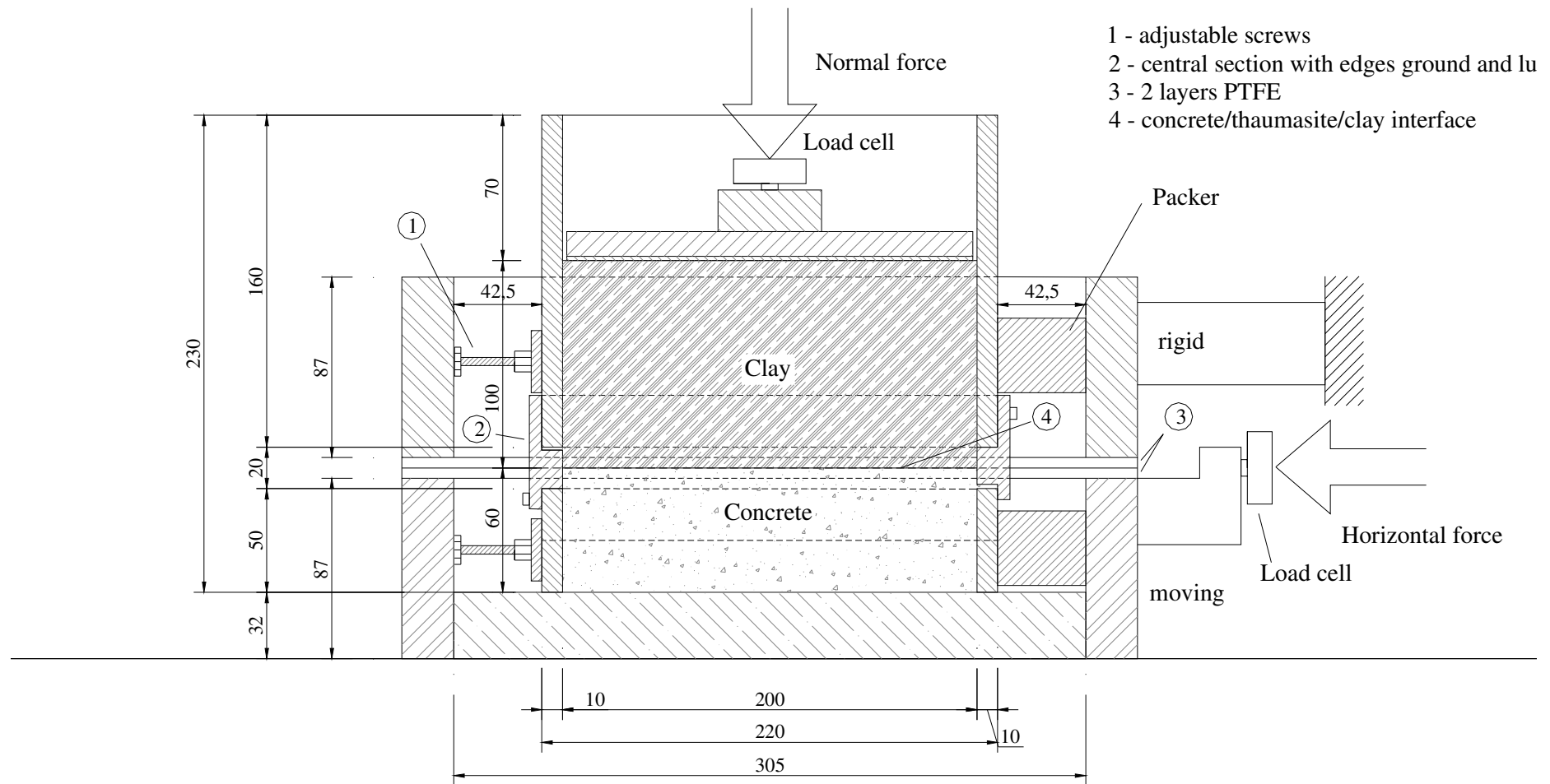
Figure 3.16 - Schematic representation of shear box with specimen [mm]

3.2.4.3   Shear Test

Before the main shear test was started the specimen was allowed to re-consolidate for an hour. This was necessary to reduce the effects of rebound of the clay and the increase in pore water pressure that occurred after removal of the pressure frame. Reconsolidation and reduction of pore pressure was assumed to be completed within an hour in order to obtain 'consolidated drained' conditions [111] where pore pressure has to be reduced to zero before test can start. However, the pore pressure was not measured.

A second parameter for this condition is that the test has to be performed very slowly to avoid development of new pore pressure. However, the test had to be completed in reasonable time and therefore a rate of 0.041402mm/min was chosen this corresponds to a displacement of 15mm in about 6 hours excluding the one hour for re-consolidation. The testing rate varied by about ±5%. Preliminary tests at different rates of 0.017018 and 0.041402mm/min were undertaken to determine the effect of rate on shear strength. During these tests it was observed that there was a slight difference in the peak shear strength as shown in Figure 3.17; however, the residual shear strength was the same for both rates, this is illustrated in Figure 3.18.
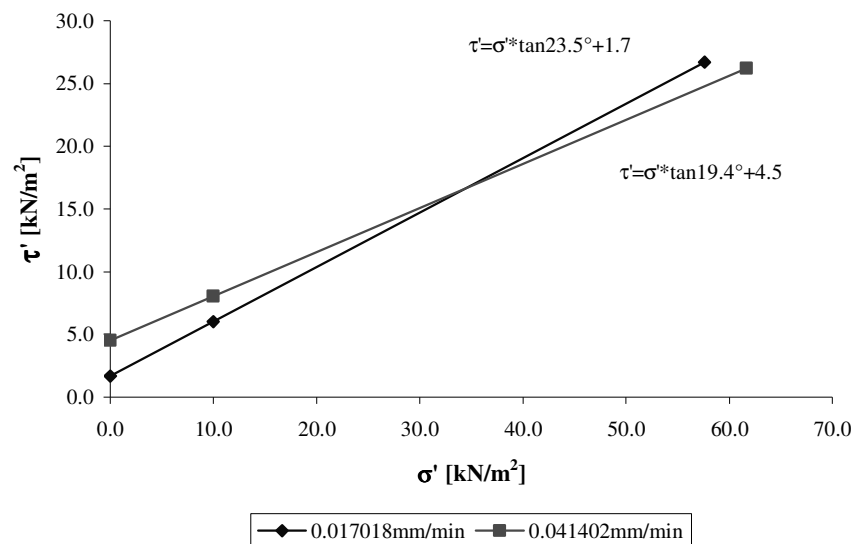
Figure 3.17 - Peak shear strength of trial tests with different rates
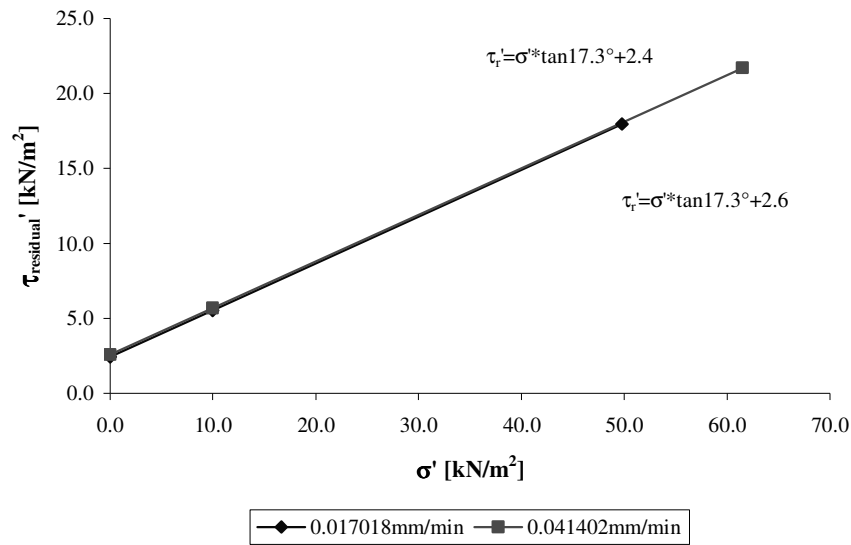
Figure 3.18 - Residual shear strength of trial tests with different rates

3.2.5 Chemical Tests

3.2.5.1 Introduction

The determination of the exchange of the SO_4^{2-}- and CO_3^{2-}- ions was performed at Series III, ion exchange samples every three months. The change of the sulfate content of the solution was measured using the Turbidimetric Method described in Section 3.2.5.2 [142] with a Hach 2100N Turbidimeter and the change of the carbonate content was determined with a Total Carbon Analyser TOC-5050 with auto sampler ASI-5000A, see Section 3.2.5.3. Additionally, the pH of the Series III exchange samples and clay adjacent to the interface in Series V specimens was measured with the Electrometric method described in Section 3.2.5.4 using a pH-meter with an accuracy of 0.01.

3.2.5.2 Sulfate Content

The principle of the Turbidimetric Method [142] is that sulfate ions (SO_4^{2-}) precipitate in an acetic acid medium with barium chloride ($BaCl_2$) and form barium sulfate ($BaSO_4$) crystals of uniform size. The light absorbance of the barium sulfate suspension

is measured by a photometer and the sulfate ion concentration is determined by comparison of the reading with a standard curve.

3.2.5.3   Carbonate Content

The principle of the carbon analyzer [146] is that: Non-purgable organic carbon (NPOC) is measured by acidifying samples to a pH less than 2.0 and sparging with CO_2 free air. A combustion/non-dispersive infrared gas analysis method is employed. High purity carrier gas, moistened by a humidifier, flows at a rate of 150 ml/min. The sample is injected into a TC (Total Carbon) combustion tube, which has been filled with oxidation catalyst and heated to 680^oC. The sample is combusted or decomposed to CO_2. The combustion product is sent through an IC reaction vessel, cooled, dried by a dehumidifier and then sent through a halogen scrubber. The NPOC component is detected for CO_2 in a non-dispersive infrared gas analyzer (NDIR). The peak area count is proportional to the NPOC concentration of the sample.

3.2.5.4   pH-Value

The pH-value of Series III solutions and Series V clay samples was measured with the electrometric method according to BS 1377-3:1990. The samples of Series III were measured immediately with an electrode after the solution was changed; however, the samples of the clay at five different depths from the interface had to be prepared before being tested. Samples were dried at 105°C and then extracted to 2.5:1 with distilled water and allowed to homogenize for at least 8 hours but preferably 24 hours in a homogenizer. The pH meter was calibrated using standard buffer solutions.
In addition to pH, the water content was also obtained at five different depths. The depths correspond to the mean of the clay zone from 0-10mm, 10-20mm, 20-30mm, 30-40mm and 40-50mm from the interface.

3.2.6   X-ray Diffraction Analysis

The mineralogical composition of deteriorated concrete samples was performed using the Siemens D5000 powder X-ray diffractometer which is a transmission instrument,

allowing very high resolution to be obtained, and is equipped with a position sensitive detector, allowing rapid data collection. Therefore it can be used for rapid 'fingerprinting' identification and characterization of the crystalline phases [147]. A semi-quantitative analysis of the reaction products determined was carried out using the software program 'DIFFRAC^{plus} EVA'.

This kind of characterisation method forms an effective tool in conjunction with polarisation microscopy for the unambiguous identification of thaumasite and ettringite, the two most common reaction products of sulfate attack. However, XRD-analysis can be problematic if reaction products are not present in sufficient quantities [68] or sampling was not representative of the distribution of the actual reaction products. Therefore sampling is a very important part of the analysis and has been discussed in Section 2.4.5.

A new specimen was used for each XRD analysis. The method used to collect the material for testing depended on the level of deterioration of the specimen. Where there was no loose or soft material, the surface of the specimen was scraped to obtain samples for analysis otherwise the loose detached material was collected. To obtain a representative distribution of the reaction products as much deteriorated material as available, however, more than 1 g, was collected and prepared for analysis, i.e. all the collected material was dried at room temperature, this was done in order to prevent temperature influenced structural changes of the compounds present, ground to less than 50μm, homogenized and then about 1g of material was analysed.

Analyses were performed on the initial Series I, II and IV specimens after 9, 15 and 21 months immersed in solution and on the additional Series I and II specimens after 9, 12 and 15 months.

3.2.7   Microscopy

The petrographic analysis was performed using a polarisation microscope at the Building Research Establishment (BRE). This represents probably the most versatile and cost effective technique for analysing sulfate attack damaged concrete samples [68]. Thin sections of about 20μm thickness from the damaged concrete produced show the distribution of the deterioration such as micro-crack development and changes in porosity. However, the distinction between the crystallographic characteristics of

thaumasite and ettringite is not possible because of their quite similar habit and density and that means that the detection and proof of thaumasite must be done by X-ray diffraction or electron microscopy (REM/ESEM) [43].

Specimens for the production of thin sections were demoulded and then dried slowly at room temperature in order to avoid the formation of drying induced microcracks and structural changes in the reaction products. After drying the samples were vacuum impregnated with a blue resin and thin sections of an area of 15x45mm^2 were produced. Sampling is as abovementioned a very important part as the thaumasite reaction starts at the surface, sampling is described in Section 2.4.5.

Clay adjacent to the interface was included when sampling from the Series IV specimens. The aim of this was to determine any progress of the thaumasite into the clay.

3.3   Materials

3.3.1   Concrete

Five different concrete mixes with two different cement contents (290 kg/m^3 and 320 kg/m^3) and three different water to cement (w/c)-ratios (0.55; 0.65; 0.75) are used, see Section 3.1.2 Table 3.1.

The mixes were designed according to BRE Report 'Design of normal concrete mixes' [148]. Before each mix the determination of the moisture content of the aggregates and the subsequent re-calculation of the aggregate parts was necessary. The batch was homogenized using a mechanical mixer followed by casting in the moulds in three layers and compacting each time using a vibrating table or small poker vibrator. The compaction of the specimens was performed until the surface became smooth and glazed. In order to check the composition of the batch, slump and density of the fresh concrete were determined according to BS 1881-102:1983. The compressive strength test according to BS 1881-116:1983, was chosen to obtain quality properties of each mix cast on different dates. A summary of the properties of the fresh and hardened concrete are shown in Appendix A: Table A-1.

All precast specimens were 'seal' cured under the given conditions (see Section 3.1.2.2) for a period of 27 days at 20 ± 2 °C after the fresh specimens were covered with polythene for the initial 24 hours. The seal curing method used by BRE is described in detail in Section 2.6.6.

3.3.1.1   Cement

The cement type used was a Portland Cement (PC) CEM I 42.5N with a C_3A content of about 8% and supplied by Lafarge from their Caldon works. Despite it was the same type of cement the chemical composition of the two charges differed in the concentration of the clinker phases. The chemical composition of the cement according to in-plant sources [149] can be found in Table 3.12. The clinker phases of the second cement charge were calculated according to the Bogue method [28].

Series I and II, Stage 1, and Series IV and V specimens were produced with the first charge of cement (Feb 2004). Series I and II, Stage 2 and Series III specimens were produced with the second cement charge (Jan 2005).

Table 3.12: Chemical composition of PC CEM I 42.5N [149]

PC CEM I 42.5N	Cement Oxidic Composition Charge: 03.02.2004	Cement Oxidic Composition Charge: 06.01.2005
SiO_2	19.41	19
Al_2O_3	5.04	5
Fe_2O_3	2.98	3
CaO	62.9	63
MgO	1.47	1.2
SO_3	3.20	3.1
K_2O	0.74	
Na_2O	0.12	
Eq Na_2O	0.61	0.61
Cl	0.023	0.033
C_3S	56.01	63
C_2S	13.39	6
C_3A	8.31	7
C_4AF	9.07	10

3.3.1.2   Aggregate

For the required carbonate-containing aggregate, Jurassic Oolitic limestone was used, in two fractions 0-4 mm and 4-20 mm. The limestone was supplied by Gill Mill Quarry in Ducklington, Oxfordshire. The aggregate fractions were graded according to BS 812-103:1985, the results are shown in Table 3.13. The absorbed water content of the limestone is 3.5% for both fractions.

Table 3.13: Sieve analysis Jurassic Oolitic limestone

Size [mm]	0-4 %-Passing	4-20 %-Passing
20		100
14		79
10		49
5	100	3
2.36	78	1
1.18	56	
0.6	39	
0.3	15	
0.15	4	
0.075	2	
0	0	

3.3.1.3   Water

The water used for the concrete mixes was ordinary tap water and the water for mixing the reaction solutions was distilled water (H_2O).

3.3.2   Clay

Two types of clay were used for the experiments, one inert clay, an English China Clay (ECC) and one sulfate-bearing clay, a Lower Lias Clay. The Lower Lias Clay was collected from a stockpile at the Moreton Valence trial site (Figure 3.19) used by BRE close to the M5. This clay was excavated in July 2001 and is currently stockpiled for oxidation of the containing sulfide minerals. According to BRE investigations the

Lower Lias Clay was classified as Sulfate Class of 2-3 and the sulfate content is 2.03 – 2.45 g SO_4^{2-}/l. The values relate to the date of sampling and collection, respectively, in June 2004, two months before starting the experiments, i.e. before immersing the specimens into sulfate solution.

Figure 3.19 - Stockpile (left) and collection pit (right) of LLC at Moreton Valence [150]
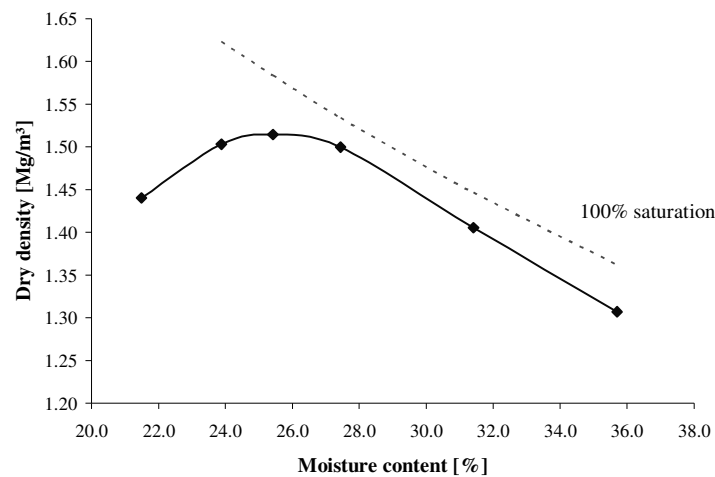
Figure 3.20 - Dry density/moisture content relationship - English China Clay
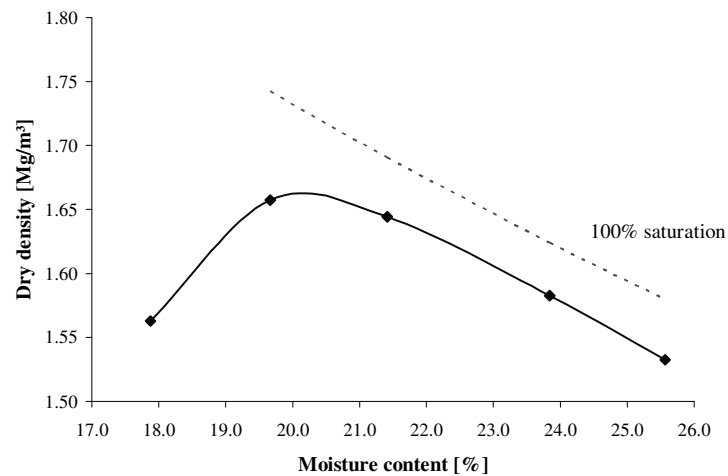
Figure 3.21 - Dry density/moisture content relationship – Lower Lias Clay

Characteristic properties of the clays used such as proctor density according to BS 1377-4:1990 is represented in Figure 3.20 and Figure 3.21. A brief chemical specification of the used Lower Lias Clay, performed by TES Bretby [150], is shown in Table 3.14 and the detailed specification is shown in Appendix A: Table A-2. The main properties are summarized in Table 3.15.

Table 3.14: Chemical specification of Lower Lias Clay

Sample / Depth	Mean Depth	Water soluble sulfates [WS]	Sulfate Class (WS re SD1[96])	pH
[m]	*[m]*	$[SO_4^{2-}\ g/l]$		
0.0 – 0.1	0.05	2.030	2	7.7
0.2 – 0.3	0.25	2.170	2	7.8
0.4 – 0.5	0.45	2.240	2	7.8
0.6 – 0.7	0.65	2.380	3	7.8
0.8 – 0.9	0.85	2.450	3	7.8

Table 3.15: Properties of clay

Type of soil	English China Clay Puraflo 50 [151]		Lower Lias Clay (BGS [152]+Lab+[27])	
Properties				
Particle size distribution	>0.02mm	1%	>2.0mm (gravel)	4%
	0.02-0.01mm	5%	2.0-0.06mm (sand)	10%
	0.01-0.005mm	18%	0.06-0.002mm (silt)	41%
	0.005-0.002mm	27%	<0.002mm (clay)	45%
	0.002-0.001mm	12%		
	<0.001mm	37%		
Mineralogical composition (XRD)	Kaolinite	64%	Kaolinite	
	Potash Mica	24%	Chlorite	
	Soda Mica	2%	Illite/mica	
	Quartz	6%	Orthoclase feldspar	
			Albite feldspar	
Optimum moisture content	25.4%		20.2%	
Maximum dry density	1510 kg/m^3		1660 kg/m^3	
ϕ'	18.1°		21.7°	
c'	12.3 kN/m^2		22.8 kN/m^2	
pH	5.4		7.7	

The percentage determination of the mineralogical composition of the Lower Lias Clay was difficult using XRD, however, the minerals present in the LLC were obtained from BGS [152] and the Halcrow Group [27]. A BGS borehole was close to the trial site and the Halcrow Group performed soil investigation after the investigation of TSA along the M5 motorway.

The particle size distribution of the inert and artificial English China Clay [151] and the reactive natural Lower Lias Clay [27] is illustrated in Figure 3.22. The ECC is a very fine grained clay whereby the natural LLC has a wider coarser particle size distribution.
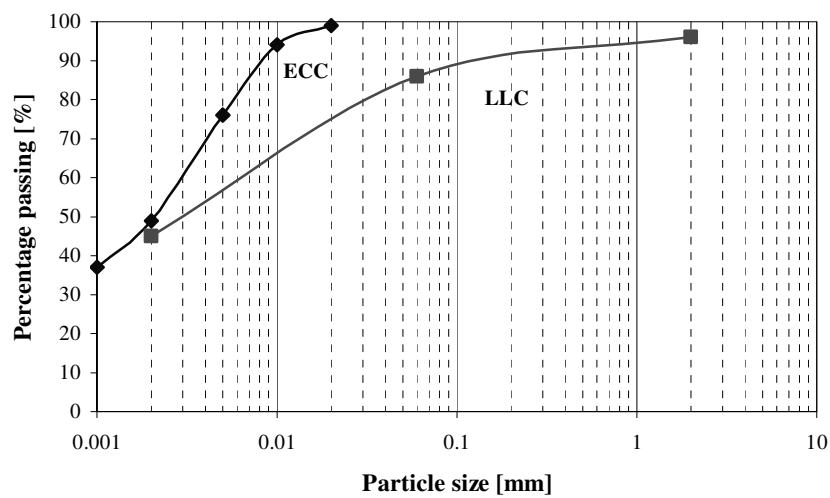
Figure 3.22 - Particle size distribution of LLC [27] and ECC [151]

3.3.3   Chemicals

Specimens where deterioration was desired were immersed in either a solution with 1.8% SO_4^{2-}/l or a combined sulfate-carbonate solution, 1.8% SO_4^{2-}/l + 370 mg CO_3^{2-}/l. Magnesium sulfate hydrate, $MgSO_4*7H_2O$, and sodium hydrogen carbonate, $NaHCO_3$, were used as the source of sulfate and carbonate, which were supplied by Fisher Scientific.

4.   Results and Discussion of TSA Acceleration

This chapter describes the results of the acceleration of the thaumasite form of sulfate attack performed on Series I, II and III specimens with several variables. Different concrete properties subjected to a variety of conditions were investigated in these different series. The results presented include properties of the concrete used, an estimation of the progress of TSA under unrestrained and restrained conditions as well as chemical interactions between concrete and solution.

The results of the interface investigations, such as the determination of the shear strength parameter, that were performed on Series IV and V specimens are described in Chapter 5.

4.1   Concrete Properties

The compressive strength test according to BS 1881-116:1983 was chosen to obtain the 28 day strength of each mix. The differences of the compressive strength within one designed mix regime were attributed mainly to variations in the aggregate moisture content despite that fact that aggregate moisture contents were measured and adjustments made at the time of mixing. Additionally, the cement came from two different batches, see Table 3.11. The compressive strengths and standard deviations of the mixes used in all series are given in Table 4.1, Table 4.2 and Table 4.3.

The compressive strength and standard deviation were calculated from a series of three cubes with an age of 28 days.

Table 4.1: Compressive strength and standard deviation of concrete used with cement batch I

Mix* c w/c	Series I, II, IV – precast		Series IV – cast in-situ	
	Compressive strength (f_{cu}) $[N/mm^2]$	Standard Deviation $[N/mm^2]$	Compressive strength (f_{cu}) $[N/mm^2]$	Standard Deviation $[N/mm^2]$
1 290 0.55	46.1	0.61	39.2	1.81
2 290 0.65	37.0	1.21	33.0	1.25
3 290 0.75	27.9	0.44	23.7	0.68
4 320 0.55	44.0	1.57	48.0	1.36
5 320 0.75	25.2	1.05	22.5	0.67
	Series V – shear test specimen – precast		Series V – shear test specimen – cast in-situ	
3 290 0.75	24.0	0.63	29.4	0.86
4 320 0.55	41.2	0.60	50.0	0.52
5 320 0.75			21.4	1.15

*c: cement content [kg/m³], w/c: water/cement ratio

Table 4.2: Compressive strength and standard deviation of concrete used with cement batch II

Mix* c w/c	Series I, II – cast in-situ[+], Series I – pressure[+], Series III – solution uptake		Series III – carbonate migration	
	Compressive strength (f_{cu}) $[N/mm^2]$	Standard Deviation $[N/mm^2]$	Compressive strength (f_{cu}) $[N/mm^2]$	Standard Deviation $[N/mm^2]$
1 290 0.55	41.6	0.87	36.4	0.27
2 290 0.65	31.2	0.79	26.5	0.42
3 290 0.75	23.0	1.25	20.3	1.42
4 320 0.55	41.1	0.47	38.8	0.20
5 320 0.75	20.4	0.90	20.4	0.61

* c: cement content [kg/m³], w/c: water/cement ratio; [+]Mixes 3, 5 only used

Table 4.3: Average strength and standard deviation of mixes

	Mix 1 *(290-0.55)*	**Mix 2** *(290-0.65)*	**Mix 3** *(290-0.75)*	**Mix 4** *(320-0.55)*	**Mix 5** *(320-0.75)*
Average strength [N/mm²]	40.8	31.9	24.7	43.8	22.0
Standard deviation [N/mm²]	3.8	4.0	3.3	4.2	2.0

4.2   Thaumasite Progress

4.2.1   Effect of the Concrete Mix

4.2.1.1   Deterioration Measurement

The main focus of this part of the investigation was the effect of the cement content and the water/cement ratio on the rate of progress of TSA. An increase in cement content and a decrease of the water/cement ratio results in a denser concrete. This would be expected to improve the resistance to TSA as for instance concluded by the TEG [1] and so it was expected that the higher w/c specimens would show more deterioration. However, the permeability of the concrete was not tested.

The test specimens used for this part of the investigation were the cylindrical Series I specimens consisting of only concrete and aggressive solution. These and the methodology adopted are described in more detail in Section 3.1.2.1.
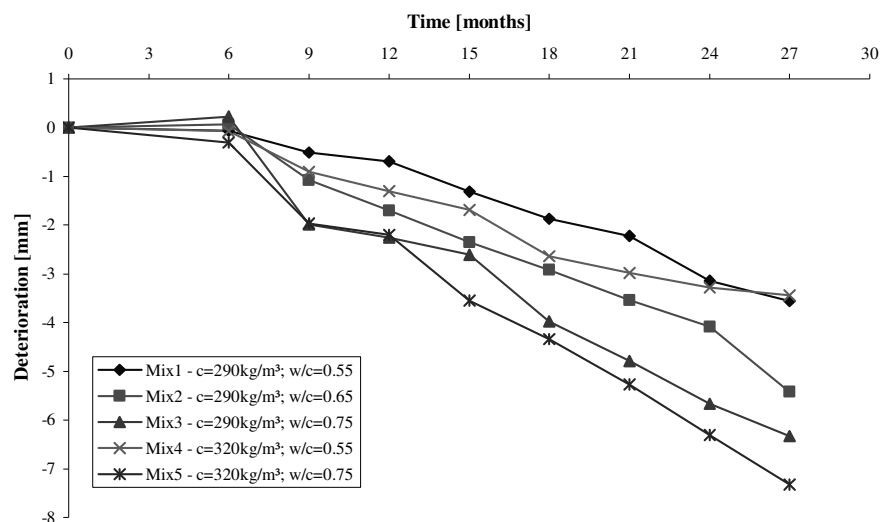
Figure 4.1 - Thaumasite progress in 1.8% sulfate solution depending on mix design

Figure 4.1 shows the deterioration due to the progress of the thaumasite formation on precast specimens depending on cement content and water/cement ratio over a period of 27 months immersed in a 1.8% SO_4-solution and stored in an environmental chamber at 6°C. The measurements made using the needle test describe the pure structural effects of the deterioration caused by TSA because the actual loss of cement matrix is measured. This corresponds to Zone 3 and 4 as described by Sibbick et al. [38, 54], and discussed in Section 2.2.2.2. From the figure it can be seen that after an initial period of six months of very little activity a linear trend of deterioration was observed. This was analysed using linear regression for all mixes and the results of this are reported in Table 4.4. This dormant period of six months was also observed by Crammond and Nixon [40] in TSA laboratory investigations. Monteiro [58] also observed dormant periods during sulfate attack in specimens with low water-cement ratio which could last up to 15 years.

It is suggested that expansion forces caused by TSA were less than the internal tensile strength of the concrete during the initial period of little activity. During this period TSA occurred under a small layer of surface concrete which was identified as a carbonated 'sound' concrete crust. This is discussed in more detail in Section 4.2.1.2. After the internal TSA expansion forces exceeded the concrete tensile strength the cement matrix started to disintegrate from beneath the surface inwards.

Table 4.4: Progress of deterioration of precast mixes in 1.8% SO_4-solution

Mix	Deterioration progress		Correlation coefficient R^2
	[mm/month]	*[mm/year]*	
1 (290-0.55)	0.18	2.1	0.9824
2 (290-0.65)	0.23	2.7	0.9797
3 (290-0.75)	0.26	3.1	0.9721
4 (320-0.55)	0.15	1.8	0.9591
5 (320-0.75)	0.31	3.7	0.9889

In the majority of cases the relationship between cement content, water/cement ratio and deterioration due to TSA was as expected with both reduction in w/c-ratio and increase in cement content resulting in an increase in resistance to TSA. The exception to this was concretes with a water-cement ratio of 0.75 where the concrete with the higher

cement content was found to have a lower resistance than that with the low cement content. It is suggested that this phenomenon is caused by the increased porosity, i.e. the increase in cement to aggregate ratio caused by increasing the cement content at a given w/c-ratio results in a relative increase in the area of cement paste in the concrete and, hence, an increased susceptible surface. However, the opposite effect which is important for structural engineering that high quality concretes are less susceptible is confirmed based on the trend of the graphs in Figure 4.2.
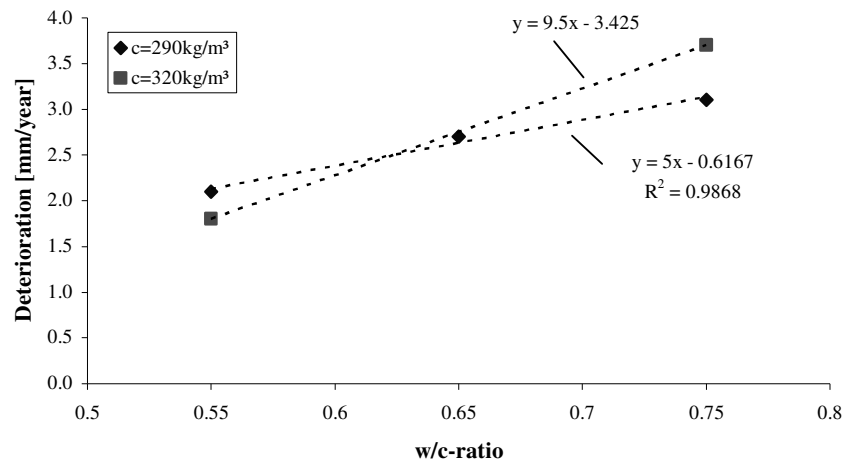
Figure 4.2 - Relationship between w/c ratio, cement content and deterioration, SO_4-solution

4.2.1.2   Macroscopical Observations

As already mentioned in the paragraph above it was observed that the formation of thaumasite started underneath an intact crust of 'sound' concrete which began to debond between the sixth and ninth month. The occurrence of the initial thaumasite front beneath an intact crust is a known phenomenon. This was described by the Halcrow Group [27] and Sibbick et al. [38] as a result of a pre-carbonated surface layer at which interface the formation starts progressing inwards, see Section 2.2.2.2. Figure 4.3 to Figure 4.6 show the presence of the formation of TSA underneath a 'sound' crust within the first nine months. The crust was observed in all specimens and developed earliest in specimens with the low quality mix designs, Mix 3 and 5, after four months. In Figure 4.7 and Figure 4.8 the development of the deterioration products formed on one specimen between the 7th and the 27th month are illustrated.

Figure 4.3 - Mix 3 (290-0.75) sample after 7months in SO$_4$-solution, top view

Figure 4.4 - Mix 3 (290-0.75) sample after 9months in SO$_4$-solution, top view

Figure 4.5 - Mix 3 (290-0.75) sample after 7 months in SO$_4$-solution, side view
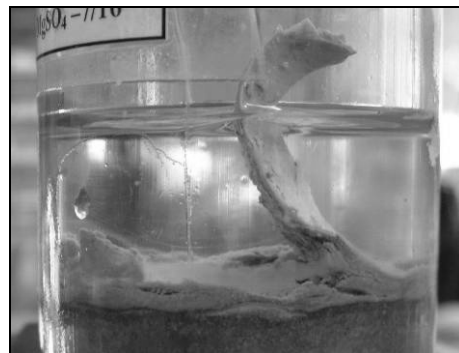
Figure 4.6 - Mix 3 (290-0.75) sample after 9 months in SO$_4$-solution, side view

Figure 4.7 - Mix 3 (290-0.75) sample after 7 months in SO$_4$-solution, side view

Figure 4.8 - Mix 3 (290-0.75) sample after 27 months in SO$_4$-solution, side view

The maximum thickness of the sharp separated layer of deterioration products in Mix 3 specimens was 19mm after 27 months and that differs to the actual concrete deterioration measured of 6.5mm due to the transformation of cement paste into a more voluminous end product. The development of this layer for each of the five mixes used is illustrated in Figure 4.9 this was determined by measuring the thickness of the thaumasite layer, as illustrated in Figure 4.8, on at least 10 samples of each set of

specimens at each needle test date. The measurements were performed at the outside of each sample at eight different points along the circumference. The trend of each mix confirms the results obtained by the needle test method. Annual progress of expansion observed in this investigation is presented in Table 4.5, this was obtained by regression of the graphs in Figure 4.9. The average factor of expansion compared to the actual depth of deterioration was calculated as 2.9 (Table 4.6) and is valid for the unrestrained conditions applied to this type of specimen.

The sharp deterioration front between the softened mass and sound concrete as described by Sibbick et al. [38] was clearly observed and also the presence of loose aggregate grains in this soft mass of deteriorated cement paste.
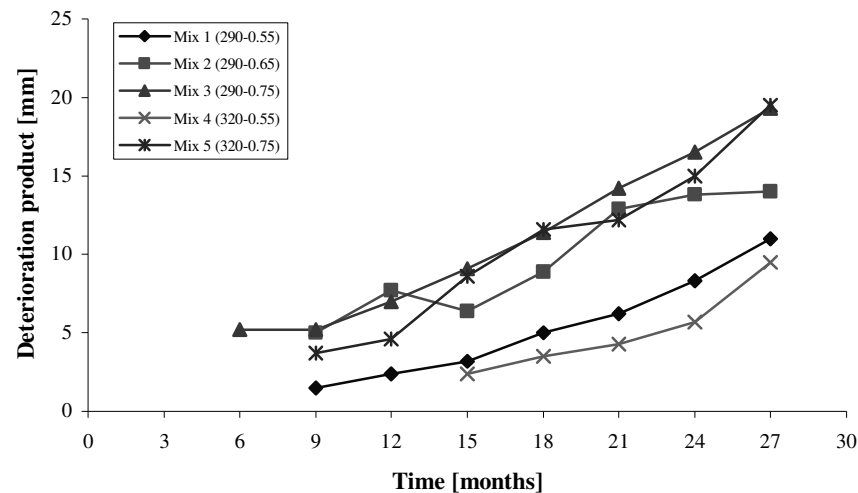
Figure 4.9 - Development of amount of deterioration product, SO_4-solution

Table 4.5: Rate of accumulation of end product layer of precast mixes in 1.8% SO_4-solution

Mix	Accumulation		Correlation coefficient R^2
	[mm/month]	*[mm/year]*	
1 (290-0.55)	0.52	6.2	0.9619
2 (290-0.65)	0.54	6.5	0.8979
3 (290-0.75)	0.71	8.5	0.9720
4 (320-0.55)	0.55	6.6	0.8904
5 (320-0.75)	0.85	10.3	0.9711

Table 4.6: Expansion factor of precast concrete mixes in 1.8% SO$_4$-solution

Mix	Actual deterioration according to Table 4.4	Accumulation according to Table 4.5	Expansion factor
	[mm/year]	*[mm/year]*	*[-]*
1 (290-0.55)	2.1	6.2	2.9
2 (290-0.65)	2.7	6.5	2.4
3 (290-0.75)	3.1	8.5	2.8
4 (320-0.55)	1.8	6.6	3.6
5 (320-0.75)	3.7	10.3	2.8
Average expansion factor:			**2.9**

The macroscopical progress of deterioration observed at the unrestrained specimens immersed in solution can be summarised in its steps as follows:

- Formation of thaumasite beneath a carbonated surface layer – crust of 'sound' concrete;
- Formation of more voluminous compounds causing cracking of the surface;
- Spalling and debonding of the crust from the thaumasite layer beneath;
- Thaumasite progress inwards towards the core with sharp deterioration front; and
- Gradual erosion of crust with remnant aggregate grains in mushy paste.

4.2.1.3   Microscopical Observations

Microscopical observations performed as part of this project by Sibbick [153] and the author using a polarisation microscope confirmed the presence of thaumasite and showed typical features of TSA. The four zones described by Sibbick et al. [38], see Section 2.2.2.2, were well developed and a sharply defined degradation front was often observed. Thaumasite occurred as TF inside cracks, patchy distributed in the matrix, around aggregate grains and as completely transformed zone extending inwards from the surface. Figure 4.10 shows the different zones occurring during attack. The top one to two millimetres can be identified as Zone 3 and 4 where the cement paste is either almost or completely transformed into thaumasite and only some small islands of

cement paste remain. Below this brighter zone and until the large horizontal crack the cement paste is less affected, however, a system of small cracks is visible. The horizontal crack can be assumed as boundary between Zone 1 and 2 because only little deposits of thaumasite (TF) which are typical of Zone 1 were found below and in a close vicinity to this crack.
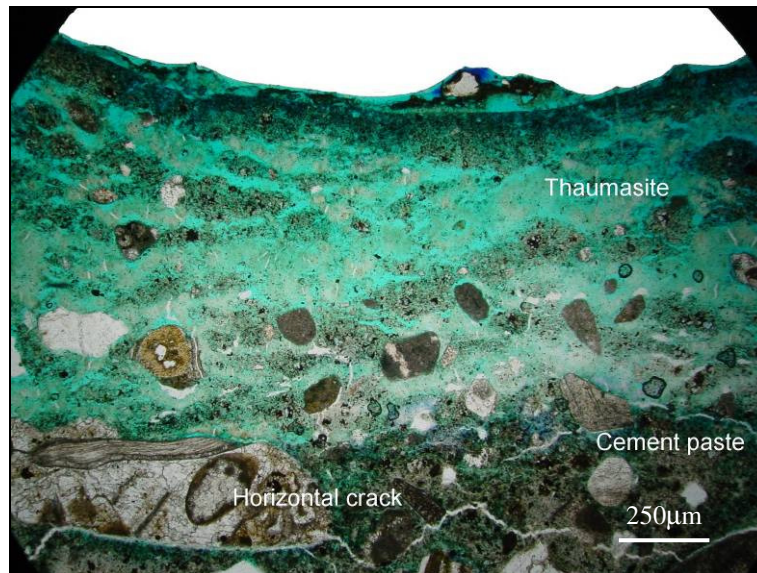
Figure 4.10 - TSA attack of surface area after 9 months, plane polarised light (PPL)

The assumption that the macroscopically observed 'sound' concrete crust was carbonated and therefore deterioration began underneath was confirmed in samples where the crust could be preserved during sampling and thin section preparation. The observed thaumasite formation under the crust and the spalling and rolling up of the crust depended on the grade of carbonation, i.e. the actual pH value in the pore solution of the cement paste. It is suggested that the rolling up (see Figure 4.5) of the crust is the consequence of the pH gradient which occurs in the partly carbonated cement paste. As suggested by Gaze and Crammond [48] thaumasite forms readily at higher pH values and is unlikely to form below the critical pH of 10.5. This led to a gradient of the formation of thaumasite at the bottom side of the crust resulting in an expansion gradient which eventually caused the rolling up.

Besides Thaumasite, gypsum crystallisation in air voids and secondary calcium hydroxide in adhesion cracks was observed, see also Appendix B. In addition thaumasite deposits with secondary calcite, PCD (Section 2.3.4), were found at samples examined after 21 months immersed in solution. The observation of PCD is evidence

that sub-aqueous carbonation of the initial formed thaumasite took place due to a decrease in stability of the thaumasite. This process can be considered as the final degradation process associated with TSA and therefore supports the statement made by Crammond [2].

4.2.1.4 X-ray Diffraction Analysis

X-ray diffraction analyses confirmed the presence of the main reaction product thaumasite in all samples tested at an ages of 9, 15 and 21 months. Besides the typical cement hydration products such as calcite, quartz and ettringite [28, 86] reaction products due to TSA such as the sulfate-bearing minerals secondary ettringite and gypsum as well as aragonite were detected. The development of a typical mineral concentration of one mix design using semi-quantitative analysis is represented in Figure 4.11. Further X-ray diffraction analyses are illustrated in Appendix C.
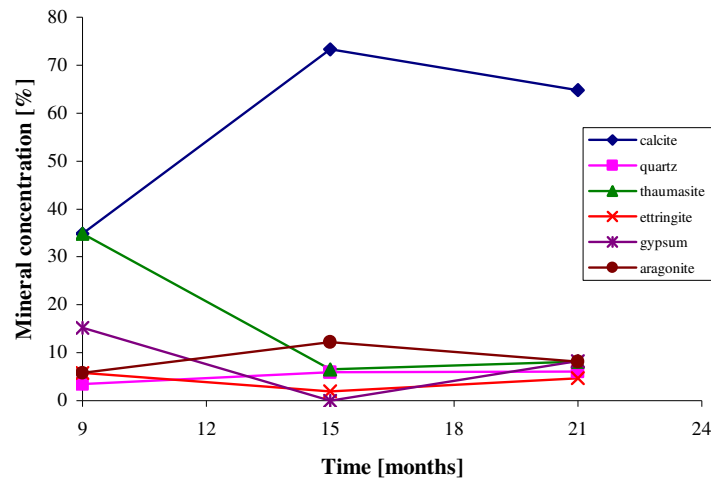
Figure 4.11 - Development of mineral concentration at Mix 2 (290-0.65) samples, SO_4-solution

The main compound found, the calcite, altered its concentration in inverse proportion to the concentrations of thaumasite and gypsum during the investigated time period. The concentration of calcite increased between the 9th and 15th months and decreased afterwards. Simultaneously thaumasite and gypsum decreased and then increased. Ettringite is mainly present in higher concentration during the early stages of the thaumasite form of sulfate attack and decreases with time. Quartz and aragonite quantities are relatively stable. It should be noted that the results obtained are based on a

semi-quantitative analysis which aims to convey the trends and relative proportions of minerals present rather than actual percentages. In addition, the analysis was performed on concrete which is a heterogeneous material.

It is assumed that a gradient of pH was present between the reaction front towards the surface of the reaction product layer facing the solution. The TSA reaction product layer was very loose so that a high gradient can be expected as it can be seen in Figure 4.8. The pH at the reaction front was still above 10.5 so that thaumasite formation could progress in optimum conditions. However, the pH decreased towards the solution so that decalcification processes of thaumasite and ettringite occurred and the concentrations of calcite and aragonite increased. Therefore reverse proportional relations of thaumasite and ettringite to calcite and aragonite are visible in Figure 4.11. The decomposition of the sulfate-bearing compounds to calcite and aragonite released sulfate ions into solution which served as additional sulfate source. Secondary calcite was also observed on the deteriorated zone using microscopy confirming the suggestions that a pH gradient was responsible for the reduction of thaumasite stability with subsequent formation of calcite. Aragonite can also be considered as a reaction product of the carbonation process of thaumasite as suggested by Freyburg and Berninger [43] and observed by Sibbick and Crammond [82].

Traces of magnesium compounds such as brucite were not found in this investigation although brucite is a frequently observed compound when concrete is exposed to magnesium-containing solutions (Section 2.3.2) and therefore magnesium sulfate attack can be excluded.

4.2.1.5   Summary

The dependency of the rate of deterioration on the w/c-ratio was observed as expected, i.e. high w/c-ratios increase the vulnerability of the concrete. The second variable the cement content confirmed the expected trend that the higher cement content ($320kg/m^3$) had a better resistance to TSA than the concrete with $290kg/m^3$ of cement. However, this was only until a certain w/c-ratio and beyond this threshold high cement contents proved to be more susceptible. The threshold was to be found between w/c=0.6 to 0.65 in the current investigation.

Macroscopical observations showed the development of a crust of 'sound' concrete above the actual layer where TSA starts to form. It is assumed that thaumasite starts to form underneath a carbonated surface layer. Further deterioration showed a linear trend with the deterioration product expanding to three times the depth of actual deterioration. Polarisation microscopy was used to verify the presence of thaumasite and to distinguish the different zones formed from the soft surface, Zone 4, to the Zone 1 and sound concrete.

X-ray diffraction confirmed the common reaction products observed during TSA, such as calcite, quartz, thaumasite, ettringite, gypsum and aragonite. The amount of thaumasite was found to decrease with further progress of TSA. It is assumed that this was caused by the carbonation of thaumasite and formation of secondary calcite.

4.2.2   Effect of Aggressive Solution

4.2.2.1   Deterioration Measurement

The aim of this part of Series I was to investigate the effect of two different aggressive solutions on the rate of TSA. The results of concrete immersed into a pure 1.8% SO_4^{2-}-solution (as $MgSO_4$) are presented in Section 4.2.1 and are extended with the use of a combined sulfate-carbonate solution (1.8% SO_4^{2-} + 370mgCO_3^{2-}/l) in this section. The progress of TSA during an observation period of 27 months is illustrated in Figure 4.12.
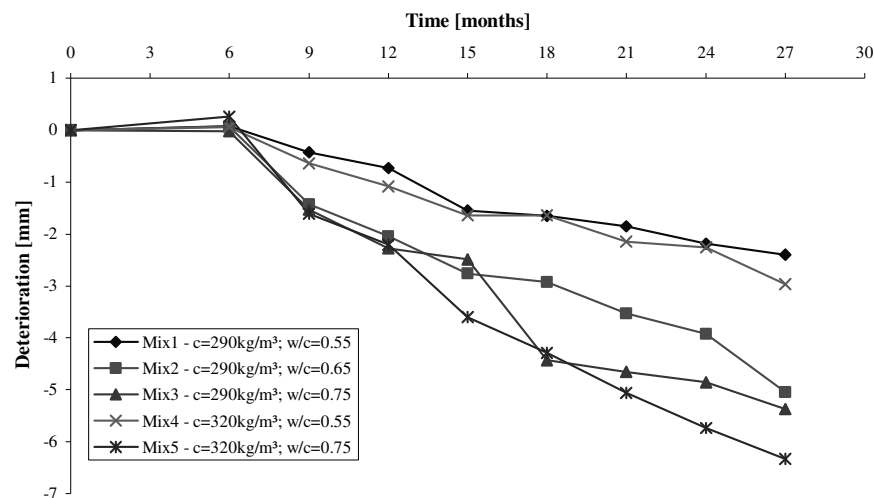
Figure 4.12 - Thaumasite progress in combined sulfate-carbonate solution depending on mix design

The progression in sulfate-carbonate solution is similar to the pure sulfate solution; however, the rate of deterioration was slower than that observed with the pure sulfate solution. Results for both solution types are compared in Table 4.7. The observation that concrete with the higher cement content ($320kg/m^3$) was more susceptible to TSA at high w/c-ratios and vice versa as described in Section 4.2.1.1 was also confirmed in specimens immersed in the combined solution. The boundary of this untypical behaviour in the case of this solution is at a w/c-ratio of 0.55 and is shifted to a slightly lower ratio than that observed with the pure sulfate solution (0.6-0.65) (Figure 4.13).

Table 4.7: Progress of deterioration of precast mixes in combined sulfate-carbonate-solution and comparison with pure sulfate solution

Mix	Deterioration progress in combined SO_4^{2-}-CO_3^{2-}-solution		Correlation coefficient R^2	Deterioration progress in 1.8% SO_4^{2-}-solution
	[mm/month]	*[mm/year]*		*[mm/year]*
1 (290-0.55)	0.11	1.3	0.9423	2.1
2 (290-0.65)	0.18	2.2	0.9711	2.7
3 (290-0.75)	0.22	2.7	0.9226	3.1
4 (320-0.55)	0.12	1.4	0.9618	1.8
5 (320-0.75)	0.27	3.2	0.9855	3.7
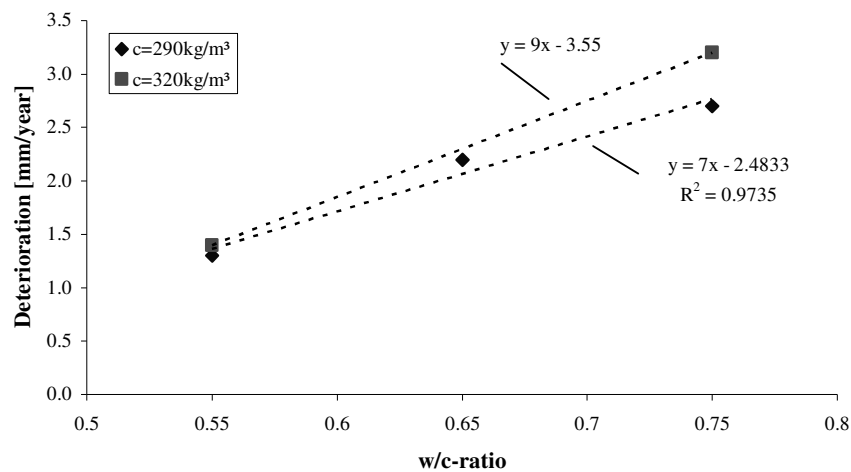
Figure 4.13 - Relationship between w/c ratio, cement content and deterioration, SO_4-CO_3-solution

The effect of mix design is the same as for specimens immersed in the pure sulfate solution, this is illustrated in Figure 4.14 where it can be seen that the deterioration rate

was reduced to 60-90% of the rate measured in the 1.8% sulfate solution. The highest reduction to 60% occurred in the Mix 1 specimens, this reduction is considered as an outlier which is clearly shown based on the regression in Figure 4.14. On the other hand Mix 1 could also show the trend of a curve. Excluding the Mix 1 value there was a clear linear dependency of the deterioration rate in the combined sulfate-carbonate solution on the compressive strength. Specimens in the combined sulfate-carbonate solution deteriorated 5% per 10N/mm^2 increasing strength slower than specimens in the pure sulfate solution, i.e. the additional carbonate decelerated the deterioration in concretes with less permeability. It is suggested that excess supply of carbonate favoured the precipitation of calcite in the concrete pores hence the density of the cement matrix increased and the transportation of aggressive sulfate ions was reduced. A lower amount of additional carbonate in solution may enhance the rate of deterioration. The optimum carbonate content in solution for the acceleration of TSA should be investigated in future work.
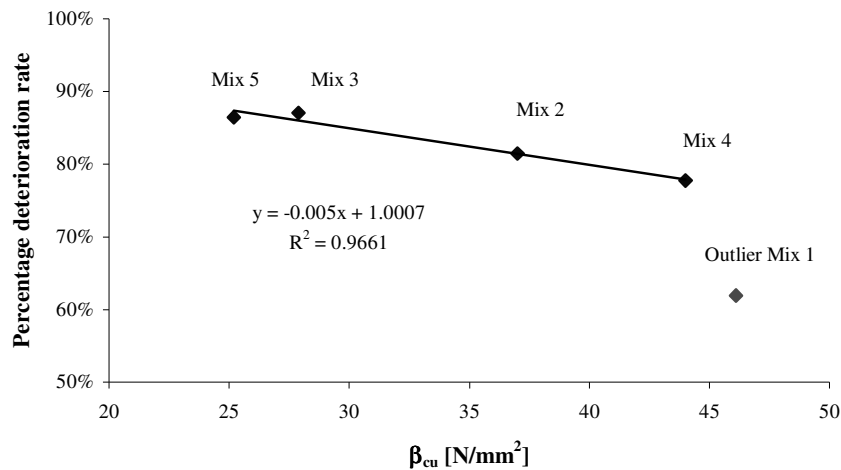
Figure 4.14 - Percentage rate of deterioration in SO_4-CO_3-solution compared to the SO_4-solution

In order to summarise the dependency between mix design, type of solution and rate of deterioration a relationship of annual deterioration to the concrete compressive strength was established. Due to the linear dependency between the rate of deterioration 'y' and w/c-ratio, $y \propto w/c$, as well as the dependency between compressive strength β and the w/c-ratio, $\beta \propto 1/w/c$, there exists a relationship between deterioration and the compressive strength, $y \propto 1/\beta$, as illustrated in Figure 4.15.
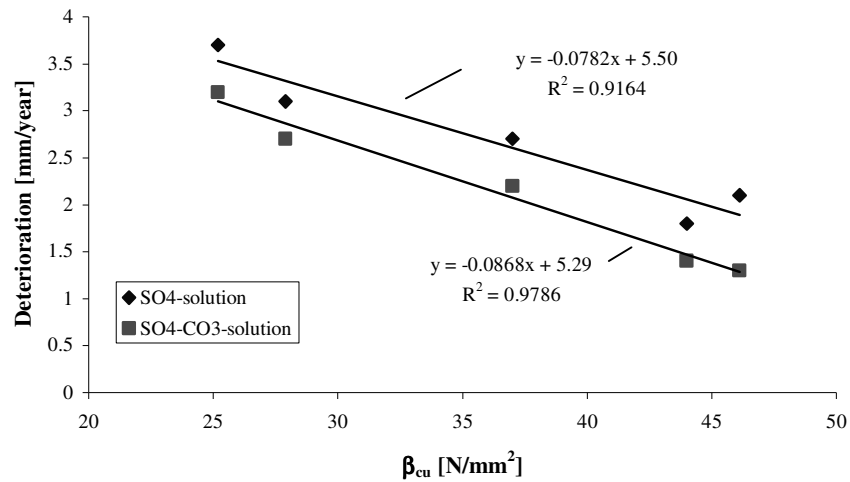
Figure 4.15 - Relationship between compressive strength and annual deterioration

The difference in the rate of deterioration in both solutions used and the linear dependency of them on the compressive strength are clearly visible in Figure 4.15. Assuming the linear extension of both trend lines deterioration should not occur when the compressive strength of the concrete exceeds $61N/mm^2$ in the case of the combined sulfate-carbonate solution and $70N/mm^2$ in the case of the more aggressive pure sulfate solution. However, an asymptotic approach is more likely but further points are not available. Furthermore it should be considered that results were obtained in highly aggressive laboratory conditions, hence it is assumed that the effect of TSA on structure material is less in the field. On the other hand economical concrete strengths are usually below this threshold of $70N/mm^2$ and therefore structures are in the vulnerable zone. In the case of the Tredington-Ashchurch and Grove Lane overbridges [27] concrete with grade C35/40 was used, however, strengths of up to $77N/mm^2$ were measured for core samples of sound concrete taken from the bridge at the time TSA was discovered (29 years after the bridge was built).

It is suggested that there is not a clear threshold regarding TSA and compressive strength and it is assumed that the rate approaches zero the higher the strength but TSA cannot be excluded. High quality concrete is able to preserve a dormant period when no attack occurs but the onset of the attack can only be postponed and not prevented in carbonate-containing concretes.

4.2.2.2   Macroscopical Observations

From the macroscopical point of view there were no obvious differences observed between the two solutions used. The onset of TSA occurred at a similar time with the same features observed such as the initial developing of a 'sound' concrete crust spalling from the surface and rolling up caused by an expansion gradient underneath the crust as described in detail in Section 4.2.1.2. Furthermore the sharp reaction illustrated in Figure 4.5-Figure 4.8 was also present in the specimens immersed in the combined sulfate-carbonate solution.

Measurements of the height of the deterioration products were undertaken and similar trends to the deterioration in pure SO_4-solution were obtained, however, the difference between Mix 3 and Mix 5, which differed in the cement content, were more significant, Figure 4.16. Mix 5 with the higher cement content exhibited lower total expansion compared to Mix 3 in the combined solution and Mix 3 and 5 in the pure sulfate solution, see Figure 4.9.
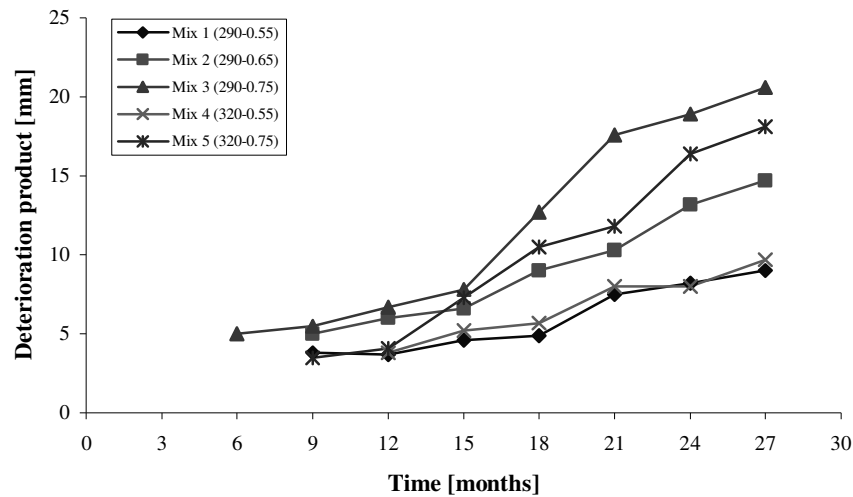
Figure 4.16 - Development of the amount of deterioration product, SO_4-CO_3-solution

The rate of accumulation of the deterioration products was determined using regression of the graphs contained in the figure above from the ninth to the 27th month and the progress is summarised in Table 4.8. This is compared to the results obtained from the specimens immersed into pure sulfate solution in Table 4.9.

Table 4.8: Rate of accumulation of end product layer of precast mixes in SO_4-CO_3-solution

Mix	Accumulation SO_4-CO_3-solution		Correlation coefficient R^2
	[mm/month]	*[mm/year]*	
1 (290-0.55)	0.33	3.9	0.9194
2 (290-0.65)	0.51	6.1	0.9136
3 (290-0.75)	0.85	10.2	0.9375
4 (320-0.55)	0.33	4.0	0.8804
5 (320-0.75)	0.87	10.4	0.9784

Table 4.9: Expansion factor of precast concrete mixes in SO_4 and SO_4-CO_3-solution

Mix	Actual deterioration *[mm/year]*		Accumulation *[mm/year]*		Expansion factor *[-]*	
	SO_4	SO_4-CO_3	SO_4	SO_4-CO_3	SO_4	SO_4-CO_3
1 (290-0.55)	2.1	1.3	6.2	3.9	2.9	3.0
2 (290-0.65)	2.7	2.2	6.5	6.1	2.4	2.8
3 (290-0.75)	3.1	2.7	8.5	10.2	2.8	3.8
4 (320-0.55)	1.8	1.4	6.6	4.0	3.6	2.8
5 (320-0.75)	3.7	3.2	10.3	10.4	2.8	3.3
Average expansion factor:					**2.9**	**3.1**

The expansion factor, which represents the relation of the actual deterioration to the accumulation of the deterioration products, showed an average value of three. However, deviations occurred within the mixes and these were probably caused by measurement errors. Therefore expansion factors less than three appear to be underestimated and more than three overestimated. It is suggested that the height of the end product layer formed is generally three times higher than the actual deteriorated zone of concrete. It should be noted that this conclusion is restricted to TSA under unrestrained conditions.

4.2.2.3   Microscopical Observations

Microscopical investigations showed the same features as described in Section 4.2.1.3 for specimens immersed into the pure sulfate solution. The presence of thaumasite and gypsum in cracks and as replacement for the cement paste was confirmed and all

characteristic deterioration zones were also well developed, see Figure 4.10, p.106. Less evidence was found for the occurrence of secondary calcite as a carbonation product of thaumasite than in samples deteriorated in the pure sulfate solution. This does not mean that it did not occur as the spalling of the crust and the difficulty in sampling this crust for testing may have resulted in the loss of any secondary calcite on the surface.

4.2.2.4   X-ray Diffraction Analysis

Less thaumasite and gypsum but an increasing amount of aragonite was detected in specimens stored in sulfate-carbonate solution than in those stored in pure sulfate solution. The concentration of calcite, quartz and ettringite was similar and relatively stable over the time period analyses were performed. Changes in the mineral concentration of Mix 2 specimens are illustrated in Figure 4.17.
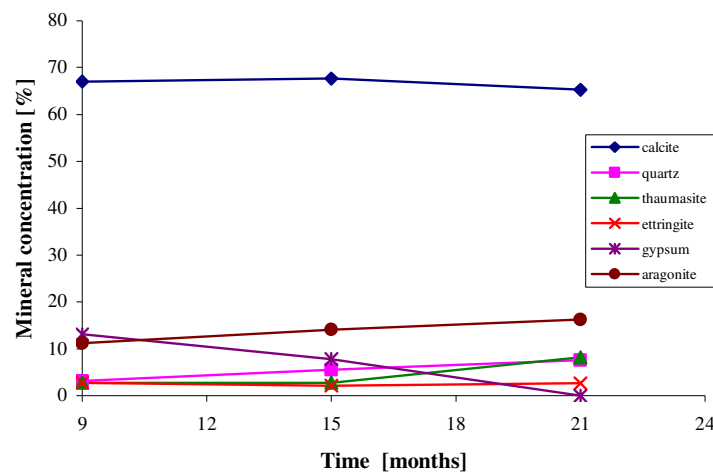
Figure 4.17 - Development of mineral concentration at Mix 2 (290-0.65) samples, SO_4-CO_3-solution

Considering all five mixes, a continuously increasing amount of thaumasite and aragonite was observed. Aragonite was the second highest concentration after calcite and then came thaumasite. The concentration of thaumasite at the first test date (nine months) was lower than the initial concentration of thaumasite detected in samples stored in the pure sulfate solution. This indicates that either less thaumasite was formed or that the rate of de-calcification of thaumasite to both secondary calcite and aragonite within the reaction products was accelerated in the combined sulfate-carbonate solution.

The proportionally increase in concentration of aragonite in the combined solution supports the latter suggestion of accelerated de-calcification processes.

It is suggested that the excess supply of bi-carbonate ions in solution favoured the de-calcification of thaumasite in the low alkaline environment. The numerical average pH of the solution surrounding the reaction products was measured with 8.5 in the combined and 8.7 in the pure sulfate solution. That means according to Crammond [2] that with reduction in alkalinity the stability of thaumasite decreased. However, the difference in pH was very low and therefore it is more likely that the presence of the additional carbonate ions resulted in the increased formation of aragonite as observed. These observations support the theory postulated by Crammond [2] that secondary calcite and aragonite are the final degradation products of TSA, see also Section 2.3.4 and Section 4.2.1.4.

4.2.2.5   Summary

The additional carbonate source in the aggressive sulfate solution did not accelerate the deterioration of the concrete samples compared to those in pure sulfate solution, however, a similar linear trend of deterioration was observed. Maximum concrete deteriorations of up to 7-8mm after 27 months were measured. The phenomenon that high cement contents at high water/cement ratios were less resistant compared to less cement contents was also observed. The threshold where high cement contents improve the resistance shifted to a w/c ratio of 0.55.

No macroscopic and microscopic differences occurred in the products between the two solutions used. However, X-ray diffraction analysis showed an increased formation of aragonite in the combined sulfate-carbonate solution.

4.2.3   Effect of Casting Position

4.2.3.1   Deterioration Measurement

The main goal of this part of the investigation (Series II) was to compare the effect of the casting position on the rate of deterioration. The rate of precast specimens (PC) undergoing TSA has been discussed in Section 4.2.1 and is compared to the rate of TSA

on the cast in-situ face (CS) of the specimens in this paragraph. Figure 4.18 shows the progress of the deteriorated softened zone using the needle test method, deterioration measured using this method is limited to the combined depth of Zone 3 and 4 (see Section 2.2.2.2).
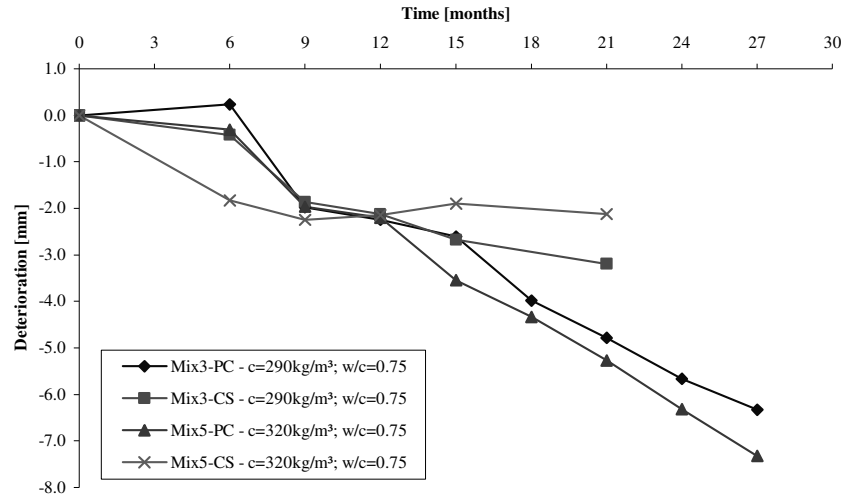
Figure 4.18 - Thaumasite progress in 1.8% sulfate solution depending on casting position

The development of deterioration of the precast (Stage 1, investigated period of 27 months) and cast in-situ (Stage 2, 21 months) specimen surfaces has a similar trend until the 15th month, however, cast in-situ Mix 5 specimens do not follow this development. Mix 5-CS specimens deteriorated faster during the first six months probably due to a very weak thin surface layer of cement paste with a high w/c-ratio and an increased calcium hydroxide $(Ca(OH)_2)$ concentration. Afterwards no further significant deterioration was measured. After the 15th month a trend of deterioration depending on the casting surface was apparent. Precast specimens show a higher deterioration rate than the same mixes cast with the in-situ method. It is suggested that the lower rate of deterioration in the CS-specimens is caused by an increase of concrete density towards to the core. A significant difference between the two types of specimens (precast and in-situ) is the deteriorating face. In the case of the precast specimen the top cast face is the deteriorating face and for the in-situ specimens it is the bottom face. The top cast face has a higher w/c-ratio, less aggregate/cement ratio and the grade of hydration is less compared to the average conditions encountered within the core. This zone of higher permeability is caused by bleeding and sedimentation processes of the fresh concrete.

The bottom cast face has a lower w/c-ratio and was able to cure under ideal curing conditions, however, there exists a thin surface layer which is enriched with cement paste and fine aggregate grains due to casting against a face. The thickness of this weaker layer is less at the cast in-situ (bottom cast) face than at the precast (topcast) face and therefore the initial deterioration is similar but afterwards the rate is decelerated at the bottom face.

The rate of deterioration of the cast in-situ specimens was estimated based on the developed trend after the initial period from the 9th month until the 21st month as it has also been performed for the results of the precast specimens, see Section 4.2.1.1. The rate of deterioration at both casting faces is represented and compared in Table 4.10.

Table 4.10: Progress of deterioration depending on casting position in 1.8% SO_4-solution

Mix		Deterioration progress		Correlation coefficient R^2
		[mm/month]	*[mm/year]*	
3-PC	290	0.26	3.1	0.9721
3-CS	0.75	0.11	1.4	0.9768
5-PC	320	0.31	3.7	0.9889
5-CS	0.75	0.01	0.1	0.1410

The results obtained consider only a maximum investigation period of 27 months, i.e. the deterioration front at the precast specimens may still be in the highly permeable zone. If testing had been continued a reduction in rate would have been expected when denser concrete was encountered. Mix 5-CS specimens did not show significant further deterioration after the first nine months. As the tests ended after twenty one months it cannot be concluded that this trend would continue indefinitely. It is assumed that the reaction is still in the dormant period in this less permeable zone after the initial weaker surface layer was deteriorated.

Field observations for instance at the Tredington-Ashchurch bridge [27] showed that the face cast directly against the clay, the so-called cast in-situ face, suffered less from TSA and only traces of TF were found. However, the concrete was cast against unweathered Lower Lias Clay where the pyrite present had not been oxidised to sulfate yet. Therefore the risk of TSA was low.

4.2.3.2   Macroscopical Observations

Macroscopical observation at the two casting faces differed in the extent of the softened and expanded zone, in both cases, however, the formation of thaumasite started underneath a crust of 'sound' concrete. This is shown in Section 4.2.1.2 in Figure 4.3-Figure 4.6 for precast specimens and in Figure 4.19 for cast in-situ specimens. The crust of PC-specimens was more friable and deteriorated faster to a soft mush, however, the expansion caused by the unrestrained transformation of cement paste into a mush (described in Section 4.2.1.2) was not observed at the cast in-situ faces, see Figure 4.20. It is suggested that is due to the higher quality of the concrete in the bottom cast zone, including curing and proportion of coarse aggregate grains despite the higher w/c-ratio.

Figure 4.19 - Mix 3-CS (290-0.75) sample after 15 months in SO_4-solution, top view
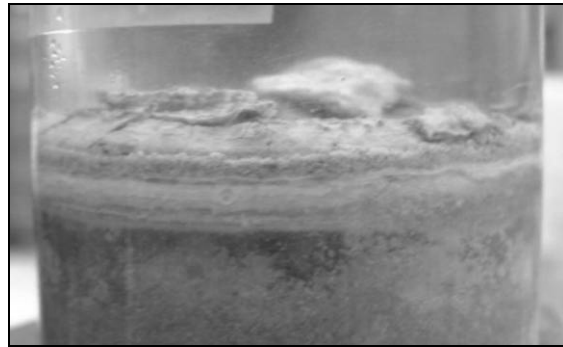
Figure 4.20 - Mix 3-CS (290-0.75) sample after 15 months in SO_4-solution, side view

4.2.3.3   Microscopical Observations

The presence of thaumasite was confirmed in all specimens using polarisation microscopy. The extent of thaumasite at the cast in-situ faces in the zone from the solid concrete inwards was very low and only patchy TF corresponding to Zone 1 was found. TSA occurred in a small layer underneath the crust causing expansion and spalling of the crust. Beyond this small layer further progress inwards was not observed and this agrees with the needle test results of the cast in-situ specimens already discussed in Section 4.2.3.1.

4.2.3.4   X-ray Diffraction Analysis

X-ray analysis confirmed the presence of the minerals calcite, quartz, thaumasite, ettringite, gypsum and aragonite in all specimens cast with both methods. The amount of thaumasite increased continuously over the investigated period from the 9th to the 15th month immersed in sulfate solution, see Figure 4.21. The main difference of the cast in-situ specimens to the precast is that aragonite was only present in traces and disappeared with time, however, calcite was strongly present as calcium carbonate compound caused by the nature of the aggregate.
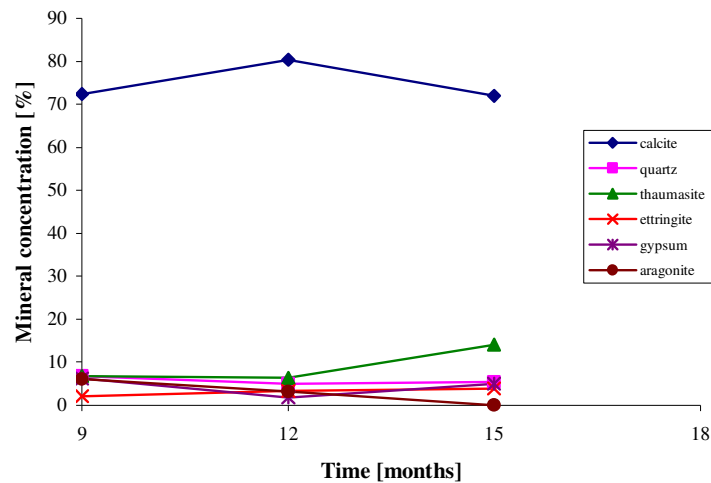
Figure 4.21 - Development of mineral concentration at Mix 5-CS (320-0.75) samples

4.2.3.5   Summary

The precast and cast in-situ method used showed a similar initial deterioration trend, however, the rate of deterioration at the cast in-situ face decelerated significantly after 12 months whereas Mix 5 returned into a dormant period without any significant deterioration. The deterioration at the precast face progressed with a stable rate after 12 months. The deterioration can be differentiated into an initial deterioration process, including initial expansion, independent on casting position and in a second stable deterioration rate which is dependent on the casting position and curing. According to

the results obtained in this investigation the cast in-situ face is the more resistant to TSA.

The formation of a crust of 'sound' concrete was observed at both casting methods, however, the final degradation of this crust was slower at cast in-situ faces. The mineral concentration of the reaction products showed particular differences in the amount of aragonite which was detected at higher concentration in precast samples and in traces in the cast in-situ samples due to the slower rate of thaumasite formation.

4.2.4   Effects of the Concrete Mix on Expansion Pressure Development

4.2.4.1   Pressure and Expansion Development

The results presented in this section describe the expansion caused by TSA under restrained conditions and gives estimations of the expansion and the pressure resulted. The specimens used for these tests were cylindrical Series I type specimens with an additional pressure application frame and are described in detail in Section 3.1.2.1.

The measurements obtained describe an almost linear expansion and pressure development after the ninth month, see Figure 4.22, however, there is a significant difference between the two casting surfaces. Considering the almost constant increase in pressure between the ninth and 15th month it was assumed that the pressure development was linear from the end of the dormant period. The linear assumption is supported by the deterioration measurements, see Section 4.2, however, the three measuring points cannot provide a clear confirmation of the trend. Extrapolations of the linear regressions between the ninth and 15th months towards the abscissa showed that the cast in-situ surface started to expand after an initial dormant period of six and a half months and the precast surface begun to expand after two months, see Figure 4.22. The regression calculations based on the results shown in the figure below are presented in Table 4.11.
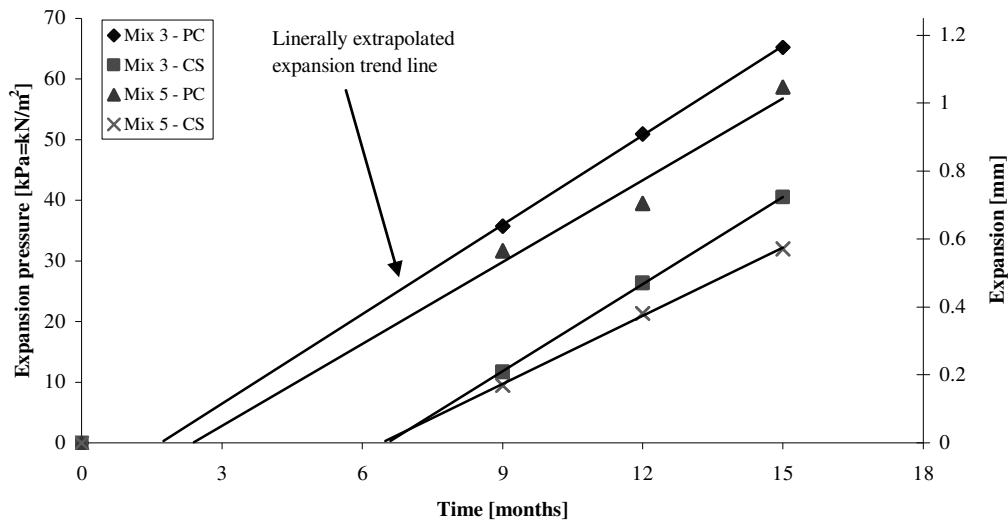
Figure 4.22 - Pressure development due to TSA

The expansion pressure developed at a similar rate on the two casting surfaces (Table 4.11), however, the onset of the expansion occurred after significant different dormant periods (PC – 2 months, CS – 6.5 months) resulting in different pressures at the end of the test period. The expansion pressure development of Mix 5-PC/CS was less than of Mix 3 whereas Mix 5-CS showed the slowest expansion rate. This is caused by the lowest permeability of the cast in-situ side of Mix 5 with a cement content of 320kg/m^3 compared to 290kg/m^3 for Mix 3.

Table 4.11: Expansion and pressure development caused by TSA in SO$_4$-solution

Mix		Expansion pressure			Expansion		
		[kPa/month]	[kPa/year]	R^2	[mm/month]	[mm/year]	R^2
3-PC	290	4.9	58.9	0.9997	0.088	1.05	0.9979
3-CS	0.75	4.8	57.6	0.9999	0.085	1.02	0.9998
5-PC	320	4.5	54.0	0.9436	0.081	0.98	0.9411
5-CS	0.75	3.8	45.0	0.9988	0.065	0.78	0.9980
Stiffness of thaumasite: **56.4 [kPa/mm]**							

The development of the pressure and amount of expansion at a concrete surface caused by the formation of more voluminous reaction products during TSA is summarised in Table 4.11. The measured annual amount of expansion of about 1mm and the measured

thickness of the deteriorated layer, which was 2 mm after one year, leads to the conclusion that under the current test conditions the relationship of actual deterioration and expansion was 1:1, i.e. the total layer formed is the double of the actual deteriorated concrete. The stiffness of the thaumasite was estimated with 56.4 kPa/mm for the four mixes investigated. The effect of varying pressures on expansion is discussed in Chapter 5. This relationship is supported by field measurements undertaken by BRE [20, 52, 53], Halcrow Group [27] and Fountain [51]. It should be noted that the pressures measured may not occur at the interface concrete/soil in the field because of the ability of the soil mass to dissipate pressure occurring due to expansion, however, any expansion that does take place will have the effect of compressing the surrounding soil.

4.2.4.2   Microscopical Observations

The formation of thaumasite was confirmed using polarisation microscopy. The top layer of about 2mm was almost completely transformed into thaumasite, corresponding to Zone 3 and 4, and below these zones thaumasite occurred patchy distributed.

4.2.4.3   X-ray Diffraction Analysis

X-ray diffraction analysis confirmed the presence of calcite, quartz, thaumasite, ettringite and gypsum but aragonite was not found either at the precast or cast in-situ surfaces. It is assumed that the increased density of the reaction product layer reduced the ingress of solution resulting reduction in pH thus preventing the formation of aragonite as the final reaction product of the de-calcification process besides secondary calcite as aragonite formed under unrestrained conditions, see Section 4.2.1.4 and 4.2.2.4. This theory is supported by the increased concentration of ettringite and thaumasite, see Figure 4.23 and Figure 4.24, compared to their concentrations detected at unrestrained conditions.

The initial high concentration of quartz is caused by the pressure distributing sand which was pushed into the deteriorated layer but with increasing formation it could be removed during sampling. Despite this influence an increasing trend in the thaumasite concentration was observed and this was enhanced at the precast samples.
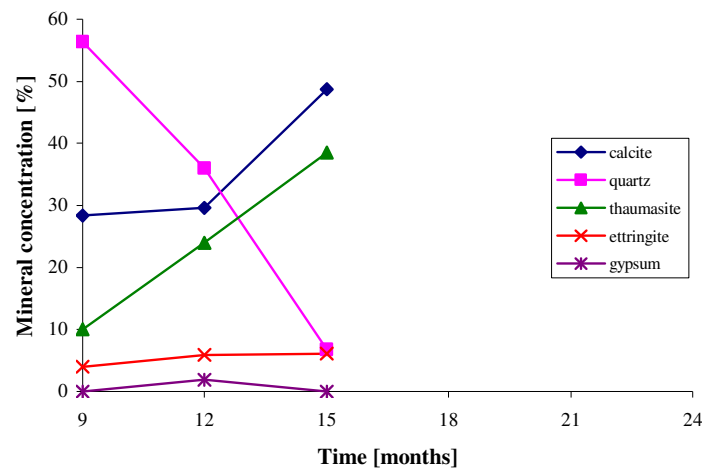
Figure 4.23 - Mineral concentration of Mix 3 - PC (290-0.75) samples, restrained
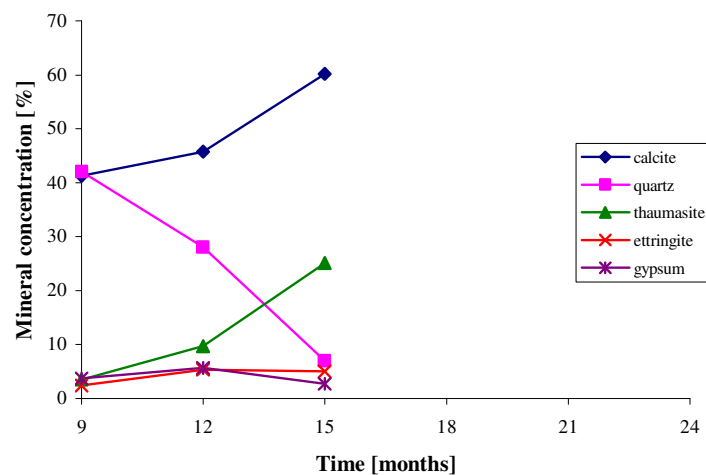
Figure 4.24 - Mineral concentration of Mix 3 - CS (290-0.75) samples, restrained

4.2.4.4   Summary

A significant pressure development caused by the formation of more voluminous reaction products was measured whereby the precast face started to expand after two months compared to six and a half months at cast in-situ faces. The rate of expansion did not depend on the casting face despite the fact that the initial dormant period was different. It is assumed that the measured increase in expansion pressure will not be present in this amount at the soil/concrete interface in the field because lateral

expansion forces dissipate in large volumes of soil. XRD analysis showed the absence of the mineral aragonite under the restrained conditions leading to the assumption that the de-calcification process resulting in the end product aragonite did not take place or was hindered compared to unrestrained conditions. That means aragonite can be assumed as one final degradation product of TSA besides secondary calcite when the ambient pH drops to low alkaline conditions.

4.3   Ion Exchange

The aim of this investigation series was to determine the sulfate and carbonate ion exchange between the aggressive solution containing sulfate and carbonate ions and the concrete to estimate the consumption of ions used by TSA. The results are supported by pH measurements of the solution.

4.3.1   Sulfate Ion Exchange

4.3.1.1   Pure Sulfate Solution

The sulfate ion exchange was measured between the aggressive solution containing 1.8% SO_4/l as magnesium sulfate and the concrete as uptaking medium. It is assumed that the sulfate present in the solution was the only available dissolved source neglecting sulfate compounds bound in the cement paste. That means the sulfate difference measured is the amount uptaken by the concrete which comprises both migration of sulfate ions into the cement matrix through penetration and the consumption of free sulfate by the formation of sulfate compounds. In this case the majority of sulfate ions were bound in the reaction products thaumasite, ettringite and gypsum of the thaumasite form of sulfate attack. However, it should be noted that thaumasite and ettringite are not a stable phase in low alkaline conditions, Gaze and Crammond [2, 48]. XRD analyses (Section 4.2.1.4) supported the instability theory of thaumasite where the amount of calcite and aragonite increased while thaumasite and ettringite decreased over the time period investigated. Based on these it is probable that the initially bound sulfate was released back into solution.

The exchange investigation was performed on specimens immersed in solution which was renewed every three months and tested at this time using the Turbidimetric Method [142], described in Section 3.2.5.2.
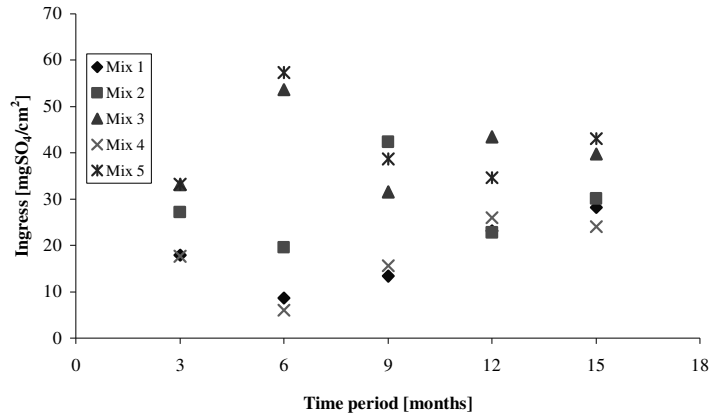
Figure 4.25 - Ingress of SO_4 over precast surface in 1.8% SO_4 solution, 3monthly
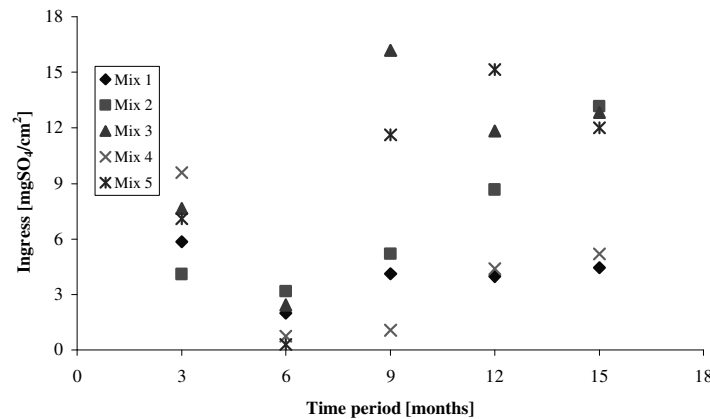
Figure 4.26 - Ingress of SO_4 over cast in-situ surface in 1.8% SO_4 solution, 3monthly

Figure 4.25 and Figure 4.26 show the difference measured in sulfate content of the solution expressed as milligram sulfate ions per cm^2 for precast and cast in-situ surfaces. The unit cm^2 was chosen in order to unify the uptaking amount from the concrete surface relative to the amount of solution. The diagrams show a significant effect of casting position and mix type, i.e. there is a direct relationship between uptake and w/c-ratio. Mixes with a high w/c-ratio and high permeability showed in general an increased uptake of sulfate ions compared to mixes with low permeability. However, few exceptions were measured. The permeability of the concrete was not measured but

it is assumed that the permeability increases with increasing w/c-ratio in accordance to general knowledge. According to Figure 4.25 and Figure 4.26 the ingress can be summarised in three different phases these are: an initial diffusion of the sulfate ions from the solution into the concrete pore structure. The second phase can be described as a dormant period with little activity. This was before expansion was sufficient to cause cracking of the matrix which would therefore increase the exposed area. As cracking begins the reaction front shifts into the concrete. This is referred to as phase 3. It is assumed that the sulfate ion concentration at the reaction front is stable and that the deteriorated layer does not possess resistance towards the diffusion mechanism. Behind the reaction front the diffusion is subjected to common diffusion laws such as applied to carbonation processes, see Figure 4.27.
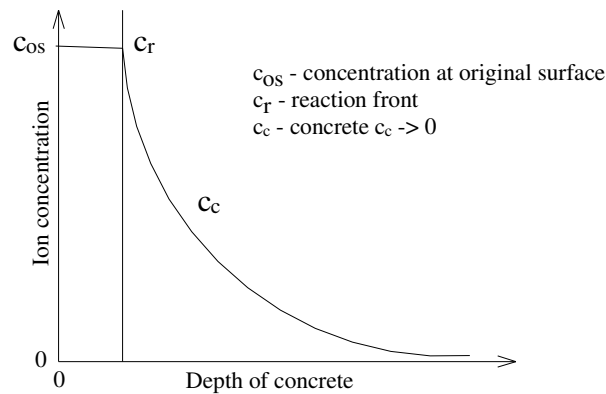
Figure 4.27 - Ion diffusion into TSA affected concrete

The dormant period has already been described during the discussion of the thaumasite progress in Section 4.2 where clear changes at the deteriorated surface and in the expansion were measured. This started between the second and ninth month. The sulfate uptake measurement supports the different onset of TSA, especially the suggested starting point of the TSA dependant on the casting face. The evaluation of the expansion pressure and the linear extrapolation towards the onset, see Figure 4.22, confirmed the abnormal uptake found at the sixth months in Figure 4.25 and Figure 4.26. Concrete with low permeability, i.e. cast in-situ surface and low w/c-ratio, differed significantly compared to the precast mixes 3 and 5 with high w/c-ratio. A dormant period with low uptake was not found in Mix 3 and 5. It is suggested that the uptake reaches a constant level depending on the mix design and density of the concrete starting with the ninth month after the weak top layer of cement paste was deteriorated.

The cumulative sulfate ingress through the precast and cast in-situ surface during a period of 15 months is illustrated in Figure 4.28 and Figure 4.29, respectively. The three uptake phases described previously are generally visible, after the initial uptake/diffusion follows a dormant period of low activity. After this a constant trend is obvious both for precast Mix 1 and 4 and all cast in-situ face mixes. Precast Mix 2, 3 and 5 do not show this trend in the graph, however, it is assumed that the dormant phase existed. The interval of measurements was too wide to show explicitly this phase. The dependency on the concrete mix is straightforward; however, the main dependent variable is the w/c-ratio. The two casting methods differed significantly in the amount of the uptaken sulfate. This can be clearly seen in the rate of ingress, Table 4.12, which was calculated for Phase 3, i.e. containing the uptake measured after the sixth month. The rate of ingress and the relating correlation coefficient are based on the uptake on three testing dates.
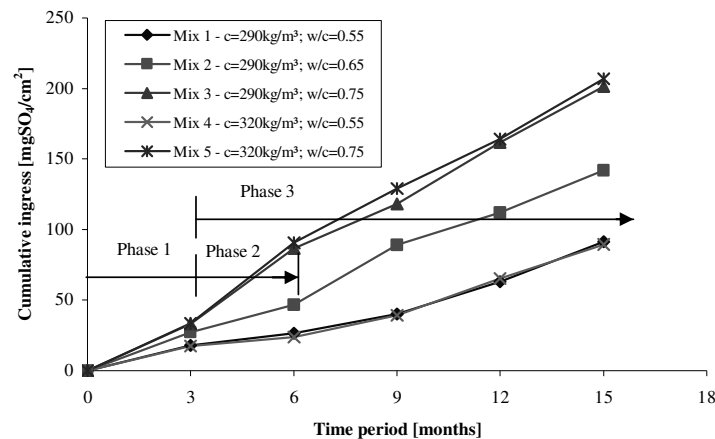
Figure 4.28 - Cumulative ingress of SO_4 over precast surface in 1.8% SO_4 solution
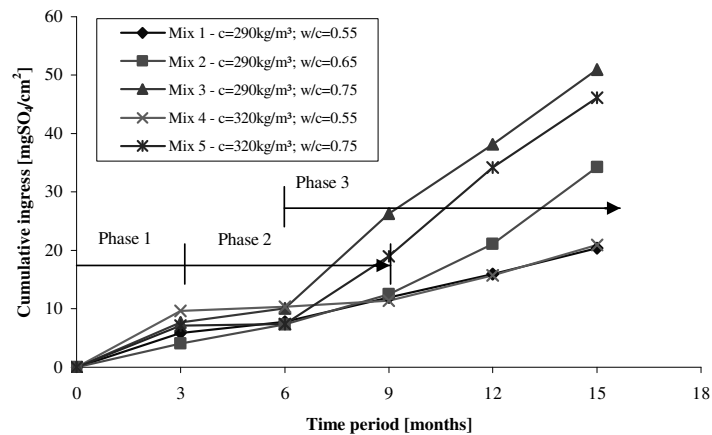
Figure 4.29 - Cumulative ingress of SO_4 over cast in-situ surface in 1.8% SO_4 solution

Table 4.12: Rate of sulfate ingress in phase 3, 1.8% SO_4 solution

Mix		Precast surface		Cast in-situ surface		Relationship precast/cast in-situ
		Rate of ingress $[mgSO_4/cm^2/month]$	Correlation coefficient R^2	Rate of ingress $[mgSO_4/cm^2/month]$	Correlation coefficient R^2	
1	290 0.55	7.3	0.9767	1.4	0.9995	5.2
2	290 0.65	10.3	0.9848	3.0	0.9616	3.4
3	290 0.75	12.9	0.9961	4.5	0.9954	2.9
4	320 0.55	7.4	0.9899	1.2	0.9347	6.2
5	320 0.75	12.8	0.9983	4.4	0.9974	2.9

The constant rate of ingress of cast in-situ Mix 5 specimens is in contrast to the observations made during the determination of the deterioration using the needle test method where Mix 5-CS did not show further deterioration after the 9th month. This period of low deterioration activity has been described as a dormant period before visible deterioration progresses. The ingress data show a continuous uptake and a linear uptake-time relationship with a significant difference in the casting position.

The relationship between the two casting surfaces describes the ingress ability, i.e. the density and porosity of the concrete. This implies that the type of casting surface becomes more relevant with increasing concrete compressive strength due to the high relation factor between the two faces. However, it is suggested that this trend was mainly related to the extent of the pore structure, the permeability, which was caused by curing. The permeability of the concrete specimens was not measured but it is generally assumed that permeability increases with increasing w/c-ratio. The cast in-situ specimens were seal cured according to Crammond et al. [63, 80] and the precast specimens were cured following this method, however, with a layer of air between surface and cling film, as described in Section 3.1.2.2.

4.3.1.2   Combined Sulfate-Carbonate Solution

In addition to the pure 1.8% sulfate solution, the sulfate ingress through the concrete was also measured with the combined 1.8% sulfate and 370mg/l carbonate solution. The results are briefly summarised and compared to those of the pure sulfate solution.
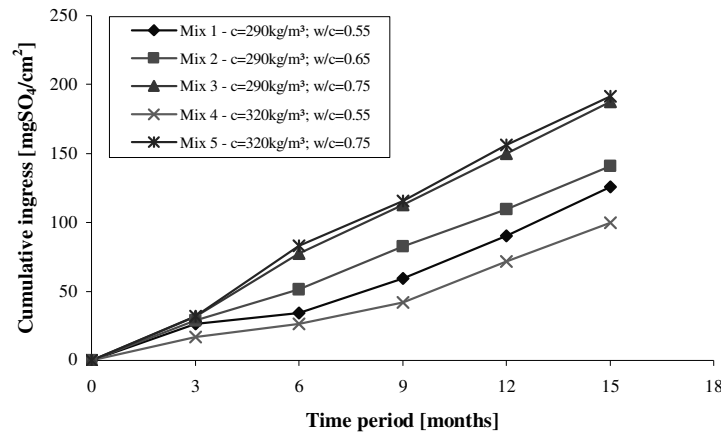
Figure 4.30 - Cumulative ingress of SO_4 over precast surface in SO_4-CO_3 solution
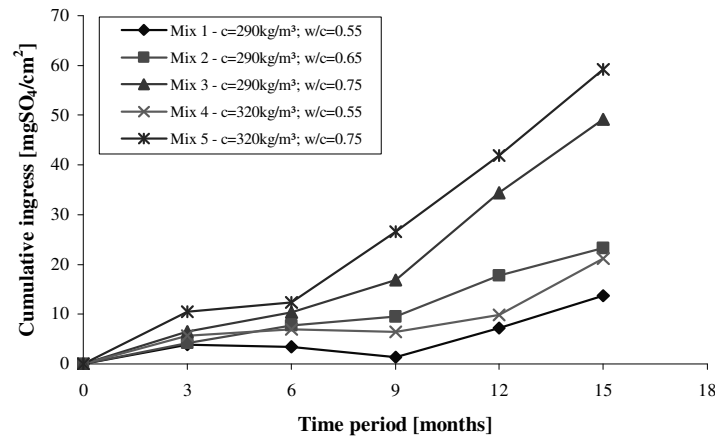
Figure 4.31 - Cumulative ingress of SO_4 over cast in-situ surface in SO_4-CO_3 solution

The sulfate ingress can also be separated into three different phases as described in Section 4.3.1.1, Phase 1 where diffusion of sulfate ions into the pore structure of the concrete took place, Phase 2 the dormant period with only slight uptakes and Phase 3 with continuous sulfate ingress as seen in Figure 4.30 and Figure 4.31. The sulfate ingress at the precast surface was very similar to the uptake measured in the pure sulfate solution; however, the dormant period at the cast in-situ surface can be considered as 3 - 6 months longer due to lower permeability. Phase 3 is represented by the constant rate of ingress and the rate estimated using regression of three testing dates is summarised in Table 4.13.

Table 4.13: Rate of sulfate ingress in phase 3, SO_4-CO_3-solution

Mix	Precast surface		Cast in-situ surface		Relationship precast/cast in-situ
	Rate of ingress [$mgSO_4/cm^2/month$]	Correlation coefficient R^2	Rate of ingress [$mgSO_4/cm^2/month$]	Correlation coefficient R^2	
1	10.2 (7.3)*	0.9938	2.1 (1.4)	0.9993	4.9 (5.2)
2	9.8 (10.3)	0.9992	2.3 (3.0)	0.9868	4.3 (3.4)
3	12.2 (12.9)	0.9998	5.4 (4.5)	0.9976	2.3 (2.9)
4	8.3 (7.4)	0.9832	2.5 (1.2)	0.9133	3.4 (6.2)
5	12.2 (12.8)	0.9982	5.4 (4.4)	0.9988	2.2 (2.9)

* Values in brackets correspond to pure sulfate solution

The rate of ingress at the precast surface was similar to that measured in specimens immersed in the pure sulfate solution, however, the rate at cast in-situ surface in the combined solution was higher and i.e. there was a continuously increased uptake after the extended dormant period reflected in the lower ratio of the relationship between precast and cast in-situ faces in Table 4.13.

Comparing the findings of the uptake with deterioration measurements at the precast surface (Section 4.2.2.1) which differed between the two solutions it is suggested that despite the fact that uptake was the same the increased deterioration in the pure sulfate solution was caused by the re-use of sulfate ions released from reaction products. It is assumed that the release of the sulfate ions took place through de-calcification of thaumasite to calcite and aragonite; however, this assumption cannot be confirmed with XRD results due to the influence of the additional source of carbonate in the combined solution.

The relationship between rate of sulfate ingress at the precast and cast in-situ surface of the pure sulfate and combined sulfate-carbonate solution and concrete compressive strength of parallel cast cubes (Table 4.1) is illustrated in Figure 4.32.
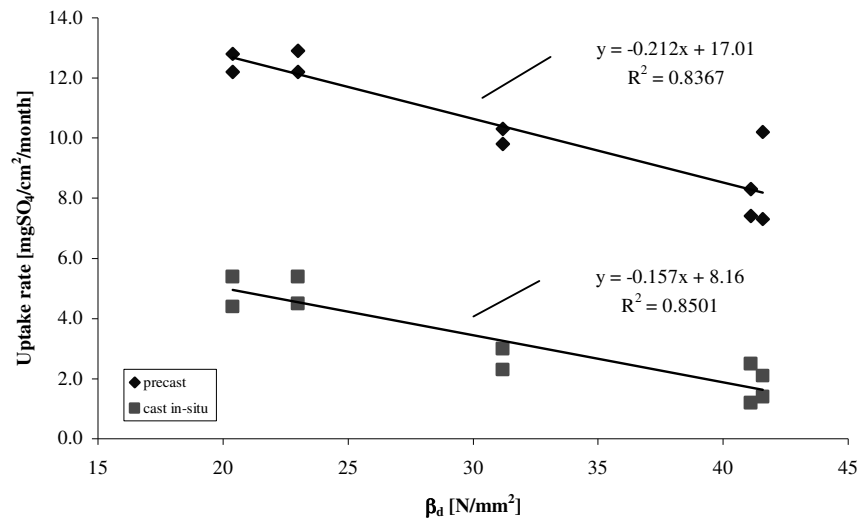
Figure 4.32 - Relationship between sulfate uptake rate and concrete compressive strength for SO_4- and SO_4-CO_3-solution

The sulfate uptake results of the two solutions were similar and a linear relationship between sulfate uptake and concrete compressive strength was obtained. It should be noted that despite the visible linear uptake-strength relationship it is assumed that the uptake tends asymptotically towards zero with increasing strength without eliminating completely any uptake and therefore deterioration reactions. The estimated cut-off point for deterioration on concrete with high permeable precast faces using linear extrapolation was determined in Section 4.2.2.1 as $70N/mm^2$ and is below the linear extrapolated uptake cut-off point of $80N/mm^2$. Sulfate ions are able to diffuse into the concrete matrix, however, without being destructive during an undefined dormant period. The cut-off point for cast in-situ surface was estimated with $52N/mm^2$ and the differences were mainly caused by surface porosity and differences in the aggregate-cement paste ratio within the bottom and top cast face, i.e. concretes with compressive strengths of over $52N/mm^2$, ideal curing conditions and complete hydration may be able to delay sufficiently TSA.

It is suggested that concrete strengths over $80N/mm^2$ extend the dormant period by hindering the uptake of sulfate so that deterioration of the concrete is stopped according to this investigation; however, deterioration cannot be completely eliminated as the Tredington-Ashchurch field case showed [27].

4.3.1.3   pH-Value

The measurements of the pH of the solution showed a slight dependency on the mix design and the pH rose from its initial level (6.3) to a numerical average in the range 8.8-9.4 during each three months exposure to a given solution. For specimens immersed in sulfate solution, the pH of the external solution in contact with precast face dropped with an increasing water/cement ratio. The pH-values measured at the precast and cast in-situ specimens immersed in 1.8% sulfate solution are shown in Table 4.14.

Table 4.14: pH-values of precast and cast in-situ specimens immersed in SO_4-solution

Mix	Test date [month]					Numerical average
Precast	**3**	**6**	**9**	**12**	**15**	
Mix 1 (290-0.55)	9.1	9.4	8.5	9.5	9.5	9.2
Mix 2 (290-0.65)	8.9	9.5	9.0	8.9	9.4	9.1
Mix 3 (290-0.75)	8.4	8.8	8.9	9.2	9.3	8.9
Mix 4 (320-0.55)	8.8	9.6	9.6	9.5	9.5	9.4
Mix 5 (320-0.75)	8.5	8.7	8.8	9.1	9.1	8.8
Cast in-situ						
Mix 1 (290-0.55)	9.1	9.2	8.9	9.5	9.2	9.2
Mix 2 (290-0.65)	9.1	9.1	9.1	9.4	9.1	9.2
Mix 3 (290-0.75)	9.2	9.2	8.7	9.2	8.8	9.0
Mix 4 (320-0.55)	9.1	9.2	9.1	9.2	9.2	9.2
Mix 5 (320-0.75)	9.2	9.3	9.2	9.0	9.2	9.2

There was an effect of concrete mix on pH evident for both the precast and cast in-situ specimens immersed in the combined sulfate-carbonate solution, see Table 4.15. However, the low pH of Mix 3 and 5 precast specimens was due to one very low value for each case and therefore it is suggested that their actual average pH were higher and that there is no actual difference in pH between the two casting positions and the mixes.

Table 4.15: pH-value of precast and cast in-situ specimens immersed in SO_4-CO_3-solution

Mix	Test date [month]					Numerical average
Precast	**3**	**6**	**9**	**12**	**15**	
Mix 1 (290-0.55)	8.6	9.6	9.5	9.6	9.4	9.4
Mix 2 (290-0.65)	9.3	9.0	9.0	9.2	9.3	9.1
Mix 3 (290-0.75)	8.6	8.3	9.0	9.0	9.0	8.8
Mix 4 (320-0.55)	9.2	9.7	9.6	9.4	9.6	9.5
Mix 5 (320-0.75)	8.5	8.2	8.0	9.3	9.0	8.6
Cast in-situ						
Mix 1 (290-0.55)	9.3	9.5	9.4	9.2	9.6	9.4
Mix 2 (290-0.65)	8.8	9.6	9.5	9.6	9.6	9.4
Mix 3 (290-0.75)	9.4	9.1	9.0	8.7	8.9	9.0
Mix 4 (320-0.55)	9.0	9.5	9.2	9.6	9.3	9.3
Mix 5 (320-0.75)	8.9	9.6	9.0	9.1	9.1	9.1

4.3.2   Carbonate Ion Exchange

The carbonate ion exchange was measured using a carbon analyser (Section 3.2.5.3) for each of the three solutions; the pure sulfate, the combined sulfate-carbonate as well as the distilled water solution and the concrete. In the first and last case the concrete was both the uptaking and the supplying medium due to the limestone aggregate. In addition to the carbonate added to the solution and the supply from the aggregate there was another carbonate source - atmospheric carbon dioxide was able to dissolve in solution. The ion exchange of interest regarding sulfate and carbonate ion exchange as well as pH is illustrated in Figure 4.33.
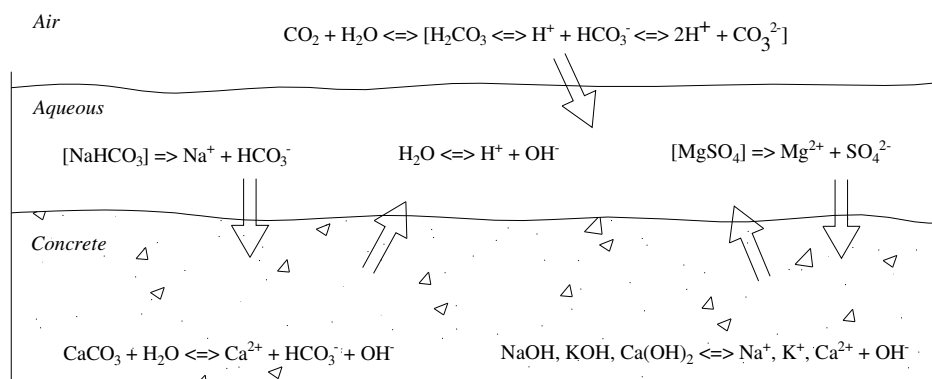
Figure 4.33 - Ion exchange 'Concrete-solution-atmosphere'

4.3.2.1   System I 'Concrete – Distilled Water – Air'

In System I 'concrete – distilled water – air' the carbonate ions measured were derived from the limestone aggregate and the atmospheric carbon dioxide. The specimens were covered with either a lid or two layers of cling film; however, it is assumed that carbon dioxide was able to reach the solution and to dissolve to an unknown extent. The solubility of the Jurassic Oolitic limestone aggregate can be assumed as $14mgCO_3/lH_2O$ at 25°C for calcite according to Perry [154]. It should be noted that the dissolved carbonate was expressed as mg per surface area and that all specimens used in the System I 'concrete – H_2O – air' tests were the precast type, i.e. the top cast face was in contact with the distilled water.
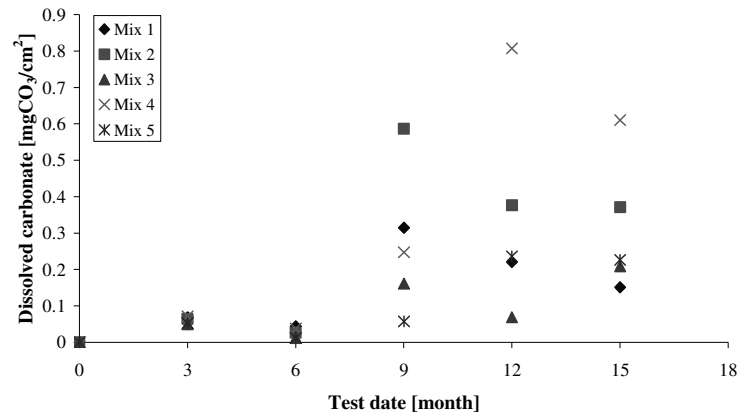
Figure 4.34 - Carbonate exchange concrete-distilled water, 3monthly renewed
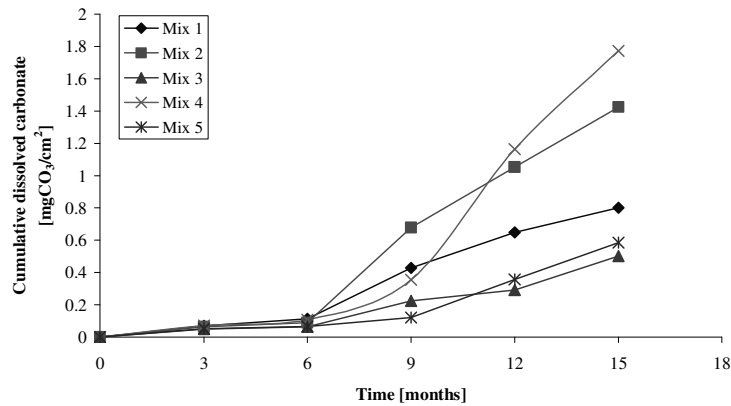
Figure 4.35 - Total carbonate exchange concrete-distilled water, 3monthly renewed
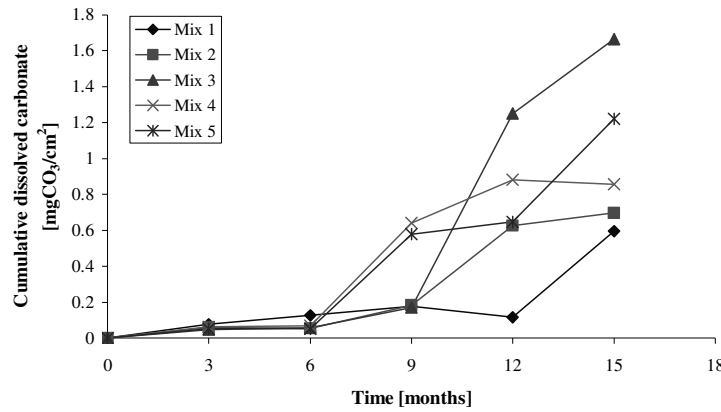
Figure 4.36 - Total carbonate exchange concrete-distilled water, no renewing

The amount of carbonate measured at each test date, i.e. the carbonate dissolved in distilled water within three months is illustrated in Figure 4.34. The carbonate dissolution increased significantly between the sixth and ninth month, this can be seen in Figure 4.35 and Figure 4.36 which show the cumulative amount of carbonate dissolved in the distilled water during the observation time of 15 months.

The results illustrated in Figure 4.35 are of specimens where the solution was renewed every three months and those in Figure 4.36 are of specimens that did not have the solution changed throughout the investigation period.

The amount of carbonate dissolved in the distilled water during the first six months was similar in both solution conditions. After this there was no obvious trend and the total amount of dissolved carbonate for each mix was very different for each of the solution conditions (renewed/not renewed). It is suspected that this may have been mainly caused by preparation and secondarily by measurement errors using the carbon analyser due to suspended matter in the solution. However, the tests were repeated and therefore the results can be assumed as valid.

The pH showed a direct dependency on the solution condition, see Table 4.16. The pH of the solution which was renewed every three months dropped with time, this was caused by the continuous leaching of the hydroxyl ions from the calcium hydroxide and the alkalis NaOH and KOH, see schematic representation of ion exchange in Figure 4.33. The pH of the solution which was not changed over the investigated time was stable in the range between 12.2 and 12.5.

The alkaline environment of the system 'concrete – H_2O – air' was not expected in the other two combinations ('concrete – SO_4-solution – air' and 'concrete – SO_4-CO_3-solution – air') because of the high concentrations of sulfate and carbonate ions in the solutions which are dominant in setting the pH, see Table 4.14 and Table 4.15.

Table 4.16: pH-values of distilled water in system 'concrete – H_2O – air'

Mix	Test date [month]				
Renewed H_2O	**3**	**6**	**9**	**12**	**15**
Mix 1 (290-0.55)	12.5	12.1	11.7	11.5	11.3
Mix 2 (290-0.65)	12.5	12.2	10.9	10.2	9.6
Mix 3 (290-0.75)	12.6	12.5	11.9	12.1	11.6
Mix 4 (320-0.55)	12.4	12.1	11.8	10.5	9.7
Mix 5 (320-0.75)	12.5	12.2	11.8	10.0	9.8
Not renewed H_2O					
Mix 1 (290-0.55)	12.5	12.4	12.5	12.5	12.4
Mix 2 (290-0.65)	12.5	12.4	12.4	12.4	12.4
Mix 3 (290-0.75)	12.6	12.5	12.4	12.4	12.3
Mix 4 (320-0.55)	12.4	12.4	12.3	12.4	12.4
Mix 5 (320-0.75)	12.5	12.5	12.2	12.4	12.3

4.3.2.2   System II 'Concrete – Sulfate Solution – Air'

System II 'concrete – SO_4-solution – air' was similar to the system discussed in the paragraph above regarding the source of carbonate. The presence of the magnesium sulfate solution with low acidity (pH=6.3) modified the system so that the dissolution ability of the present compounds was influenced by Mg^{2+}, SO_4^{2-} ions and pH. This allowed TSA and further reaction mechanisms to take place. The carbonate ion exchange mechanism is described in the following paragraphs. A final quantitative interpretation of the carbonate consumed due to TSA has not been possible. This is caused by various reaction mechanisms which affected the system such as popcorn calcite decalcification and carbonate precipitation and the aggregate solubility in the alkaline environment of the cement matrix.

Ion exchange was measured in specimens where either the precast or the cast in-situ surface was in contact with the solution. The carbonate exchange is represented by milligrams of carbonate per square centimetre of exchange surface. The amount measured is composed of carbonate ions dissolved in the solution such as carbon dioxide and ions derived from the aggregate migrating from the cement matrix. The initial carbonate ion migration was towards the solution but due to use of carbonate within TSA and de-calcification processes carbonate ions migrated back to the concrete. That mechanism can be described as a cycle with an additional outer source, the atmospheric CO_2.

Figure 4.37 illustrates the carbonate ion content which was measured in the initial pure sulfate solution after being in contact with the precast surface and then changed every three months. The carbonate ion content of the solution in contact with the cast in-situ surface is illustrated in Figure 4.38. A significant difference is obvious in the amount of carbonate measured in the solution of each of the two casting surfaces. The solution in contact with the cast in-situ surface contained up to twice the amount of carbonate as that in contact with the precast surface. Although the carbonate amounts were different for the two surface types the trends were the same with high content at three months low content at 6 months and then fairly constant values at 9, 12 and 15 months. The carbonate exchange between concrete and solution can be also split into three phases based on Figure 4.37 and Figure 4.38 assuming carbon dioxide dissolution was constant: the initial diffusion towards the solution, the dormant period with low exchange (except precast Mix 4 where was a significant high amount of carbonate measured) and then a continuous stable diffusion towards the solution which settled after the sixth month. It is assumed that the ion exchange stabilised as did the rate of deterioration and sulfate ingress, see Section 4.2 and 4.3.1.

Comparing the measured carbonate amounts in system I (Figure 4.34) and system II (Figure 4.37 and Figure 4.38) it appears that the effect of inclusion of Mg^{2+} and SO_4^{2-} ions and the associated reduction of pH is to remove the initial dormant period observed in the system I tests.
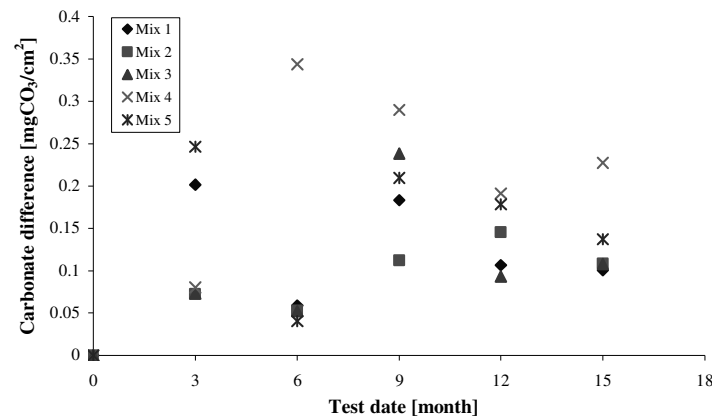
Figure 4.37 - Change of carbonate content in System II, precast surface
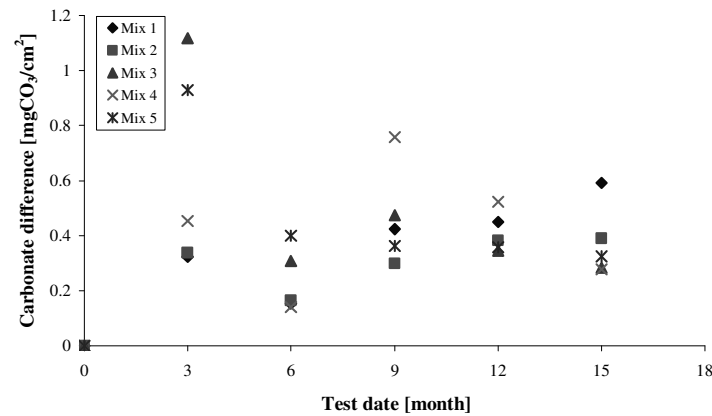
Figure 4.38 - Change of carbonate content in System II, cast in-situ surface

The three different diffusion phases which occur before the third, between the third and sixth and after the sixth month are illustrated in Figure 4.39 and Figure 4.40 which show the total amount of dissolved carbonate measured in the solution during the investigation period. It is assumed that the diffusion of carbonate ions from the concrete to the solution lead to an accumulation of ions in the solution which were in equilibrium with the carbonate ions dissolved in the pore solution of the concrete. However, it was not possible to define the amount of carbonate ions bound in the reaction products of TSA and related reactions due to two unquantifiable processes beside the unknown uptake of atmospheric carbon dioxide which was assumed to be constant and therefore neglected. The first process was the diffusion from the concrete towards the solution. The second process was the migration backwards to the concrete where the ions were bound in solid reaction products and the balance was lowered. Both processes depended

on the porosity/permeability, the water/cement ratio and cement content. It is suggested that the differences in the balance between the five mixes derived from the amount of ions bound during reaction, i.e. the higher the porosity the more carbonate was released. This statement is supported by the amount of carbonate being in balance which was expressed as the rate of ions dissolving in the solution during phase 3 starting from the sixth month. However, this statement is not applicable to the difference in behaviour between precast and cast in-situ specimens. The rate of the carbonate ion diffusion for each mix design and casting surface is given in Table 4.17 which was calculated via regression for each three test dates.
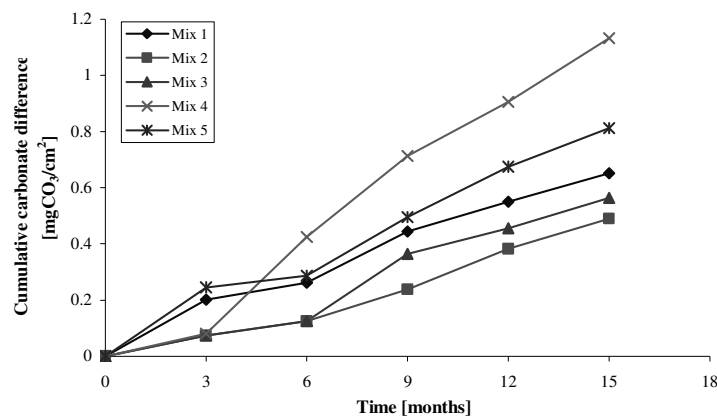
Figure 4.39 - Total carbonate exchange in System II, precast surface
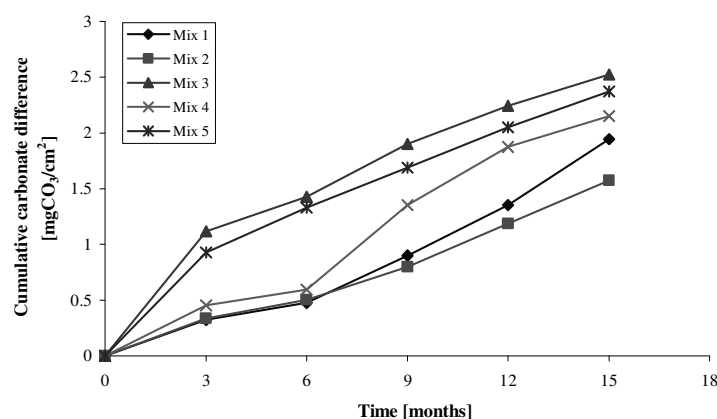
Figure 4.40 - Total carbonate exchange in System II, cast in-situ surface

Table 4.17: Rate of carbonate dissolution towards the solution in System II

Mix	Precast (High porosity)		Cast in-situ (Low porosity)	
	Rate of carbonate increase in solution [$mgCO_3/cm^2/year$]	Correlation coefficient R^2	Rate of carbonate increase in solution [$mgCO_3/cm^2/year$]	Correlation coefficient R^2
Mix 1 (290-0.55)	0.51	0.9763	1.94	0.9935
Mix 2 (290-0.65)	0.50	0.9968	1.44	0.9963
Mix 3 (290-0.75)	0.56	0.9474	1.46	0.9862
Mix 4 (320-0.55)	0.93	0.9930	2.08	0.9589
Mix 5 (320-0.75)	0.70	0.9916	1.40	0.9994

The differences in the rate between the two casting surfaces reflect the amount of deterioration at the precast and cast in-situ surface which depended on the actual porosity of the exposed face (w/c-ratio), curing and aggregate distribution. These factors of the exposed face were assumed and not experimentally determined.

4.3.2.3   System III 'Concrete – Sulfate-Carbonate Solution – Air'

System III 'concrete – SO_4-CO_3-solution – air' differed from the other combinations in that carbonate was present in the initial solution. This system contained three sources of carbonate, namely: limestone aggregate in the concrete, the carbon dioxide from the atmosphere and $370mgCO_3^{2-}/l$ dissolved as $NaHCO_3$ in the solution. The additional carbonate and Na^+, Mg^{2+} and SO_4^{2-} ions and the increased pH of 8.1 determined the differences of the ambient conditions in the system. It is assumed that the additional carbonate ions favoured the precipitation of carbonate containing compounds as shown in XRD-analyses in Section 4.2.2.4 where an increased amount of aragonite was detected, however, the additional carbonate did not favour an accelerated deterioration of the concrete as it was discussed in Section 4.2.2.1. It is intended to represent the ion exchange in this system based on the carbonate concentration in the aggressive solution, without defining the actual amount being dissolved in solution and bound during reactions as thaumasite or de-calcification end products. The ion exchange was measured at the precast and cast in-situ surface of the specimens and represented the amount of carbonate migrating between solution and concrete.

The difference of the carbonate ion content in the solution regarding the initial amount of $370 mgCO_3^{2-}/l$ is illustrated in Figure 4.41 for the precast surface and in Figure 4.42 for the cast in-situ surface. The proposed three phases ion exchange process is again visible; however, it is not as distinct as observed in System I and II.
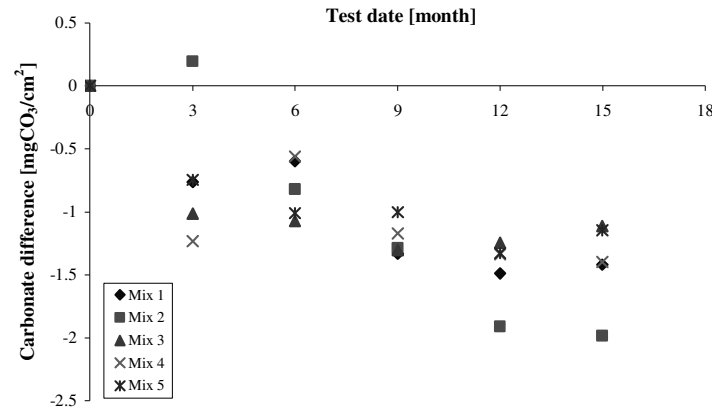
Figure 4.41 - Change of carbonate content in System III, precast surface
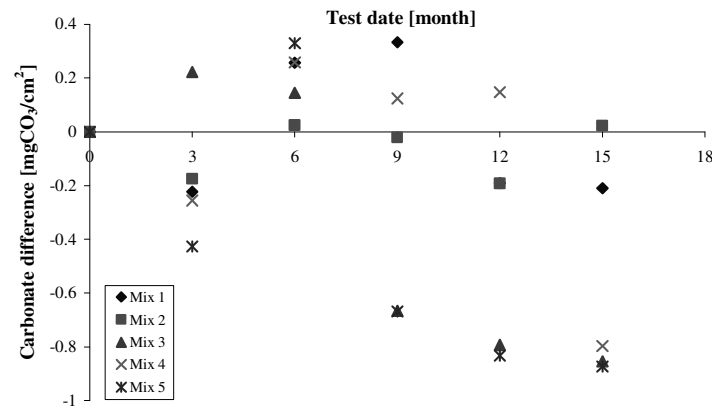
Figure 4.42 - Change of carbonate content in System III, cast in-situ surface

The main difference observed in this system was the preferred diffusion direction from the solution towards the concrete which was the opposite process to System I and II. That means that the actual consumption of carbonate ions due to TSA lay within the difference measured since it is assumed that the difference split into one part diffusing into the cement matrix and one part being a reactant for TSA and calcite/aragonite precipitation. It should also be noted that due to the high content of carbonate in solution the dissolution of atmospheric carbon dioxide was hindered since only a certain

amount of CO_2 can be dissolved in water depending on temperature, pH and further factors. The effect on the carbon dioxide dissolution ability of these further factors such as the presence of Mg^{2+}, Na^+, SO_4^{2-} is unknown, however, it is known that $0.82 mgCO_2/l$ ($p_{CO_2} = 0.3 \cdot 10^{-3} atm$) dissolves at 6°C according to Edvardsen [in 28] and the presence of carbon dioxide in solutions, low temperatures as well as low pH favour the dissolution of $CaCO_3$ [28].
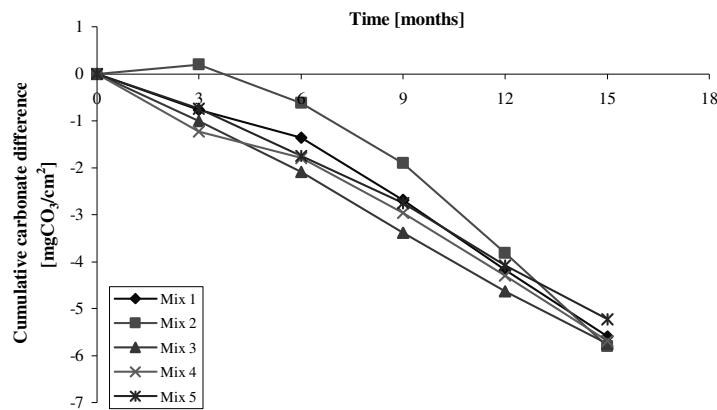
Figure 4.43 - Cumulative carbonate difference in System III , precast surface
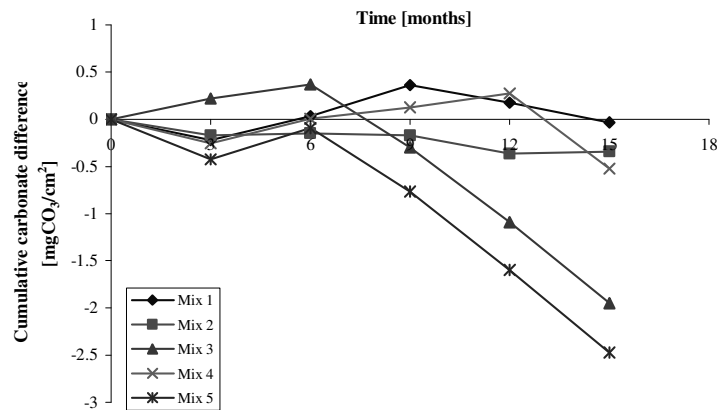
Figure 4.44 - Cumulative carbonate difference in System III, cast in-situ surface

Figure 4.43 and Figure 4.44 illustrate the cumulative amount of carbonate migrating into the concrete and which was partly used as reactant during TSA. The total difference measured at the precast surface show a constant increase of the carbonate consumed by each mix so that the migration can be expressed as for System I and II as rate as shown in Table 4.18.

Table 4.18: Rate of carbonate migration towards the concrete in System III

Mix	Precast		Cast in-situ	
	Rate of carbonate decrease in solution $[mgCO_3/cm^2/year]$	Correlation coefficient R^2	Rate of carbonate decrease in solution $[mgCO_3/cm^2/year]$	Correlation coefficient R^2
Mix 1 (290-0.55)	-5.7	0.9996		
Mix 2 (290-0.65)	-7.0	0.9911		
Mix 3 (290-0.75)	-4.9	0.9987	-3.1	0.9970
Mix 4 (320-0.55)	-5.2	0.9985		
Mix 5 (320-0.75)	-4.7	0.9974	-3.2	0.9964

It should be noted that the ingress, the negative change of carbonate content, was expressed as a negative rate to symbolise the way of ion migration. As Figure 4.44 illustrates it was not justifiable to calculate the rate of ingress at the cast in-situ surface for Mix 1, 2 and 4 because of the low permeability and fluctuations in values. The rate of uptake was estimated for Mix 3 and 5 and compared with the consumption at the precast surface. The precast surface mixes showed an increased rate of ingress, i.e. more carbonate was bound in compounds and deterioration progressed faster due to the higher porosity at this surface. A significant trend and a clear dependency of the mix design on the rate were not found.

4.3.3   Summary

The sulfate ion exchange was quantitatively determined due to one assumed source of sulfate ion which was externally available; however, the exact amount consumed by TSA could not be identified. The sulfate uptake was split into the sulfate consumed by TSA and sulfate ions being present in the cement matrix. The rate of sulfate ingress was decreased in proportion to the compressive strength of concrete and the linearly extrapolated cut-off point was similar to the cut-off point obtained for the rate of deterioration. Therefore it was concluded that deterioration and sulfate uptake are hindered over a concrete compressive strength of 80N/mm^2; however, it is suggested that in reality uptake will approach gradually zero as neither uptake or deterioration can be completely stopped, however, increasing concrete strength does have the effect of extending the dormant period and this effect may be used to ensure that TSA does not

affect a structure during a prescribed service life. The dependency of the rate of ingress on the mix design and casting surface, i.e. density/permeability, was clearly present but not proven.

The ion exchange was estimated between the three different sources of carbonate which were relating to the concrete internal such as the limestone aggregate and external such as the atmospheric carbon dioxide and carbonate that was present in the initial solution. The experiments showed two ways of carbonate migration, firstly the diffusion from the concrete towards the solution and secondly the opposite migration direction, the principal migration direction depended on the carbonate ion concentration level in the solution. The amount of carbonate diffusing into the concrete depended on the properties of exposed face, i.e. the denser the concrete the more external carbonate migrated into the concrete. It is concluded that dense concrete uses mainly external sources of carbonate whereas less dense concrete uses more the internal supply, i.e. as long as sufficient ions can diffuse through the concrete pore structure to the reaction front external carbonate is only the secondary source. However, deterioration measurements did not confirm this statement. Additional carbonate hindered the deterioration compared to the pure sulfate solution.

The ion exchange process can be generally expressed in three different phases, Phase 1 consists of initial ion absorption and diffusion into the concrete structure, Phase 2 can be described as dormant with little activity of ion ingress and Phase 3 shows a constant ion exchange. The length of the dormant phase depends on the permeability of the concrete, i.e. the density and strength govern further uptake caused by deterioration mechanism.

4.4   Summary - TSA Acceleration

The findings and observations made during the acceleration of the thaumasite form of sulfate attack are summarised as follows:

- Deterioration consisted of two stages – an initial expansion process and subsequent constant deterioration.

- The extent of thaumasite deterioration was directly dependent on the mix design, however, increased cement content of 320kg/m^3 only had an improved resistance below w/c=0.55-0.65 compared to concrete with 290kg/m^3 of cement, otherwise they were more susceptible. The threshold depended on the solution.

- Precast (top cast) and cast in-situ (bottom cast) surfaces showed similar initial deterioration, however, the deterioration rate of cast in-situ surfaces decreased afterwards. Pressure measurements confirmed this and also showed a longer dormant period in case of cast in-situ faces. The cast in-situ surface was more resistant due to increased density and less permeability.

- A crust of 'sound' concrete formed in unrestrained specimens, was less distinct and sometimes absent under restrained conditions.

- TSA under unrestrained conditions formed as an incohesive loose mass whereas in restrained conditions it formed as a compacted cohesive mass but was without binding abilities. The TSA reaction product layer was twice and three times the thickness of the actual concrete deterioration depth at restrained and unrestrained conditions, respectively.

- Thaumasite, ettringite, gypsum, quartz, calcite and aragonite were found as reaction products under unrestrained conditions and absence of aragonite and reduction of gypsum was observed under restrained conditions.

- Additional source of carbonate in solution did not accelerate TSA despite that the same sulfate consumption was observed, i.e. combined sulfate-carbonate solution was less aggressive but favoured the formation of aragonite.

- Sulfate uptake decreased in proportion to the compressive strength/permeability and the linear extrapolated sulfate cut-off point was similar to the deterioration cut-off point so that TSA should be hindered with strengths over 80N/mm^2; however, it is assumed that TSA cannot be completely stopped.

- Ion exchange consisted of three phases: Phase 1 – ion absorption and diffusion into the concrete pore structure, Phase 2 – dormant period with little activity depending concrete density/porosity, Phase 3 – constant ion uptake.

5   Interface Behaviour

This chapter deals with the behaviour of the structure/soil interface affected by the thaumasite form of sulfate attack. The characteristics of the behaviour are split into three main sections which describe firstly the interface deterioration in Series IV and Series V specimens, secondly the physical interactions affected by TSA and thirdly chemical interactions occurring within the clay adjacent to the concrete.

5.1   Interface Deterioration

The concrete/soil interface deterioration was monitored on the cylindrical Series IV specimens and determined on the Series V shear box specimens after the shear tests were performed. The Series IV specimens provided a link between the TSA investigations on unrestrained specimens, discussed in Chapter 4, and the Series V specimens used to investigate the shear strength at the concrete/soil interface affected by TSA under restrained conditions. This series of tests had two main purposes, the first was to monitor the progress of TSA in restrained samples and the second was to monitor the rate of deterioration in samples containing clay. This was not possible in the shear strength specimens as they could not be disturbed prior to shear testing.

Series V specimens were mainly used for the determination of the physical and chemical interface interactions, however, it was necessary to determine the amount of thaumasite formed and the effect of different earth pressures on the interface.

5.1.1   Interface Thaumasite Formation

5.1.1.1   Cylindrical Series IV - Link Specimens

The thaumasite layer measured comprises the actual concrete deterioration and the expansion relative to the original surface caused by the formation of the more voluminous reaction products. According to the expansion observed in Section 4.2.4 it is assumed that 50% of the measured thickness of the thaumasite layer corresponded to the actual depth of deteriorated concrete and 50% was associated with expansion. The effect of TSA on the two casting positions, precast and cast in-situ, for the cylindrical

Series IV specimens confirmed the observations made with unrestrained specimens as discussed in Section 4.2. One significant difference was observed which was not expected in that the acidic non-sulfate containing English China Clay (ECC), pH=5.4, favoured TSA more than the reactive sulfate containing Lower Lias Clay (LLC), pH=7.7. However, the literature [1] has described the LLC as a very aggressive stratum in the field. The thaumasite layers measured are presented in Table 5.1.

Table 5.1: Thickness of thaumasite layer at Series IV specimens after 21 months in 1.8% SO_4-solution

Mix	Lower Lias Clay		English China Clay	
	Precast surface	**Cast in-situ surface**	**Precast surface**	**Cast in-situ surface**
1 (290-0.55)	1-2mm	1-2mm	3-4mm	0mm
2 (290-0.65)	1-2mm	1-2mm	5-6mm	0mm
3 (290-0.75)	2-3mm	1-2mm	5-6mm	2-3mm
4 (320-0.55)	1-2mm	1-2mm	3-4mm	0mm
5 (320-0.75)	2-3mm	1-2mm	6-7mm	0mm

The specimens were restrained so that a pressure of 100mm of clay was present at the concrete/clay interface, i.e. it did not correspond to the pressure applied at Series I, Stage 2 specimens (Section 4.2.4) and Series V, shear strength specimens which corresponded to 0.5m, 2.0m and 3.5m of clay. Therefore the measured thaumasite thickness differed between the Series IV – 'link'-specimens and Series I specimens as well as being influenced by the type of clay adjacent to the concrete as observed within this group of specimens.

5.1.1.2   Series V - Shear Strength Specimens

The mix design of the concrete was the ruling factor for the formation of thaumasite at the interface of Series V – shear specimens as observed in cylindrical Series I specimens, see Section 4.2. Due to the variety of variables in this complex system of concrete/clay/solution the effects of the mix design were not clearly observed, which is shown by the not existing correlation to the measured thaumasite thickness, Table 5.2. This relationship between thaumasite formation and mix design was observed at the

boundary with English China Clay. However, the denser concrete Mix 4 (c=320 kg/m^3; w/c=0.55) was more susceptible at the Lower Lias Clay boundary than the more porous Mix 3 (290-0.75) and Mix 5 (320-0.75).

Differences between the two casting positions, precast and cast in-situ, were clearly observed; the cast in-situ surface was more resistant to TSA due to less permeability/porosity of the surface, see Section 4.2.3. The inert (non-sulfate-containing) English China Clay appeared to be more aggressive at both the precast and cast in-situ surface as already observed at the cylindrical Series IV specimens. However, the enhanced aggressiveness of ECC was not valid at Mix 4-CS specimens, the mix with the densest surface. It should be noted that the values for the thaumasite thickness given in Table 5.2 consist of a series of eight to ten readings at each of the two specimens with the same pressure. In one set of specimens there were six specimens with each two for one pressure. The depth of deterioration was within the readings and the two specimens were similar. The expansion pressure is shown in Appendix F.

Table 5.2: Thaumasite layer depending on clay, casting surface, pressure and mix at age of 27 months

Thickness of thaumasite layer at boundary [mm]						
Lower Lias Clay						
Mix		**Precast surface with pressure of**			**Cast in-situ surface with pressure of**		
		10 kPa	*40 kPa*	*70 kPa*	*10 kPa*	*40 kPa*	*70 kPa*
Mix 3	290 0.75	6	2.75	2.75	3.5	2	1
Mix 4	320 0.55	12.5	6	4.5	7	1.5	2.5
Mix 5	320 0.75				3	3.5	5
English China Clay						
Mix		**Precast surface with pressure of**			**Cast in-situ surface with pressure of**		
		10 kPa	*40 kPa*	*70 kPa*	*10 kPa*	*40 kPa*	*70 kPa*
Mix 3	290 0.75	24	14	11.5	10.5	7	4
Mix 4	320 0.55	16	8.5	9.5	3	0	0
Mix 5	320 0.75				10	5	2
Mix 3*	290 0.55	10.5	5.5	5	1	1	0.5

* Thaumasite reaction time of 18 months instead of 27 months

The rate of deterioration for restrained and unrestrained specimens showed significant differences, see Table 4.9, p.114, and Table 5.3. The determination of the rate was based on the thaumasite layer measured and the assumption that expansion was equal to the actual deterioration so that "deterioration + expansion = thickness". The rate of deterioration for Mix 3/ECC with a reaction period of 18 and 27 months in the case of the lowest restraint (10 kPa) was higher than the rate at unrestrained Series I and II specimens. The rate was estimated using the most conservative approach assuming constant deterioration during the whole reaction time and neglecting a dormant period. Differences in the compactness of the thaumasite depending on the interface pressure were observed (Section 5.1.2); nonetheless they were neglected in this approach due to the comparison of the rates within the same applied pressure.

The presence of clay and the increased pH at the interface accelerated TSA. However, it should be noted that the amount of TSA was primarily controlled by the type of clay and secondarily by the pH. The pH at the boundary with Lower Lias Clay (pH 11.1) was higher but less thaumasite was observed than at the boundary with the English China Clay (pH 9.3-10.5), see Section 5.3.3. Comparing the set of Mix 3/ECC specimens with different ages significant differences in the estimated rates were observed (Table 5.3) apparently related to the time of the application of the restraint. The reaction period at the 27 months old specimens comprised 9 months of formation without additional pressure but 100mm upload of clay and 18 months with the additional restraint. Mix 3* deteriorated under applied pressure over the whole reaction time of 18 months. The two sets differed in the type of sulfate penetration. Absorption and diffusion occurred at the specimens immediately immersed in aggressive solution. Diffusion was the predominant transportation process of Mix 3* specimens. These were saturated with H_2O for nine months before being immersed in aggressive sulfate solution. The diffusion process is slower than the sulfate ingress through the combined initial absorption and subsequent diffusion which resulted in higher sulfate concentration within the cement matrix. Furthermore it is suggested that the difference in the rates was also caused by the many unknown variables in this system and that the deterioration rate may have increased with time. This suggests the rate of deterioration was not linear, as observed under unrestrained conditions, nonetheless this cannot be supported by further results since thaumasite measurements could only be performed at the end of the reaction time.

Table 5.3: Rate of thaumasite deterioration at restrained and unrestrained conditions in [mm/year]

Mix	Restraint at precast surface of			Restraint at cast in-situ surface of		
(290-0.75)	*10 kPa*	*40 kPa*	*70 kPa*	*10 kPa*	*40 kPa*	*70 kPa*
Mix 3/ECC-27months	5.3	3.1	2.7	2.2	1.6	0.9
Mix 3*/ECC-18months	3.3	2.0	1.7	0.33	0.33	0.17
	Unrestrained – without clay			**Unrestrained – without clay**		
Mix 3- (Table 4.9)	3.1			1.4		

The dependency of the pressure at the concrete/clay interface on thaumasite formation is clearly visible, from Figure 5.1-Figure 5.4. In precast specimens the thaumasite layer reduced with an increase of pressure from 10 to 40 kPa but above this no discernible changes were observed; see Figure 5.1 and Figure 5.3. In the case of cast in-situ specimens (Figure 5.2 and Figure 5.4) the thaumasite layer at Mix 3/LLC/ECC specimens decreased constantly with increasing pressure. Cast in-situ mixes 4 and 5 did not show a uniform trend depending on pressure. Mix 5 showed an increasing thaumasite layer with increasing pressure at the boundary to LLC but the layer decreased in the case of ECC. The layer on Mix 4/LLC decreased towards a pressure of 40 kPa and then increased again at 70 kPa. In the case of Mix 4/ECC the initial thaumasite layer at 10 kPa reduced to zero at 40 kPa showing the dependency of the dormant period on the onset of TSA. It is suggested that the differences at the cast in-situ surface are a result of the higher importance of fluctuations within the microclimate at the interface at low permeability surfaces.

Crammond [2] reported that the majority of TSA affected concretes in the UK have been completely buried at depths of up to 5m below ground. However, this threshold has mainly been described with the characteristics of the soil, i.e. the present source of soluble sulfate.
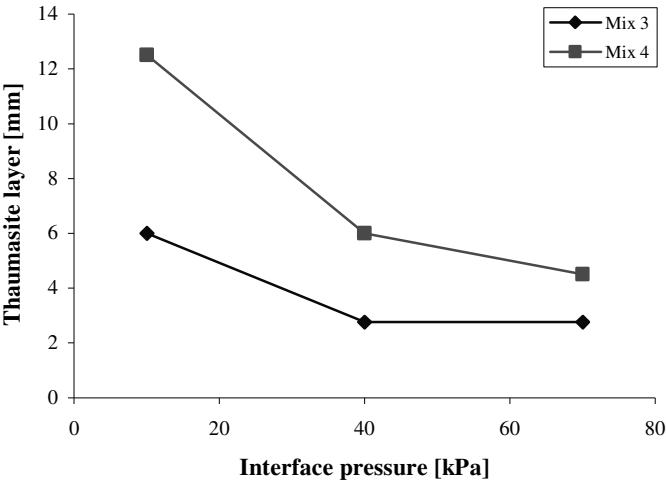
Figure 5.1 - Relationship thaumasite formation-pressure at 27th month, LLC-precast
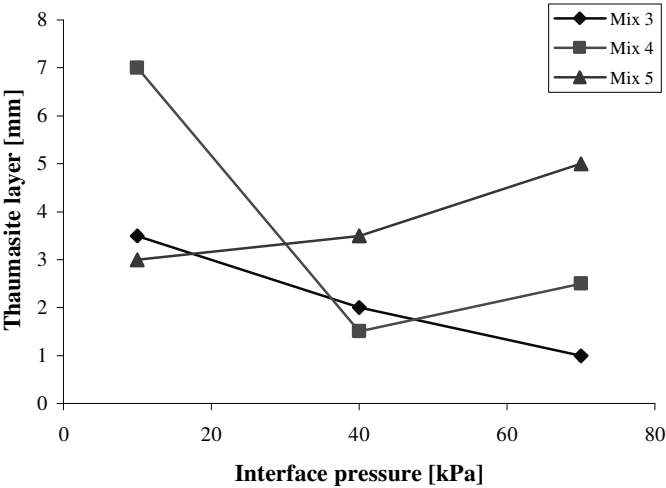
Figure 5.2 - Relationship thaumasite formation-pressure at 27th months, LLC-cast in-situ
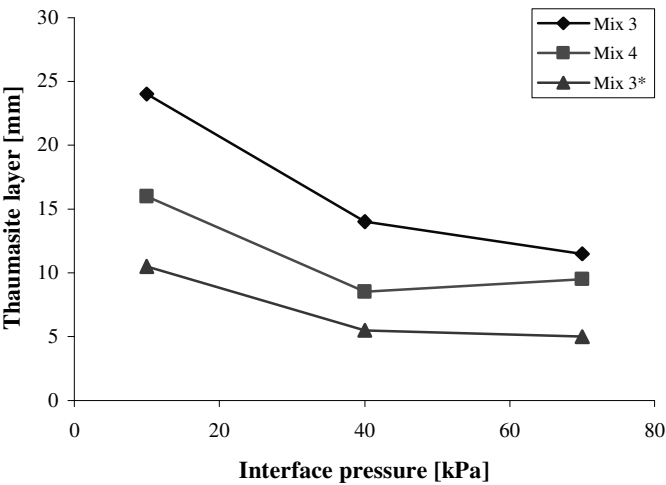
Figure 5.3 - Relationship thaumasite formation-pressure at 27th month, ECC-precast ([*18th month])
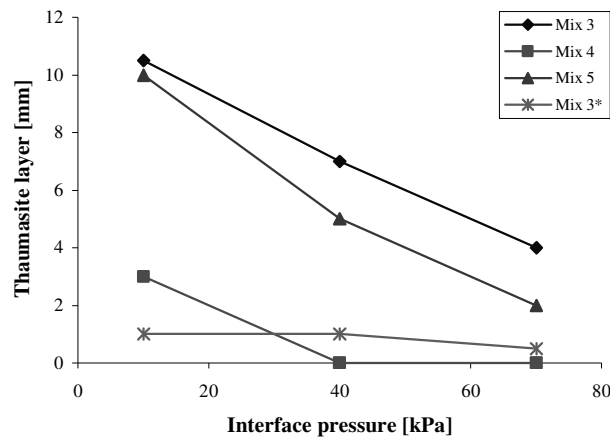
Figure 5.4 - Relationship thaumasite formation-pressure at 27th month, ECC-cast in-situ ([*18th month])

It is suggested that the thickness of the thaumasite layer depended on the time of onset of TSA, the rate of deterioration and the bulk density of the layer. Observations showed that the thaumasite layer was softer and looser at lower restraints. The formation of thaumasite with its accompanied products causes an increase in volume. The bulk density (compactness) of the reaction products is governed by the pressure and therefore the compactness increases with increasing pressure until the optimum bulk density is reached. Further increase of pressure will not affect the compactness. Observations on unrestrained and restrained Series I specimens (Section 4.2) showed an 'actual deterioration-expansion' ratio of 1:2 and 1:1, respectively.

The thaumasite formation at the two interface specimens developed to a different extent which is assumed to be caused by the design of the specimens. The cross section of the cylindrical Series IV specimens appeared to be too small to experience the same aggressive conditions as were present at the square Series V specimens. Furthermore the reservoir for the sulfate solution also seemed to be too low to supply a sufficient source of aggressive ions. Therefore the thickness of the thaumasite layer could not be included in the pressure dependency description and further analyses. Evaluations regarding the amount of thaumasite will be based on the results of Series V specimens but macroscopical and microscopical observations did not depend on the amount after a layer formed.

5.1.1.3   Comparison to Field Results

The extent of TSA attack at clay restrained specimens has been evaluated using the 'wear rating' method introduced by BRE [63], see Table 5.4, and compared to the results of the parallel laboratory trial to the Shipston-on-Stour field trial (Table 5.5) [2, 108]. Wear rating is discussed in Section 2.2.2.4. Crammond stated that the field observations correlated well with the laboratory results obtained after three years.

The level of attack measured in this investigation was converted into wear ratings; however, actual wear ratings have to be considered as greater in magnitude. The enhanced deterioration of the corners was neglected and equal deterioration on each side of a 100mm cube was assumed so that an idealised square deteriorated cube was obtained. To compare the ratings obtained with the results from BRE [108] deteriorations, Mix 4 specimens with comparable mix design (w/c=0.55; c=320kg/m^3) are used. This mix design conforms to the concrete used by BRE during the parallel laboratory field trial. Specimens were not subjected to any pressure and were not in contact with clay. The wear rating values of the lowest restraint in this investigation are used for comparison and were interpolated to 12 months assuming linear deterioration.

The wear ratings are up to 5 and are similar to the ratings from BRE; however, the increased vulnerability of the corners was not included. Therefore it is assumed that the actual wear ratings are slightly higher, despite there being a good correlation between the deterioration on Series V specimens and the cubes tested at BRE.

The deterioration rates obtained from Series I precast specimens, see Section 4.2, converted into wear ratings are summarised in Table 5.6. The rating for Mix 4 does not correlate well with the results obtained in Series V and the ratings provided by BRE. Series IV specimens showed the least attack during the period of 27 months and have therefore not been converted into a wear rating.

Table 5.4: Wear ratings of Series V specimens

Wear-ratings of attacked Series V specimens [mm]						
Lower Lias Clay						
Mix		**Precast surface with pressure of**			**Cast in-situ surface with pressure of**		
		10 kPa	*40 kPa*	*70 kPa*	*10 kPa*	*40 kPa*	*70 kPa*
Mix 3	290 0.75	*1.9*	0.9	0.9	*1.1*	0.6	0.3
Mix 4	320 0.55	***3.9***	1.9	1.4	***2.2***	0.5	0.8
Mix 5	320 0.75				*0.9*	1.1	1.6
English China Clay						
Mix		**Precast surface with pressure of**			**Cast in-situ surface with pressure of**		
		10 kPa	*40 kPa*	*70 kPa*	*10 kPa*	*40 kPa*	*70 kPa*
Mix 3	290 0.75	*7.5*	4.4	3.6	*3.3*	2.2	1.3
Mix 4	320 0.55	***5.0***	2.7	3.0	***0.9***	0.0	0.0
Mix 5	320 0.75				*3.1*	1.6	0.6
Mix 3*	290 0.55	*3.3*	1.7	1.6	*0.3*	0.3	0.2

* Thaumasite reaction time of 18 months instead of 27 months

Table 5.5: Wear ratings of cubes in laboratory exposure for one year, BRE [108]

Binder Type	Free w/b-ratio	Aggregate	Seal-cured cubes wear rating
PC (10% C_3A)	0.58	Carboniferous limestone	3.5; 4.0
PC (7% C_3A)	0.58	Carboniferous limestone	4.5; 5.0

Table 5.6: Wear rating of Series I specimens, 1.8% SO_4-solution

Mix	Rate of deterioration *[mm/year]*	Wear rating
Mix 1 (290-0.55)	2.1	1.5
Mix 2 (290-0.65)	2.7	1.9
Mix 3 (290-0.75)	3.1	2.2
Mix 4 (320-0.55)	1.8	*1.3*
Mix 5 (320-0.75)	3.7	2.6

Wear ratings do not fully express the features of TSA and can be affected by deterioration caused by conventional sulfate attack, Crammond [63]. The conversion of actual deteriorated depth on the surface was combined with problems incorporating the damage to the more vulnerable corners. Therefore the actual depth of deterioration should be reported to allow comparison within the literature.

5.1.2   Macroscopical Observations

The formation of a crust of 'sound' concrete was not observed in the cylindrical cast in-situ specimens, however, a very thin crust was observed at some specimens with a precast face. That suggests that carbonation governed the onset of TSA and therefore the thickness of the crust. The larger shear specimens showed that the density of the thaumasite layer depended on the applied pressure. Differences in the hardness of the thaumasite were also observed but not measured for the two casting surfaces. Thaumasite at the precast surfaces appeared to be softer and mainly without a hard crust which was often observed at cast in-situ surfaces which disagrees with the findings of the cylindrical Series IV specimens. It is suggested that the hard crust on the shear specimens was mainly caused by the pressure at the interface and secondly by carbonation since this can be precluded at cast in-situ faces.

The most important difference between unrestrained and restrained specimens was that in the restrained specimens the thaumasite formed attached as a cohesive mass of reaction products as shown in Figure 5.5 and Figure 5.6. The attached thaumasite had a soft surface and was often covered with a crust as in the case of Series V cast in-situ specimens. The thaumasite mass is described as a cohesive soft white 'mush' without binding abilities; however, it was so compacted through the pressure that it could not be compared with the incohesive mass observed in the unrestrained specimens. The thaumasite mass became very brittle and had a distinct white colouration after the sample was dried.

According to the observations made on Series IV specimens, it was concluded that a distinct thaumasite layer had developed in the Series V specimens after 21 months storage in an aggressive environment. This ensured that the concrete/clay interface deteriorated sufficiently to investigate the effects of TSA on skin friction. This

assumption was confirmed with the thaumasite found after shear tests were performed, see Section 5.1.1.2.

Figure 5.5 - Thaumasite layer at precast - LLC

Figure 5.6 - Thaumasite layer at precast - LLC, after sampling

The main observation of the thaumasite layer on the shear specimens was that precast samples with more than 5mm of reaction product layer and a boundary with English China Clay showed a different colouration, see Figure 5.7. The top layer was orange/reddish and the bottom layer close to the concrete had a greyish colouration. The greyish part of the layer was about 2-4mm and the rest of the thaumasite layer above was converted into the orange/reddish appearance. This implies the TSA-reaction products underwent a further process which is discussed in more detail in Section 5.1.4.
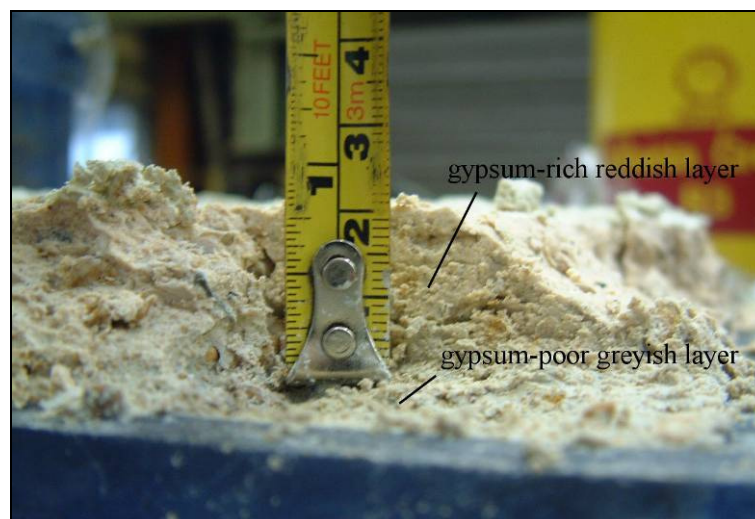
Figure 5.7 - Coloured TSA reaction product layers

5.1.3   Microscopical Observations

Microscopical observations performed by Sibbick [153] and the author on cylindrical Series IV specimens confirmed the degradation of the cement paste due to TSA in the precast specimens. The cast in-situ surface revealed less attack and only thaumasite formation (TF) occurred. This was particularly noticeable for the cast in-situ specimens with adjacent English China Clay in the case of the cylindrical Series IV specimens, see Table 5.1. ECC was found to be more aggressive than LLC towards porous surfaces of Series V specimens but the opposite was observed with low permeable surfaces such as Mix 4. Severe degradation was mainly found at the precast surface zone as shown in Figure 5.8 and underneath this degraded layer a fully carbonated zone was observed, see Figure 5.9. The fully carbonated zone particularly occurred at specimens with both a precast surface and a cast in-situ surface exposed to English China Clay. Initial carbonation was excluded as the cause since the cast in-situ specimens were cast directly against the clay and for that reason were completely sealed. It is assumed that carbonation could have taken place while the samples were dried for the preparation of thin sections. Nonetheless dissolved carbonate ions could also have favoured neutralisation processes in the decreased alkaline environment around the reaction front.
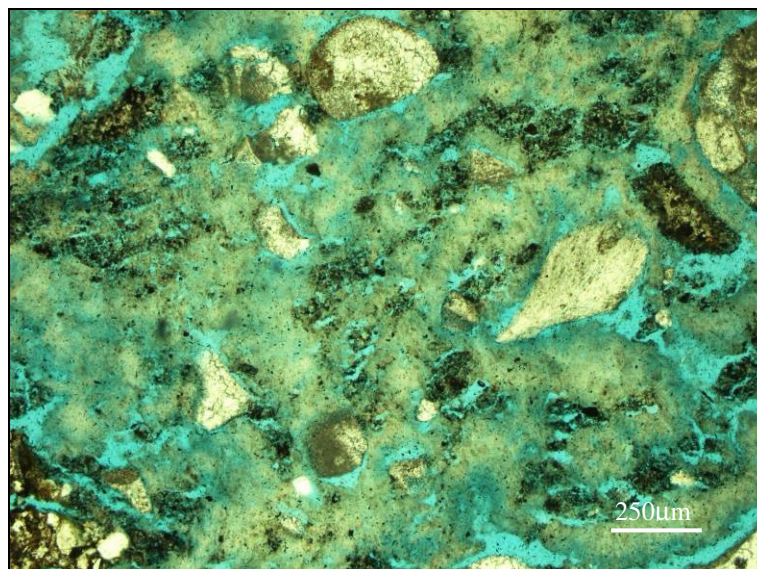
Figure 5.8 - Severe TSA at precast sample in contact with ECC after 15 months, plane polarised light (PPL)

The pH of the pure ECC was 5.4 compared to pH 7.7 for the LLC and pH measurements of the clay adjacent to the interface revealed values between 9.3 and 10 for ECC and pH 10.3 to 11.2 for LLC, see Section 5.3.3. It is suggested that this difference in pH favoured carbonation processes in the cement paste since dissolved bi-carbonate ions HCO_3^- were available, due to the dissolution of the limestone aggregate in pore solution. That would mean that thaumasite was able to form within the carbonated zone and even enhanced TSA, as the measured thickness of the thaumasite layer (Table 5.1) and the observations using the polarisation microscope showed. This disagrees with the formation conditions proposed by Gaze and Crammond [48] who suggested that thaumasite does not appear to form at a pH below 10.5. Carbonated areas possess a pH of circa 9 [28]. On the other hand microscopy showed heavily carbonated degraded zones without any residual thaumasite. It is assumed that de-calcification processes caused by the pH of the ECC carbonated the TSA/TF degraded cement paste since it was mainly observed at concrete surfaces in contact with ECC.

Further features observed were the presence of gypsum at the boundary with the clay, mainly with the Lower Lias Clay, and carbonate at the boundary with the English China Clay.
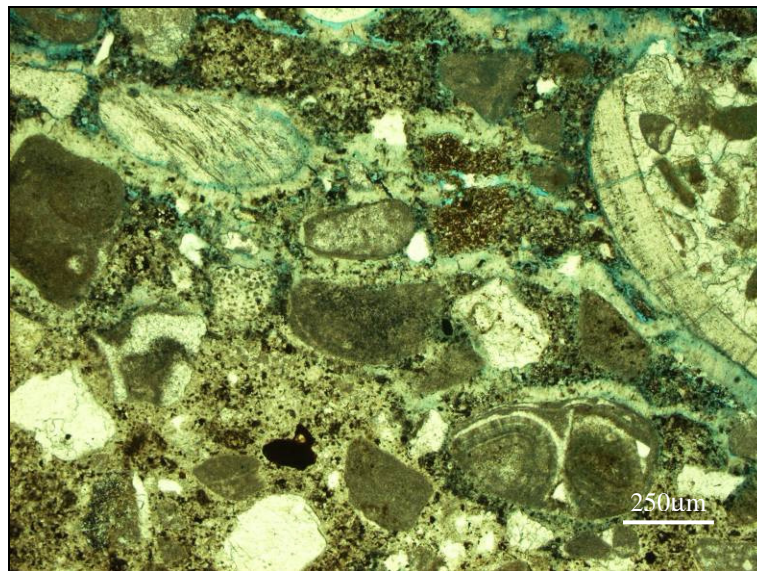
Figure 5.9 - Fully carbonated zone underlying degraded concrete surface at precast sample in contact with ECC after 15 months, plane polarised light (PPL)

5.1.4   X-ray Diffraction Analysis

XRD analyses on Series IV confirmed the presence of calcite, quartz, thaumasite and ettringite. Gypsum was detected in significant amounts in cast in-situ surfaces in contact with English China Clay and in traces in a few samples with precast surfaces in contact with ECC. Gypsum was not detected in deteriorated concrete in contact with Lower Lias Clay. Aragonite and brucite were rarely detected in any samples. Typical concentration distributions of the four major minerals detected are illustrated in Figure 5.10 and Figure 5.11.

Figure 5.10 and Figure 5.11 show the relationship between the mineral concentration and reaction time of specimens adjacent to Lower Lias Clay in aggressive 1.8% sulfate solution. The proportion of the thaumasite within the reaction products was significantly increased compared to the concentration observed at the unrestrained specimens as discussed in Section 4.2.1.4. Ettringite and quartz had similar concentrations regarding restrained and unrestrained specimens. This observation and the measured pH of the adjacent LLC of pH 10.3-11.2 supported the thaumasite stability theory of Gaze and Crammond [48] that the stability of thaumasite decreases with decreasing pH and that aragonite and in this case calcite are the final reaction products. The concentration of thaumasite was generally inversely proportional to the concentration of calcite but cast in-situ specimens in contact with LLC where high proportions of quartz were found. Therefore there was a direct relationship between the concentrations of thaumasite and calcite whereby ettringite and quartz were independent of this development.

Figure 5.10 - Development of mineral concentration at Mix2/PC/LLC (290-0.65)
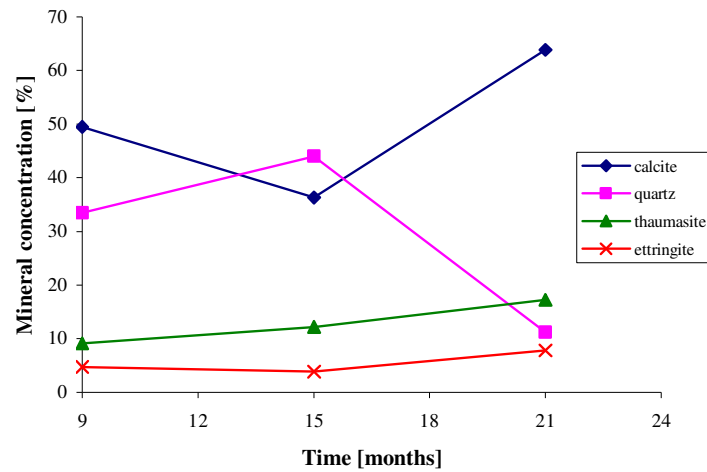
Figure 5.11 - Development of mineral concentration at Mix2/CS/LLC (290-0.65)

Further support for the decreased thaumasite stability was given by the mineral concentrations detected at samples in contact with the acidic English China Clay, see Figure 5.12 and Figure 5.13, where the zone of clay adjacent to the concrete had a pH of 9.3 to 10.0. The decreased thaumasite concentration and the presence of gypsum in the case of the cast in-situ surface confirmed the findings of Sahu [44] and Zhou et al. [57]. Sahu observed the co-existence of thaumasite and gypsum at pH of 10-11 and Zhou et al. [57] observed gypsum as the dominant degradation product by acidic conditions, see Section 2.3.3.
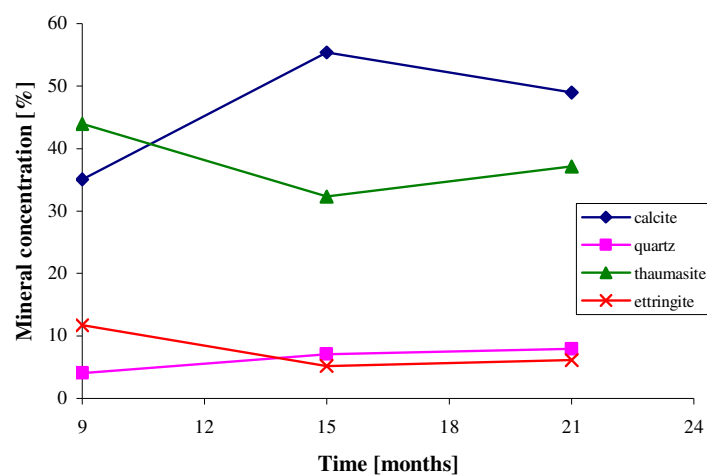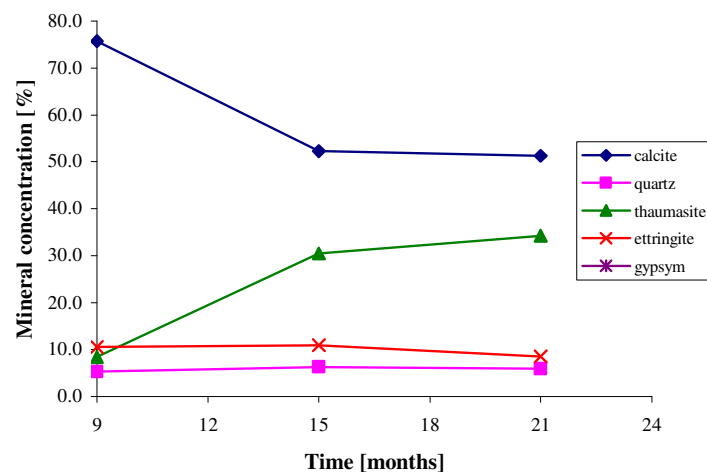

Figure 5.12 - Development of mineral concentration at Mix2/PC/ECC (290-0.65)
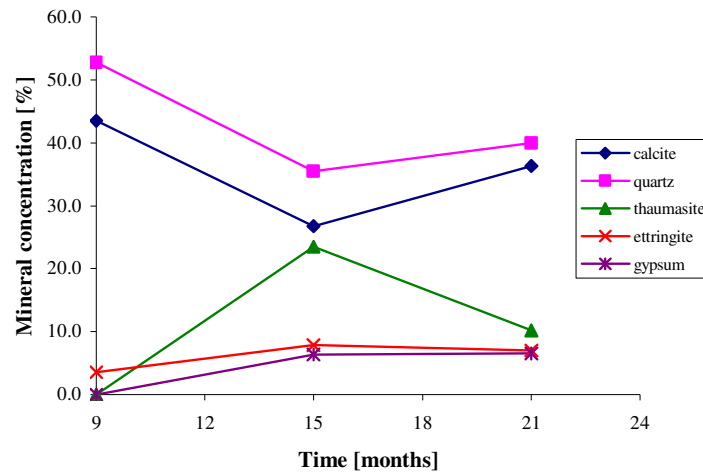
Figure 5.13 - Development of mineral concentration at Mix2/CS/ECC (290-0.65)

The absence of aragonite and, for the most part, gypsum except for CS-ECC-interfaces, formed the main difference in the XRD pattern between unrestrained and restrained surfaces being under attack. The pH value of the ambient conditions was assumed to be the responsible factor.

X-ray diffraction analysis of the TSA reaction products at the interface of the shear specimens also detected the presence of calcite, quartz, thaumasite, ettringite and traces of gypsum confirming the reaction products found at Series IV-specimens. The two different coloured TSA reaction product layer showed different concentration distributions which are semi-quantitatively illustrated in Figure 5.14. The greyish layer close to the 'sound' concrete had similar mineral concentrations as the TSA mass at the specimens where no colouration was observed. However, the reddish coloured layer showed a significantly increased amount of gypsum which indicates that the reaction products, particularly thaumasite, underwent a further reaction process. The differences in the concentrations of thaumasite and gypsum are more clearly represented in Figure 5.15 which excludes the detected amount of calcite. The increased amount of aggregate grains caused calcite dominance in the greyish layer close to the 'sound' concrete. The concentration of gypsum increased significantly in favour of the thaumasite and ettringite leading to the conclusion that thaumasite and ettringite were less stable in the present conditions than gypsum. The two layers occurred particularly at the boundary with ECC where a substantial deterioration occurred and a pH of 9.7-10.0 was

measured. It is assumed that the pH within the product layer dropped gradually from the concrete/thaumasite to the thaumasite/clay interface. Therefore it is suggested that the TSA reaction products of the greyish layer can be considered as initial or intermediate reaction products which react/carbonate to form gypsum and secondary calcite depending on the alkaline environment. Gypsum and secondary calcite are considered as the final degradation products of the thaumasite form of sulfate attack as suggested by Crammond [2].

Figure 5.14 - Reaction product distribution of the two layers
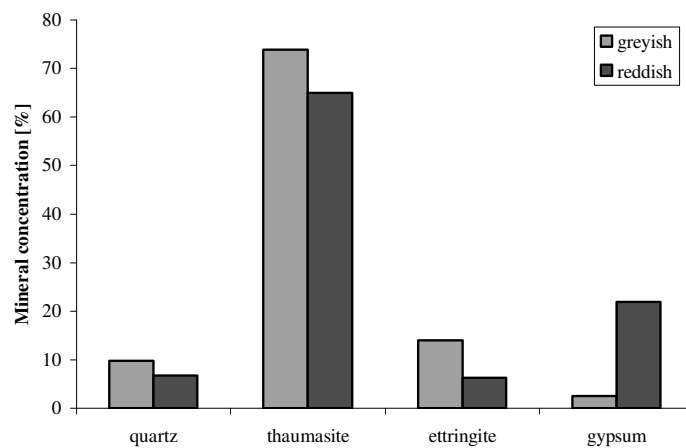
Figure 5.15 - Reaction product distribution of the two layers, excluding calcite

The observation by Zhou et al. [57] that gypsum was the dominant degradation product in acidic conditions supports the present results that thaumasite and ettringite

decompose in favour of gypsum. It is concluded that the decomposition process takes place immediately in acidic conditions after thaumasite deterioration occurred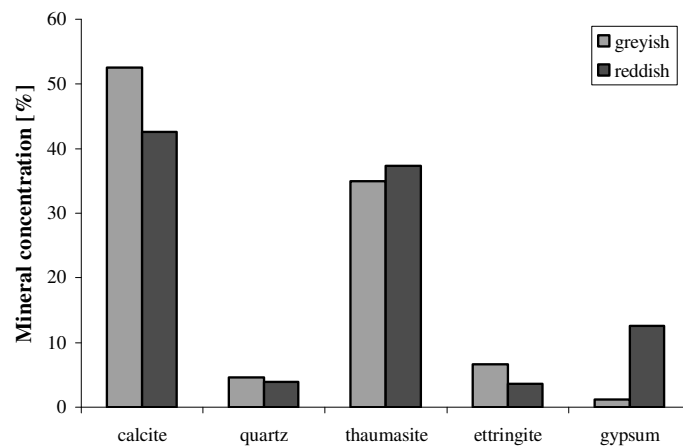 in the alkaline environment of the concrete pore solution. This is caused by the exposure of the reaction products to acidic conditions due to increased accessibility.

5.1.5   Summary

TSA under clay-restrained conditions formed a compacted cohesive mass of reaction products which was attached to the concrete. The amount of thaumasite formed differed significantly between the cylindrical Series IV and Series V shear specimens so that Series V specimens are used for further evaluation processes. It was assumed that enhanced aggressive conditions were present in the square shear strength specimens. These showed a maximum thaumasite layer of up to 25mm whereas up to 7mm were measured at Series IV specimens. The design of the cylindrical Series IV specimens was most probably not appropriate for an acceleration of TSA for clay-restrained conditions. The comparison of the deterioration depths with wear ratings from BRE laboratory investigations correlated well in the case of Series V specimens. Converted Series I specimens showed significantly lower wearing ratings for a period of one year.

The non-sulfate containing ECC favoured TSA at the highly susceptible precast surface whereas TSA was lower at the low susceptible cast in-situ surface. Series V specimens with a highly permeable surface showed a relatively thick thaumasite layer of up to 10mm. The typical 'sound' concrete crust was rarely found but dependencies of the compactness of the thaumasite layer on the pressure were observed.

Carbonated zones were mainly observed at the precast face with a boundary to ECC, where the cement paste and TSA reaction products were heavily carbonated. Due to the nature of the carbonated zone, in that it was found behind the reaction front, it was assumed that thaumasite was able to form within this zone. Subsequently thaumasite was decomposed to calcite and gypsum caused by the de-calcification processes. Therefore thaumasite can be considered as an intermediate reaction product and not the final degradation product, agreeing with Crammond [2].

X-ray diffraction analyses on Series IV specimens supported these observations, with the detection of a decreasing concentration of thaumasite and an additional formation of gypsum when concrete was in contact with acidic English China Clay. The ambient

interface conditions revealed a pH of 9.3-10. Furthermore the different colouration within thaumasite layer in the shear specimens showed an increasing amount of gypsum towards the clay boundary. This confirms the suggestion that thaumasite is an intermediate reaction product. The concentration of thaumasite decreased with a decreasing pH and the amount of calcite and gypsum increased simultaneously. Aragonite was only observed in traces and so it is assumed that aragonite forms mainly in unrestrained conditions.

5.2   Physical Interactions

5.2.1   Shear Strength

The shear strength at the concrete/thaumasite/clay interface was determined according to BS 1377-7:1990 by the direct shear test with consolidated drained conditions using a direct shear box apparatus, see Section 3.2.4. The shear tests for one set of specimens were performed using three different pressures (10, 40, 70 kPa) with each of two specimens. One set of specimens is related to one combination of concrete mix, casting position and clay. The typical shear stress curves obtained for one set of specimens are illustrated in Figure 5.16 and as it can be observed, the peak shear stress and the residual shear stress were clearly developed. It was assumed that the residual shear stress was developed within 15mm of displacement and that further reductions in shear stress were mainly caused by the constant loss of shear area.

Despite the interface being differentially affected by the formation of thaumasite, the shear strength parameters were calculated according to the standard method, BS 1377-7:1990. Thaumasite formed to a different extent at the interface caused by the three normal loads, as can be seen in Table 5.2.

In the following discussion on the shear strength parameters, φ' and δ' represent the internal friction of the clay and skin friction at the interface, respectively. The term skin friction (δ') is mainly used in connection with interface investigations. The expression for cohesion is generally used for the shear strength both within the clay c' and at the interface c_a' despite that it involved adhesion. According to the definition of the term,

adhesion describes the force between two different materials, i.e. when shearing occurs directly at the interface.
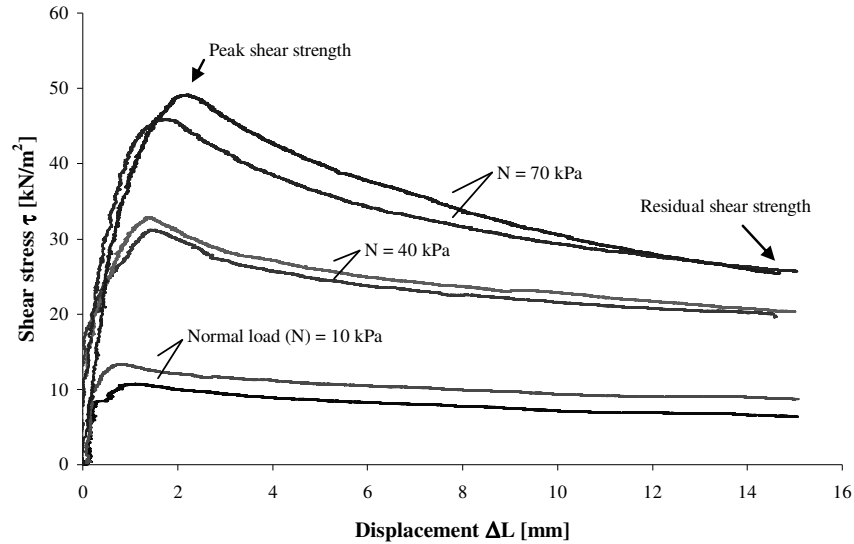
Figure 5.16 - Shear stress - displacement curves for concrete/soil interface with 3 different normal loads, Specimen set: Mix 3/PC/LLC (290-0.75)

The shear strength parameters δ' and c_a' were obtained by plotting the peak and residual shear stress from the direct shear test curves, Figure 5.16, against the effective normal load. The data are based on the initial shear area of $200 \times 200 mm^2$. This is illustrated in Figure 5.17 and Figure 5.18 for the peak and the residual shear strengths, respectively. In addition to the concrete/thaumasite/clay interface results, those for the pure clay tests are also plotted. In the case of Mix 3-PC-LLC both the peak shear stress diagram (Figure 5.17) and the residual shear stress diagram (Figure 5.18) show that the skin friction δ' increased and the cohesion c_a' decreased significantly at the TSA affected interface. However, the effect of TSA on skin friction and cohesion is based on the relation to unaffected concrete/clay control interfaces. The parameters for the concrete/LLC control interface were estimated using the relationship of internal to skin friction for the pure ECC to concrete/ECC interface which was experimentally obtained. It was assumed that this relationship of internal friction to skin friction is similar in the case of ECC and LLC. Therefore no control specimens were produced for the interface concrete/LLC condition.
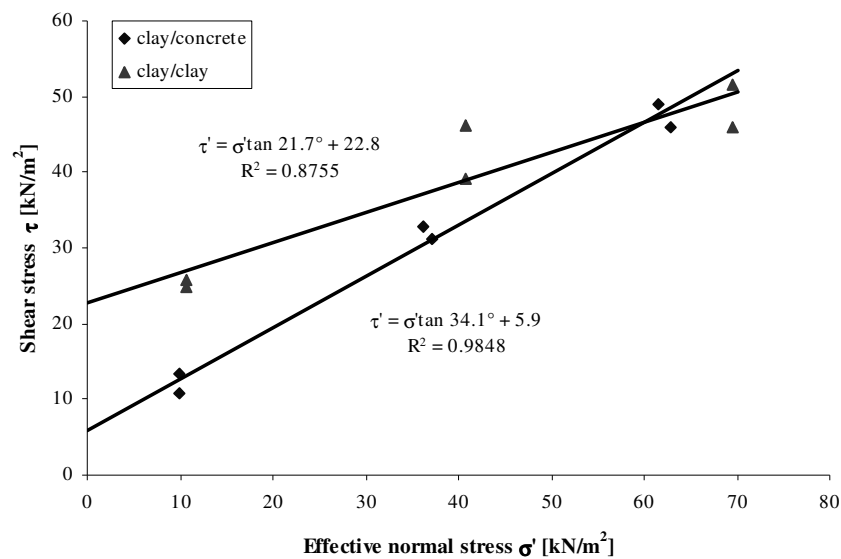
Figure 5.17 - Relationship between peak shear stress and effective normal stress of TSA affected specimen set: Mix3/PC/LLC (290-0.75), 27 months, and pure LLC/LLC interface
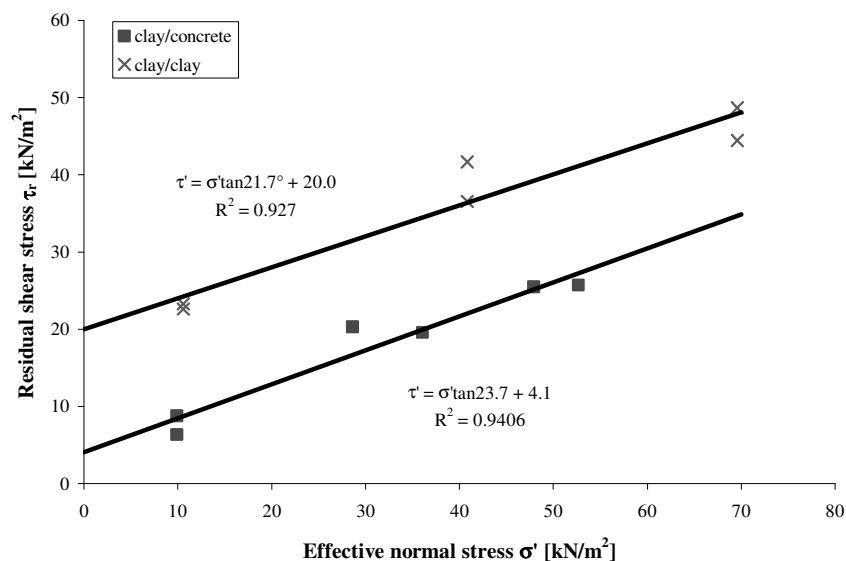
Figure 5.18 - Relationship between residual shear stress and effective normal stress of TSA affected specimen set: Mix 3/PC/LLC (290-0.75), 27 months, and pure LLC/LLC interface

The shear strength parameters for all the variations investigated are shown in Table 5.7, including the age of the interface, the peak shear stress, the residual shear stress and the water content present at the interface. The latter affects the shear strength such that an increase in the interface water content reduces the shear strength. However, it was intended to obtain similar water contents for each set of specimens to minimise this

influence. The water content at the interface of each set of specimens was found to be similar hence this factor is not discussed further.

Table 5.7: Direct shear test results of the samples used

Sample series	Age	Shear stress		Residual shear stress		Water content interface
	[months]	φ' or δ [°]	c' or c_a' [kN/m²]	φ_r' or δ_r' [°]	c_r' or $c_{a,r}'$ [kN/m²]	w [%]
Interface – Lower Lias Clay						
Clay/clay	-	21.7	22.8	21.7	20.0	26.2
Estimated control - precast	-	*26.6*	*4.1*	*20.1*	*6.3*	-
Mix 3-precast	27	34.1	5.9	23.7	4.1	27.9
Mix 4-precast	27	31.5	9.6	23.5	6.6	28.7
Estimated control - cast in situ	-	*27.8*	*5.4*	*25.2*	*6.3*	-
Mix 3-cast in-situ	27	32.0	10.0	27.0	5.6	36.7
Mix 4-cast in-situ	27	33.2	10.3	34.4	2.3	28.2
Mix 5-cast in-situ	27	37.0	4.6	31.9	2.2	35.1
Interface – English China Clay						
Clay/clay	-	18.1	12.3	16.0	10.1	31.8
Control Mix 3-precast	6	22.2	2.2	14.7	3.2	40.8
Mix 3-precast	18	30.7	11.6	20.2	5.5	33.6
Mix 3-precast	27	25.0	16.7	23.0	7.5	35.7
Mix 4-precast	27	26.4	12.8	19.4	9.6	37.6
Control Mix 3-cast in-situ	6	23.2	2.9	18.4	3.2	37.3
Mix 3-cast in-situ	18	27.7	5.4	19.5	5.2	31.9
Mix 3-cast in-situ	27	21.4	12.4	12.9	9.9	32.5
Mix 4-cast in-situ	27	27.8	4.2	23.5	3.1	32.9
Mix 5-cast in-situ	27	26.1	10.0	16.4	9.8	33.5

Changes of the shear strength parameters, depending on the amount of thaumasite formed at the interface, are analysed using the ratio of the shear strength parameters affected by TSA to the parameters obtained at the control specimens, these being

$$\delta'_{TSA} \Big/ \delta'_{control} \quad \text{and} \quad c'_{a\,TSA} \Big/ c'_{a\,control} \, .$$

Potyondy [122] used a similar approach of comparing the shear strength of clay φ' with the skin friction δ' (see Section 2.9.4.2, Figure 2.7). The main aim of the investigation was to determine the effect of TSA on skin friction at the interface and therefore the skin friction at the control interface was used for comparison. It should be noted that estimated shear strength parameters were used for the LLC interface based on the ECC ratios obtained. The amount of thaumasite relating to the ratio of TSA shear strength parameters to control parameters is the average value of the thaumasite formed for one set of specimens. One set consists of six specimens with three different pressures. The mean values of two specimens with the same pressure within one set are represented in Table 5.2. This type of representation was chosen to show detailed changes of the skin friction δ' and the cohesion c_a'. The influence of the different thicknesses of thaumasite within one set of specimens had to be neglected in this approach and an average value was assumed.

The skin friction ratio $\delta'_{TSA} \Big/ \delta'_{control}$ was generally scattered above 1 with one exception where $\delta'_{TSA} \Big/ \delta'_{control} = 0.92$, as can be seen in Figure 5.19. A clear trend line for thaumasite influenced changes on skin friction in the Lower Lias Clay and English China Clay interfaces was not possible to obtain. However, a generally increased skin friction was observed when thaumasite occurred. Skin friction generally increased by 10% in the case of thaumasite formation with the one exception. It is suggested that this one value can be considered as the result of a reduction of normal load during testing. Because of limitations with the equipment some loss of normal load occurred during the majority of tests, however, this was generally in the order of 5-10% whereas in this case 30% of the original load was lost.

Concrete and clay are inhomogeneous materials and a good correlation at their interface is not expected. In the case of this investigation the trend is of importance.
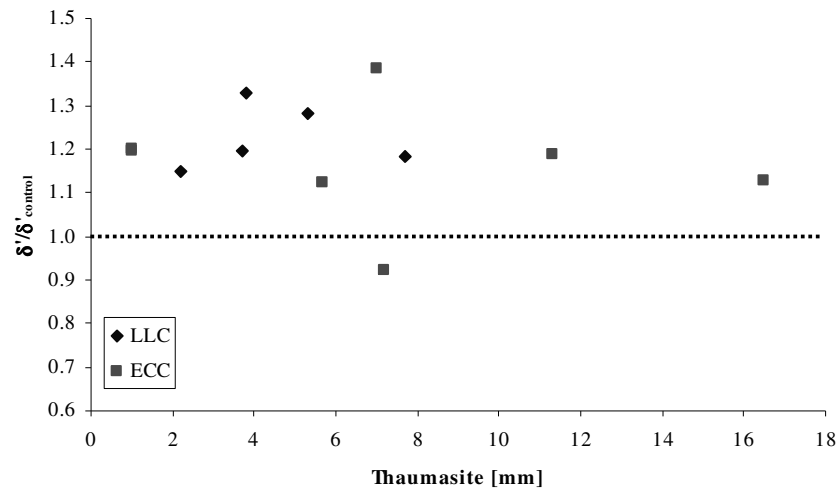
Figure 5.19 - Thaumasite influenced changes of skin friction δ' for all specimen sets, age 27 months
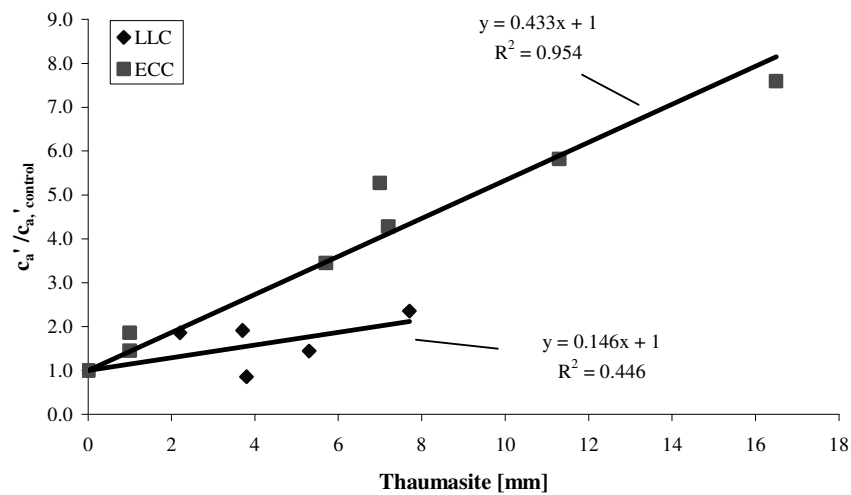
Figure 5.20 - Thaumasite influenced changes of cohesion c_a' for all specimens sets, age 27 months

The influence of the thaumasite formation on the shear strength parameters was greater for the cohesion c_a', see Figure 5.20. A significant positive effect of TSA was observed at the ECC interface which showed an increase of cohesion of around 40% per millimetre of thaumasite. The cohesion at the Lower Lias Clay interface increased with each millimetre of thaumasite up to 14% but one outlying result was found with 0.86. However, it should be noted that the shear plane mainly occurred within the clay in specimens with the artificial very fine grained English China Clay adjacent to the concrete. At the interface with the naturally coarse grained Lower Lias Clay, the shear

plane was predominantly observed at the interface of the thaumasite/clay and within one millimetre of the clay from the interface. Shearing at the control samples occurred directly at the interface which was rarely observed at the TSA affected interfaces, see Section 5.2.2. Additionally, it is suggested that cementation/stabilisation processes within the clay adjacent to the interface contributed as a positive effect on the shear strength parameters. These processes will be described in more detail in Section 5.3.3.

The evaluation of the residual shear strength parameters did not create a clear regression with regard to the dependency of the change of the parameters on the formed thaumasite; see Figure 5.21 and Figure 5.22. Two outlying results were encountered in the evaluation of the residual skin friction, Figure 5.21, and five within the residual cohesion, Figure 5.22. Nonetheless it is obvious that there is a positive trend in the enhancement of the shear strength rather than a negative trend causing reduction of skin friction at TSA affected concretes. The residual cohesion values decreased until an amount of thaumasite of 4mm and subsequently increased steadily.

The poor regressions obtained during the evaluation of the shear strength parameters δ' and c_a' may be caused by the use of specimens with different amounts of thaumasite formed under three pressures. This evaluation method is based on BS 1377-7:1990 and several sources of specialist guidance [111, 112, 113] for unaffected soil/structure interfaces. Guidelines for testing deteriorated interfaces do not exist.
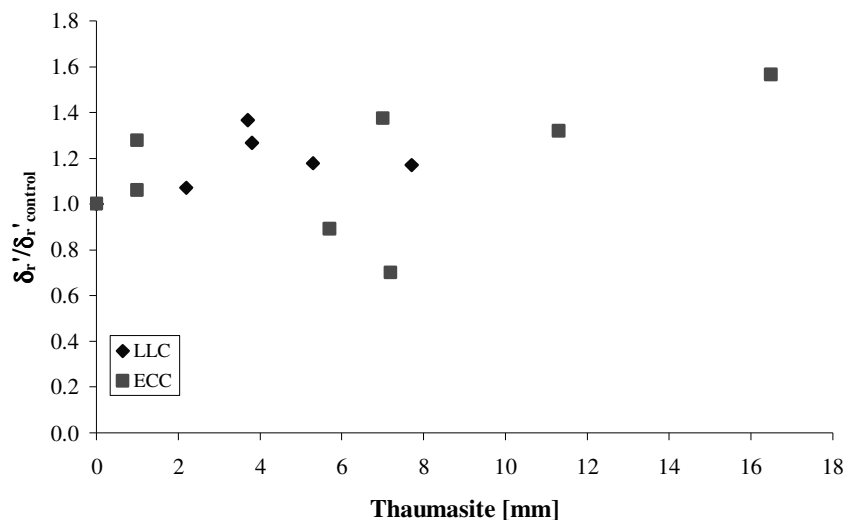
Figure 5.21 - Thaumasite influenced residual skin friction δ_r', all specimen sets, 27 months
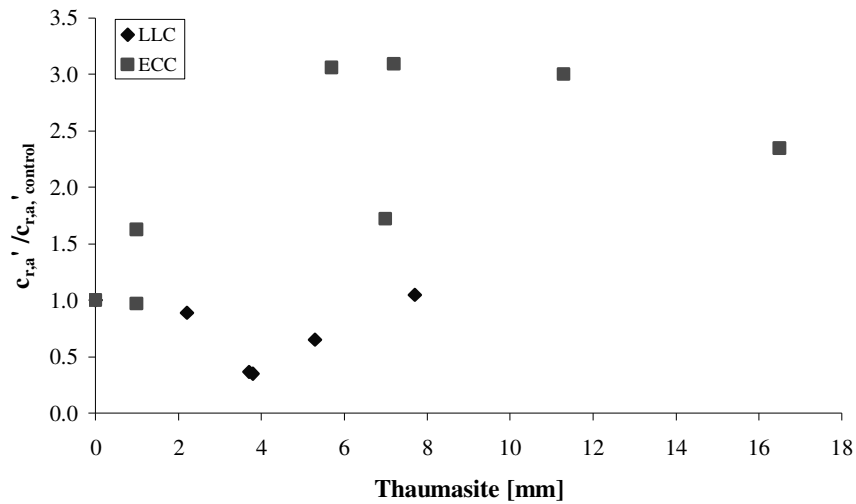
Figure 5.22 - Thaumasite influenced residual cohesion $c_{r,a}'$, all specimen sets, 27 months

Based on the standard evaluation, the results showed a general positive effect of TSA on skin friction. The effects of TSA on the interface behaviour were also assessed by a second method. This method involved changes of the shear stress directly dependent on the thaumasite formed and it was intended to obtain more expressive values for the residual shear strength.

The idea was to determine the influence of TSA on the shear strength for each interface which was characterised through the upload and resulting thickness of thaumasite. Each interface was independently evaluated from its set of specimens as used above. The factor of change, 'TSA-factor', was calculated from the ratio between the measured shear stress affected by TSA to the shear stress of the control sample at equal normal stress. The TSA-factor was determined at each interface for both the peak shear strength, $\tau_{TSA}/\tau_{control}$ and the residual shear strength $\tau_{r,TSA}/\tau_{r,control}$ which are summarised in Table 5.8.

Table 5.8: Factor for shear strength change of TSA affected/control sample of each test, age 27 months

Sample	Pressure	Precast			Cast in-situ		
		$\dfrac{\tau_{TSA}}{\tau_{control}}$	$\dfrac{\tau_{TSA_{residual}}}{\tau_{r,control}}$	Thaumasite	$\dfrac{\tau_{TSA}}{\tau_{control}}$	$\dfrac{\tau_{TSA_{residual}}}{\tau_{r,control}}$	Thaumasite
	[kPa]	*[-]*	*[-]*	*[mm]*	*[-]*	*[-]*	*[mm]*
Interface – Lower Lias Clay							
Mix 3 (290-0.75)	10	1.39	0.85	6	1.52	0.97	3.5
	40	1.37	1.01	2.8	1.33	1.02	2
	70	1.36	1.06	2.8	1.28	1.04	1
Mix 4 (320-0.55)	10	1.74	1.10	12.5	1.58	0.82	7
	40	1.42	1.14	6	1.37	1.19	1.5
	70	1.35	1.15	4.5	1.33	1.24	2.5
Mix 5 (320-0.75)	10	-	-	-	1.13	0.76	3
	40	-	-	-	1.31	1.05	3.5
	70	-	-	-	1.35	1.15	5
Interface – English China Clay							
Mix 3* *18months (290-0.75)	10	2.81	1.58	10.5	1.49	1.34	1
	40	1.87	1.47	5.5	1.32	1.20	1
	70	1.74	1.46	5	1.29	1.16	0.5
Mix 3 (290-0.75)	10	3.43	2.02	24	2.30	1.88	10.5
	40	1.86	1.79	14	1.40	1.20	7
	70	1.63	1.75	11.5	1.24	1.06	4
Mix 4 (320-0.55)	10	2.85	2.26	16	1.32	1.14	3
	40	1.75	1.79	8.5	1.26	1.23	0
	70	1.57	1.66	9.5	1.25	1.25	0
Mix 5 (320-0.75)	10	-	-	-	2.08	1.96	10
	40	-	-	-	1.48	1.36	5
	70	-	-	-	1.36	1.18	2

The TSA-factor of the peak shear strength and the residual shear strength is illustrated graphically in Figure 5.23 to Figure 5.26. The trends for the Lower Lias Clay and the English China Clay showed increases of shear strength of up to 8% per millimetre of thaumasite formed for both the peak shear strength and the residual shear strength. The best regressions were obtained for the artificial fine grained English China Clay with an increase of up to 8% per millimetre for the peak shear strength and up to 5% for the residual shear strength. The positive effect of TSA on skin friction at the boundary to the natural coarse grained Lower Lias Clay was less, whereby an increase of 3% for the peak shear strength was calculated despite no correlation. The residual shear strength trend of the LLC interface was considered as positive. Nonetheless a percentage

increase of skin friction has not been calculated because of the wide distribution of the data and the subsequent not existing correlation coefficient of R^2=0.053.

The differences between the correlation coefficients for the LLC and ECC interface were most likely caused by the characteristics of the clays, particularly by the particle size distribution; see Section 3.3.2, Figure 3.22. The lower correlation for the natural LLC was caused by the wider particle size distribution compared to the narrow distribution of the artificial English China Clay. Oversize particles and other inhomogeneous material might have additionally affected the correlation. The narrowly distributed ECC is essentially homogeneous. It is suggested that the trends seen in the graphs of the artificial ECC reflect the effects of TSA on skin friction. Natural soils behave differentially and quantitative statements to the increase in skin friction caused by TSA should be considered carefully.
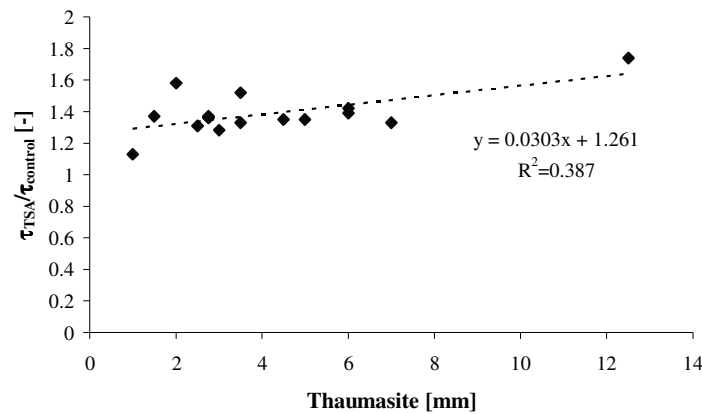
Figure 5.23 - Relationship TSA-factor/thaumasite for LLC samples, peak strength, 27 months
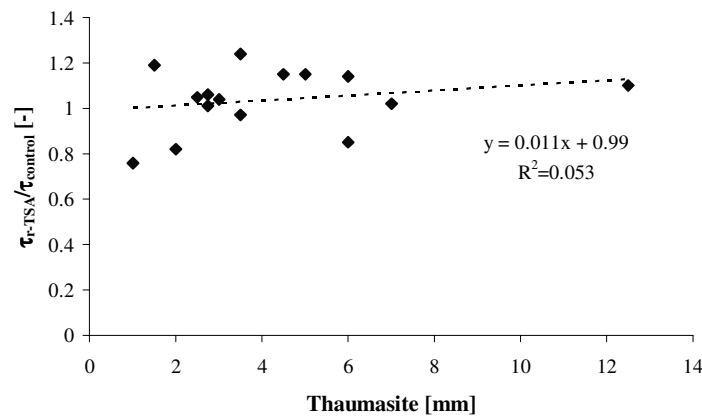
Figure 5.24 - Relationship TSA-factor/thaumasite for LLC samples, residual strength, 27 months
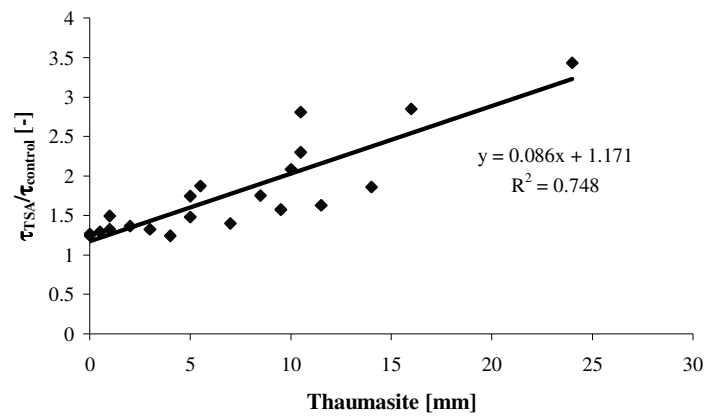
Figure 5.25 - Relationship TSA-factor/thaumasite for ECC samples, peak strength, 27 months
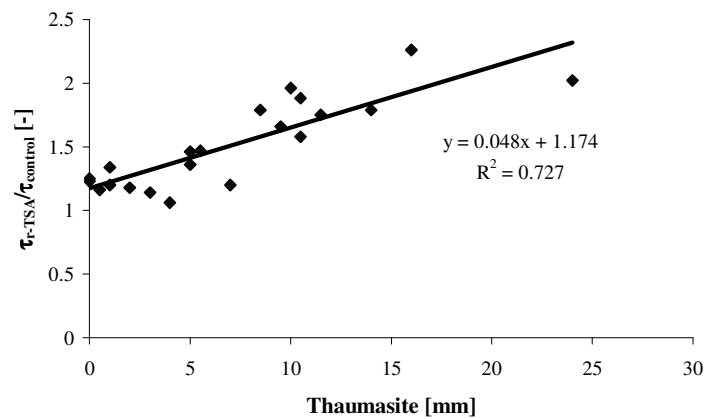
Figure 5.26 - Relationship TSA-factor/thaumasite for ECC, residual strength, 27 months

The evaluation of the shear strength including the two methods employed is summarised in Table 5.9, however, as already noted, the positive trend is more significant than the actual increase.

Table 5.9: Summary of percentage effect of TSA on shear strength

Interface	Shear strength parameter evaluation		Shear strength	
	δ	c_a'	τ	$\tau_{residual}$
LLC	10%	14%/mm$_{th.}$	3%/mm$_{th.}$	±0%
ECC	10%	40%/mm$_{th.}$	8%/mm$_{th.}$	5%/mm$_{th.}$

The relationship between skin friction and internal clay friction was investigated, amongst others, by Potyondy [122] and Lee [126]. The results obtained in this

investigation showed an increased skin friction in the control samples compared to the internal friction of the clay adjacent to the concrete, Table 5.10. This was in contrast to the findings of Potyondy [122] who observed that the skin friction at the interface between clay and concrete, steel and wood was mainly less, or in the case of smooth concrete, almost equal to the internal friction of the clay, see Section 2.9.4.2. Therefore Potyondy [122] concluded that the skin friction values should be reduced in cases where the skin friction is responsible for the bearing capacity. Nonetheless Lee [126] observed an increase in skin friction with increasing curing time whereby the skin friction exceeded the internal friction of the clay itself. That indicates that chemical interactions caused the increase, as suggested, for example, by Burland and Twine [155]. The long time curing effect on skin friction was considered as a contributor besides TSA increasing the skin friction and in particular the cohesion as already discussed above. The difference of the cohesion factor at TSA unaffected interfaces to Potyondys' [122] results were most probably caused by the high interface moisture content. However, Chandler [116] and Burland [117] considered a loss of cohesion at an unaffected interface compared to the internal clay cohesion and neglected the influence of cohesion c' for the reason of it being destroyed during pile installation.

Table 5.10: Relationship between shear strength and skin friction of clay unaffected by TSA

Friction on	δ'/φ'	c_a'/c'	Moisture content w [%]
Clay/concrete-PC	1.23	0.18	40.8
Clay/concrete-CS	1.28	0.24	37.3
Clay/smooth concrete [122]	0.97	0.57	22.8
	0.82	0.52	26.1

It is suggested that the expansion of the surface with the connected compaction of the clay adjacent to the concrete (Figure 5.27) was the second and main contributor to the increase of skin friction besides the curing effect. This conclusion derives from the percentage increase of skin friction per millimetre of thaumasite, see Table 5.9. Nonetheless this occurred under laboratory conditions and therefore it is suggested that this effect is much less in field conditions. The pressure distribution zone is significantly increased in the field.
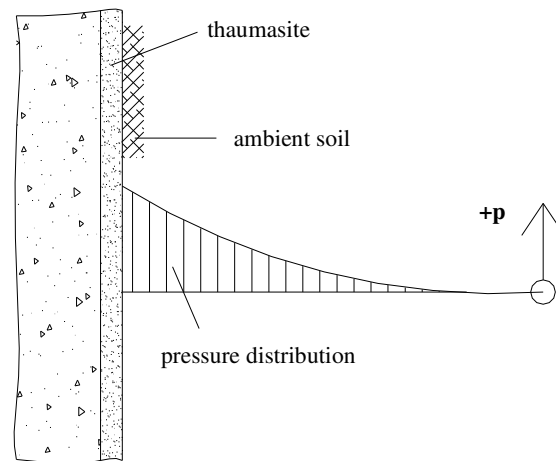
Figure 5.27 - Expansion pressure distribution in adjacent soil caused by TSA

5.2.2   Shear Plane

The shear plane symbolises the weakest point within the interface system 'concrete-thaumasite-clay' which was able to form at three main locations. These were the thaumasite, at the interface thaumasite/clay and within the clay. Two additional shear planes were observed. These were a zone of clay close to the interface and a combination of the three main shear planes where shearing occurred within thaumasite, interface and clay, see Figure 5.28 and Figure 5.29. The shear planes observed in the specimens (PC/CS, LLC/ECC) are summarised in Table 5.11.

Figure 5.28 - Combined interface shear plane, clay view

Figure 5.29 - Combined interface shear plane, concrete view

Table 5.11: Percentage location of shear plane

Specimens	Shear plane located within			
	Interface	**Interface-clay**	**Clay**	**Specimens**
Control				
ECC-PC	33%	33%	33%	6
ECC-CS	0%	0%	100%	6

	Thaumasite	**Interface thaumasite/clay**	**Thaumasite-interface-clay**	**Interface close clay zone**	**Clay**	**Specimens**
TSA						
ECC-PC	0%	11%	33%	0%	56%	18
ECC-CS	0%	0%	0%	17%	83%	24
LLC-PC	0%	8%	67%	8%	17%	12
LLC-CS	0%	0%	0%	72%	28%	18

It is clearly visible from Table 5.11 that the weakest point of the interface system 'concrete-thaumasite-clay' was not the 'mushy' thaumasite layer which did not possess any binding ability. The shear plane mainly occurred in two scenarios. The first one with shearing occurred within the clay, either very close to the actual thaumasite-clay interface (1-2mm from the interface for LLC-CS) or further into the clay (>5mm for

ECC-PC/CS). The second can be described as a combination of thaumasite-interface-clay shearing whereby the interface formed the main shear plane (LLC-PC). A strong dependency of the shear plane was observed on the casting position. Concrete-clay boundaries with precast surface sheared preferentially at the interface and with cast in-situ surface shearing occurred mainly within the clay. The artificial fine grained ECC formed mainly the point of weakness compared to the natural LLC where shearing preferred to occur around the interface, see Table 5.12.

Table 5.12: Main location of shear plane depending on clay and casting position

Dependency of clay		Dependency of casting surface	
ECC	**LLC**	**Precast**	**Cast in-situ**
Shear plane in clay	Shear plane in interface close areas	Shear plane mainly in interface	Shear plane mainly in clay and interface close areas

The surface roughness is a major factor for the development of skin friction. Additionally the roughness is responsible for the location of the shear plane which is transferred into the clay dependent upon the roughness of the surface, as suggested by Zong-Ze et al. [119] and by Useugi and Kishida [128]. It is assumed that the different shear planes depend partly on the additional compaction, caused by expansion, and partly on the smoothness of the thaumasite layer, however, that cannot be clearly confirmed. Despite the smooth nature of thaumasite, aggregate grains embedded in the surface increase the roughness. The observed shear planes were in disagreement with the assumption of Potyondy [122] that the interface is the weakest point, although they confirmed the possible shear plane descriptions of Zong-Ze et al. [119], see Section 2.9.4.2.

5.2.3   Settlement

The settlement of the clay was measured at two subsequent stages during the process of the shear box test. An initial settlement was measured after the specimens were installed in the shear box and underwent the pre-test consolidation phase, while the second stage of settlement monitoring was performed during the shear test. Settlements depended on

the load, the storage consolidation stage before the specimen was installed and on the rebound of the clay during the preparation of the specimen. The storage consolidation stage was additionally affected by the amount of thaumasite formed. The settlements did not undergo a particular trend due to these variables. However, as the normal load increased, settlement also increased leading to a loss in normal load which was accommodated in the shear strength calculations.

5.3   Chemical Interactions

Chemical interactions between concrete and clay were determined by the investigation of up to 50mm of the clay adjacent to the interface. The main aims were to determine the change of moisture content and pH within this area. Additionally the effect of TSA on the mineralogical composition of the clay was investigated.

5.3.1   Macroscopical Observations

Different macroscopical clay structures were observed during sampling. The first approximately 10mm of clay showed a friable structure which was mostly separated by cracks from the main body, see Figure 5.30 and Figure 5.31. This zone also appeared drier than the samples further into the clay. However, the moisture content of this zone was higher than further into the clay, see Section 5.3.2.
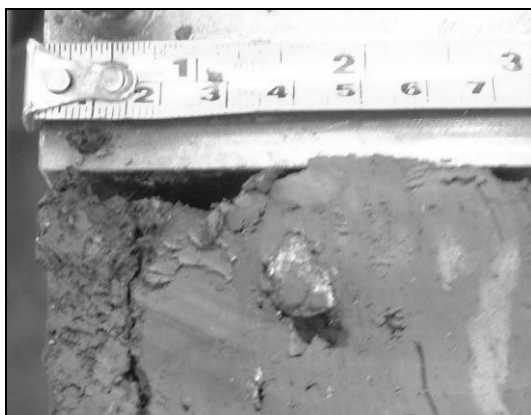
Figure 5.30 - Interface adjacent macroscopical
clay structure, LLC

Figure 5.31 - Interface adjacent macroscopical
clay structure, ECC

5.3.2   Water Content

The typical moisture content distribution of the clay adjacent to the interface is illustrated in Figure 5.32, also see Appendix G. It is clearly visible that the moisture content at the interface was significantly increased compared to the relatively consistent moisture content measured afterwards. Measurements were performed at clay layers with a thickness of 10mm and therefore the interface moisture at 5mm refers to the moisture content of the zone 0-10mm from the interface. A slight dependency of the interface pressure on the moisture content was visible caused by the different compaction, however, a direct dependency due to this or the casting position is not clearly defined.
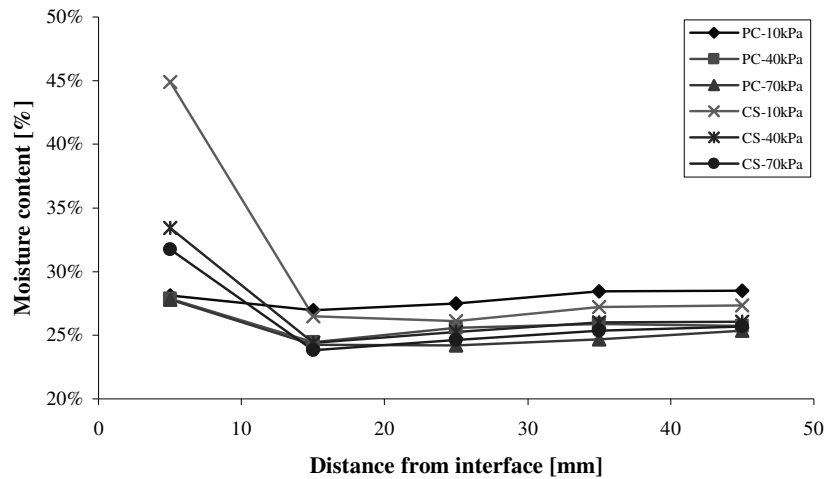
Figure 5.32 - Relationship moisture content - interface distance, Mix 3-LLC (290-0.75)

Several authors such as Lee [126] and Milititsky et al. [138] investigated the moisture behaviour towards the concrete and observed an increase towards the soil/structural interface. The Halcrow Group [27] reported the same characteristic towards TSA affected concrete/soil interfaces and this was confirmed through laboratory results. A slight difference in the interface moisture depending on the age of the specimens was observed at the ECC control and TSA specimens. This confirms the observations made by Lee [126] that the interface water content reduces slightly with time, see Section 2.9.5.

Shearing occurred at the zone of clay with increased moisture or directly at the interface (see Section 5.2.2) describing the dependency of the failure plane on the moisture

content. Shear strength decreases with increasing moisture content as for example demonstrated by Potyondy [122] and shown in Table 5.10.

5.3.3   pH-Values

The pH-value was measured at the same distance from the interface as the moisture content. There was a significant dependency of the distance from the interface as well as the storage age. The pH was measured with a range of 9.3-11.2 and 10.3-11.1 at the interface for English China Clay and Lower Lias Clay, respectively. Therefore it is concluded that the actual pH of the clay was determined mainly by the time dependent changes at the interface.

The pH distribution within LLC adjacent to the interface is illustrated in Figure 5.33 where no significant differences between the casting positions occurred. This distribution was typical for all the specimens investigated. The pH at the interface was high and reduced linearly inwards, however the rate of levelling depended on the age of the specimen. This is demonstrated by the significantly different pH affected area as observed at the ECC-control specimens and the 18 months old specimens, see Figure 5.34 and Figure 5.35. The actual pH of the Lower Lias Clay was 7.7 and of the English China Clay 5.4.
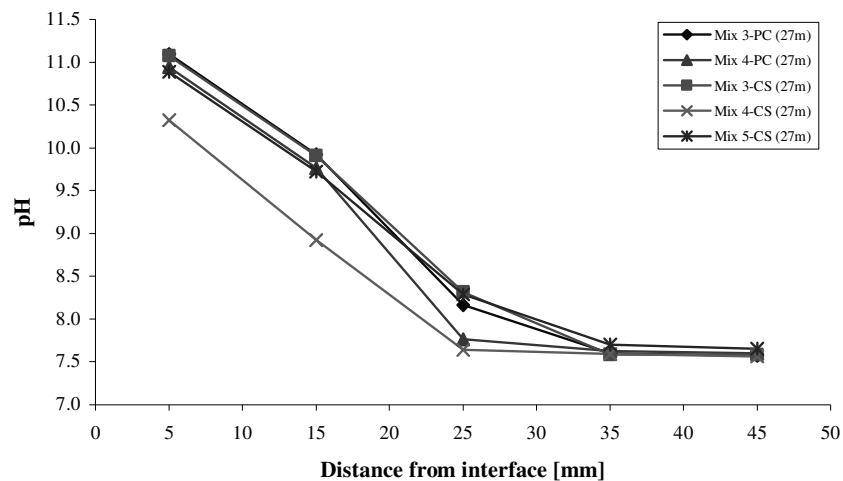
Figure 5.33 - pH-value distribution at adjacent clay, interface PC/CS-LLC

The reduction of the pH to the natural soil value was not in agreement with the point where the moisture levelled to a constant value which was also observed by Lee [126].

It is suggested that both the moisture and the pH are independent from each other but both have the same increasing trend towards the concrete as also observed by the Halcrow Group [27] in connection with TSA cases.

The pH at the interface of both clays indicated that TSA formation conditions differed. The LLC interface generated a pH-range of 10.3-11.1 and at the ECC interface there was a range of 9.5-10.0, which is less favourable for TSA. Despite this, thaumasite formed at both interfaces. The consequences of the different pH-values regarding the formation of thaumasite have been discussed in Section 5.1.1.
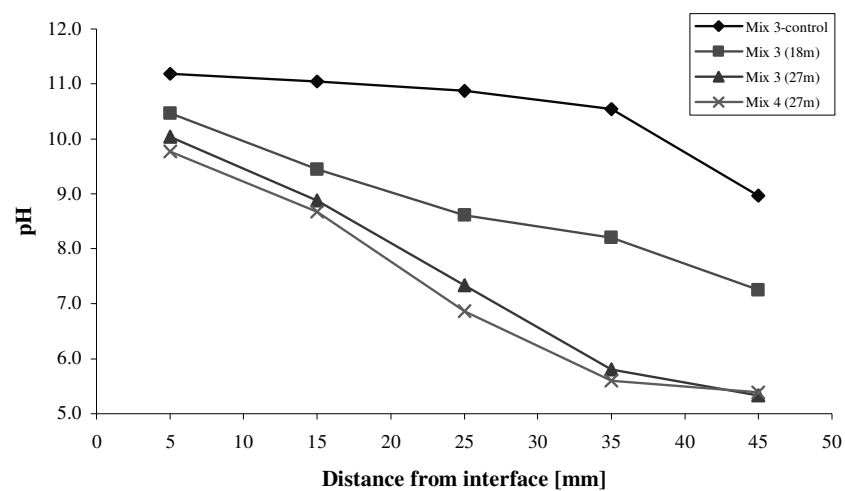
Figure 5.34 - pH-value distribution at the adjacent clay, interface PC-ECC
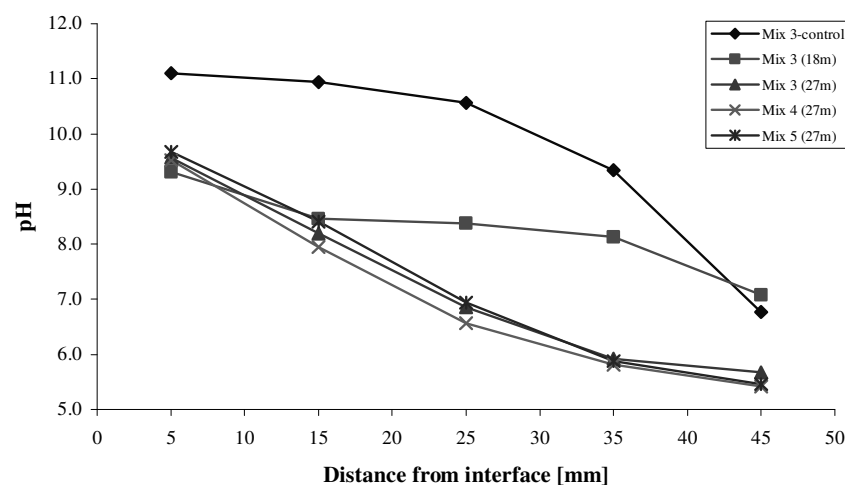
Figure 5.35 - pH-value distribution at the adjacent clay, interface CS-ECC

The increase of pH in the clay adjacent to concrete is derived from ion diffusion processes, such as alkali (Na^+, K^+) and hydroxyl ions (OH^-), within the concrete and soil pore solution leading to a sequence of reactions as stated by Webster and Sheary [135]. These reactions culminated in the flocculation of clay particles to make the clay more friable, as has been observed. Furthermore the optimum moisture content was increased and an increase of the strength and stability occurred which was mainly caused by the presence of hydroxyl ions. This favoured solidification processes as a result of pozzolanic reactions where calcium silicate hydrates (CSH) and calcium aluminate hydrates (CAH) formed in the clay as shown by Sherwood [136], see Section 2.9.5.

5.3.4   Mineralogical Changes

Mineralogical changes of the clay adjacent to the interface were identified in the case of the English China Clay compared to pure clay samples where traces of brucite were detected in the zone next to the interface, see Figure 5.36. However, it is suggested that this brucite was attached at the clay sample and derived from the thaumasite formation process at the interface. Further changes in the mineralogical composition depending on the distance from the interface were not found.
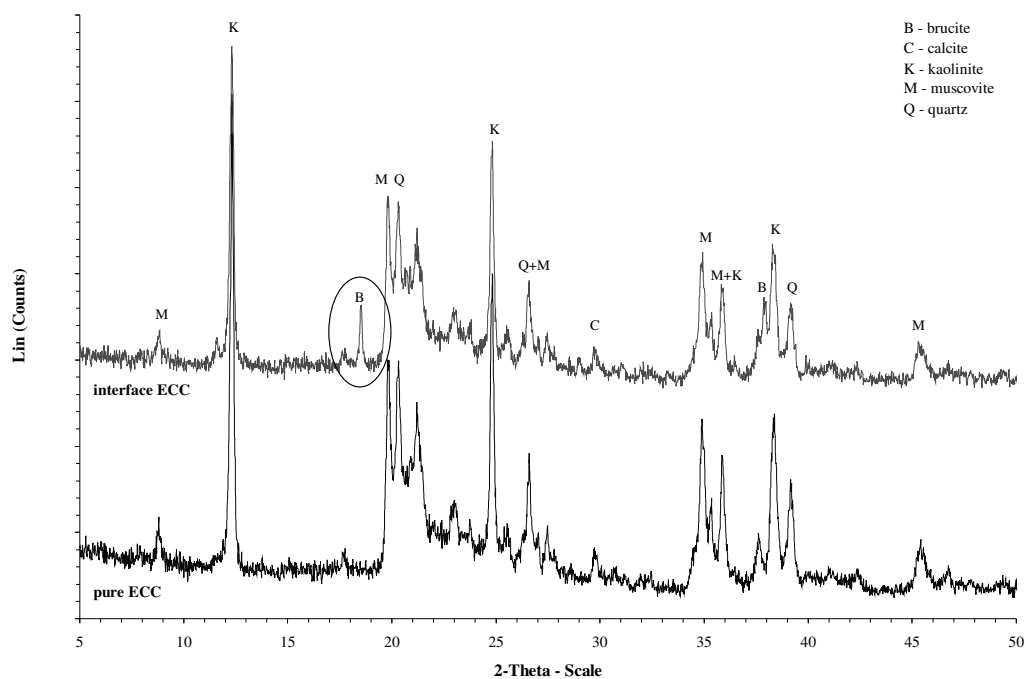
Figure 5.36 - Mineralogical composition of pure and interface ECC clay

Significant differences in the mineralogical composition between the natural Lower Lias Clay and the LLC adjacent to the concrete were not identified, see Figure 5.37. Therefore it is concluded that no significant changes of the mineralogy of the clay at the interface occurred. Microscopical investigations at the boundary concrete/thaumasite/clay confirmed this statement and traces of TSA reaction products were not found in the clay using polarisation microscopy and XRD. Furthermore differences in gypsum and pyrite concentrations depending on the extent of attack as described by the Halcrow Group [27], see Section 2.9.6, were not detected using XRD. This is due to the extensive supply of sulfate ions through the highly concentrated and aggressive magnesium sulfate solution.
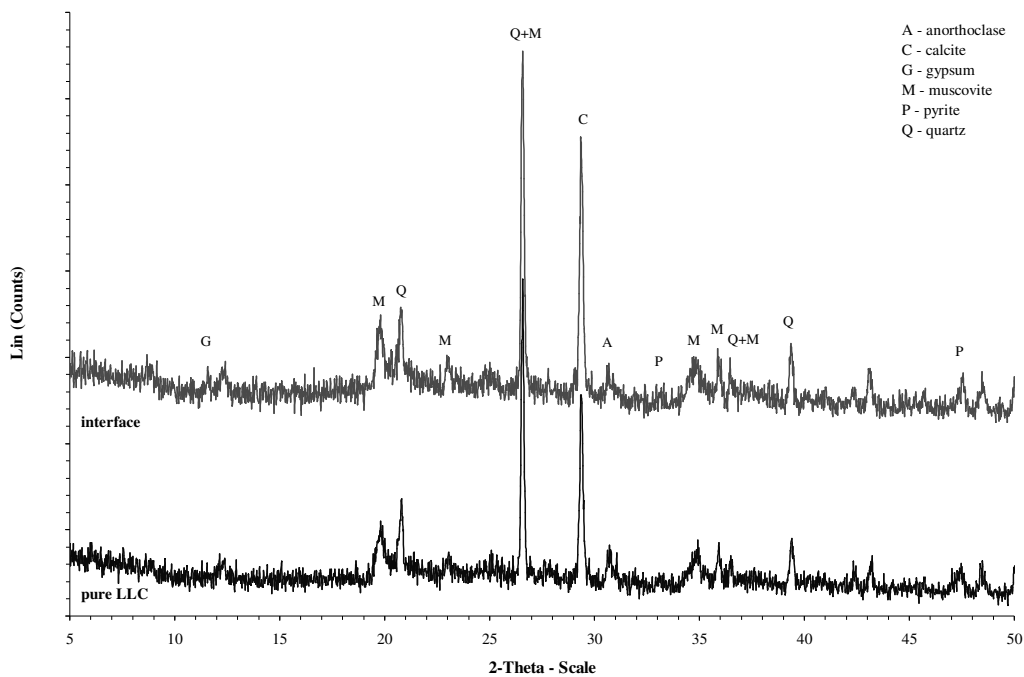
Figure 5.37 - Mineralogical composition of pure and interface LLC clay

5.4   Summary - Interface Behaviour

The findings and observations made during investigations of the TSA affected concrete/clay interface are summarised as follows:

- No reduction of skin friction/shear strength was detected at TSA affected interfaces which was caused by curing effects and the compaction of clay adjacent to concrete through thaumasite expansion.

- The effect of TSA on the shear strength parameters at the interface was evaluated using two methods: Method 1 evaluated changes in the shear strength using the two separate parameters for skin friction δ' and cohesion c_a'. Method 2 evaluated the effect of TSA on the interface shear strength according to the peak and residual shear strength τ.

- The effect of TSA on skin friction δ' was generally positive and an increase in skin friction of up to 10% at the natural Lower Lias Clay (LLC) - boundary was measured when thaumasite occurred. The effect at the boundary to the artificial English China Clay was similar. The cohesion increased significantly due to the formation of thaumasite. An increase of 14% per millimetre of thaumasite at the LLC-boundary and of 40% at the ECC-boundary was measured. Nonetheless, this significant positive effect should not be taken into account.

- Both peak and residual shear strength increased with increasing thaumasite. The peak shear strength at the LLC-boundary increased by 3% per millimetre of thaumasite and by 8% at the ECC-boundary. The residual shear strength increased by 5% at the ECC-interface and did not change at the LLC interface.

- Concrete/clay skin friction was higher than internal clay friction, though the cohesion was significantly less at the interface.

- The shear plane occurred mainly in clay and zones of clay close to the interface or within a combination of thaumasite/interface/clay. The failure plane never occurred within the thaumasite layer. LLC favoured shearing around the interface and ECC favoured shearing within the clay.

- TSA was more severe in clay-restrained Series V specimens than in unrestrained conditions and TSA was enhanced at the interface to artificial non-sulfate containing ECC. This acidic English China Clay was more aggressive than Lower

        Lias Clay at highly permeable surfaces and less at surfaces with a low permeability.

- Thaumasite, ettringite, quartz and calcite were mainly found as reaction products. Gypsum was detected at the boundary of the acidic English China Clay with a pH<10.

- The decomposition of thaumasite and ettringite in favour of mainly gypsum within the formed reaction product layer at the ECC interface (pH 9.7-10) supports the hypothesis of thaumasite being an intermediate reaction product during TSA. Whereas no increased amount of gypsum was observed at the LLC interface (pH 10.3-11.1).

- An increase of moisture and pH towards the interface was observed which reduced with time.

- Changes in the clay mineralogy were not detected within the clay adjacent to the interface.

6   Practical Influence

The following section focuses on the practical influence of the thaumasite form of sulfate attack, considering both pure structural effects and concrete/soil interface effects.

6.1   Pure Structural Influence

Pure structural effects of TSA can be considered as loss of concrete cross-sectional area leading to an increased slenderness of the structural element, loss of cover concrete potentially leading to premature corrosion of reinforcement and a reduction of the bond between reinforcement and concrete. The latter effect was investigated by Gorst and Clark [110] and discussed in Section 2.8.1. The extent of the loss of concrete cross-sectional area and of cover concrete is discussed in this section. The findings are based on the results obtained in this investigation as discussed in Chapter 4 and 5.

The mixes used in the investigation which are most relevant to practice are 1, 2 and 4, these mixes had w/c-ratios in the range 0.55 to 0.65 and concrete strength class C25/30 to C30/37. Comparing the observed rates of deterioration of unrestrained (Table 6.1) and restrained specimens (Table 6.2) it is clear that the deterioration progresses faster on clay-restrained specimens, which represent buried concrete structures. The results of Mix 4 specimens, with a cement content of 320 kg/m^3 and w/c-ratio 0.55 and restrained with Lower Lias Clay (LLC) and English China Clay (ECC) have been used to predict worst case deterioration rates that might be encountered in the field.

Table 6.1: Deterioration rate on unrestrained specimens

Mix	Deterioration progress in 1.8% SO$_4$ –solution [mm/year]		Deterioration progress in combined SO$_4$-CO$_3$-solution [mm/year]	Compressive strength f$_{cu}$ [N/mm^2]
	Precast	*Cast in-situ*	*Precast*	
1 (290-0.55)	*2.1*	*-*	*1.3*	43.9
2 (290-0.65)	*2.7*	*-*	*2.2*	34.1
3 (290-0.75)	3.1	1.4	2.7	25.5
4 (320-0.55)	*1.8*	*-*	*1.4*	42.6
5 (320-0.75)	3.7	0.1	3.2	22.8

Lower and upper bound values were estimated for the rate of deterioration of clay restrained specimens. The lower bound and upper bound were determined according to the assumption that linear deterioration took place within 27 months in aggressive solution. A possible dormant period was neglected in this approach. Figure 6.1 illustrates the lower and upper bound in case of Mix 4 concrete with a boundary to English China Clay at a depth of 0.5m below ground. Deterioration was linearly extrapolated for the upper bound values. In the case of the lower bound it is assumed that the rate of deterioration decreases towards the core, however, experimental data for the start and extent of this decrease are not available. The decrease of deterioration rate is caused by the gradient of increasing density through a highly permeable surface zone until a uniform pore structure is encountered. The upper bound of a possible linear deterioration is used for the worst case scenario because it is the only evidence.

Table 6.2: Lower and upper bound for annual deterioration on clay restrained specimens

| Lower and upper bound deterioration rate at boundary [mm/year]						
Lower Lias Clay						
Mix		**Precast surface with pressure of**			**Cast in-situ surface with pressure of**		
		10 kPa	*40 kPa*	*70 kPa*	*10 kPa*	*40 kPa*	*70 kPa*
Mix 3	$\frac{290}{0.75}$	1.3 – 1.7	0.6 – 0.8	0.6 – 0.8	0.8 – 1.0	0.4 – 0.6	0.2 – 0.3
Mix 4	$\frac{320}{0.55}$	*2.8 – 3.6*	*1.3 – 1.7*	*1.0 – 1.3*	*1.6 – 2.0*	*0.3 – 0.4*	*0.6 – 0.7*
Mix 5	$\frac{320}{0.75}$	-	-	-	0.7 – 0.9	0.8 – 1.0	1.1 – 1.4
English China Clay						
Mix		**Precast surface with pressure of**			**Cast in-situ surface with pressure of**		
		10 kPa	*40 kPa*	*70 kPa*	*10 kPa*	*40 kPa*	*70 kPa*
Mix 3	$\frac{290}{0.75}$	5.3 – 6.9	3.1 – 4.0	2.6 – 3.3	2.3 – 3.0	1.6 – 2.0	0.9 – 1.1
Mix 4	$\frac{320}{0.55}$	*3.6 – 4.6*	*1.9 – 2.4*	*2.1 – 2.7*	*0.7 – 0.9*	*0*	*0*
Mix 5	$\frac{320}{0.75}$	-	-	-	2.2 – 2.9	1.1 – 1.4	0.4 – 0.6
Mix 3*	$\frac{290}{0.75}$	3.3 – 5.3	2.0 – 2.8	1.7 – 2.5	0.3 – 0.5	0.3 – 0.5	0.2 – 0.3
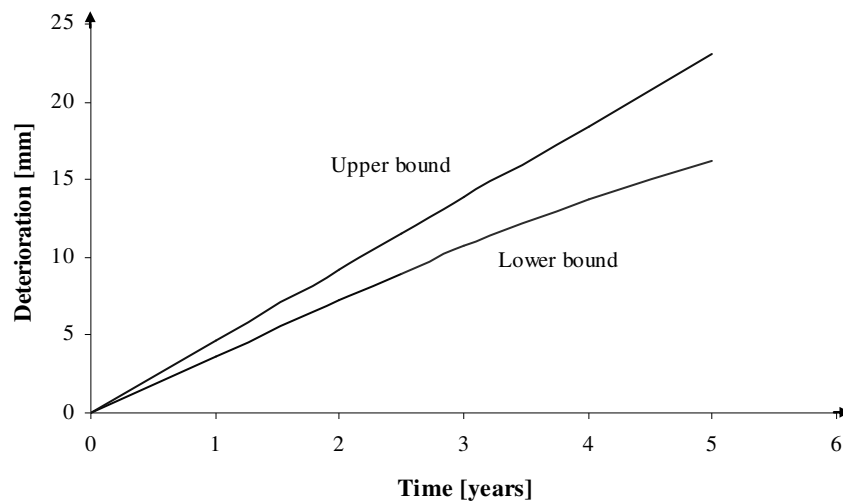
Figure 6.1 - Lower-upper bound deterioration in Mix 4/PC-ECC-10kPa samples

With predictions based on the laboratory results, a deterioration of up to nearly 5mm per year is possible when Portland cement and limestone aggregate C30/37 concrete is used. Deterioration rate and onset have been shown to be dependent on earth pressure. An annual deterioration of 5mm or greater was observed in the field in the Canadian Arctic where the columns of a building had to be replaced two years after construction [20]. In the case that TSA occurs in deeper strata a real deterioration of about 2.5mm (Table 6.2) can be assumed for the worst case scenario based on the results presented in Chapter 5. It should be noted that deterioration in the field has generally been observed to occur below a top layer of about one metre which contains either a reduced sulfate content or no sulfate source. This is caused by mineral leaching processes whereby sulfate ions are transported to deeper strata until the soil permeability is too small.

For an annual deterioration of 2.5mm in a circular concrete pile, the loss of cross-sectional area is illustrated in Figure 6.2. For example, deterioration on a 300mm diameter pile caused by TSA may lead to a loss of the cross-sectional area of about 13% after four years in the worst case scenario. Therefore cross-sectional loss is the main structural effect of TSA for concrete piles (≤750mm diameter) and may cause substantial loss of load capacity. The confinement effect of the expanding thaumasite layer might be beneficial and compensates the cross-sectional loss.

It is suggested that existing superstructures based on piles with a low diameter at TSA risk should be strengthened or additional measures should be taken into account if any

appearance of TF is observed. Substructures built according to current regulations, such as BRE Special Digest 1 [96], should be ensured against severe TSA. Nonetheless piles with greater diameter are installed or additional sacrificial concrete is used in term of an increased safety factor in critical cases. The safety factor is currently 2 or greater as stated by the TEG [1].
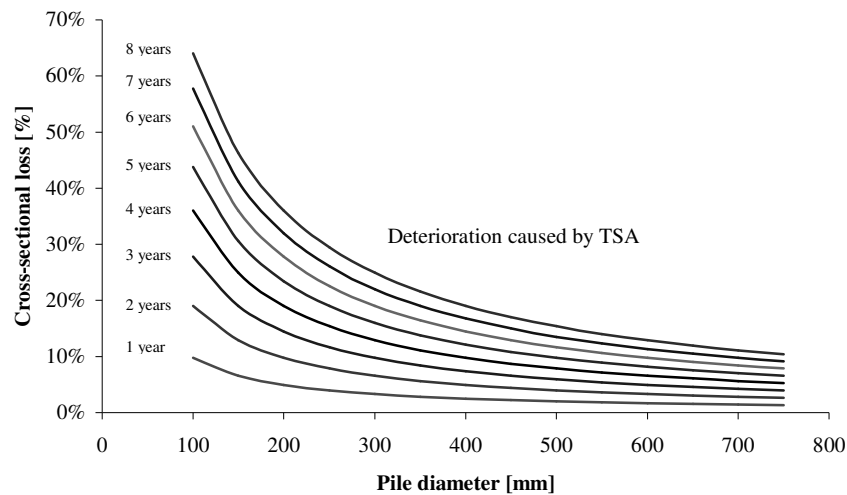
Figure 6.2 - Cross-sectional loss depending on pile diameter and thaumasite

The annual rate of deterioration of 2.5 millimetres can cause substantial loss of cover concrete, hence, initiating corrosion of the reinforcement if insufficient cover concrete was considered. Corrosion may be induced through chlorides contained in de-icing salts which are used on carriageways, however, the oxygen availability in the ground is low and this reduces the rate of corrosion. These processes may result in a change of the designated end conditions of elements of the substructure. This was observed by Wallace [109] who reported a change in the designated 'fixed end' condition of a buried reinforcement lap to a less effective 'pinned end' caused by loss of bond strength.

Structures designed according to current guidance should be capable of resisting TSA and its structural effects. However, structures built according to early guidelines prior to an awareness of TSA may be of concern. Those structures at risk should be subject to investigation and if necessary, strengthened with the assumption that the worst case scenario of cross-sectional loss may occur. Despite the suggested worst case scenario, loss of the structural integrity has been encountered in the field only in one case. The columns of a building in the Canadian Arctic had to be replaced two years after construction [20]. The structural integrity of the M5 overbridges was not affected

despite severe TSA was encountered. In this case several columns were replaced, however, this was due to investigative reasons and the lack of knowledge about TSA.

6.2 Concrete/Soil Interface Effects

Soil/structural effects of TSA caused by softening of the concrete surface can be divided into a change of pile friction reducing the load capacity, a change of sliding resistance of base foundations to lateral loads and damage of the superstructure due to settlements. The structural stability of both piles subjected to vertical loads and base foundations subjected to lateral loads is mainly determined by the skin friction between soil and structural material. The second shear strength parameter, the cohesion, is neglected for stability calculations according to BS EN 1997-1:2004. Chandler [116] and Burland [117] have previously suggested that this should be the case because of the likelihood that the cohesion is destroyed during pile installation.

The findings of Chapter 5, summarised in Table 6.3, show that there was no negative effect of TSA on either skin friction or cohesion. In addition, the approach using the total shear strength of the interface did not reveal negative effects. The results listed in Table 6.3 describe the percentage increase of the shear strength parameters δ' and c' when thaumasite occurs and both the cohesion and the shear strength per millimetre of thaumasite. The values were obtained using two different approaches, firstly by the evaluation of the shear strength parameters and secondly by evaluation of the shear strength. The two methods and results are discussed in Section 5.2.1. A quantitative statement about a percentage increase in skin friction per millimetre of thaumasite was not possible. However, an increase of at least 10% in skin friction was observed when thaumasite occurred. The evaluation was based on changes relating to unaffected interfaces which showed a greater skin friction than the internal clay friction.

Table 6.3: Percentage effect of TSA on shear strength

Interface	Shear strength parameter evaluation		Shear strength	
	δ	c_a'	τ	$\tau_{residual}$
LLC	10%	14%/mm$_{th.}$	3%/mm$_{th.}$	±0%
ECC	10%	40%/mm$_{th.}$	8%/mm$_{th.}$	5%/mm$_{th.}$

It was anticipated that the effect of thaumasite would be to decrease the shear strength at the soil/structure interface. This assumption was not confirmed and reverse effects were observed. Furthermore the soft thaumasite did not serve as the weak point during shearing; which was observed at both the thaumasite/clay interface and within the clay. Therefore it is suggested that the current practical guidance with its assumptions for surface roughness and the current safety factors offer a potential degree of safety combined with guidelines dealing with TSA. The traditional safety factor for the installation of piles is 2, however, it can be reduced with increased pile testing. Guidance for the design of foundations, BS EN 1997-1:2004, differentiates with regard to surface roughness for the skin friction coefficient δ between the methods of casting, precast or cast in-situ. However, if TSA occurs and forms a soft surface then changes of the surface roughness are expected. The roughness might decrease where cement paste transforms into thaumasite but on the other hand increase due to mechanical interlocking with solid embedded aggregate grains. The findings of this investigation lead to the conclusion that the roughness is not negatively affected and the skin friction coefficients depending on casting face in accordance with BS EN 1997-1:2004 are sufficient. These coefficients are as follows:

$$\delta = \varphi\left(\max.35°\right) \qquad \text{cast in-situ elements}$$

$$\delta = \frac{2}{3}\varphi \qquad \text{precast elements}$$

However, further investigation of the concrete surface roughness in an in-situ concrete/thaumasite/clay system might be of interest. Furthermore the expansion process may distribute in the bulk of the soil and the positive effect observed may disappear. If this confining effect, caused by the expansion of the thaumasite layer, is lost then the results of this investigation may not applicable to the field. It is necessary to validate the findings of this investigation with measurements of the confining effect at TSA affected piles in the field, as discussed in Section 5.2.1.

Structures built according to current guidelines, taking TSA into account in accordance with BRE Special Digest 1 [96], provide a high resistance against TSA and should preserve the initial surface. TSA cannot be precluded but safety factors provide

sufficient resistance to prevent significant damage to superstructures. Structures at potential risk are structures built according to former guidelines which were not aware of TSA and located in aggressive environments. The extent of risk can be estimated through desk studies and if signs of TSA occur it is suggested that the deterioration is monitored until the structural integrity is endangered and remediation is necessary. The absence of significantly damaged structures due to loss of skin friction supports the findings that skin friction is preserved and safety factors have been adequate.

The second and often neglected shear strength parameter, cohesion, undergoes a significant increase caused by thaumasite expansion. This expansion results in the compaction of the clay adjacent to the concrete and chemical interactions favouring cementation processes. The compaction effect on the cohesion might be lost due to the distribution of the expansion pressure in the bulk soil. These effects are not taken into account during design but they may offer an additional reserve of safety.

Due to the expansion processes and the stability of the thaumasite layer it can be concluded that settlements and resulting damage of the superstructure can be considered as very unlikely to occur. It is more likely that the expansion forces cause a slight heaving. However, TSA can most probably be precluded at the bottom face of the structure due to the large foundation pressures being present and unweathered clay in contact with concrete. Observations at the base of the Tredington-Ashchurch Bridge [27] showed very small amounts of thaumasite on the base compared to the severely deteriorated sides of the foundation.

6.3   Summary

The practical implications of the effects of TSA can be separated into pure structural effects and soil structure interaction effects.

Based on the results of the current investigation the effects of TSA on pure structural behaviour are likely to be negative. Loss of cross-section and cover concrete with progressing deterioration will result in reduction in strength, increase in slenderness and reduction in restraint at supports.

The effect is not the same for soil-structure interaction, the results revealed generally positive effects with little or no change of skin friction at the interface and limited or no

further damage resulting from settlement. The overall positive effects were caused by cementation and confinement of the soil adjacent to the interface and a possible increase of roughness of the surface due to mechanical interlocking of aggregate grains embedded in the thaumasite layer. The effects of confinement in the field may not be the same as in small scale experimental samples used in this as it is possible that some of the pressure generated due to the production of expansive deterioration products will dissipate into the surrounding soil. Further work is required to determine this effect at larger scale specimens. New structures built according to current guidelines are expected to be able to withstand TSA and the usual skin friction coefficients according to BS EN 1997-1:2004 can therefore be used.

7 Conclusions and Recommendation for Further Research

7.1 Conclusions

This section presents the conclusions of the main objectives of this research project, the acceleration of the thaumasite form of sulfate attack and its effects on skin friction at the soil/concrete interface. The conclusions of the accompanying investigations are included, which belong to the macroscopic deterioration, TSA reaction products and the ion exchange between attacked concrete and environment.

7.1.1 Acceleration and Deterioration Progress of TSA

- It is possible to achieve significant amounts of TSA in a relatively short period of time if;

  $\Rightarrow$ susceptible concrete mixes are used (high permeability, high water/cement ratio and susceptible Portland cement binder with 8% C_3A, Jurassic Oolitic limestone as coarse and fine aggregate),

  $\Rightarrow$ the curing method minimises carbonation, in this case an adapted version of the 'seal-curing' method developed by the BRE was used and,

  $\Rightarrow$ specimens are stored in a highly aggressive environment, i.e. immersed in a highly concentrated magnesium sulfate or a magnesium sulfate/carbonate solution and stored at the optimum deterioration temperature of 5-6°C.

- The observed deterioration caused by TSA separated into two distinct phases the first being an initial period of low activity, the dormant period, and a subsequent period when the deterioration rate was constant and dependent on the mix design.

- In general increasing the compressive strength and reducing the permeability resulted in a decreased rate of attack. Increasing cement content only causes an improvement in resistance when the w/c-ratio is less than 0.55-0.6. In concretes with w/c-ratios greater than these limits increasing the cement content results in an increase in susceptibility. It is suggested that this is due to the relative increase in susceptible surface area, caused by increasing the cement to aggregate ratio in concretes with high w/c ratio.

- Increasing concrete strength and decreasing surface permeability increase the dormant period, however, the occurrence of TSA cannot be completely precluded in a lifetime of a structure.

- The rate of deterioration depends on the density of the concrete and reduces with decreasing porosity. Therefore a constant linear rate of deterioration is not expected to be present from surface towards the core.

- Pure magnesium sulfate solutions are more aggressive than combined magnesium sulfate/carbonate solutions because of increased de-calcification processes taking place.

- Thaumasite forms attached on the concrete under restrained conditions.

- TSA was found to be more severe in restrained conditions than in unrestrained concrete specimens which were directly in contact with solution. The reason for this is that one of the effects of the restraining material is to limit the ability of the alkalinity to diffuse away from the concrete surface.

- At low water cement ratios specimens in contact with English China Clay (ECC) showed lower deterioration than those in contact with Lower Lias Clay (LLC), however this reversed in specimens with high water/cement ratios (0.75). The ECC is acidic, hence, rate of TSA is not directly dependent on interface pH.

- Comparison of deterioration data obtained with wear-ratings published by BRE is difficult due to the lack of knowledge of the corner deterioration.

7.1.2   Macroscopical Deterioration Observations

- A crust of 'sound' concrete forms on specimens under unrestrained conditions and this crust is less apparent and sometimes absent under restrained conditions.

- TSA forms as an incohesive loose mass under unrestrained conditions and changes to a compacted cohesive mass; however, without binding abilities, under restrained conditions.

- The effect of increasing the pressure at the interface is to extend the dormant period

- The TSA reaction product layer is two to three times the actual depth of concrete deterioration under restrained and unrestrained conditions, respectively. That indicates that under restrained conditions the extent of expansion caused by TSA

from the original surface is equal to the depth of the actual deterioration. A minimum expansion of 100% occurs when thaumasite forms and is able to increase towards 200% under no restraint.

- The extent of the thaumasite layer depends on the pressure on the interface, i.e. the onset of TSA is shifted, the dormant period extended, with increasing pressure as long as mobile sulfate ions are available in the ground.

7.1.3   TSA Reaction Products

- Thaumasite, ettringite, gypsum, quartz, calcite and aragonite are the main reaction products on specimens under unrestrained conditions. Restrained conditions hinder the formation of aragonite and partly of gypsum. However, gypsum forms predominantly at clay boundaries with pH<10.

- The relative amount of thaumasite within the TSA reaction product layer decreases with progressing TSA and the amount of calcite increases due to the de-calcification of thaumasite towards secondary calcite and aragonite. Aragonite forms predominantly as de-calcification product in the presence of additional carbonate such as in the solution.

- Thaumasite is able to form within a carbonated environment or at low alkaline interfaces but serves as an intermediate reaction product and almost immediately decomposes to gypsum, secondary calcite and aragonite because of de-calcification processes taking place in this low alkaline environment. Therefore thaumasite is the final degradation product within TSA, however, the de-calcification process follows consequently and the onset of this depends on the alkalinity of the affected zone and environment. In the overall deterioration process thaumasite is not the final degradation product, secondary calcite and aragonite form the definite stable end-phase.

7.1.4   Ion Exchange between Solution and Concrete

- The ion exchange process can be separated into three phases: Phase 1 can be considered pure ion diffusion into the concrete pore structure; Phase 2 describes a

dormant period with low activity depending on the concrete density/porosity; and Phase 3 shows a constant ion uptake by the concrete.

- The sulfate uptake decreases in proportion to the compressive strength/permeability of the concrete and linear extrapolation indicates that sulfate uptake will cease when compressive strength reaches $80N/mm^2$, however, it is assumed that the sulfate uptake will approach zero non-linearly because diffusion cannot be stopped.

- Carbonate ions migrate in both directions with ions entering the solution from dissolution of the limestone aggregate and of atmospheric carbon dioxide. Migration from the solution into the concrete consists of initial absorption, diffusion and the consumption of carbonate in the TSA reaction. The extent of the migration direction mainly depends on the carbonate available in the solution and on the permeability of the concrete.

7.1.5   Physical Interface Effects of TSA

- The skin friction at the concrete/clay interface exceeded the internal friction of the clay alone; however, cohesion is significantly less at the interface, hence, the cohesion should be neglected during load capacity calculations.

- The effect of TSA on the shear strength parameters at the interface was evaluated using two methods: Method 1 evaluated changes in the shear strength using the two separate parameters for skin friction δ' and cohesion c_a'. Method 2 evaluated the effect of TSA on the interface shear strength according to the peak and residual shear strength τ.

- The effect of TSA on skin friction δ' was generally positive and an increase in skin friction of up to 10% at the natural Lower Lias Clay (LLC) - boundary was measured when thaumasite occurred. The effect at the boundary to the artificial English China Clay was similar. The cohesion increased significantly due to the formation of thaumasite. An increase of 14% per millimetre of thaumasite at the LLC-boundary and of 40% at the ECC-boundary was measured. Nonetheless, this significant positive effect should not be taken into account.

- Both peak and residual shear strength increased with increasing thaumasite. The peak shear strength at the LLC-boundary increased by 3% per millimetre of

thaumasite and by 8% at the ECC-boundary. The residual shear strength increased by 5% at the ECC-interface and did not change at the LLC interface.

- TSA does not cause reduction of skin friction/shear strength at affected interfaces because of curing effects affecting the clay adjacent to the interface such as solidification processes caused by an increased presence of hydroxyl ions and the confining effect caused by the restrained expansion of the deterioration products. The difference in surface roughness of precast and cast in-situ reduces due to the transformation of cement paste into a soft mass of TSA reaction products.

- The TSA affected interface zone is not the weakest zone within the concrete/thaumasite/clay interface this is evidenced by the fact that the shear plane occurs mainly in the clay and in the clay close to the interface or within a combination of thaumasite/interface/clay with greater than 60% in the interface. The failure plane is not expected to occur within the thaumasite layer as the investigations showed. Within the current investigation the location of the shear plane was found to depend on the particle size distribution of the clay adjacent to the interface; the wider grained the clay the closer shearing occurs to the interface.

7.1.6   Chemical Interface Effects of TSA

- The clay within 10mm of the interface is more friable than elsewhere despite having an increased moisture content which is caused by flocculation of clay particles.

- Within a distance of 10-15mm from the concrete a moisture content gradient exists with moisture content increasing towards the interface, however, the percentage moisture increase is time related and decreases with time.

- The pH increases towards the interface but both area affected by increased pH and the increase in pH itself decrease with time.

- A relationship between moisture content and pH was not apparent.

7.1.7   Practical Influence

- TSA can result in a significant loss of cross section and cover concrete. Based on the results of the experimental programme reported here an annual loss of

concrete of up to 2.5mm is possible, in practice this could result in a significant increase in slenderness of piles.

- The surface roughness of both precast and cast in-situ faces changes so that besides the formation of the soft 'mush' an exposure of embedded aggregate grains occurs and the roughness might increase. Negative implications regarding load capacity due to change of skin friction were not observed and therefore are practically not to be expected at structures affected by TSA. TSA accompanying processes, such as expansion and cementation, are beneficial and the shear plane was mainly observed close to the interface within the clay. Therefore substructures built under guidance not considering TSA are supposed to be stable according to this investigation and new structures are sufficiently protected for the occurrence of TSA due to concrete specifications. But TSA cannot be precluded and positive side effects may disappear.

- Settlements, caused by TSA and the resulting transformation of the concrete into a soft mass at the bottom face of structure are very unlikely because TSA will not tend to form when the clay in contact with the concrete is of unweathered clay and because of the large foundation pressures.

7.1.8   General Conclusion

The thaumasite form of sulfate attack has been successfully accelerated in laboratory conditions, a large number of variables such as cement content, water/cement ratio, casting position, aggressive solution and clay have been assessed and consequently optimum combinations to accelerate TSA depending on the compressive strength have been identified. Thaumasite forms attached to the concrete when it is allowed to form under restrained conditions and forms detached from the surface when samples are immersed in aggressive solution without restraint.

A technique, the needle test, was developed to measure the rate of ingress and deterioration of TSA under laboratory conditions, however, the calibration of the results against field data could not be realised through the non availability of comparable results obtained from the field. The findings obtained correspond to a possible worst practical scenario in a highly aggressive environment which may cause pure structural deterioration in the annual extent of up to 2.5mm in buried concretes. Structures may be

mainly affected by cross-sectional loss and loss of cover concrete causing increase in slenderness, corrosion and loss of bond. Concretes with a compressive strength of over $80N/mm^2$ should resist TSA at the lower bound as cut-off points for deterioration and sulfate uptake were obtained using extrapolation. However, the upper bound for deterioration and uptake may be significantly higher but such high strength concretes are not commonly used.

The main objective of this investigation the effect of TSA on the skin friction at the concrete/clay interface was performed using a specimen developed to meet the following requirements:

- simulation of underground conditions during the period of attack,
- ability to be transferred to the shear test equipment, a large shear box, without disturbing the concrete/thaumasite/clay interface.

The effect of TSA on skin friction and sliding resistance is not negative despite that the roughness of the surface changed. The skin friction and the cohesion increase with increasing thaumasite and therefore existing structures under attack can still fulfil their designated purpose and structural damage of the superstructure is not to be expected. Furthermore skin friction at unaffected interfaces exceeds the interface friction of the clay because of cementation processes of the clay adjacent to the interface. Shearing within the system concrete/thaumasite/cemented-clay occurs within the clay or in the clay close to the interface and is not expected to occur within the thaumasite layer which can be considered as not having any binding ability. The risk of settlements due to the transformation of concrete into the soft mass is very unlikely, caused by the significant expansion pressure of the new minerals formed. Furthermore it is very unlikely that TSA occurs on the bottom side of the concrete and causes heave.

Current guidance, relating to TSA, provides the resistance of concrete structures against TSA by concrete specifications which should prevent significant deterioration. Pure structural effects of TSA are likely to occur at structures built according to former regulations and being located in aggressive environments. Case studies should estimate the risk and deterioration using the progression rate of the worst case scenario from this investigation and if necessary strengthen the structure.

In general a reduction of skin friction is not expected despite that the fact that the roughness of the concrete surface changes. Skin friction and cohesion are not negatively affected by TSA and current regulations for designing structure appear to be sufficient.

7.2   Further Work

The results of the current investigation have highlighted some points which are worthy of further investigation:

- Data about the linear relationship between compressive strength/permeability and rate of deterioration have been obtained in the range between 20-50 N/mm^2. Further investigation is needed to confirm the proposed linearity towards concrete with higher compressive strength and lower permeability.

- It is suggested to improve the developed needle test method using an ultra sonic bath to remove all loose concrete and aggregate grains before measurements are taken.

- The use of an additional source of carbonate showed less aggressiveness. Therefore it is suggested to determine the influence of different amounts of external carbonate on the aggressiveness of a combined sulfate-carbonate solution.

- The TSA progress at clay-restrained conditions could not be explicitly determined. Data about the rate were not found and the long term deterioration rate should be investigated. The length of the dormant period under clay-restrained conditions and the dependency on the pressure should be investigated more closely.

- The skin friction was determined using two different clays; however, it is suggested to validate the skin friction test results using both model pile tests and a variety of soils with different particle size distributions.

- The formation of thaumasite changes the roughness of the interface for both precast and cast in-situ surface. A reduction in skin friction caused by changes in roughness were not observed, however, the friction coefficient should be determined in order to validate the skin friction coefficient, δ, for precast and cast in-situ surfaces according to BS EN 1997-1:2004.

- Few field data about the extent of TSA have been found and, for instance, deterioration data of the BRE field trial at Shipston-on-Stour were published using 'wear-rating' as test method which does not explicitly expressed deterioration caused by TSA. Conversion of data obtained into wear-ratings was difficult due to

the unknown corner deterioration. The extent of deterioration on the surface of field concrete should be determined using another method showing the actual deterioration and expansion in order to compare with laboratory data obtained in this investigation.

- This investigation showed an increase of skin friction and cohesion depending on the expansion pressure of the thaumasite formed. There are no data about the distribution of the pressure within the clay adjacent to the interface in the field and there is no evidence if laboratory observed pressure can be confirmed in the field. The pressure distribution caused by thaumasite expansion should be investigated at different distances from the interface in order to validate the increase of skin friction depending on the amount of thaumasite formed.

- Data are available for effects of chemical interactions at the interface for a period of 28 days but the long term benefits on the shear strength parameter at unaffected interfaces have not been investigated yet.

- The loss of the cover concrete due to the formation of thaumasite affects the diffusion resistance towards the reinforcement, however, there is a lack of knowledge of the change of the permeability coefficient for the in-situ system of TSA affected concrete and compacted soil adjacent to the interface. The compaction of the soil may increase the diffusion way so that the diffusion of aggressive ions, such as chloride, might not be favoured.

References

[1]   Department of the Environment, Transport and the Regions: The thaumasite form of sulfate attack: risks, diagnosis, remedial works and guidance on new construction. Report of the Thaumasite Expert Group, DETR, London, January 1999

[2]   Crammond, N.J.: The thaumasite form of sulfate attack in the UK. Cement & Concrete Composites 25, 2003, pp.809-818

[3]   Bickley, J.A.; Hemmings, R.T.; Hooton, R.D. and Balinsky, J.: Thaumasite related deterioration of concrete structures. Proceedings of Concrete Technology: Past, Present and Future ACI SP: 144–8, 1995. pp.159–175

[4]   Skalny, J.P. and Thaulow, N.: Sulfate attack in North America. Proceedings of the 1.International Conference on Thaumasite, BRE, London, 2002

[5]   Ma, Baoguo; Gao, Xiaojian; Byars, Ewan A. and Zhou, Qizhi: Thaumasite formation in a tunnel of Bapanxia Dam in Western China. Cement & Concrete Research 36, 2006, pp.716-722

[6]   Mingyu, Hu; Fumei, Long and Mingshu, Tang: The thaumasite form of sulfate attack in concrete of Yongan Dam. Cement & Concrete Research 36, 2006, pp.2006-2008

[7]   Erikson, K.: Thaumasite attack on concrete at Marbjerg Waterworks. Cement & Concrete Composites 25, 2003, pp.1147-1150

[8]   Lachaud, R.: Thaumasite and ettringite in building materials. Ann ITBTP, 1979, 370:3

[9]   Leifeld, G.; Muenchberg, W. and Stegmaier, W.: Ettringit und Thaumasite als Treibursache in Kalk-Gips-Putzen. ZKG International 23, 1970, pp.174-177

[10]   Ludwig, U. and Mehr, S.: Destruction of historical buildings by the formation of ettringite or thaumasite. Proceedings of the 8th International Congress on the Chemistry of Cement, Rio de Janeiro, 1986, Vol.5, pp.181-188

[11]   Berra, M. and Baronio, G.: Thaumasite in deteriorated concretes in the presence of sulfates. In: Scanlon, J.M.: editor. Proc. of Katherine and Bryant Mather International Conference on Concrete Durability. Atlanta, 1987. American Concrete Institute, SP-100, 2; 1987, pp.2073-2089

References

---

[12]   Hagelia, P.; Sibbick, R.G.; Crammond, N.J. and Larsen, C.K.: Thaumasite and secondary calcite in some Norwegian concretes. Cement & Concrete Composites 25, 2003, pp.1131-1140

[13]   Strupi Suput, J.; Mladenovic, A.; Cernilogar, L. and Olensek, V.: Deterioration of mortar caused by the formation of thaumasite on the limestone cladding of some Slovenian railway tunnels. Cement & Concrete Composites 25, 2003, pp.1141-1145

[14]   Oberholster, R.E.; Van Aardt, J.H.P. and Brandt, M.P.: Durability of cementitious systems. In: Barnes, P.; editor. Structure and Performance of Cements. New York: Applied Science Publishers; 1983, pp.365-413

[15]   Romer, M.; Holzer, L. and Pfiffer, M.: Swiss tunnel structures: concrete damage by formation of thaumasite. CCC 25, 2003, pp.1111-1117

[16]   Erlin, B. and Stark, D.C.: Identification and occurrence of thaumasite in concrete. Symposium on the effects of aggressive fluids in concrete. Highway Research Record 11, 1965, pp.108-113

[17]   Van Hees, R.P.J.; Wijffels, T.J. and van der Klugt, L.J.A.R.: Thaumasite swelling in historic mortars: field observations and laboratory research. Cement & Concrete Composites 25, 2003, pp.1165-1171

[18]   Stark, D.C.: Occurrence of thaumasite in deteriorated concrete. Cement & Concrete Composites 25, 2003, pp.1119-1121

[19]   Bensted, J.: Some problems with ettringite and thaumasite in the gypsum plaster/cement contact area. In: Proceedings of the International RILEM Symposium on Calcium Sulfates and Derived Materials, France, 1977, pp.479-487

[20]   Crammond, N.J. and Halliwell, M.A.: The thaumasite form of sulfate attack in concretes containing a source of carbonate ions – microstructural overview. In: Advances in Concrete Technology, 2nd CANMET/ACI Symposium on Advances in Concrete Technology, Las Vegas, 1995, pp.357-380

[21]   Crammond, N.J.: The occurrence of thaumasite in modern construction – a review. Cement & Concrete Composites 24, 2002, pp.393-402

[22]   Crammond, N.J. and Dunster, A.D.: Avoiding the deterioration of cement-based building materials; Lessons from case studies 1. BRE Lab. Report BR 324. UK: Construction Research Communications Ltd (CRC); 1997

References

[23]   Bracegirdle, A.; Jefferis, S.A., Tedd, P.; Crammond, N.J.; Chudleigh, I. and
        Burgess, N.: The investigation of acid generation within the Woolwich and
        Reading Beds at Old Street and its effects on tunnel linings. Proceedings of the
        International Symposium on Soft Ground Tunnelling, City University, London,
        Balkema, 1996

[24]   Crammond, N.J.; Dunster, A.M. and Hollinshead, K.: Avoiding deterioration
        of cement-based building materials; Lessons from case studies 2. BRE Lab.
        Report BR 357. UK: Construction Research Communications Ltd (CRC); 1999

[25]   Department of the Environment, Transport and the Regions: Thaumasite
        Expert Group One-Year Review. Report of the Thaumasite Expert Group,
        DETR, London, 2000

[26]   Department of the Environment, Transport and the Regions: Thaumasite
        Expert Group Three-Year Review. Report of the Thaumasite Expert Group,
        DETR, London, 2000

[27]   Halcrow Group Ltd.: Halcrow Thaumasite Investigation – Final Interpretative
        Report. 2000

[28]   Stark, J. and Wicht, B.: Dauerhaftigkeit von Beton – Der Baustoff als
        Werkstoff (Durability of concrete). F. A. Finger-Institut für Baustoffkunde der
        Bauhaus-Universität Weimar. Birkhäuser Verlag Basel, 2001 (in German)

[29]   Mehta, P.K. and Monteiro, P.J.M.: Concrete – Microstructure, Properties, and
        Materials. 3rd Edition, McGraw-Hill Book Professional., New York, 2006

[30]   Candlot, E.: Sur les propriétés des produits hydrauliques. Bull. Soc. Encour.
        Ind. Nat. 89, 1890, pp.682-689

[31]   Michaelis, W.: Der Cementbacillus. Tonindustrie-Zeitung 16, 1892, Vol.6,
        pp.105-106

[32]   Brown, P.W.: Thaumasite formation and other forms of sulfate attack – Guest
        Editorial. Cement & Concrete Composites 24, 2002, pp.301-303

[33]   Sims, I. and Huntley, S.A.: The thaumasite form of sulfate attack – breaking
        the rules. Cement & Concrete Composites 26, 2004, pp.837-844

[34]   The EUROMIN project: http://euromin.w3sites.net/mineraux/THAUMASITE.
        html, February 2007

[35]   Crammond, N.J.: Thaumasite in failed cement mortars and renders. Cement &
        Concrete Research 15, 1985, pp.1039-1050

References

---

[36]   Moore, A.E. and Taylor, H.F.W.: Crystal structure of thaumasite. Acta Crystallographica, Section B 26, 1970, pp.386-393

[37]   Edge, R.A. and Taylor, H.F.W.: Crystal structure of thaumasite. Acta Crystallographica, Section B 27, 1971, pp.594-601

[38]   Sibbick, R.G.; Crammond, N.J. and Metcalf, D.: The microscopical characterisation of thaumasite. Cement & Concrete Composites 25, 2003, pp.831-837

[39]   Collett, G.; Crammond, N.J.; Swamy, R.N. and Sharp, J.H.: The role of carbon dioxide in the formation of thaumasite. Cement & Concrete Research 34, 2004, pp.1599-1612

[40]   Crammond, N.J. and Nixon, P.J.: Deterioration of concrete foundation piles as a result of thaumasite formation. Proceedings of the 6th Durability Building of Materials Conference, Omiya Sonic Complex, Tokyo, Japan, 1993

[41]   Barnett, S.J.; Macphee, D.E.; Lachowski, E.E. and Crammond, N.J.: XRD, EDX and IR analysis of solid solutions between thaumasite and ettringite. Cement & Concrete Research 32, 2002, pp.719-730

[42]   Hobbs, D.W.: Thaumasite sulfate attack in field and laboratory concretes: implications for specifications. Cement & Concrete Composites 25, 2003, pp.1195-1202

[43]   Freyburg, E. and Berninger, A.M.: Field experience in concrete deterioration by thaumasite formation: possibilities and problems in thaumasite analysis. Cement & Concrete Composites 25, 2003, pp.1105-1110

[44]   Sahu, S.; Badger, S. and Thaulow. N.: Mechanism of thaumasite formation in concrete. Proceeding of 1st International Conference on Thaumasite, BRE, London, 2002

[45]   Lipus, K. and Sylla, H.-M.: Investigations in Germany of the thaumasite form of sulfate attack. Proceedings of 1st International Conference on Thaumasite, BRE, London, 2002

[46]   Irassar, E.F.; Bonavetti, V.L.; Trezza, M.A. and González, M.A.: Thaumasite formation in limestone filler cements exposed to sodium sulfate solution at 20°C. Cement & Concrete Composites 27, 2005, pp.77-84

References

---

[47]   Oberholster, R.E.: Deterioration of mortar, plaster and concrete: South-African laboratory and field case studies. Proceedings of 1st International Conference on Thaumasite, BRE, London, 2002

[48]   Gaze, M.E. and Crammond, N.J.: The formation of thaumasite in a cement:lime:sand mortar exposed to cold magnesium and potassium sulfate solutions. Cement & Concrete Composites 22, 2000, pp.209-222

[49]   Bellmann, F.: On the formation of thaumasite: Part I. Advances in Cement Research 16, 2004, pp.50-60

[50]   Bellmann, F.: On the formation of thaumasite: Part II. Advances in Cement Research 16, 2004, pp.89-94

[51]   Fountain, E.J.: The myth of TSA. Proceedings of the 1st International Conference on Thaumasite, BRE, London, 2002

[52]   Nixon, P.J.; Longworth, T.I. and Matthews, J.D.: New UK guidance on the use of concrete in aggressive ground. Cement & Concrete Composites 25, 2003, pp.1177-1184

[53]   Crammond, N.J.; Longworth, T.I. and Sibbick, R.G.: Report on occurrence of thaumasite form of sulfate attack to concrete foundation at Abbeymead, Gloucestershire. BRE, Watford, UK, Report No 80414; 1999

[54]   Sibbick, R.G. and Crammond, N.J.: Two case studies into the development of the thaumasite form of sulfate attack (TSA) in hardened concretes. Proceeding of the 7th Euroseminar on Microscopy Applied to Building Materials, Delft, Netherlands, 1999, pp.203-212

[55]   Loudon, N.: A review of the experience of thaumasite sulfate attack by the UK Highways Agency. Cement & Concrete Composites 25, 2003, pp.1051-1058

[56]   Slater, D.; Floyd, M. and Wimpenny, D.E.: A summary of the Highways Agency Thaumasite Investigation in Gloucestershire: the scope of work and main findings. Cement & Concrete Composites 25, 2003, pp.1067-1076

[57]   Zhou, Q.; Hill, J.; Byars, E.A.; Cripps, J.C.; Lynsdale, C.J. and Sharp, J.H.: The role of pH in thaumasite sulfate attack. Cement & Concrete Research 36, 2006, pp.160-170

[58]   Monteiro, P.J.M.: Scaling and saturation laws for the expansion of concrete exposed to sulfate attack. Proceedings of the National Academy of Science 31, USA, 2006, pp.11467-11472

References

[59]   Bensted, J.: Mechanism of thaumasite sulfate attack in cements, mortars and concretes. ZKG International 53, 2000, pp.704-709

[60]   Mulenga, D.M.; Nobst, P. and Stark, J.: Praxisnahes Pruefverfahren zum Sulfatwiderstand von Moertel und Beton mit und ohne Flugasche. Beitraege zum 37. Forschungskolloquium des Deutschen Ausschusses fuer Stahlbeton am 7. und 8.10.1999 an der Bauhaus Universität Weimar. Weimar, 1999, pp.197-213 (in German), Beuth-Verlag, Berlin, Germany

[61]   Slater, D.; Knights, J.C. and Wimpenny, D.E.: Sulfate and chloride profiles and the visual characteristics with depth from the face in buried concrete subject to TSA. Proceedings of 1st International Conference on Thaumasite, BRE, London, 2002

[62]   Tsivilis, S.; Sotiriadis, K. and Skaropoulou, A.: Thaumasite form of sulfate attack (TSA) in limestone cement pastes. Journal of the European Ceramic Society 27, 2007, pp.1711-1714

[63]   Crammond, N.J.; Halliwell, M.A. and Higgins, D.D.: The use of ground blastfurnace slag to avoid the thaumasite form of sulfate attack: four-year results. Proceedings of International Conference in Sustainable Construction into the Next Millennium, João Pessoa, Brazil, Nov 2000

[64]   Czerewko, M.A.; Cripps, J.C.; Duffell, C.G. and Reid, J.M.: The distribution and evaluation of sulfur species in geological materials and manmade fills. Proceedings of 1st International Conference on Thaumasite, BRE, London, 2002

[65]   White, S.J.; Smy, R.H. and Lynch, M.: Highways Agency Area 2: Managing the threat of thaumasite sulfate attack. Proceedings of 1st International Conference on Thaumasite, BRE, London, 2002

[66]   Longworth, T.I.: Contribution of construction activity to aggressive ground conditions causing the thaumasite form of sulfate attack to concrete in pyritic ground. Cement & Concrete Composites 25, 2003, pp.1005-1013

[67]   Floyd, M.; Czerewko, M.A.; Cripps, J.C. and Spears, D.A.: Pyrite oxidation in Lower Lias Clay at concrete highway structures affected by thaumasite, Gloucestershire, UK. Cement & Concrete Research 25, 2003, pp.1015-1024

[68]   Eden, M.A.: The laboratory investigation of concrete affected by TSA in the UK. Cement & Concrete Composites 25, 2003, pp.847-850

References

---

[69]   Chandler, R.J.: Lias Clay weathering processes and their effects on shear strength. Geotechnique 22, 1972, pp.403-431

[70]   Torres, S.M.; Lynsdale, C.J.; Swamy, R.N. and Sharp, J.H.: Microstructure of 5-year-old mortars containing limestone filler damaged by thaumasite. Cement & Concrete Research 36, 2006, pp.384-394

[71]   Thomas, M.D.A.; Rogers, C.A. and Bleszynski, R.F.: Occurrences of thaumasite in laboratory and field concrete. Cement & Concrete Composites 25, 2003, pp.1045-1050

[72]   Nobst, P. and Stark, J.: Grundlagenuntersuchungen zur Thaumasitbildung in Zementsteinpasten. Proceedings of 15th IBAUSIL, Finger Institute fuer Baustoffkunde, Weimar, 2003, Vol.2, pp.0685-0700

[73]   Hobbs, D.W. and Taylor, M.G.: Nature of thaumasite sulfate attack mechanism in field concrete. Cement & Concrete Research 30, 2000, pp.529-533

[74]   Wimpenny, D. and Slater, D.: Evidence from the highways agency thaumasite investigation in Glouchestershire to support or contradict postulated mechanisms of thaumasite formation (TF) and thaumasite sulfate attack (TSA). Cement & Concrete Composites 25, 2003, pp.879-888

[75]   Bensted, J.: Thaumasite – direct, woodfordite and other possible formation routes. Cement & Concrete Composites 25, 2003, pp.873-877

[76]   Bonen, D. and Cohen, M.D.: Magnesium sulfate attack on Portland cement paste – I. Microstructural analysis. Cement & Concrete Research 22, 1992, pp.169-180

[77]   Bonen, D. and Cohen, M.D.: Magnesium sulfate attack on Portland cement paste – II. Chemical and mineralogical analyses. Cement & Concrete Research 22, 1992, pp.707-718

[78]   Koehler, S.; Heinz, D. and Urbonas, L.: Effect of ettringite on thaumasite formation". Cement & Concrete Research 36, 2006, pp.697-706

[79]   Bensted, J.: Thaumasite – a deterioration product of hardened cement structures. II Cemento 85, 1988, pp.3-10

[80]   Crammond, N.J.; Collett, G.W. and Longworth, T.I.: Thaumasite field trial at Shipston on Stour: three-year preliminary assessment of buried concretes. Cement & Concrete Composites 25, 2003, pp.1035-1043

[81]   Brown, P.W. and Doerr, A.: Chemical changes in concrete due to the ingress of aggressive species. Cement & Concrete Research 30, 2000, pp.411-418

[82]   Sibbick, R.G. and Crammond, N.J.: The petrographical examination of popcorn calcite deposition (PCD) within concrete mortar, and its association with other forms of degradation. Proceedings of 9th Euroseminar on Microscopy Applied to Building Materials, Trondheim, Norway, Sep 2003

[83]   Hartshorn, S.A.; Sharp, J.H. and Swamy, R.N.: The thaumasite form of sulfate attack in Portland-limestone cement mortars stored in magnesium sulfate solution. Cement & Concrete Composites 24, 2002, pp.351-359

[84]   Hill. J.; Byars, E.A.; Sharp, J.H.; Lynsdale, C.J.; Cripps, J.C. and Zhou, Q.: An experimental study of combined acid and sulfate attack of concrete. Cement & Concrete Composites 25, 2003, pp.997-1003

[85]   Lee, S.T.; Moon, H.Y.; Hooton, R.D. and Kim, J.P.: Effect of solution concentrations and replacement levels of metakaolin on the resistance of mortars exposed to magnesium sulfate solution. Cement & Concrete Research 35, 2005, pp.1314-1323

[86]   Taylor, H.F.W.: Cement Chemistry. 2nd Edition, 1997, Thomas Telford Publishing, London

[87]   Wimpenny, D. and Slater, D.: Evidence from the highways agency thaumasite investigation in Glouchestershire to support or contradict postulated mechanisms of thaumasite formation (TF) and thaumasite sulfate attack (TSA). Cement & Concrete Composites 25, 2003, pp.879-888

[88]   Thaulow, N. and Jacobsen, U.H.: Deterioration of concrete diagnosed by optical microscopy. Proceedings of the 6th Euroseminar on Microscopy Applied to Building Materials, Reykjavik, Iceland, 1997, pp.282-296

[89]   Sibbick, R.G. and Crammond. N.J.: Microscopical investigations into recent field examples of the thaumasite form of sulfate attack. Proceedings of the 8th Euroseminar on Microscopy Applied to Building Materials, Athens, Greece, 2001, pp.261-269

[90]   Bromley, A.V. and Pettifer, K.: Sulfide-related degradation of concrete in Southwest England. Building Research Laboratory Report, BR325. CRC Ltd. Watford, 1997, pp.13-29

References

---

[91]   Thaulow, N.; Lee, R.J.; Wagner, K. and Sahu, S.: The form, extent and significance of carbonation. In 'Calcium hydroxide in Concrete' published by the Materials Science of Concrete, Wiley Europe Ltd., Chichester, 2000, pp.191-202

[92]   French, W.J.: Sub-aqueous carbonation and the formation of thaumasite in concrete. Proceedings of the 20th IOM[3] Cement and Concrete. Science Conference, Sheffield University, Sep 2000, Published by IOM[3], London

[93]   Nobst, P. and Stark, J.: Investigations on the influence of cement type on thaumasite formation. Cement & Concrete Composites 25, 2003, pp.899-906

[94]   St John, D.A.; Poole, A.W. and Sims, I.: Concrete Petrography – A handbook of investigative techniques. Published by Arnold, London, 1998

[95]   Bellmann, F. and Stark, J.: Ein Beitrag zum Chemismus der Thaumasitbildung. Proceeding of 15th IBAUSIL, Finger Institute fuer Baustoffkunde, Weimar, 2003, Vol. 2, pp.659-671

[96]   Building Research Establishment: Concrete in aggressive ground. Special Digest 1, BRE, Watford, (CRC Ltd., London), UK, 2005

[97]   Building Research Establishment: Sulfate and acid resistance to concrete in the ground. Digest 363, BRE, Watford, (CRC Ltd., London), UK, 1996

[98]   Lipus, K. and Punkte, St.: Sulfatwiderstand unterschiedlich zusammengesetzter Betone (Teil 1). Beton, Verlag Bau+Technik, Duesseldorf, 2003, pp.97-100 (in German)

[99]   Lipus, K. and Punkte, St.: Sulfatwiderstand unterschiedlich zusammengesetzter Betone (Teil 2). Beton, Verlag Bau+Technik, Duesseldorf, 2003, pp.153-157 (in German)

[100]   Blanco-Varela, M.T.; Aguilera, J. and Martinez-Ramirez, S.: Effect of cement C_3A content, temperature and storage medium on thaumasite formation in carbonated mortars. Cement & Concrete Research 36, 2006, pp.707-715

[101]   Herfort, D.; Porsborg, A.T.; Grundvig, S.; Jakobsen, H.J. and Skibsted, J.: Hydrate phase assemblages of Portland cement pastes stored at 5 and 20°C. Proceedings of the 20th IOM[3] Cement and Concrete. Science Conference, University of Sheffield, Sep 2000, Published by IOM[3], London

[102] Crammond, N.J. and Halliwell, M.A.: The thaumasite field trial, Shipston-on-Stour: Details of the site and specimen burial. Client Report: CR68/94, BRE, 1998

[103] Crammond, N.J. and Halliwell, M.A.: The thaumasite form of sulfate attack in laboratory-prepared concretes. BRE Report, Watford, 1996

[104] Halliwell, M.A. and Crammond, N.J.: Avoiding the thaumasite form of sulfate: two-year report. BRE DETR Report, Watford, 2000

[105] Building Research Establishment: Concrete in Sulfate-bearing Soils and Groundwaters. Digest 250, BRE, Watford, (CRC Ltd., London), UK, 1981

[106] Wittekindt, W.: Sulfatbestaendige Zemente und ihre Pruefung. Zement-Kalk-Gips 13, 1960, pp.565-571

[107] Tesch, V. and Middendorf, B.: Occurrence of thaumasite in gypsum lime mortars for restoration. Cement & Concrete Research 36, 2006, pp.1516-1522

[108] Crammond, N.J.: Thaumasite field trial at Shipston-on-Stour – One year results from parallel laboratory study, Report No.80006, 1999, BRE

[109] Wallace, J.: Finding thaumasite sulfate attack – Consequences for works in progress. Proceedings of 1st International Conference on Thaumasite, BRE, London, 2002

[110] Gorst, N.J.S. and Clark, L.A.: Effects of thaumasite on bond strength of reinforcement in concrete. Cement & Concrete Composites 25, 2003, pp.1089-1094

[111] Cernica, J.N.: Geotechnical Engineering: Soil Mechanics. Published by John Wiley & Sons, Inc., New York, Chichester, 1995

[112] Cernica, J.N.: Geotechnical Engineering: Foundation design. Published by John Wiley & Sons, Inc., New York, Chichester, 1995

[113] Das, B.M.: Principles of Foundation Engineering. 5th Edition, Published by Brooks/Cole-Thomson Learning, Pacific Grove, California, 2004

[114] Ruetz, D.; Schmidt, H.-G.; Wendt, R. and Witt, K.J.: Wissensspeicher Geotechnik. Bauhaus-Universität Weimar, 15th Edition, Weimar, 2004

[115] Meyerhof, G.G. and Murdock, L.J.: An Investigation of the Bearing Capacity of Some Bored and Driven Piles in London Clay. Geotechnique 3, 1953, pp.267-282

[116]   Chandler, R.J.: The Shaft Friction of Piles in Cohesive Soils in terms of Effective Stress. Civil Engineering Public Works Review 63, 1968, pp.48-51

[117]   Burland, J.B.: Shaft Friction of Piles in Clay. A Simple Fundamental Approach. Ground Engineering 6, 1973, pp.30-42

[118]   Haraldsson, A. and Wriggers, P.: A strategy for numerical testing of frictional laws with application to contact between soil and concrete. Computer Methods in Applied Mechanics and Engineering 190, 2000, pp.963-977

[119]   Zong-Ze, Yin; Hong, Zhu and Guo-Hua, Xu: A Study of Deformation in the Interface between Soil and Concrete. Computers and Geotechnics 17, 1995, pp.75-92

[120]   Tabsh, S.W.; O'Neill, M.W.O. and Nam, M.S.: Shear strength of drilled shafts with minor flaws. Engineering Structures 27, 2005, pp.736-748

[121]   Matthews, M.C.: The engineering application of direct and simple shear testing. Ground Engineering 21, 1988, pp.13-21

[122]   Potyondy, J.G.: Skin friction between various soils and construction materials. Geotechnique 11, 1961, pp.339-353

[123]   Clough, G.W. and Duncan, J.M.: Finite Element Analyses of Retaining Wall Behaviour. Journal of the Soil Mechanics and Foundation Division 97, ASCE, 1971, pp.1657-1673

[124]   Peterson, M.S.; Kulhawy, F.H.; Nucci, L.R. and Wasil, B.A.: Stress-Deformation Behaviour of Soil-Concrete Interface. Contract Report B-49 to Niagara Mohawk Power Corporation, Syracuse, New York, 1976

[125]   Lemos, L.J.L. and Vaughan, P.R.: Clay-interface shear resistance. Geotechnique 50, 2000, pp.55-64

[126]   Lee, Lin: Soil-pile interaction of bored and cast in-situ piles. PhD-Thesis, University Of Birmingham, 2001

[127]   Frost, J.D.; DeJong, J.T. and Recalde, M.: Shear failure behaviour of granular-continuum interfaces. Engineering Fracture Mechanics 69, 2002, pp.2029-2048

[128]   Uesugi, M. and Kishida, H.: Frictional resistance at yield between dry sand and mild steel. Soils and Foundations 26, 1986, pp.139-149

[129]   Chandler, R.J. and Martins, J.P.: An experimental study of skin friction around piles in clay. Geotechnique 32, 1982, pp.119-132

References

[130]   Johnston, I.W.; Lam, T.S.K. and Williams, A.F.: Constant normal stiffness direct shear testing for socketed pile design in weak rock. Geotechnique 37, 1987, pp.83-89

[131]   Rojas, E.: Static behaviour of model friction piles. Ground Engineering, 1993, pp.26-30

[132]   Rojas, E.; Valle, C. and Romo, M.P.: Soil-pile interface model for axially loaded single piles. Soils and Foundations 39, 1999, pp.35-45

[133]   Chandler, R.J. and Hamilton, P.S.: On the measurement of the undrained strength of discontinuities in the direct shear box. Geotechnique 49, 1999, pp.615-620

[134]   Rao, K.S.S.; Allam, M.M. and Robinson, R.G.: Drained Shear Strength of Fine-Grained Soil-Solid Surface Interfaces. Geotechnical Engineering 143, 2000, pp.75-81

[135]   Webster, J.D. and Sheary, V.J.: Stabilisation of Clays and other Fine Grained Materials. Australian Road Research Board, Vol.1, Part 2, 1962, pp.223-250

[136]   Sherwood, P.T.: Soil stabilisation with cement and lime. London: HMSO, 1993

[137]   El-Rawi, N.M. and Awad, A.A.: Permeability of lime stabilized soils. Transportation Engineering Journal 107, 1981, pp.25-35

[138]   Mililitsky, J.; Jones, J.R. and Clayton, C.R.I.: A radiochemical method of studying the moisture movement between fresh concrete and clay. Geotechnique 32, 1982, pp.271-275

[139]   Chuang, J.W. and Reese, L.C.: Studies of shearing resistance between cement mortar and soil. University of Texas at Austin, Research report 89-3, 1969

[140]   O'Neill, M.W. and Reese, L.C.: Behaviour of axially loaded drilled shafts in Beaumont clay. University of Texas at Austin, Research report 89-8, 1970

[141]   Yong, K.Y.: A laboratory study of the shaft resistance of bored piles. PhD-thesis, University of Sheffield, 1979

[142]   Clesceri, L.; Greenberg, A. and Eaton, A.: Standard Methods for the Examination of Water and Wastewater, 20th Edition, American Public Health Association, Atlanta, 1998

[143]   Email correspondence with Norah Crammond, Building Research Establishment, Watford, UK, 2004-2005

[144]   http://www.concrete-catalog.com/soil_compaction.html, February 2007

References

[145]   Disc spring information sheet of Belleville Washers, 2005

[146]   Shimadzu TOC-5050 Total Organic Carbon Analyzer – Manual book: http://snobear.colorado.edu/cgi-bin/Kiowa/Kiowa.con.pl?shimadzu5050a.doc.html, August 2006

[147]   University of Birmingham, Centre for Chemical and Biochemical Analysis: http://www.chem.bham.ac.uk/chemanalysis/X.htm, August 2006

[148]   Teychenné, D.C.; Franklin, R.E. and Erntroy, H.C.: Design of normal concrete mixes. Building Research Establishment report, Department of the Environment, 1988

[149]   Email correspondence with Ian Heritage, Lafarge cement, 2005

[150]   Email correspondence with Ian Longworth, Building Research Establishment, Watford, UK, April 2007

[151]   Puraflo 50 – Data sheet obtained from WBB Devon Clays Ltd., 2005

[152]   Email correspondence with Deborah Boote, British Geological Survey – Natural Environment Research Council, Nottingham, UK, March 2007

[153]   Private communication with R.G. Sibbick, September 2006

[154]   Perry, J.H.: Chemical Engineers Handbook. McGraw-Hill Professional, New York, 1963

[155]   Burland, J.B. and Twine, D.: The Shaft Friction of Bored Piles in Terms of Effective Strength. Proceedings of the Seminar on Deep Foundation on Bored and Auger Piles, Van Impe(ed), Balkema, Rotterdam, 1988

Standards

BRE Digest 250   Building Research Establishment: Concrete in Sulfate-bearing Soils and Groundwaters. Digest 250, BRE, Watford, (CRC Ltd., London), UK, 1981

BRE Digest 363   Building Research Establishment: Sulfate and acid resistance to concrete in the ground. Digest 363, BRE, Watford, (CRC Ltd., London), UK, 1996

References

BRE Special Digest 1	Building Research Establishment: Concrete in aggressive ground, Special Digest 1, BRE, Watford, (CRC Ltd., London), UK, 2005
BS EN 197-1:2004	Cement – Part 1: Composition, specifications and conformity criteria for common cements.
BS EN 206-1:2001	Concrete – Part 1: Specification, performance, production and conformity.
BS 812-103:1985	Sieve Tests
BS 882:1992	Specification for aggregates from natural sources for concrete.
BS 1377-3:1990	Methods of test for 'Soils for civil engineering purposes – Part 3: Chemical and electro-chemical tests
BS 1377-4:1990	Methods of test for 'Soils for civil engineering purposes – Part 4: Compaction related test
BS 1377-7:1990	Methods of test for 'Soils for civil engineering purposes – Part 7: Shear strength tests (total stress).
BS 1881-102:1983	Methods for determination of slump
BS 1881-116:1983	Methods for determination of compressive strength of concrete cubes
BS EN 1992-1-1:2004	Eurocode 2: Design of concrete structures – Part 1-1: General rules and rules for buildings.
BS EN 1997-1:2004	Eurocode 7: Geotechnical design – Part 1: General rules.
BS 4027:1996	Specification for Sulfate-resisting Portland cement.
BS 5328-1:1997	Concrete – Part 1: Guide for specifying concrete.
BS 5328-2:1997	Concrete – Part 2: Methods for specifying concrete mixes.
BS 5328-3:1990	Concrete – Part 3: Specification for the procedures to be used in producing and transporting concrete.
BS 5328-4:1990	Concrete – Part 4: Specification for the procedures to be used in sampling, testing and assessing compliance of concrete.
BS 8500-1:2002	Concrete – Complementary British Standard to BS EN 206-1 – Part 1: Method of specifying and guidance for the specifier.

References

BS 8500-2:2002   Concrete – Complementary British Standard to BS EN
                        206-1 – Part 1: Specification for constituent materials and
                        concrete.

Appendix

Table A- 1: Physical properties of mixed concrete

Specimen type	Mix	Calculated density [g/dm³]	Measured density [g/dm³]	Slump [mm]	Compressive strength	
					7 days [N/mm²]	28 days [N/mm²]
Series I, II, IV-precast	1	2342.7	2342.9	20	37.5	46.1
	2	2296.3	2312.3	90	28.6	37.0
	3	2249.3	2288.1	210	20.8	27.9
	4	2321.4	2323.4	40	36.4	44.0
	5	2219.0	2286.2	260	18.8	25.2
Series IV-cast in-situ	1	2342.7	2343.9	55	31.5	39.2
	2	2296.3	2290.6	160	26.0	33.0
	3	2249.3	2272.8	225	16.9	23.7
	4	2321.4	2361.6	25	40.0	48.0
	5	2219.0	2242.6	255	16.4	22.5
Shear test specimen-precast	3	2249.3	2290.6	235	18.6	24.0
	4	2321.4	2340.3	40	34.9	41.2
Shear test specimen-cast in-situ	3	2249.3	2282.4	225	22.2	29.4
	4	2321.4	2341.7	20	40.9	50.0
	5	2219.0	2229.1	270	15.1	21.4
Solution uptake, Thaumasite-pressure*, Series I, II CS-needle*	1	2342.7	2361.6	10	31.6	41.6
	2	2296.3	2308.3	80	23.9	31.2
	3	2249.3	2258.6	225	17.0	23.0
	4	2321.4	2352.8	20	31.3	41.1
	5	2219.0	2290.6	235	14.7	20.4
Carbonate migration specimens	1	2342.7	2359.9	20	27.5	36.4
	2	2296.3	2329.7	160	17.6	26.5
	3	2249.3	2278.2	230	14.6	20.3
	4	2321.4	2352.8	20	29.8	38.8
	5	2219.0	2283.5	240	14.8	20.4

*Mixes 3; 5 only used

Table A- 2: Detailed chemical specification of Lower Lias Clay (Moreton Valence) [149]

Sample / Depth	Mean Depth	TS	TPS	WS	AS	OS	OS/TPS	Sulfate Class (WS re SD1[23])	In 2:1 Water extract				pH	ACa
									WMg	WNa	WK	WCa		
m	m	S %	SO₄ %	SO₄ g/l	SO₄ %	SO₄ %			Mg g/l	Na g/l	K g/l	Ca g/l		Ca%
	07.06.2004	Tested by TESB by 15 July 2004												
0.0-0.1	0,05	1,286	3,858	2,030	1,960	1,898	49,20	2	0,056	0,016	0,033	0,589	7,7	7,82
0.2-0.3	0,25	1,131	3,393	2,170	1,120	2,273	66,99	2	0,120	0,014	0,040	0,560	7,8	10,80
0.4-0.5	0,45	1,823	5,469	2,240	7,740	-2,271	-41,52	2	0,144	0,034	0,027	0,561	7,8	8,99
0.6-0.7	0,65	1,139	3,417	2,380	1,580	1,837	53,76	3	0,146	0,073	0,034	0,528	7,8	8,00
0.8-0.9	0,85	1,243	3,729	2,450	1,880	1,849	49,58	3	0,127	0,115	0,035	0,535	7,8	8,84

Py	Pyrite determination by the acidified chromium reduction method
TS (MD)	Total sulfur determined by microwave digestion method (as % of sample dry mass)
TS	Total sulfur determined by the LECO combustion method as BR279 (as % of sample dry mass)
C	Total carbon determined by the LECO combustion method (as % of sample dry mass)
OS	Calculated oxidisable sulfides (as % of sample dry mass)

Water extract

WS	Water soluble sulfates SO₄ determined on 2:1 water/soil extract by ion chromatography as BR279
WMg	Magnesium in 2:1 water/soil extract by AAS as BR279
WNa	Sodium in 2:1 water/soil extract by AAS as BR279
WK	Potassium in 2:1 water/soil extract by AAS as BR279
WCa	Calcium in 2:1 water/soil extract by AAS as BR279
pH	pH determined AS BR 279 on 2.5:1 water:soil extract as BR279 and BS1377

Acid extract

AS	Acid soluble sulfate SO₄ as BR279 (as % of sample dry mass)
ACa	Total calcium Ca²⁺ determined by AAS on HCl acid extract (as % of sample dry mass)
AMg	Total magnesium Mg²⁺ determined by AAS on HCl acid extract (as % of sample dry mass)

British Geological Survey:
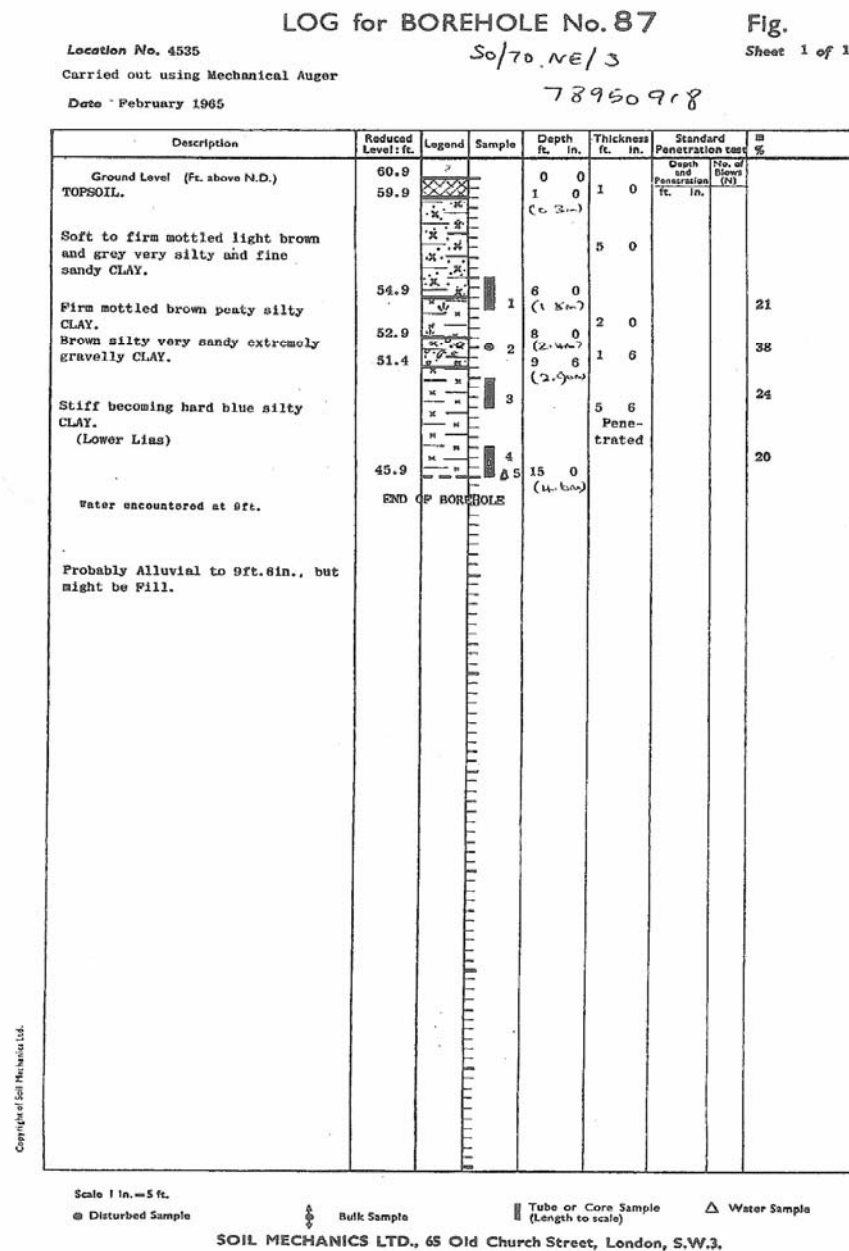
Figure A-1: Log for borehole No. 87 close to Moreton Valence trial site

TSA Assessment performed by R.G. Sibbick

Table A-3: Microscopical assessment of TSA affected concrete samples [153]

Slide – Description and number	Age [Months] In sulfate solution at 6°C	Visual assessment of TSA/TF zone depths	Comments
Mix 3 – SO_4 – 3/16	9	None	Adhesion crack with secondary CH crystals –2mm depth. Paste microcracks autogeneous shrinkage cracks. No TSA or TF
Mix 3 – SO_4 – 5/16	15	Zone 1- 4.5mm Zone 2 – 4.0mm Zone 3 – 3.5mm Zone 4 - >3mm	Uneven surface. Lifted off carbonated surface overlying Zone 4 deposit makes thickness approximate.
Mix 3 – SO_4 – 7/16	21	Zone 1- 3.5mm Zone 2 – 2.5 to 3.0mm Zone 3 – ~3.0mm Zone 4 – 2 to 5mm	TSA degradation patchy. Large CH crystals in adhesion cracks on coarse aggregate. Gypsum crystallization in air void. Sharply defined degradation (not an usual feature). Zone 4 – mainly 2mm locally 5mm.
Mix 3 – SO_4-CO_3 – 3/16	9	Zone 1 –11mm Zone 2 – 2mm Zone 3 – 1.5mm Zone 4 - ~1mm	Patchy TSA development. Surface material loss. Possible gypsum crystallization also noted. Surface Thaumasite low birefringence increasing with increased depth.
Mix 3 – SO_4-CO_3 – 5/16	15	Zone 4 material separated from remaining concrete	Surface incomplete – desiccation/ prep cracks carbonated. No intermediate degradation remains lost by prep and m/c development
Mix 3 – SO_4-CO_3 – 7/16	21	Zone 1- 3.5mm Zone 2 – 3.5mm Zone 3 – 3.0mm Zone 4 - traces	Uneven concrete surface + some loss of material. Possible gypsum crystal in microcracks in paste and aggregates with TSA affected zone.

Mix 3 / PC / LLC – 3/12 Clay attached	9	None	Carbonated edge 2-4mm Gypsum at boundary with clay. Post prep impregnation M/c. large secondary CH crystals in AC on CA
Mix 3 / PC / LLC – 5/12 No clay attached	15	Zone 1 – 2.5mm Zone 2 – 2mm Zone 3-4 - <0.5mm	Top surface of concrete cut off?
Mix 3 / PC / ECC – 2/12 Clay attached	9	None	Heavily carbonated degraded zone = Possible TSA/TF no residual Thaumasite observed. Traces possible zone 4 at 1-2mm . Not clear
Mix 3 / PC / ECC – 4/12 No clay attached	15	Zone 1- None Zone 2 – 3.0 to 3.5mm Zone 3 – 3.0mm Zone 4 – 2 to 2.5mm	Sharp TSA degradation front. No significant intermediate degradation or TF zones detected.
Mix 3 / CS / LLC – 3/12 Clay attached	9	Zone 1- 2.5 to 3mm Zone 2 – None Zone 3 – None Zone 4 - 2mm	No microcracks developed just bulk cement paste consumption observed.
Mix 3 / CS / LLC – 5/12 No clay attached	15	Zone 1- None Zone 2 - None Zone 3 – 1 to 2mm Zone 4 – trace to 1.5mm	TSA Sharp front to sound concrete. Empty prep induce crack. Poorly compacted concrete.
Mix 3 / CS / ECC – 2/12 Clay attached	9	None	No concrete degradation – carbonated to 2mm depth below clay layer. Carbonate at clay boundary layer with concrete.
Mix 3 / CS / ECC – 4/12 No clay attached	15	Zone 1 - <1mm Zone 2 Zone 3 Zone 4	Heavily carbonated. Probably only TF. Large secondary CH crystals in AC on CA

Mix 4 – SO$_4$ – 2/16	9	Zone 1 - 2mm Zone 2 – 2mm Zone 3 – 0.5-0.75mm Zone 4 - None	Uneven surface. Thick slide. Secondary surface calcite deposits 50 microns thick. Developing over normal carbonation. Thaumasite edge deposits on aggregate adhesion cracks (TF). No degradation in most areas.
Mix 4 – SO$_4$ – 4/16	15	None	Surface lost by thin section wedging in prep.
Mix 4 – SO$_4$ – 6/16	21	Zone 1 – 3.5mm max Zone 2 – 1 to 3mm Zone 3 - 1 to 3mm Zone 4 – Trace to 1mm	Mechanically induced M/c at depth. Thaumasite deposit thin with PCD
Mix 4 – SO$_4$-CO$_3$ – 2/16	9	Zone 1- 2.0mm Zone 2 – 2.0mm Zone 3 – 1.0mm Zone 4 - None	Microcracks at 3mm depth show no Thaumasite or gypsum deposits. Mechanical crack at depth
Mix 4 – SO$_4$-CO$_3$ – 4/16	15	Zone 1- 11mm Zone 2 – ~2mm Zone 3 – ~2mm Zone 4 – 1½ mm	Uneven surface plus some loss of material. Incomplete TSA sequence in parts not an uncommon occurrence. Zone 4 sharp front
Mix 4 – SO$_4$-CO$_3$ – 6/16	21	Zone 1- 5.0 to 5.5mm Zone 2 – 4-to 5.5mm Zone 3 – 4 to 5.5mm Zone 4 – 2.5 to 3mm	Incomplete surface. Sharp degradation boundary at last crack observed. No strong evidence for TF development.
Mix 4 / PC / LLC – 2/12 Clay attached	9	Zone 1- 3 to 3.5mm Zone 2 – 3mm Zone 3 – 3mm Zone 4 – 3mm	Slide prep patchy in area of interest. Parallel m-c system at 2-3mm depth probably TSA related but no associated Thaumasite deposits.
Mix 4 / PC / LLC – 4/12 No clay attached	15	Zone 1- 3.5 to 4mm Zone 2 – 2 to 3mm Zone 3 – 2 to 3mm Zone 4 – 1 to 2mm	Void fill determined for zone 1 (TF) identification.

Mix 4 / PC / ECC – 2/12 Clay attached	9	None	Well-carbonated surface. Void 1mm from surface edged with ettringite. Cracks below surface carbonated layer.
Mix 4 / PC / ECC – 4/12 No clay attached	15	Zone 1- 0mm Zone 2 – 7mm Zone 3 – 5 to 6mm Zone 4 – 6mm or greater	Severe TSA. Underlying degraded concrete surface is fully carbonated. Cracks observed at depth below TSA affected zone. Adhesion crack on coarse aggregate at depth edged with CH crystals
Mix 4 / CS / LLC – 2/12 Clay attached	9	Zone 1- 1mm max Zone 2 –1mm max Zone 3 –1mm max Zone 4 –1mm max	Clay with heavy desiccation cracking. Borderline detection mainly as fill deposits of air voids and adhesion cracks on coarse aggregate. Some microcracks and paste consumption in first 0.5mm.
Mix 4 / CS / LLC – 4/12 No clay attached	15	Zone 1- 1 to 2mm Zone 2 – None Zone 3 – None Zone 4 – None	Adhesion crack fill of Thaumasite on coarse aggregate edges. No TSA. Autogeneous paste shrinkage microcracks
Mix 4 / CS / ECC – 2/12 Clay attached	9	None	Ettringite filled air void at 0.5mm depth. Void at 8mm filled with 'clay'? No sulfate attack (TSA) related microcracks or TF detected.
Mix 4 / CS / ECC – 4/12 No clay attached	15	None	Sharp boundary overlain with clay? Incomplete retension of clay

XRD-Analyses:
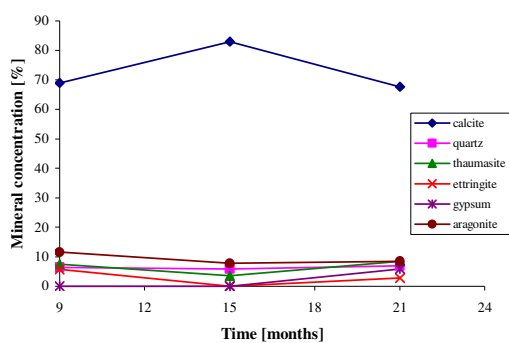
Figure A-2 - Mix 1/PC - SO$_4$-solution
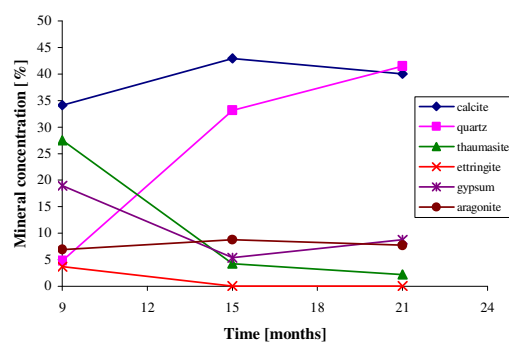
Figure A-3 - Mix 3/PC - SO$_4$-solution
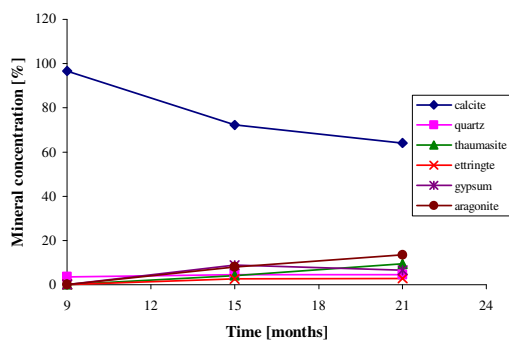
Figure A-4 - Mix 4/PC - SO$_4$-solution
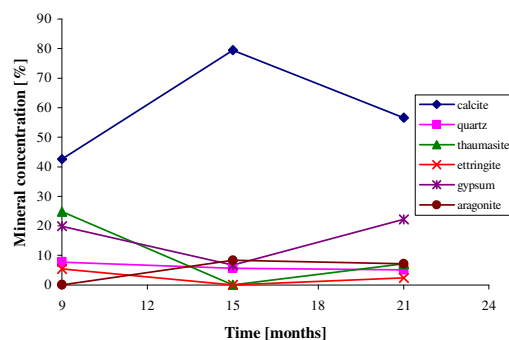
Figure A-5 - Mix 5/PC - SO$_4$-solution
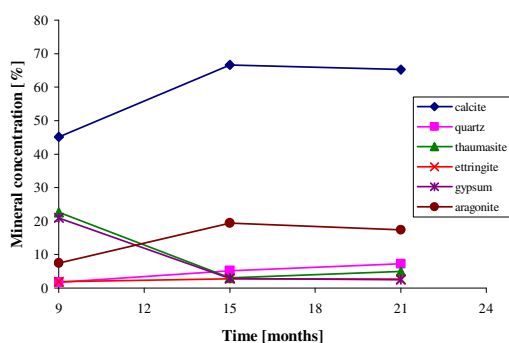
Figure A-6 - Mix 1/PC - SO$_4$-CO$_3$-solution
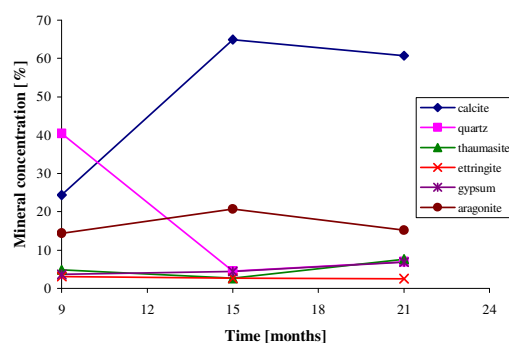
Figure A-7 - Mix 3/PC - SO$_4$-CO$_3$-solution
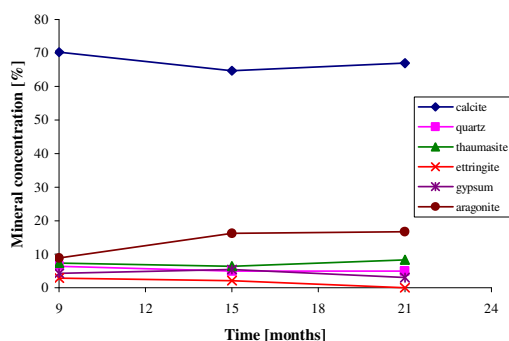
Figure A-8 - Mix 4/PC - SO$_4$-CO$_3$-solution
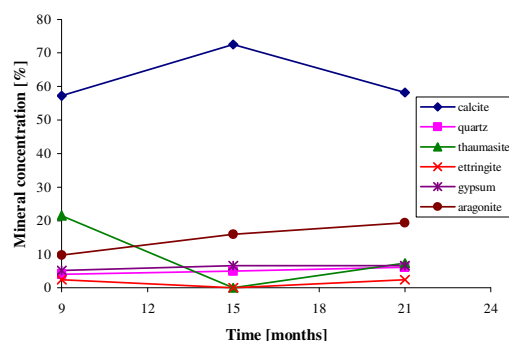
Figure A-9 - Mix5/PC - SO$_4$-CO$_3$-solution
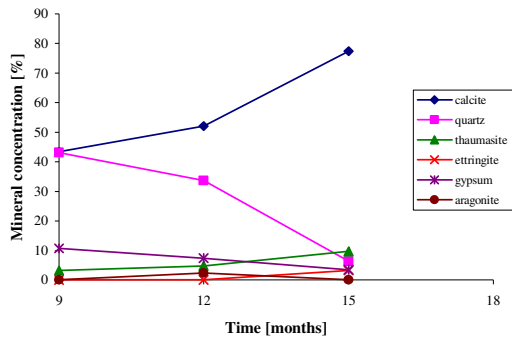
Figure A-10 - Mix 3/CS - SO$_4$-solution
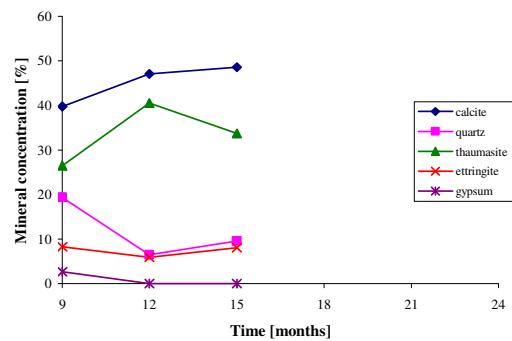
Figure A-11 - Mix 5 – PC, restrained, SO$_4$-solution
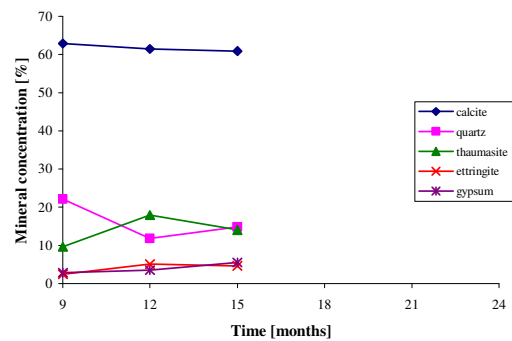
Figure A-12 - Mix5 - CS, restrained, SO$_4$-solution
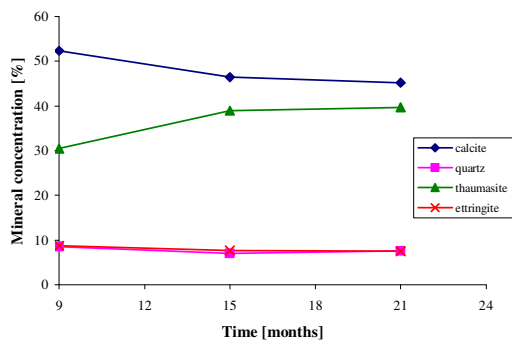
Figure A-13 - Mix1/PC/LLC
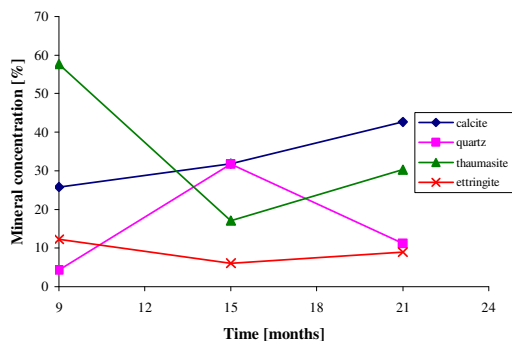
Figure A-14 - Mix3/PC/LLC
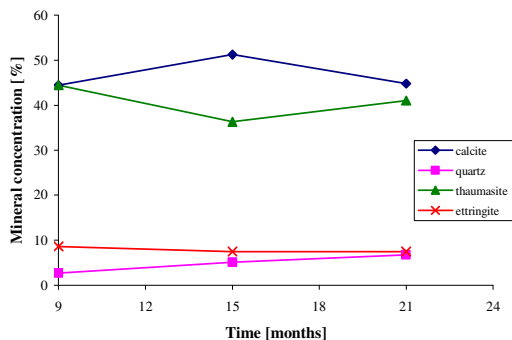
Figure A-15 - Mix4/PC/LLC
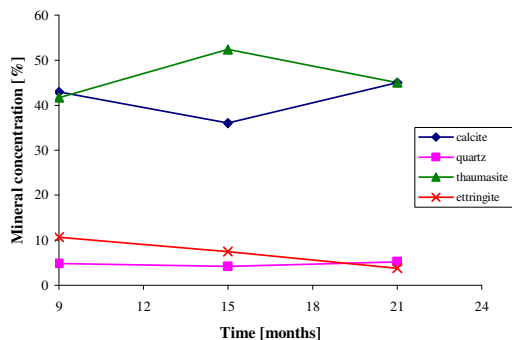
Figure A-16 - Mix5/PC/LLC
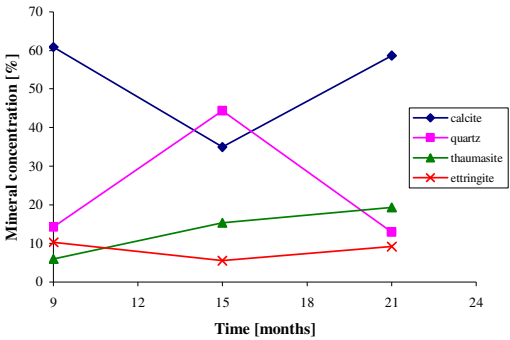
Figure A-17 - Mix1/CS/LLC
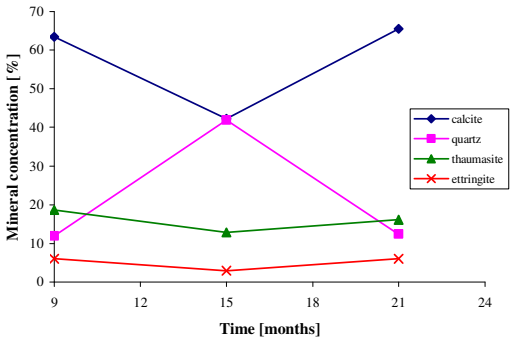
Figure A-18 - Mix3/CS/LLC
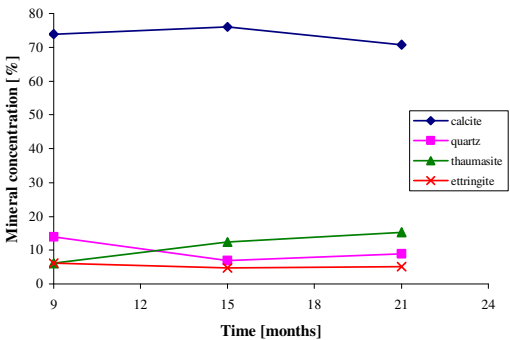
Figure A-19 - Mix4/CS/LLC
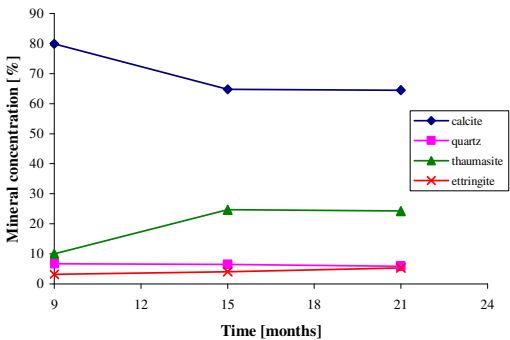
Figure A-20 - Mix5/CS/LLC
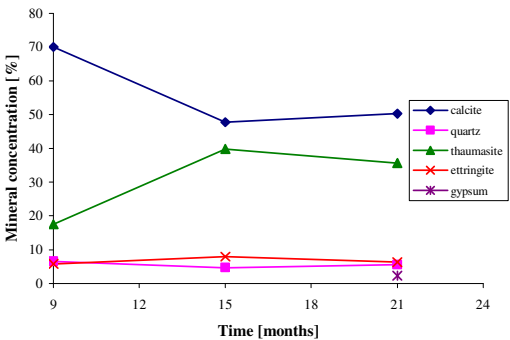
Figure A-21 - Mix1/PC/ECC
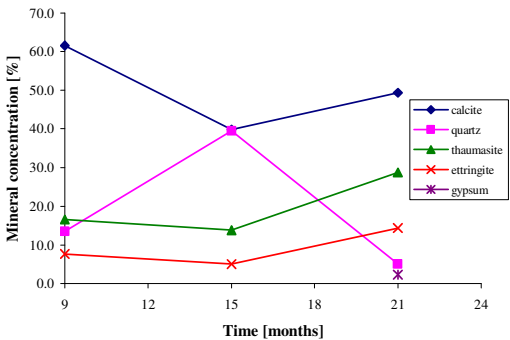
Figure A-22 - Mix3/PC/ECC
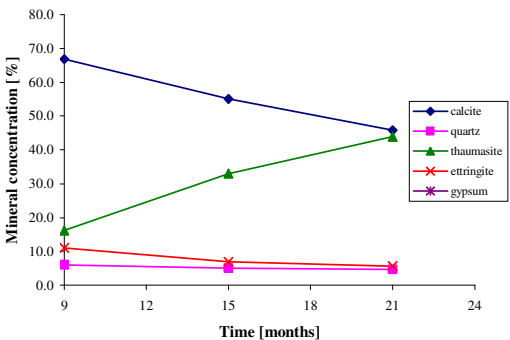
Figure A-23 - Mix4/PC/ECC
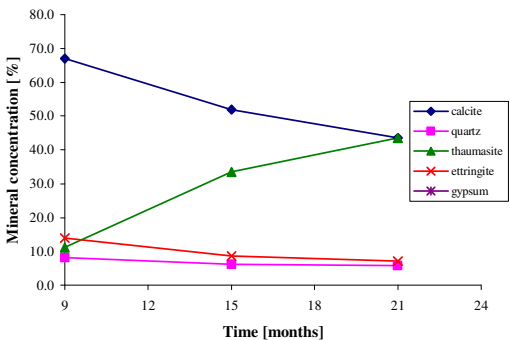
Figure A-24 - Mix5/PC/ECC
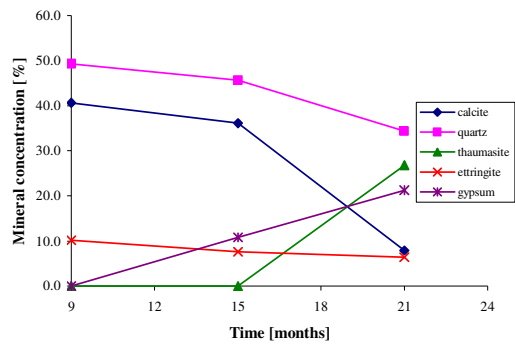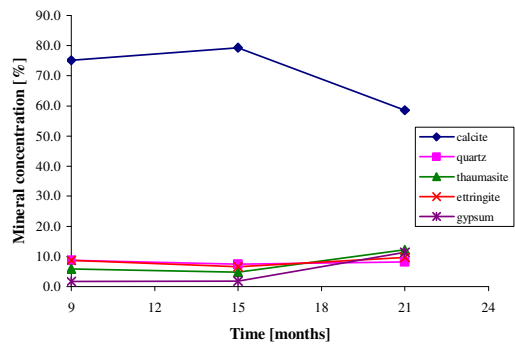
Figure A-25 - Mix1/CS/ECC
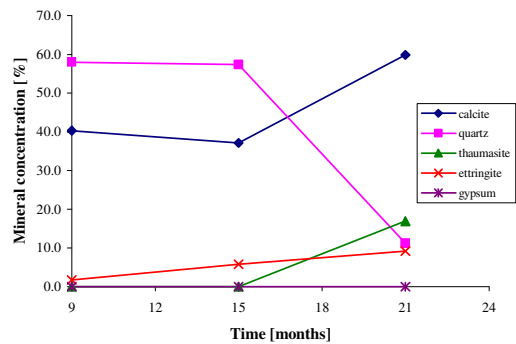
Figure A-26 - Mix3/CS/ECC

Figure A-27 - Mix4/CS/ECC

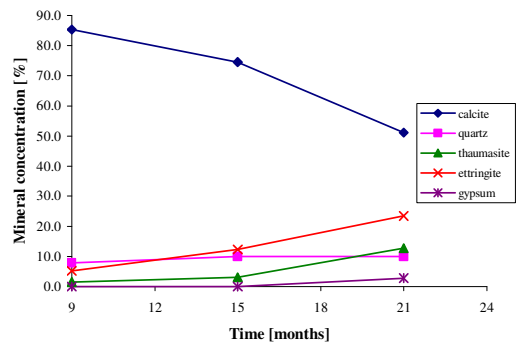

Figure A-28 - Mix5/CS/ECC

Series I – Pressure Development and Expansion

The figure shows the development of pressure and the expansion caused determined at sub-specimens belonging to Series I, Stage 2. A physical barrier consisting of a layer of filter paper was installed at the interface between concrete and pressure distributing quartz sand to prevent the ingress of TSA reaction products into the sand. However, the filter paper was too soft and thick so that it allowed expansions which could not be measured.
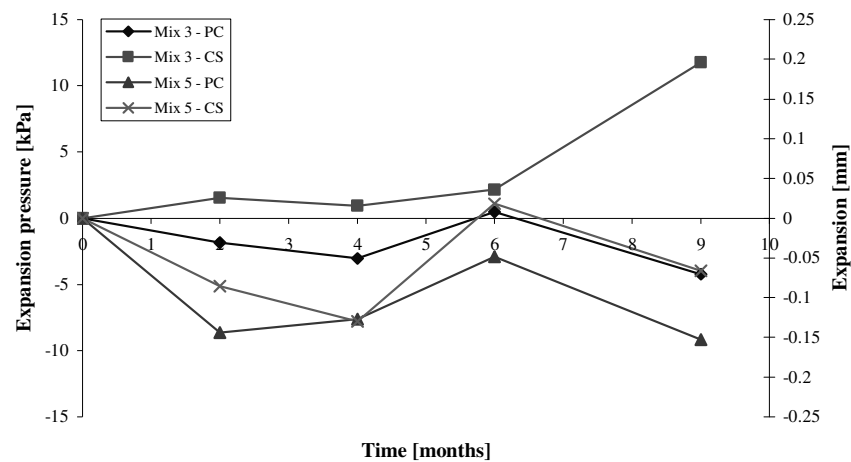

Figure A-29 - Pressure development due to TSA at sub-type with physical barrier
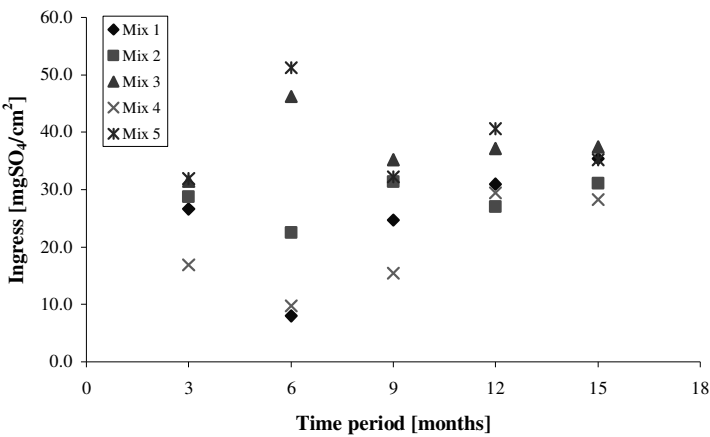
Sulfate Uptake:

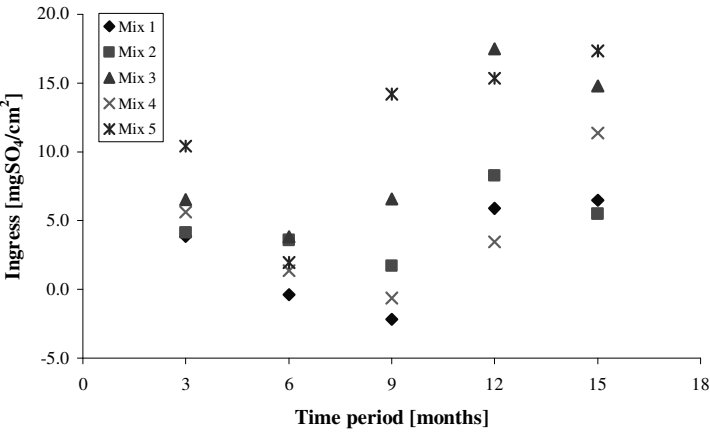**Figure A-30-** Ingress of SO_4 over precast surface in SO_4-CO_3 solution

Figure A-31 - Ingress of SO_4 over cast in-situ surface in SO_4-CO_3 solution

Series V – Expansion Data

Table A-4 - Summary of thaumasite expansion data for Series V - specimens - Lower Lias Clay

Lower Lias Clay							
Pressure at interface: 10kPa – 0.5m							
Mix	**Precast surface**				**Cast in-situ surface**		
	Thaumasite	**Expansion**			**Thaumasite**	**Expansion**	
		Springs		**Clay**		**Springs**		**Clay**
	[mm]	[kPa]	[mm]	[mm]	[mm]	[kPa]	[mm]	[mm]
Mix 3	6.0	3.95	1.5	-1.6	3.5	2.15	0.6	-1.2
Mix 4	12.5	5.35	2.7	-3.6	7.0	3.85	1.5	-2.0
Mix 5					3.0	4.7	2.2	-0.7
Pressure at interface: 40kPa – 2.0m							
Mix	**Precast surface**				**Cast in-situ surface**		
	Thaumasite	**Expansion**			**Thaumasite**	**Expansion**	
		Springs		**Clay**		**Springs**		**Clay**
	[mm]	[kPa]	[mm]	[mm]	[mm]	[kPa]	[mm]	[mm]
Mix 3	2.75	10.6	0.4	-1.0	2.0	2.45	0.1	-0.9
Mix 4	6.0	10.6	0.7	-2.4	1.5	1.05	0.1	-0.7
Mix 5					3.5	9.85	0.5	-1.3
Pressure at interface: 70kPa – 3.5m							
Mix	**Precast surface**				**Cast in-situ surface**		
	Thaumasite	**Expansion**			**Thaumasite**	**Expansion**	
		Springs		**Clay**		**Springs**		**Clay**
	[mm]	[kPa]	[mm]	[mm]	[mm]	[kPa]	[mm]	[mm]
Mix 3	2.75	11.4	0.5	-0.9	1.0	2.75	0.1	-0.4
Mix 4	4.5	5.9	0.3	-2.0	2.5	7.4	0.3	-1.0
Mix 5					5.0	3.75	0.2	-2.4

Table A-5 - Summary of thaumasite expansion data for Series V - specimens – English China Clay

English China Clay								
Pressure at interface: 10kPa – 0.5m								
Mix	**Precast surface**				**Cast in-situ surface**			
	Thaumasite	**Expansion**			**Thaumasite**	**Expansion**		
		Springs		**Clay**		**Springs**		**Clay**
	[mm]	[kPa]	[mm]	[mm]	[mm]	[kPa]	[mm]	[mm]
Mix 3	24	6.85	3.5	-8.5	10.5	-0.8	-0.3	-0.8
Mix 4	16	4.55	1.8	-6.3	3	4.45	1.7	-3.6
Mix 5					10	-1.5	-0.6	-2.1
Mix 3*	10.5	4.5	1.9	-3.4	1	5.3	2.4	-2.6
Pressure at interface: 40kPa – 2.0m								
Mix	**Precast surface**				**Cast in-situ surface**			
	Thaumasite	**Expansion**			**Thaumasite**	**Expansion**		
		Springs		**Clay**		**Springs**		**Clay**
	[mm]	[kPa]	[mm]	[mm]	[mm]	[kPa]	[mm]	[mm]
Mix 3	14	36.3	1.8	-5.3	7	15.15	0.9	-2.7
Mix 4	8.5	11.7	0.6	-3.7	0	-0.57	-0.3	-0.3
Mix 5					5	5.45	0.3	-2.3
Mix 3*	5.5	17.2	0.8	-2.0	1	-1.95	-0.2	-0.7
Pressure at interface: 70kPa – 3.5m								
Mix	**Precast surface**				**Cast in-situ surface**			
	Thaumasite	**Expansion**			**Thaumasite**	**Expansion**		
		Springs		**Clay**		**Springs**		**Clay**
	[mm]	[kPa]	[mm]	[mm]	[mm]	[kPa]	[mm]	[mm]
Mix 3	11.5	19.35	0.75	-5.0	4	2.5	0.1	-1.9
Mix 4	9.5	12.25	0.4	-4.4	0	-17.7	-0.7	-0.7
Mix 5					2	-8.65	-0.4	-1.4
Mix 3*	5	19.65	0.7	-1.9	0.5	-9.35	-0.4	-0.6

*Reaction time 18months instead of 27months

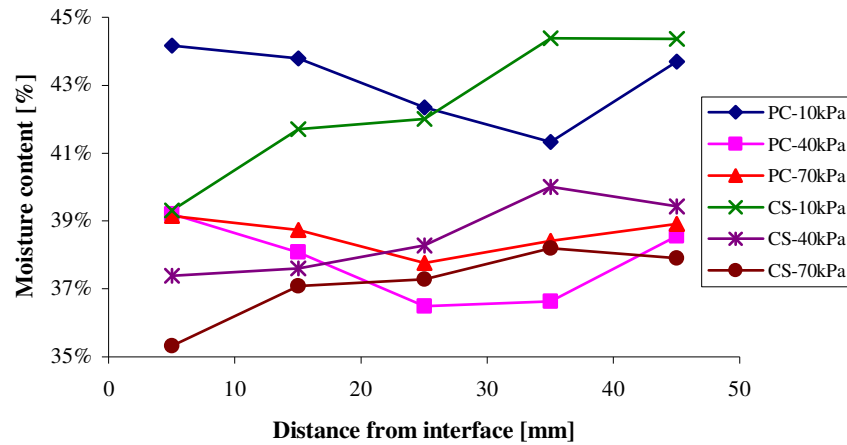## Moisture Content Development towards the Concrete/TSA/Clay Interface
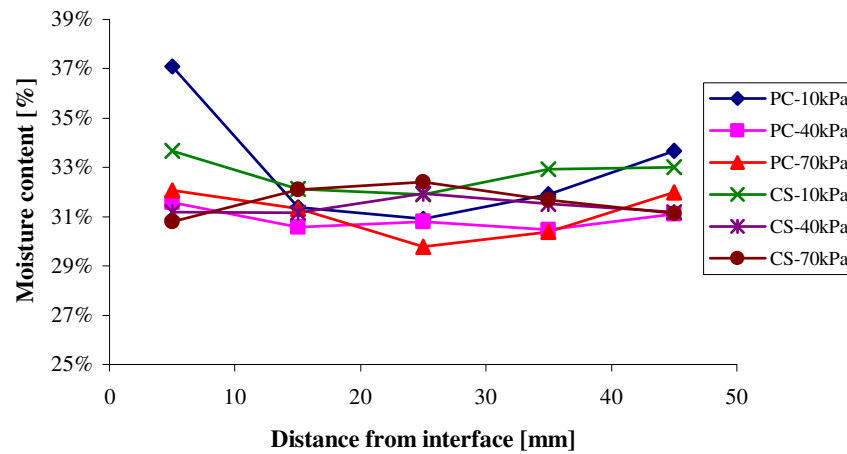

Figure A-32 - Mix 3 - ECC-control
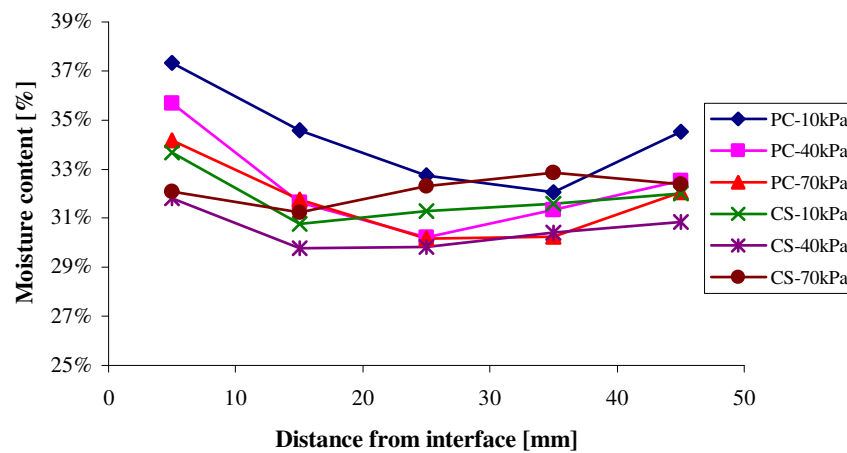

Figure A-33 - Mix 3 - ECC - 18months

Figure A-34 - Mix 3 - ECC - 27months
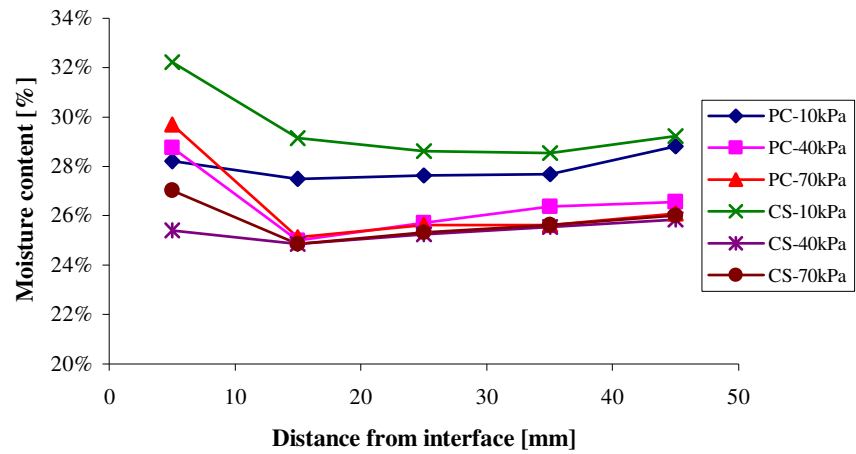
Figure A-35 - Mix 4 - LLC - 27months
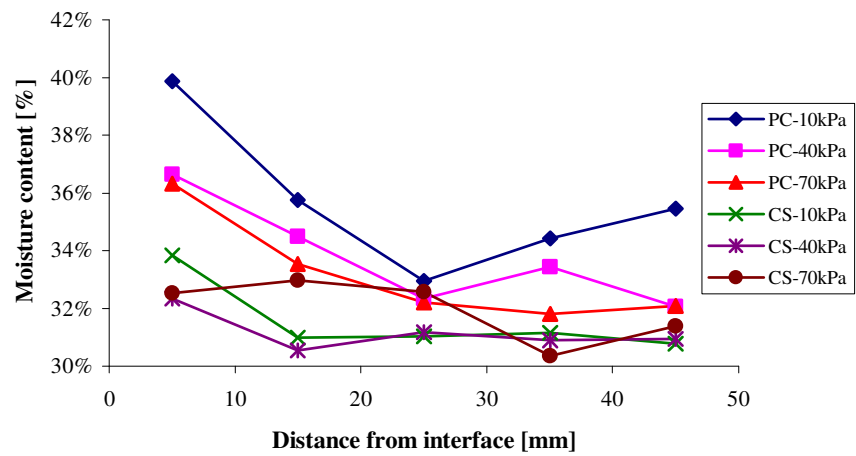
Figure A-36 - Mix 4 - ECC - 27months

Figure A-37 - Mix 5 - LLC - 27months
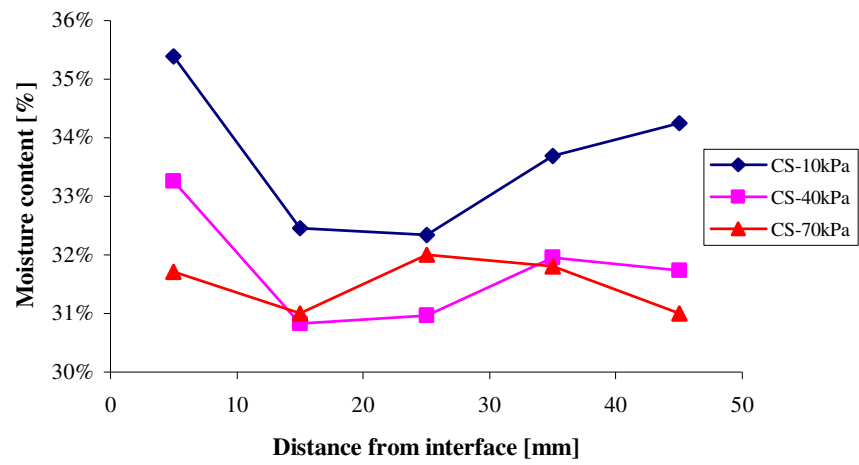
Figure A-38 - Mix 5 - ECC - 27months